GDAŃSK UNIVERSITY OF TECHNOLOGY
FACULTY OF CHEMISTRY

The author of the PhD dissertation: **Weronika Grąźlewska**
Scientific discipline: **Chemistry**

DOCTORAL DISSERTATION

Title of PhD dissertation: Novel monovalent and multivalent recombinant proteins of *Borrelia burgdorferi* sensu lato with potential diagnostic value – construction and biotechnological production

Title of PhD dissertation (in Polish): Nowe monowalentne i multiwalentne rekombinowane białka *Borrelia burgdorferi* sensu lato o potencjalnej przydatności diagnostycznej – konstrukcja i produkcja biotechnologiczna

Supervisor *signature*
Dr Eng. Lucyna Holec-Gąsior

Gdańsk, year 2023

GDAŃSK UNIVERSITY OF TECHNOLOGY
FACULTY OF CHEMISTRY

STATEMENT

The author of the PhD dissertation: Weronika Grąźlewska

I, the undersigned, agree that my PhD dissertation entitled: ,,Novel monovalent and multivalent recombinant proteins of *Borrelia burgdorferi* sensu lato with potential diagnostic value – construction and biotechnological production" may be used for scientific or didactic purposes.[1]

Gdańsk, 27.06.2023 .....

signature of the PhD student

Aware of criminal liability for violations of the Act of 4th February 1994 on Copyright and Related Rights (Journal of Laws 2006, No. 90, item 631) and disciplinary actions set out in the Law on Higher Education (Journal of Laws 2012, item 572 with later amendments),[2] as well as civil liability, I declare, that the submitted PhD dissertation is my own work.

I declare, that the submitted PhD dissertation is my own work performed under and in cooperation with the supervision of Doctor Lucyna Holec-Gąsior.

This submitted PhD dissertation has never before been the basis of an official procedure associated with the awarding of a PhD degree.

All the information contained in the above thesis which is derived from written and electronic sources is documented in a list of relevant literature in accordance with art. 34 of the Copyright and Related Rights Act.

I confirm that this PhD dissertation is identical to the attached electronic version.

Gdańsk, 27.06.2023 .....

signature of the PhD student

I, the undersigned, agree to include an electronic version of the above PhD dissertation in the open, institutional, digital repository of Gdańsk University of Technology, Pomeranian Digital Library, and for it to be submitted to the processes of verification and protection against misappropriation of authorship.

Gdańsk, 27.06.2023 .....

signature of the PhD student

[1] Decree of Rector of Gdansk University of Technology No. 34/2009 of 9th November 2009, TUG archive instruction addendum No. 8.

[2] Act of 27th July 2005, Law on Higher Education: Chapter 7, Criminal responsibility of PhD students, Article 226.

GDAŃSK UNIVERSITY OF TECHNOLOGY
FACULTY OF CHEMISTRY

DESCRIPTION OF DOCTORAL DISSERTATION

The Author of the PhD dissertation: Weronika Grążlewska
Title of PhD dissertation: Novel monovalent and multivalent recombinant proteins of *Borrelia burgdorferi* sensu lato with potential diagnostic value – construction and biotechnological production

Title of PhD dissertation in Polish: Nowe monowalentne i multiwalentne rekombinowane białka *Borrelia burgdorferi* sensu lato o potencjalnej przydatności diagnostycznej – konstrukcja i produkcja biotechnologiczna

Language of PhD dissertation: English

Supervision: Dr Eng. Lucyna Holec-Gąsior

Date of doctoral defense:

Keywords of PhD dissertation in Polish: Borelioza, *Borrelia burgdorferi* sensu lato, serodiagnostyka, białka rekombinowane, białka chimeryczne

Keywords of PhD dissertation in English: Lyme disease, *Borrelia burgdorferi* sensu lato, serodiagnostics, recombinant proteins, chimeric proteins

Summary of PhD dissertation in Polish:

Zróżnicowana budowa antygenowa *Borrelia burgdorferi* sensu lato (s.l.) oraz niski stopień zakonserwowania sekwencji białek pomiędzy genogatunkami sprawia, że serodiagnostyka boreliozy ma wiele ograniczeń.

Z wykorzystaniem systemów ekspresyjnych opartych o *Escherichia coli* wyprodukowano pięć monowalentnych białek rekombinowanych *B. burgdorferi* s.l. tj. BB0108, BB0126, BB0298, BB0323, BB0689 (każde w trzech wariantach otrzymanych z *Borrelia afzelii*, *Borrelia burgdorferi* sensu stricto, *Borrelia garinii*) oraz cztery multiwalentne białka chimeryczne złożone z fragmentów antygenów BmpA, BBK32 i BBA64. Do projektowania białek chimerycznych wykorzystano dane uzyskane z analizy bioinformatycznej sekwencji aminokwasowej i mapowania epitopów liniowych z wykorzystaniem macierzy polipeptydowej. Następnie za pomocą Western blot (WB) i ELISA określono reaktywność otrzymanych antygenów ze swoistym przeciwciałami anty-*B. burgdorferi* s.l. zawartymi w surowicach ludzkich.

Otrzymane wyniki wskazują, że BB0108 i BB0323 wykazują umiarkowaną reaktywność ze swoistymi IgG i IgM w WB i ELISA, niezależnie od stosowanego wariantu antygenu. Natomiast otrzymane białka chimeryczne wykazywały wysoką reaktywność z IgG w WB. Ponadto wykazano, że mapowanie epitopów może być przydatne w projektowaniu białek chimerycznych wykazujących reaktywność z określonym izotypem przeciwciał w celu zwiększenia skuteczności serodiagnostyki boreliozy.

Summary of PhD dissertation in English:

The diverse antigenic structure of *Borrelia burgdorferi* sensu lato (s.l.) and the low degree of protein sequence conservation between genospecies causes many limitations in serodiagnosis of Lyme disease (LD).

Using expression systems based on *Escherichia coli*, five monovalent *B. burgdorferi* s.l. recombinant proteins were produced. i.e., BB0108, BB0126, BB0298, BB0323, BB0689 (each in three variants derived from *Borrelia afzelii*, *Borrelia burgdorferi* sensu stricto, *Borrelia garinii*) and four multivalent chimeric proteins containing fragments of BmpA, BBK32 and BBA64 antigens. Data obtained from bioinformatic analysis of the amino acid sequence and linear epitope mapping with polypeptide array were used to design chimeric proteins. Subsequently, Western blot (WB) and ELISA determined the reactivity of the obtained antigens with specific anti-*B. burgdorferi* s.l. antibodies contained in human sera.

The results indicate that BB0108 and BB0323 show moderate reactivity with specific IgG and IgM in WB and ELISA, regardless of the antigen variant used. At the same time, the obtained chimeric proteins showed high reactivity with IgG in WB. In addition, it has been shown that epitope mapping can be useful in the design of chimeric proteins that exhibit reactivity with a specific antibody isotype to increase the effectiveness of Lyme disease serodiagnosis.

I would like to express my deepest gratitude to my supervisor, doctor Lucyna Holec-Gąsior for her guidance, and encouragement throughout my doctoral studies. Her extremely valuable advice and unwavering support have shaped my scientific career.

I am also grateful to the scientists from IREC, especially Professor José de la Fuente and Dr. Marinela Contreras Rojo for the warm welcome and care during the research internship, and the advice that contributed to improving the value of my research.

I would also like to thank my colleagues from the Department of Molecular Biotechnology and Microbiology for creating a friendly atmosphere that allowed me to persevere during the ups and downs of my doctoral studies.

Finally, I would like to thank my parents and my husband for everything, because without them I certainly would not have reached this joyful point in my life.

Table of contents

ABBREVIATION

Ab	- Antibody
ACA	- Acrodermatitis chronica atrophicans
APS	- Ammonium persulfate
AUC	- Area under the curve
B/32-G	- BmpA-BBK32-G
B/32-M	- BmpA-BBK32-M
B19V	- Parvovirus B19
BL	- Borrelial lymphocytoma
BLASTp	- Protein basic local alignment search tool
BmpA	- Basic membrane protein A
BSA	- Bovine serum albumin
CSF	- Cerebrospinal fluid
Dbp	- Decorin-binding protein
EBV	- Epstein-Barr virus
ELISA	- Enzyme-linked immunosorbent assay
ELISA-B/32-G	- ELISA based on BmpA-BBK32-G protein
ELISA-B/32-M	- ELISA based on BmpA-BBK32-M protein
ELISA-BB0108	- ELISA based on BB0108 protein
ELISA-BB0323	- ELISA based on BB0323 protein
EM	- Erythema migrans
FHL-1	- Factor-H-like 1 protein
GAG	- Glycosaminoglycans
GST	- Glutathione S-transferase domain
HGA	- Human granulocytic anaplasmosis
IF	- Immunodominant fragments
Ig	- Immunoglobulin
IgG-ELISA	- ELISA targeted for IgG detection
IgG-WB	- Western blot targeted for IgG detection
IgM-ELISA	- ELISA targeted for IgM detection
IgM-WB	- Western blot targeted for IgM detection
IL	- Interleukins
IR	- Invariant regions
LA	- Lyme arthritis
LBA	- Luria Bertani agar
LB	- Luria Bertani medium

LBRF - Lice-borne fever *Borrelia*

LD - Lyme disease

MBP - Maltose-binding protein

MAC - Membrane attack complex

NCBI - National center for biotechnology information

ORF - Open reading frames

OMPs - Outer membrane proteins

PCR - Polymerase chain reaction

PLS - post-Lyme syndrome

RA - Restriction analysis

RB - Round bodies

RE - Restriction enzyme

RF - Rheumatoid factor

RF *Borrelia* - Relapsing fever *Borrelia*

ROC - Receiver operating characteristic

SDS - Sodium dodecyl sulfate

SPPS - Solid phase peptide synthesis

SUMO - Small ubiquitin-related modifier

TB - Terrific broth medium

TBRF - Tick-borne relapsing fever *Borrelia*

TrxA - Thioredoxin 1 protein

TSLPI - Tick salivary lectin pathway inhibitor

TTT - Two-tiered testing

TNF - Tumor necrosis factor

VlsE - Variable major protein-like sequence expressed

WB - Western blot

WB-BB0108 - Western blot based on BB0108 protein

WB-BB0126 - Western blot based on BB0126 protein

WB-BB0298 - Western blot based on BB0298 protein

WB-BB0323 - Western blot based on BB0323 protein

WB-BB0689 - Western blot based on BB0689 protein

WCL - Whole cell lysates

YOPs - *Yersinia* outer proteins

1. INTRODUCTION

1.1. Characteristics of *Borrelia burgdorferi* sensu lato

1.1.1. Taxonomy and occurrence

The *Borrelia burgdorferi* sensu lato (s.l.) complex is a group of bacteria with a worldwide distribution (Figure 1.1). These microaerophilic, Gram-negative bacteria belonging to the phylum Spirochaetes are the etiological agent of Lyme disease (LD), the most common tick-borne disease in the northern hemisphere (Table 1.1).

Table 1. 1 Taxonomic classification of *B. burgdorferi* s.l. [*www.itis.gov*]

Kingdom	Bacteria
Subkingdom	Negibacteria
Phylum	Spirochaetae
Class	Spirochaetes
Order	Spirochaetales
Family	Spirochaetaceae
Genus	*Borrelia*
Species	*Borrelia burgdorferi*

Currently, on the basis of phylogenetic similarity, about 20 genospecies are distinguished within the *B. burgdorferi* s.l. complex. However, due to the attempts to identify and describe new strains, it is believed that this number is not final (Lohr et al., 2018; Steinbrink et al., 2022). So far, undeniable pathogenicity for humans has been confirmed for 6 genospecies, i.e. *Borrelia burgdorferi* sensu stricto (s.s.), *Borrelia afzelii*, *Borrelia spielmanii*, *Borrelia garinii*, *Borrelia bavariensis* and *Borrelia mayonii*. Human pathogenicity is very probable but still remains under debate, for *Borrelia valaisiana, Borrelia lusitaniae*, *Borrelia bissettiae*, *Borrelia turdi*, *Borrelia kurtenbachii*, and *Borrelia yangtzensis*. All of the species that have been recognized to be pathogenic to humans, except *B. mayonii*, are found in Europe. *B. burgdorferi* s.s., *B. mayonii* and the probable pathogenic *B. bissettiae* are present in the USA. In Asia, however, all the genospecies mentioned are common except for *B. burgdorferi* s.s. and *B. mayonii* (Steinbrink et al., 2022).

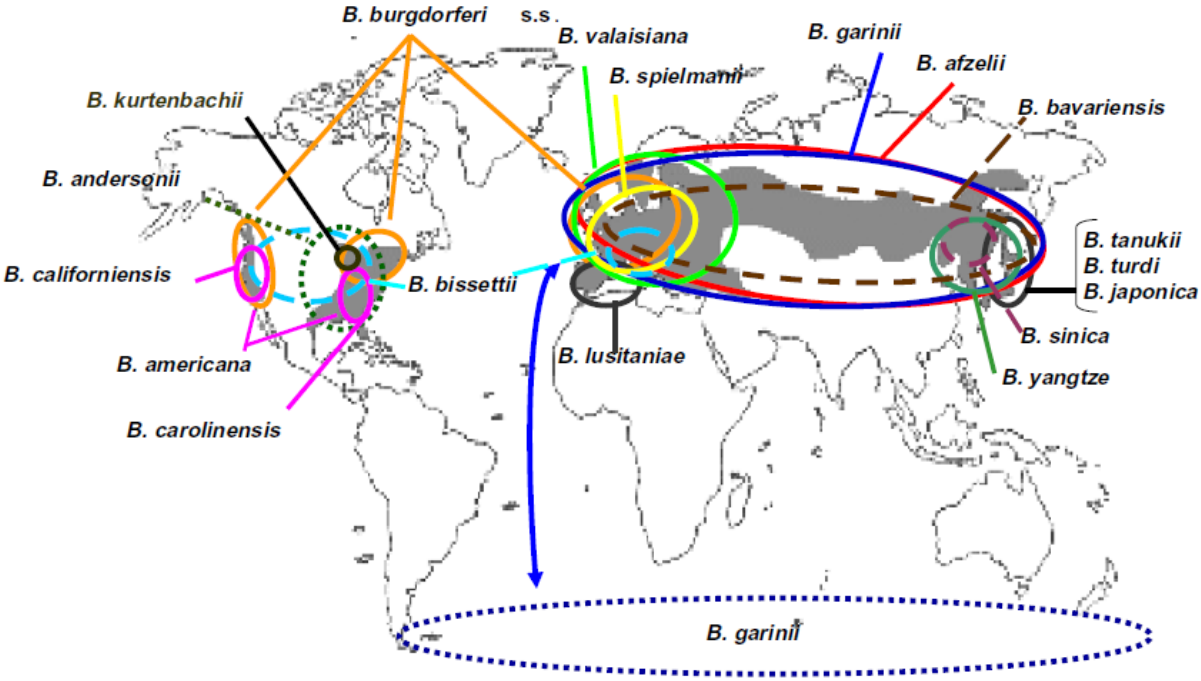

Figure 1. 1 Map of the distribution of genospecies belonging to the complex of *B. burgdorferi* s.l. (Margos et al., 2011).

1.1.2. Cell structure

B. burgdorferi s.l. cells are spiral, and their length ranges from 10 to 30 μm, while the width ranges from 0.2 to 0.5 μm. In the structure of the cell, the following elements are distinguished: outer and inner lipid membrane, protoplasmic cylinder, and periplasmic space, within which the flagella are located (Figure 1.2). Due to the presence of the outer and inner cell membranes, *B. burgdorferi* s.l. is classified as Gram-negative bacteria, but their structure differs significantly from typical representatives of this group. One of the differences is the lack of lipopolysaccharide in the outer cell membrane, instead, there are immunoreactive glycolipids, mainly composed of galactose (Goldstein et al., 1996; Meriläinen et al., 2015). Another uncommon feature is the location of the flagella - while other bacteria usually have them outside the cell - in *B. burgdorferi* s.l. are inside it. Each cell contains about 7-10 flagella, built of three elements: filament, hook, and the basal body. Flagella are arranged in a single ribbon that wraps around the periplasmic cylinder, giving the cell its characteristic spiral shape and allowing it to move in response to signals from the environment (Goldstein et al., 1996; Hyde, 2017).

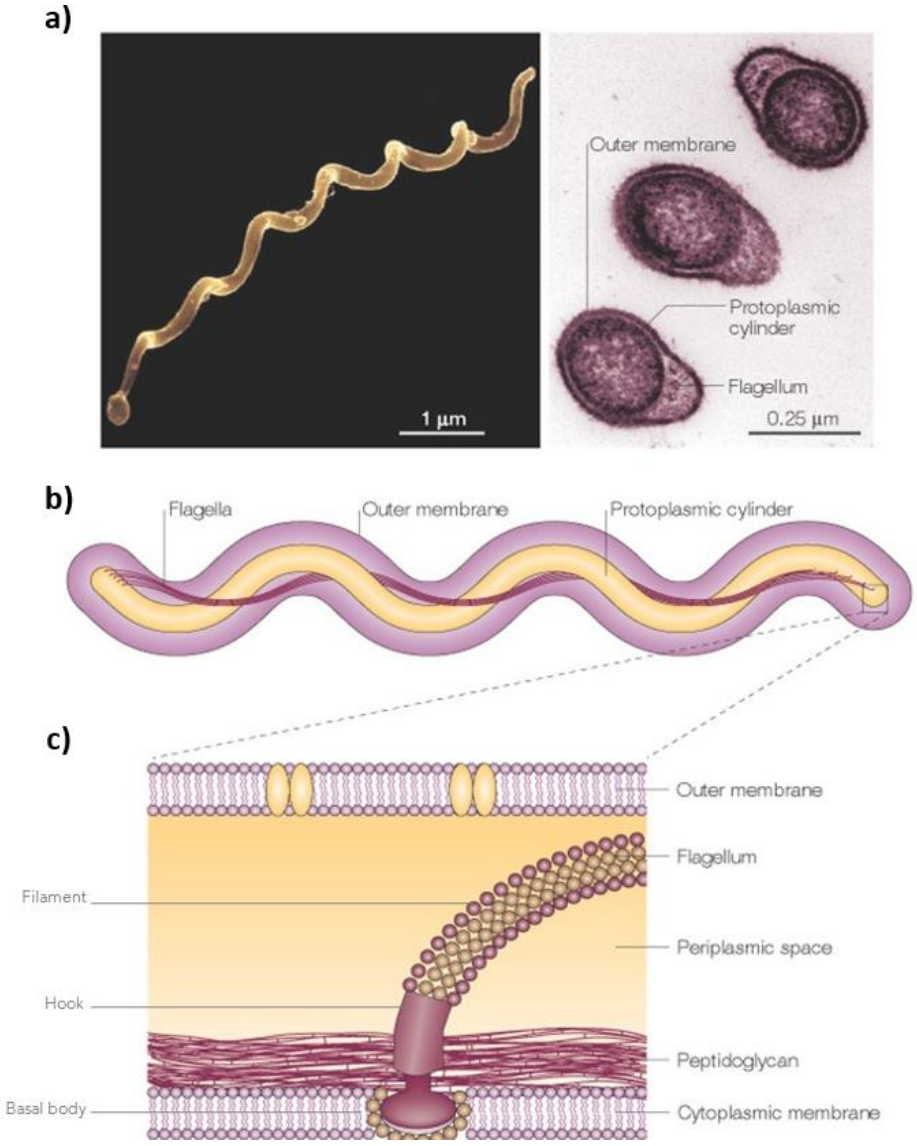

Figure 1. 2 Structure of *B. burgdorferi* s.l. cell. a) electron microscopy photos; b) scheme of cell; c) detailed scheme of periplasmic space and flagellum (Rosa et al., 2005).

Bacteria belonging to the *B. burgdorferi* s.l. complex are pleomorphic, meaning they are able to change their morphology in response to environmental conditions (Berndtson, 2013; Meriläinen et al., 2015). Four pleomorphic forms of *B. burgdorferi* s.l. are known:

- spirochaete - vegetative spiral form;
- blebs - form with a diameter of 1.3±0.43 µm;
- round bodies (RB) also called cell wall deficient - a form without a cell wall with a diameter of 2.8±0.46 µm;
- biofilm like - a colony composed of spirochetes, spherical forms and blebs, containing an extracellular polymeric substance in the matrix (Moniuszko-Malinowska et al., 2016).

Maintaining spirochetes in a vegetative (spiral) form requires favorable environmental conditions. In response to environmental stress (antibiotics, elements of the complement system), there is a transformation from the spiral form to the RB form, which facilitates survival in unfavorable conditions. Due to the lack of a cell wall, this form is insensitive to antibiotic therapy. In addition, the antigenic structure of the outer membrane of the RB is significantly different from that of the vegetative form - which helps it avoid specific antibodies (Ab). When environmental conditions improve, *B. burgdorferi* s.l. can easily revert to a vegetative form (Meriläinen et al., 2015; Moniuszko-Malinowska et al., 2016).

Blebs are also formed in response to physiological stress, but they are much smaller than RB, and unlike, they are unable to convert back to the spirochetal form. Therefore, the presence of blebs is of no clinical importance as this form is the end stage of pathogens (Meriläinen et al., 2015; Moniuszko-Malinowska et al., 2016).

1.1.3. Genome structure

Bacteria of the genus *Borrelia* are not closely related to any other microorganisms, including other spirochetes. The genome of *B. burgdorferi* s.l. has one of the most unique and intricate structures among bacteria. It is possible that this is related to the diversity of environmental conditions of their existence, which requires significant changes in the pattern of gene expression in order to survive (Brisson et al., 2012; Fraser et al., 1997). The *B. burgdorferi* s.l. genome consists of a linear chromosome with a size in the range of 905-922 kbp and numerous low-copy plasmids (at least 9 circular and 12 linear) in the 5-220 kbp size range. Not all *B. burgdorferi* s.l. isolates contain the full set of plasmids, the number varies from 7 to 21 (Casjens et al., 2000; Fraser et al., 1997).

The length of the constant regions of the chromosomes was found to be approximately 903 kb, and the differences in their sequence between *B. burgdorferi* s.l. genospecies were less than 1%, while the calculated distances between species ranged from 2.8% to 8% (Jacquot et al., 2014; Mongodin et al., 2013).

The chromosome encodes mainly housekeeping genes, but their set seems to be minimal to ensure cell survival and replication. These include genes for cell wall biosynthesis (but not lipopolysaccharide synthesis); protein export and lipidation; biosynthesis of DNA, RNA, and proteins; DNA repair; nucleotide metabolism (but not *de novo* synthesis); biosynthesis of membrane lipids and phospholipids; glycolysis and several enzymes that provide substrates for the glycolytic pathway, the only way bacteria produce ATP. *B. burgdorferi* s.l. does not have genes encoding enzymes necessary for the synthesis of amino acids, nucleotides, and fatty acids. They were probably lost as a

result of the spirochete's adaptation to a parasitic lifestyle. On the other hand, *B. burgdorferi* s.l. has many genes (at least 52) encoding various types of transport and binding proteins responsible for providing the bacterial cell with the necessary metabolites. In addition, a large and complete set of genes required for motility and chemotaxis is also present (Brisson et al., 2012; Casjens et al., 2000, 2012; Fraser et al., 1997; Ohnishi et al., 2001).

The large number of plasmids, unparalleled in other bacteria, makes *B. burgdorferi* s.l. show considerable variability within genospecies and throughout the life cycle, as not all strains of spirochaetes have a full set of plasmids. In addition, the nucleotide sequences of the individual plasmids are low conserved within the *B. burgdorferi* s.l. group. Only the cp26, cp32 and lp54 plasmids are necessary for the survival of the bacteria in the environment, therefore, they are present in all *B. burgdorferi* s.l. isolates and show a relatively high degree of conservation of the nucleotide sequence. The rest of the plasmids is quite easily lost, which is associated with difficulty in laboratory cultivation of fully virulent strains of *B. burgdorferi* s.l. (Brisson et al., 2012; Casjens et al., 2017; Ohnishi et al., 2001).

The *B. burgdorferi* s.l. contains single copies of plasmids, in which the average proportion of coding sequences ranges from 30 to 92% (Brisson et al., 2012). These plasmids are unusual compared to most bacterial plasmids in that they contain many paralogous sequences, a large number of pseudogenes, and in some cases, also essential genes. In addition, many plasmids have features that indicate they are prophages. By performing sequence homology analysis, the role of 10% of genes has so far been identified, and none of the described functions overlap with the virulence mechanisms observed in other microorganisms. Genes located on plasmids encode mainly proteins responsible for the interaction of bacteria with host tissues, thus determining the pathogenicity and virulence of *B. burgdorferi* s.l. Generally, plasmids are not required for the growth in culture however, they are necessary to establish infection in a vertebrate or tick. The only exception is cp26 which is needed for growth of spirochetes in culture medium (Fraser et al., 1997; Schwartz et al., 2021).

Studies using *B. burgdorfei* s.l. have shown that the plasmids lp25, lp28-1, lp36, lp54 and cp26 are essential for pathogenesis in mice, while lp25, lp28-1 and lp28-4 are critical for establishing infection in ticks. As many as 15% of genes located on plasmids are responsible for coding surface lipoproteins, which are a key group of proteins responsible for the transmission of the spirochete, its spread and survival in the host's organism (Casjens et al., 2017; Schwartz et al., 2021).

B. burgdorferi s.l. genes expression is strictly regulated in response to changes in environmental conditions as the production of different proteins is required during the

life of *B. burgdorferi* s.l. in the tick or host, and during transmission. Spirochetes are able to alter the expression of multiple genes involved in cell metabolism, motility, and interaction with host- and tick-derived molecules. The expression of *B. burgdorferi* s.l. genes is mainly affected by changes in temperature and environmental pH, and to a lesser extent by the content of nutrients, carbon dioxide, oxygen, heavy metals and cell density (Steinbrink et al., 2022).

1.1.4. Antigenic structure of *B. burgdorferi* s.l.

B. burgdorferi s.l. is characterized by a very high proteome heterogeneity. As mentioned, individual isolates may contain different plasmids and therefore also differ in antigenic composition. In addition, due to the multitude of environments in which *B. burgdorferi* s.l. must survive, the set of proteins produced changes at different stages of the spirochete's life cycle. The conditions in the body of ticks and mammals are completely different, which is why *B. burgdorferi* s.l. has many genes that are only transcribed in one of the hosts. The production of proteins necessary for mammalian entry and colonization usually begins in response to changing conditions during a blood meal by ticks. An increase in temperature and a decrease in pH are a signal to start the migration of spirochetes to the salivary glands of arachnids and the production of new proteins needed for transmission (Figure 1.3) (Casjens et al., 2017; Ojaimi et al., 2003).

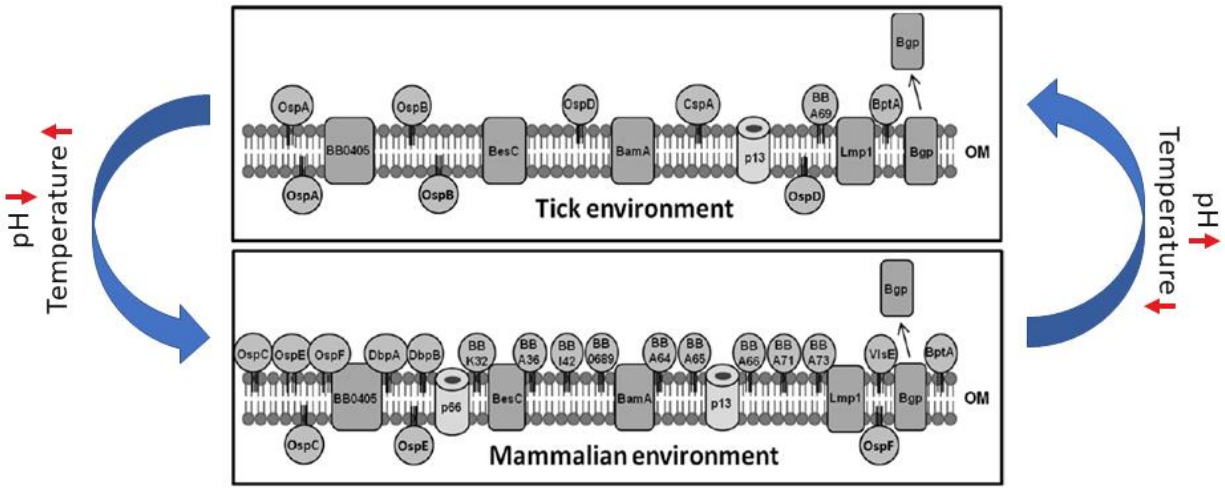

Figure 1. 3 Comparison of *B. burgdorferi* s.l. surface antigens expressed during life in the tick and in the mammalian host (OM - outer membrane) (Kenedy et al., 2012).

The proteins mainly involved in the establishment of infection in both ticks and vertebrate hosts are surface antigens. They are characterized by the greatest diversity during the life cycle of spirochetes because they are responsible for direct interactions with host tissues (DbpA, BBK32), enable *B. burgdorferi* s.l. to take up essential nutrients and avoid the immune system response (VlsE, OspE-related proteins) (Table 1.2). Their diversity is further enhanced by reports that *B. burgdorferi* s.l. produces a different set of

surface proteins depending on the type of mouse tissue in which it is found, what may be related to the tissue tropism of the spirochetes (Kenedy et al., 2012; Norris, 2006). In addition, research by Jacobs et al. (2005) suggests that different proteins are produced by different genospecies of *B. burgdorferi* s.l. under the same conditions, which may explain the different course of pathogenesis.

B. burgdorferi s.l. surface proteins fall into two main categories: lipoproteins, which are anchored to the outer membrane by N-terminal lipid moieties, and integral outer membrane proteins (OMPs), which are anchored by transmembrane domains (Kenedy et al., 2012).

OMPs are relatively well conserved among *B. burgdorferi* s.l., which is influenced by the location of almost all known genes encoding OMPs on the chromosome. They are mainly responsible for functions necessary for the survival of the bacterial cell, such as obtaining nutrients or antibiotic resistance (Fraser et al., 1997; Kenedy et al., 2012). *B. burgdorferi* s.l. contains a relatively low abundance of integral OMPs compared to other bacteria. For example, *Escherichia coli* has 10-fold more OMPs localized in the outer membrane. This shortage of integral membrane-spanning surface proteins, combined with the rather low antigenicity of OMPs hindered their identification, therefore, relatively few *B. burgdorferi* s.l. OMPs have been characterized (Kenedy et al., 2012).

Lipoproteins predominate on the surface of the spirochetes, most of which are encoded by plasmids, which makes them relatively low-conserved within *B. burgdorferi* s.l. However, there are exceptions, including BmpA, whose gene is located on a chromosome. The expression pattern of plasmid-encoded lipoproteins changes throughout the life cycle of the spirochete in response to various environmental conditions. These observations indicate that surface lipoproteins play an important role in virulence and host-pathogen interactions, and have also been shown to be involved in host immune response evasion. This opinion is supported by the observation that the loss of plasmids correlates with the decrease in *B. burgdorferi* s.l. infectivity (Kenedy et al., 2012; Purser and Norris, 2000; Schwan et al., 1995).

Throughout its complex zoonotic cycle, *B. burgdorferi* s.l. must adhere to the diverse tissues of many hosts (primarily ticks and mammals, but also birds and lizards). For this reason, spirochetes are able to express a diverse set of adhesins, which are involved in pathogenicity and virulence. Environmental cues tightly regulate the production of many of these adhesion proteins, and they aid in tissue colonization as well as support *B. burgdorferi* s.l. survival in host's blood. It has been shown that the lack of such adhesins as DbpA, BBK32 or OspC, BB0323 hinders or prevents the establishment or persistence of mammalian infection. *B. burgdorferi* s.l. encodes more than 19 adhesive outer surface proteins, both lipoproteins, and OMPs. These adhesins

have an affinity for host cells or components of the extracellular matrix. The most popular ligands for *B. burgdorferi* s.l. are fibronectin, glycosaminoglycans (GAG), decorin, integrins, lamin, plasminogen, and collagen. Additionally, several others bind to host complement regulatory factors (Table 1.2) (Caine and Coburn, 2016) .

The expression of highly specialized proteins is required to survive *B. burgdorferi* s.l. in ticks. While the complete picture of what proteins are crucial in this process is still unknown, studies have identified several required for spirochete survival in ticks. The best-known surface protein produced during this life stage of *B. burgdorferi* s.l. is lipoprotein BptA, a critical regulator of spirochete virulence and persistence in the tick, although its mechanism of action is still unknown. Also important are the proteins that support the multi-month existence of *B. burgdorferi* s.l. in the intestines of an unfed tick, when the availability of nutrients is limited. One of them is BB0690, the Dps protein produced at high levels during the life of *B. burgdorferi* s.l. in ticks, and its deficiency prevents long-term survival in unfed arachnids. In other bacteria, Dps proteins prevent DNA degradation and protect against oxidative stress. BB0690 does not bind DNA or protect against oxidative stress *in vitro*, but it does bind to iron and copper, which helps protect *B. burgdorferi* s.l. from superoxide stress (Helble et al., 2021).

1.1.4.1. VlsE (Variable major protein-like sequence expressed)

VlsE is a lipoprotein encoded by the linear plasmid lp28-1, with a molecular mass of approximately 35 kDa (Lawrenz et al., 1999; Zhang et al., 1997). The locus occupied by the *vlsE* gene consists of an expression site and 15 silencing cassettes within which there are six variable regions (VR1 to VR6) separated by invariant regions (IR) (Figure 1.4a). During mammalian infection, regions of the expressed *vlsE* cassette are replaced with regions of the silent cassettes through a gene conversion mechanism that led to the generation of billions of clones, each expressing a different VlsE variant, thus avoiding the immune response (Norris, 2015; Zhang et al., 1997). It was noted that *B. burgdorferi* s.l. grows *in vitro* or persistence in ticks retain the parental *vlsE* sequence, and sequence variation in immunocompetent mice occurred at a higher frequency compared to *vlsE* variation in SCID mice. These data suggest that antigenic variation depends on mammalian factors and that selection of VlsE variants occurs in the presence of an efficient immune system (Zhang et al., 1997).

VlsE is a strong immunogen that induces the production of immunoglobulin M and G (IgM and IgG) in the early stages of infection. A deeper study of VlsE revealed that there is a highly conserved 26-amino acid region (IR6) within it. It has also been shown that this fragment of the VlsE protein is the main antigen leading to the production of antibodies (Goettner et al., 2005; Liang and Philipp, 2000).

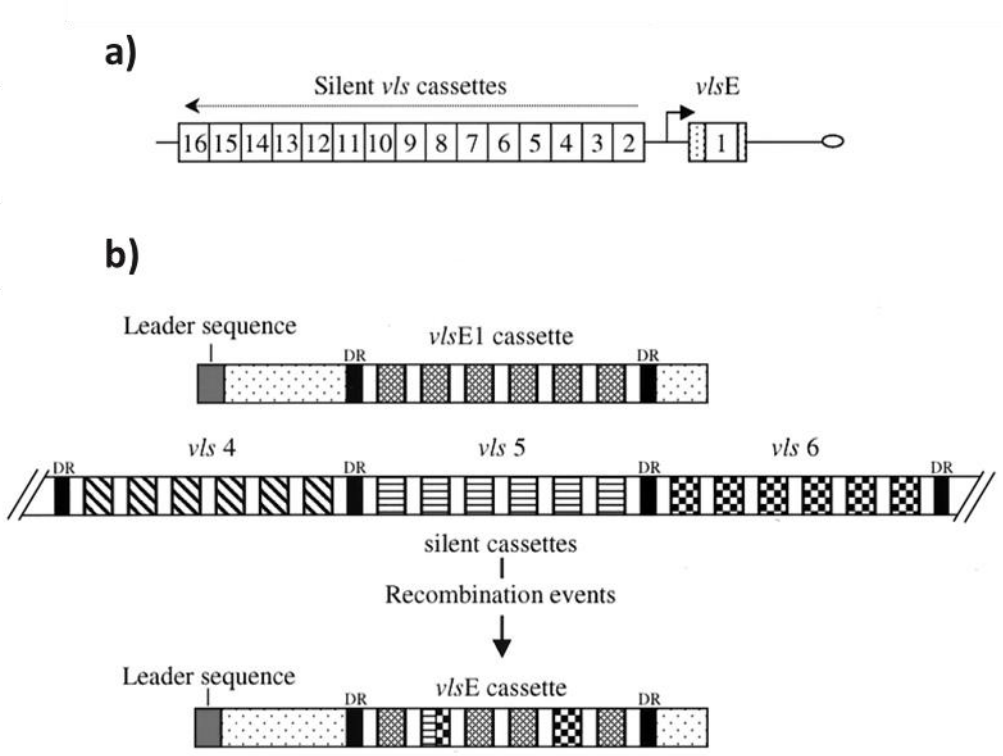

Figure 1. 4 *vlsE* structure: a) arrangement of *vls* locus in *B. burgdorferi* s.s. B31; b) mechanism of antigenic variation between the *vlsE* expression site and silencing cassettes (Lawrenz et al., 1999).

1.1.4.2. Dbp (Decorin-binding protein)

DbpA and DbpB are encoded by the *dbpB/A* operon, located on the lp54 plasmid (Hagman et al., 1998). Their production increases with a decrease in pH and an increase in temperature to 37°C, i.e., changes in the conditions accompanying the transmission of the pathogen from a tick to a mammal. These proteins are responsible for the adhesion of bacteria to host tissues by binding decorin - a proteoglycan interacting with collagen fibers. DbpA and DbpB have been shown to play a key role in the later stages of infection: spreading and maintaining the spirochete in the mammalian body. Their vast role in the development of infections may be evidenced by the fact that strains of *B. burgdorferi* s.l. those lacking the lp54 plasmid are avirulent (Fischer et al., 2003; Ojaimi et al., 2003). Particularly immunogenic is the DbpA, which induces the production of IgG (Goettner et al., 2005).

Analysis of the amino acid sequences of DbpA of various members of the *B. burgdorferi* s.l. group showed a relatively low (40-60%) degree of their conservation. DbpA from different genospecies was found to bind to dermatan sulfate with different affinities, which may account for the differences observed in the clinical manifestations of *B. garinii*, *B. burgdorferi* s.s. and *B. afzelii* infection (Caine and Coburn, 2016). DbpB

is characterized by a much more conserved amino acid sequence among representatives of *B. burgdorferi* s.l. (Salo et al., 2011).

1.1.4.3. Flagella proteins

At least 25 gene products are required to build functional *B. burgdorferi* s.l. flagella. FlaA and FlaB are among the best-studied flagella proteins. Both are encoded by genes located on the chromosome. The FlaB protein (41 kDa) builds the core, while FlaA (37 kDa) is the flagellar sheath. The genes encoding the FlaA protein are expressed at much lower levels than those encoding the FlaB protein. The surface of the flagella may be only slightly covered with the FlaA protein, leaving a large proportion of the FlaB proteins exposed (Ge et al., 1998; Panelius et al., 2001). Comparisons of the amino acid sequence of the FlaB protein have shown that it is highly conserved among a wide range of microorganisms (e.g., *Bacillus subtilis, Salmonella typhimurium, Treponema pallidum*), especially the edge fragments of the protein (Johnson et al., 1996; Wallich et al., 1990).

Very interesting is the FliL protein, also chromosomally encoded, which is probably responsible for the orientation of the periplasmic flagella, as the *fliL* mutants exhibited a significant defect in motility. Unfortunately, its function has not yet been determined due to the low degree of conservation of *B. burgdorferi* s.l. FliL sequences with its homologs in other bacteria (Motaleb et al., 2011). In addition, FilL appears to be highly immunogenic as in studies by Barbour et al. (2008), antibodies against it were detected more often in mice than those specific for FlaB, which is commonly used in diagnostics.

1.1.4.4. OspA and OspB (Outer surface protein A and B)

OspA and OspB are surface lipoproteins with molecular weights of 31 kDa and 34 kDa, respectively. They are transcribed from a single promoter located on the linear lp54 plasmid (Fraser et al., 1997; Howe et al., 1986; Kenedy et al., 2012). These proteins are characterized by a high degree of similarity in their amino acid sequences, amounting to about 50%. OspA and OspB are necessary for the survival of the spirochete in the midgut of the tick. Therefore their production occurs mainly during the life of the bacteria in the arachnid's body. OspA, binds to the tick midgut receptor TROSPA, thus enabling the bacterium to invade its tick host (Norris, 2006). The expression of the *ospB/A* is stopped when the tick begins to feed, allowing the *B. burgdorferi* s.l. to detach from the tick gut and enter the salivary glands for transmission to the host. However, the OspA protein is still present on the surface of mammalian cells. This is evidenced by the antibodies directed against this antigen, which can be detected in the serum of patients (Aguero-Rosenfeld et al., 2005). It is also worth noting that the OspA protein was a

component of the only human vaccine against Lyme disease used until 2002. It was effective since specific antibodies bound OspA in the tick gut during feeding, preventing spirochetes' transmission (Aguero-Rosenfeld et al., 2005; Kenedy et al., 2012).

1.1.4.5. OspD (Outer surface protein D)

OspD is a surface lipoprotein with a molecular weight of 28 kDa. The expression of the *ospD* gene depends on temperature changes in the *B. burgdorferi* s.l. habitat and specific signals from the mammalian organism. *OspD* expression peaks soon after feeding and tick detachment from the host. The recombinant antigen obtained in the laboratory has the ability to bind to the epithelial cells of the arachnid intestine. However, studies conducted on *B. burgdorferi* s.l. mutants have shown that the lack of OspD lipoprotin does not affect the ability of spirochetes to transmit to the tick and colonize the vector. It is therefore believed that this lipoprotein plays a secondary role in tick infection (Kenedy et al., 2012; Li et al., 2007).

1.1.4.6. BptA (*Borrelia* persistencein tick protein A)

BptA surface lipoprotein is expressed by the *bbe16* gene located on the lp25 linear plasmid. Comparative analyzes of amino acid sequences showed that the BptA shows high conservatism (over 88% similarity and 74% identity) within the *B. burgdorferi* s.l. complex. This allows us to conclude that this protein plays an essential role in maintaining the spirochete's circulatory cycle in nature. Studies have shown that tick larvae infected with *B. burgdorferi* s.l. with a silenced *bptA* gene, after molting to the nymph stage, contained 92% less bacteria compared to wild-type spirochetes, which proves the critical role played by the BptA protein during colonization of the arachnid by the pathogen. *B. burgdorferi* s.l. reach the highest level of expression of the *bbe16* gene when ticks feed on vertebrates (Revel et al., 2005).

1.1.4.7. BBA64

The surface antigen BBA64 (also known as p35) is a lipoprotein with a molecular weight of approximately 35 kDa. The *bba64* gene encoding this protein is located on the lp54 plasmid. Its expression depends on changes in temperature and pH value in the spirochete's environment. Transcriptional activity of the gene is observed both during the blood meal by the tick and during the colonization of host tissues by the spirochete. The exact function of the BBA64 protein has not yet been characterized, but it is believed that it plays an important role in the transmission of the spirochete from the tick to the mammal. Because mutants of *B. burgdorferi* s.l. lacking the ability to produce the BBA64 protein have been shown to be unable to infect mice through a tick bite. However, they were still fully virulent in the needle challenge (Gilmore et al., 2010; Kenedy et al., 2012).

Due to the fact that BBA64 plays an essential role during transmission, and in addition, anti-BBA64 antibodies show bactericidal abilities, it was considered a good candidate for a vaccine against Lyme disease. However, although mice inoculated with BBA64 developed high titers of specific antibodies, they were not protected against *B. burgdorferi* s.l. infection either by natural tick infection or challenged by needle inoculation of culture-grown spirochetes (Brandt et al., 2014).

1.1.4.8. OspC (Outer surface protein C)

OspC is a lipoprotein with a molecular weight of 20 to 25 kDa, depending on the *B. burgdorferi* s.l. genospecies. It is encoded by a locus located on the cp26 plasmid. Its production begins after the arachnid draws blood, and it replaces the OspA protein produced during the existence of the spirochete inside the tick. OspC is necessary for the transmission of *B. burgdorferi* s.l. from the tick to the mammal (Carrasco et al., 2015; Schwan and Piesman, 2000). Deleting the *ospC* gene from *B. burgdorferi* s.l. also negatively affects establishing of infection in mice. This may be due to the antiphagocytic properties of OspC, the underlying activity has not yet been elucidated *in vivo*. In addition, OspC has been shown to bind to plasminogen *in vitro*, which may also influence the pathogenesis of *B. burgdorferi* s.l. (Caine and Coburn, 2016).

OspC is one of the most immunogenic proteins in the early phase of *B. burgdorferi* s.l. infection. Many studies have shown that OspC (along with flagellum proteins) is the main diagnostic antigen detecting specific IgM (Goettner et al., 2005; B. Wilske et al., 1993). However, this protein is characterized by very high heterogeneity among different strains of *B. burgdorferi* s.l., only at its ends are highly conserved sequences. A 20 amino acid fragment covering amino acids 11 to 30 (OspC1 peptide) was located at the N-terminus (Arnaboldi et al., 2013). The fragment located at the C-terminus is shorter and consists of only 10 amino acids (C10 peptide) (Bacon et al., 2003; Mathiesen et al., 1998). This makes it challenging to design widely effective OspC-based diagnostics tools or vaccines. OspC is often used to type strains of *B. burgdorferi* s.l. So far, approximately 25 OspC serotypes have been identified in *B. burgdorferi* s.l. complex (Schwartz et al., 2021).

1.1.4.9. BBK32

BBK32 is an adhesin with a molecular weight of 47 kDa, coded by plasmid lp36. It is expressed on the surface of *B. burgdorferi* s.l. cells in feeding ticks and during the residence of the spirochete in the mammalian body. This protein has the ability to bind fibronectin and glycosaminoglycan, allowing pathogens to attach to the extracellular matrix. In addition, BBK32 has been shown to potently and specifically inhibit the classical pathway by binding with high affinity to the initiating C1 complex of complement.

It suggests that it may be an important virulence factor, however, mutants lacking *bbk32* retained full pathogenicity in mice, regardless of whether the mice were infected by syringe inoculation or naturally by tick bite (Garcia et al., 2016; Xie et al., 2019).

Serological studies have shown that BBK32-specific immunoglobulins commonly appear in patient sera during infection. In addition, a higher IgG titer on BBK32 correlates with a milder course of Lyme disease. These results indicate the diagnostic value of BBK32 and its potential as a vaccine candidate, which have been demonstrated experimentally (Li et al., 2006). Antibodies against BBK32 protect mice from experimental syringe-borne infection by *B. burgdorferi* s.l. and reduce number of spirochetes in ticks inhibiting their transmission during moulting (Fikrig et al., 2000).

1.1.4.10. BmpA (Basic membrane protein A)

bmpA gene is located on the *B. burgdorferi* s.l. chromosome adjacent to three paralogous genes named *bmpB*, *bmpC,* and *bmpD*, forming a complex operon (Simpson et al., 1994). The BmpA (also known as p39) is a lipoprotein located in the bacterial cell membrane and has a molecular weight of approximately 36 kDa. BmpA is characterized by a high degree of conservation of the amino acid sequence among *B. burgdorferi* s.l., which is probably related to the location of the gene. The study results indicate that the BmpA protein binds the components of the extracellular matrix, mainly lamin, which enables the spirochetes to adhere to mammalian cells. Patients during the early stages of infection often develop an immune response against this antigen, and it is considered to be specific for the diagnosis of Lyme disease (Roessler et al., 1997a; Verma et al., 2009).

It is believed that BmpA and its paralogs play a significant role in inducing an immune response in the cells of the synovial membrane of the joint capsule, which leads to the development of Lyme arthritis (LA). Their expression is up-regulated during the presence of spirochetes in the joints and the skin of mice, however, in the latter case, this phenomenon is at a much lower level. *B. burgdorferi* s.l. lacking *bmpA*/*B* were infectious to mice but could not survive in joints and did not lead to the development of LA. In addition, the results show that the BmpA can induce pro-inflammatory cytokine responses in synovial cells, further linking this antigen to the pathogenesis of LA (Yang et al., 2008).

1.1.4.11. BB0323

BB0323 is essential for *B. burgdorferi* s.l. virulence, persistence, and transmission through the whole enzootic cycle. The antigen has an estimated molecular mass of 44 kDa and is highly conserved among *B. brurgdorferi* s.l. Studies have shown variable expression of *bb0323* throughout the zoonotic cycle of the spirochete, with the

highest production levels during tick-mouse transmission. The *bb0323* deletion did not affect the survival of microorganisms *in vitro*, despite significant changes in growth kinetics and cell morphology. However, the *bb0323* mutants were unable to infect either mice or ticks and were rapidly eliminated from immunocompetent and immunodeficient hosts and the vector within the first few days after inoculation. This means that BB0323 is involved in establishing infection in both mammalian hosts and ticks, so inhibition of BB0323 function can interrupt the infectious cycle of spirochetes (Zhang et al., 2009).

BB0323 has in its sequence the LysM domain present in many prokaryotic and eukaryotic enzymes whose function is related to the degradation of the cell wall. LysM is also present on surface receptors involved in the host-pathogen interaction, thus contributing to the virulence of microbes as one of its main functions is peptidoglycan binding. The *bb0323* mutants show changes in cell shape and membrane organization, which indicates the involvement of this protein in the building of the spirochete membrane and cell fission. In a cell, BB0323 is cleaved into distinct N- and C-terminal polypeptides with separate functions. Spirochetes expressing only the C-terminal fragment of BB0323 exhibit normal cell membrane structure and cleavage but remain non-infectious in mice. Only the complete form of the protein ensures the infectivity of *B. burgdorferi* s.l. in mice (Kariu et al., 2015; Zhang et al., 2009).

1.1.4.12. P66

P66 is a chromosomally encoded integral membrane porin with a molecular mass of 66 kDa. It is exposed on the bacterial surface and expressed in the feeding tick before transmission and during life in the mammalian host. It has been shown that this antigen is important for the establishment of mammalian infection. P66 also acts as an adhesin, binds to β3-chain integrins, and is involved in bacterial dissemination from the site of inoculation in the skin (Caine and Coburn, 2016; Kenedy et al., 2012). P66 is also a component antigen in many Lyme disease serodiagnostic assays. However, it has been shown to contain many linear epitopes that are not specifically recognized by antibodies (Arnaboldi and Dattwyler, 2015).

Table 1. 2 Characteristics of selected proteins of *B. burgdorferi* s.l.

***Bb*sl life cycle stage**	**Protein**	**Gene localization**	**Information**	**References**
Ticks	OspA	Plasmid lp54	• Essential for the survival of *Bb*sl in the tick • A component of the only used human Lyme disease vaccine • Bind to TROSPA	(Norris, 2006; Yang et al., 2004)
	OspB	Plasmid lp54	• Essential for the survival of *Bb*sl in the tick	(Norris, 2006; Yang et al., 2004)
	OspD	Plasmid lp38	• Bind to the epithelial cells of the tick's intestine • Peak production shortly after feeding and detachment of the tick from the host	(Li et al., 2007)
	BptA	Plasmid lp25	• Highly conserved - over 74% amino acid identity • Play an important role during tick colonization	(Revel et al., 2005)
Transmisson	OspC	Plasmid cp26	• Necessary for *Bb*sl transmission from tick to mammal • Production begins when the tick takes blood meal • Bind plasminogen and Salp 15	(Caine and Coburn, 2016; Carrasco et al., 2015; Schwan and Piesman, 2000)
	BBA64 (P35)	Plasmid lp54	• Production begins when the tick take blood meal • Necessary for *Bb*sl transmission from tick to mammal	(Brandt et al., 2014; Gilmore et al., 2010)
	CspA (CRASP-1)	Plasmid lp54	• Bind factor H, factor H-like protein 1 and complement components C7, C8 and C9 • Evading the host's immune response (blocking the complement system) • Probably ensure serum resistance in the tick vector during the initial blood meal	(Anderson and Brissette, 2021; Brooks et al., 2003; Kraiczy et al., 2004a; McDowell et al., 2006)

Mammals	DbpA/B	Plasmid lp54	• Bind decorin and GAGs • Involved in the spread and maintenance of the spirochete in the mammalian body	(Caine and Coburn, 2016; Schulte-Spechtel et al., 2006)
	BBK32	Plasmid lp36	• Bind fibronectin, GAGs and complement component C1r • Involved in the spread and maintenance of the spirochete in the mammalian body (vascular and joint colonization) • Inhibit the classical pathway of complement	(Caine and Coburn, 2016; Garcia et al., 2016; Xie et al., 2019)
	VlsE	Plasmid lp28-1	• A *vls* locus contains a *vlsE* expression site and 15 silencer cassettes • Evading the host's immune response (antigenic variation) • Contain a highly conserved - IR6 region	(Panelius et al., 2003; Zhang et al., 1997)
	BmpA	Chromosome	• Bind lamin • Highly conserved • Necessary for the presence *Bb*sl in joints, play role in the development of LA	(Roessler et al., 1997a; Verma et al., 2009; Yang et al., 2008)
	BB0323	Chromosome	• Peak of production during tick-mouse transmission • Involved in establishing infection in mammals and ticks	(Kariu et al., 2015; Zhang et al., 2009)
	RevA	Plasmid cp32	• Bind fibronectin • Involved in heart colonization	(Byram et al., 2015; Carroll et al., 2001)
	OspE-releated proteins (ErpA, ErpC, ErpP)	Plasmid cp32	• Bind factor H, factor H-related proteins and plasminogen • Evading the host's immune response (blocking the complement system)	(Coburn et al., 2013; Kraiczy et al., 2004a; Stevenson et al., 2002)
	CspZ (CRASP-2)	Plasmid lp28-3	• Bind factor H, factor H-like protein 1 • Evading the host's immune response (blocking the complement system)	(Coleman et al., 2008; Kraiczy et al., 2004a)
	P66	Chromosome	• Integral membrane porin • Involved in bacterial dissemination, bind to β3-chain integrins	(Arnaboldi and Dattwyler, 2015)
	p83/100 (BB0744)	Chromosome	• Located in the periplasm • Play a role in the colonization of heart tissue	(Wager et al., 2015)

Ticks and mammals	FlaA	Chromosome	• Build a flagellum sheath • Production is on a low level	(Ge et al., 1998; Panelius et al., 2001)
	FlaB	Chromosome	• Build the flagellum core • Highly conserved among a wide range of microorganisms	(Johnson et al., 1996; Wallich et al., 1990)
	FliL	Chromosome	• Responsible for the orientation of the flagella • Low conserved among other microorganisms	(Barbour et al., 2008; Motaleb et al., 2011)

*Bb*sl - *B. burgdorferi* sensu lato

1.1.5. Zoonotic cycle of *B. burgdorferi* s.l.

The vectors that transmit *B. burgdorferi* s.l. are ticks of the genus *Ixodes*, and the area of their natural occurrence determines the Lyme disease existence zone (Figure 1.5). There are 4 main species of ticks that transmit Lyme disease to humans: *Ixodes scapularis* in the eastern USA and Canada, *Ixodes pacificus* in the western USA, *Ixodes ricinus* in Europe and Asia, and *Ixodes persulcatus* found only in Asia (Margos et al., 2011). It should be remembered that *B. burgdorferi* s.l. has also been detected in other species of hard ticks, e.g., *Dermacentor reticulatus* and *Haemaphysalis concinna*, but it has been experimentally confirmed that they are not competent vectors (Eisen, 2020).

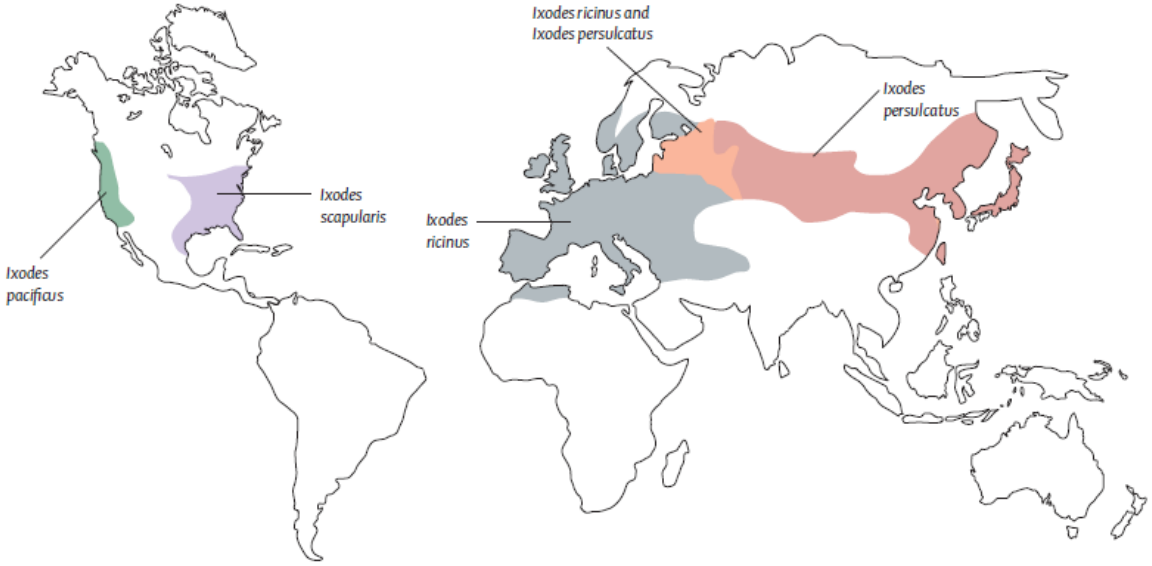

Figure 1. 5 Worldwide spread of *Ixodes* ticks (Stanek et al., 2012).

A tick goes through 4 developmental stages during life: egg, larva, nymph, and adult form (imago) (Figure 1.6). Each of these forms takes one blood meal during its life to molt (larva, nymph) or lay eggs (adult female). Uneaten ticks attach themselves to the vertebrate's skin with specialized mouthparts as the hosts pass through vegetation. After feeding for several days (about 3 days for larvae, 5 days for nymphs, and 7 days for adult females), the ticks detach from the host, and the next place of residence is the soil surface. There, the ticks stay for several months to move on to the next life stadium or, in the case of adult females (adult males do not feed on blood), to lay about 2 000 eggs. Depending on geographic regions and microclimatic conditions, the larvae are active approximately from the end of April to the end of October. In northern and central Europe, nymphs and adults are active from March to November, with a peak in April or May and a decline during warm and dry periods. The length of the tick life cycle varies from 2 to 6 years, depending on climate and host availability (Eisen, 2020; Stanek et al., 2012; Steinbrink et al., 2022).

B. burgdorferi s.l. mainly infects ticks when they feed on vertebrate reservoirs. In rare cases, spirochetes are also transmitted from the adult female to the next generation, called transovarial transmission. Rodents are the main reservoir for *B. burgdorferi* s.s. and *B. afzelii*, birds for *B. garinii*. It also seems that lizards are the main reservoir for *B. lusitaniae*, genospecies potentially pathogenic to humans. Competent reservoirs overlap across genospecies but are not yet fully described, and due to the wide host range of *Ixodes*, their potential list is very long (Eisen, 2020; Steinbrink et al., 2022).

After *B. burgdorferi* s.l. enters the arachnid's body with blood, the spirochetes localize in its midgut and are transferred to the next developmental stages of the tick by transstadial transmission. The increase in temperature and the change in pH inside the tick, accompanying the blood collection, are a stimulus for *B. burgdorferi* s.l. to start expressing a new gene pool. This allows the spirochetes to migrate from the midgut to the tick's salivary glands, from where they enter the body of a new vertebrate host (including humans) with the saliva (Eisen, 2020; Mannelli et al., 2011). Humans are unimportant in the enzootic cycle and are considered hosts of dead ends.

Due to the time required for the production of many new proteins by *B. burgdorferi* s.l., the transmission of spirochetes takes place with some delay. Studies on animal models have shown that infection with the pathogen occurs after about 16 hours of arachnid feeding. Unfortunately, so far it has not been possible to determine the minimum time of feeding by the tick necessary for transmitting the pathogen. This is a challenging task, especially since the rate of transmission seems to depend on the *B. burgdorferi* s.l. genospecies. It is widely believed that removing the arachnid from the human body within 24 hours prevents the development of Lyme disease. However, there are a few reports of patients becoming infected within hours of being bitten by a tick (Cook, 2014; des Vignes et al., 2001; Hynote et al., 2012).

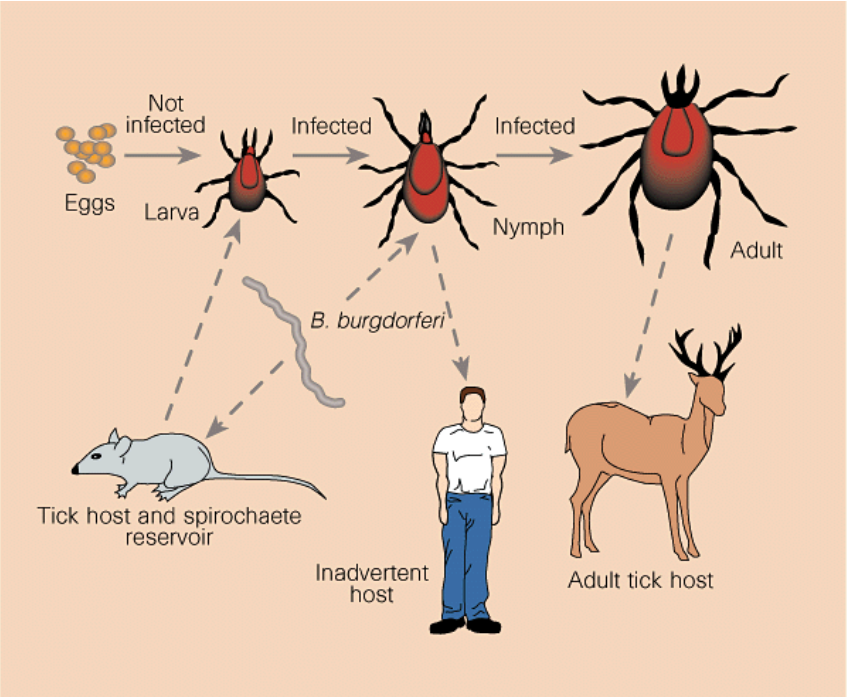

Figure 1. 6 Scheme of the life cycle of *Ixodes* ticks and circulation of *B. burgdorferi* s.l. in the environment (Barbour and Zuckert, 1997).

1.2. Lyme disease in humans

1.2.1. Epidemiology

Lyme disease was first described in the population of Lyme, Connecticut, USA. Rheumatoid-like arthritis was noted in them, mainly affecting children (Allen et al., 1977). However, for many years the etiology of this disease was unknown. It was not until the early 1980s Willy Burgdorfer was the first to discover a new species of spirochete occurring in ticks and link it to Lyme disease (Burgdorfer et al., 1982). Currently, Lyme disease is the most common tick-borne disease in the northern hemisphere. The increasing number of cases is mainly related to climate change, which leads to an increase in ticks and an extension of their feeding time. However, this phenomenon should also be associated with improving the effectiveness of laboratory diagnostics and better surveillance organization (Rizzoli et al., 2011; Strand et al., 2017).

The greatest activity of ticks falls in May-June and September-October, which increases the number of Lyme disease cases in this period. The risk of contracting Lyme disease after a single tick bite is estimated at less than 1%. However, it increases significantly with the time of the tick's meal, when the tick is attached for at least 4 days, the risk increases to 5.2% (Hofhuis et al., 2017). The severity of the problem Lyme disease prevalence is evidenced by the fact that many countries carry out epidemiological surveillance of Lyme disease (Blanchard et al., 2022). There are approximately 85 000 cases of LD per year in Europe (Sykes and Makiello, 2017).

In Poland, since 1996, doctors have been obliged to report cases of Lyme disease to state sanitary and epidemiological stations. According to data published by the National Institute of Public Health, the number of reported cases of Lyme disease in 2021 was 12,427 (incidence 32.7 per 100 000 population) (Figure 1.7). This was a similar result to that of 2020, but it differed significantly from the data obtained in 2016-2019, where over 20 000 cases were reported annually. This visible decrease may be related to the SARS-CoV-2 pandemic, so the diagnosis of Lyme disease was not prioritized. In Poland, the highest percentage of infected *B. burgdorferi* s.l. is observed in Podlasie, Mazowsze, and the south-eastern part of the country (Figure 1.8) (data National Institute of Public Health, wwwold.pzh.gov.pl/oldpage/epimeld/index_p.html).

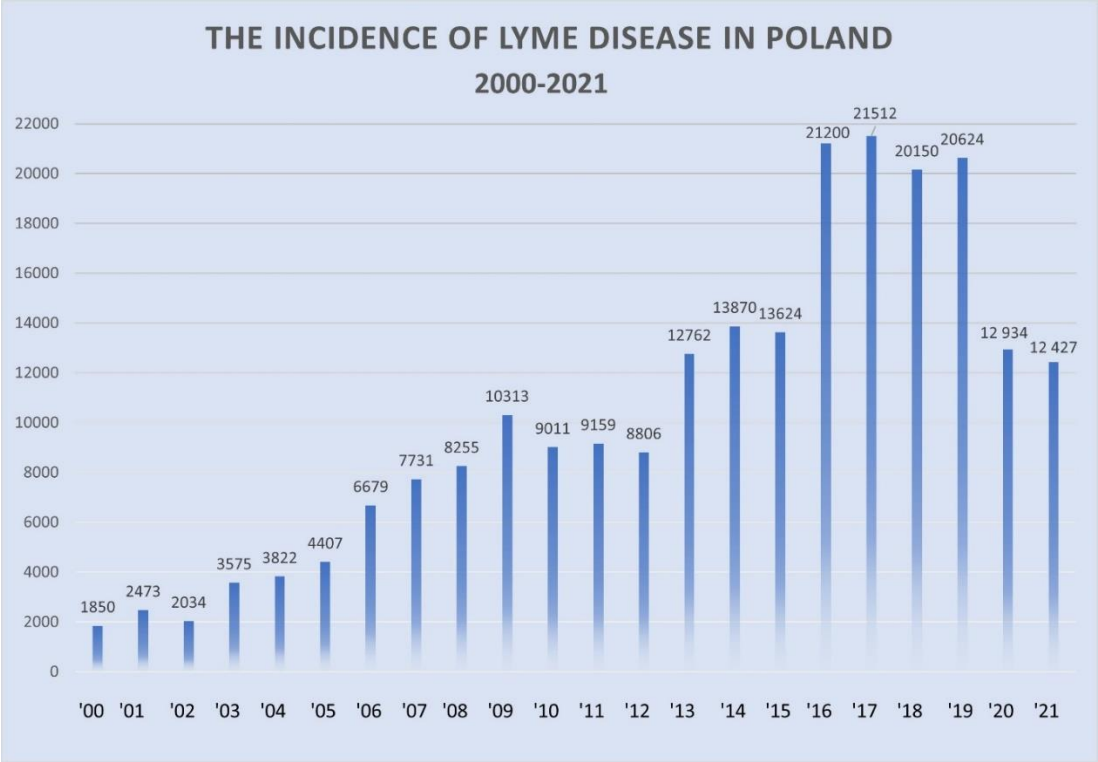

Figure 1. 7 Number of reported cases of Lyme disease in 2000-2021 in Poland (based on data National Institute of Public Health).

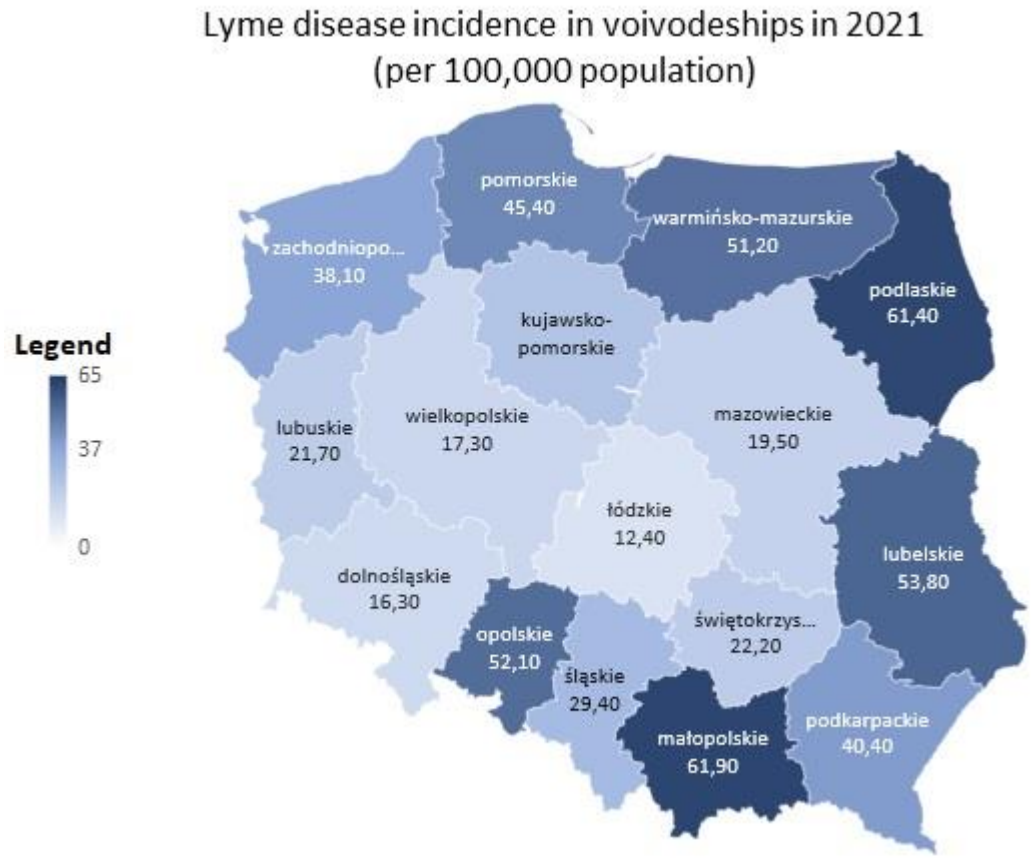

Figure 1. 8 Lyme disease incidence in voivodeships (per 100 000 population) (based on data National Institute of Public Health).

1.2.3. Immune response and pathogenesis

After *B. burgdorferi* s.l. enters the mammalian body through the tick bite site, the pathogen must face the mechanisms of the vertebrate host's innate and adaptive immune response.

The complement system is part of the innate immune system and its function is to create pores membrane attack complex (MAC) that disrupt the cell membrane causing cell lysis. There are three known ways of complement activation. The first is called the classical complement pathway, mediated by antibodies that recognize the surface of the pathogen and recruit complement component C1q molecules, which then activate a cascade of enzymatic cleavage. The second way is based on binding by mannose present in serum lectin located on pathogens' surface, leading to an activation complement cascade in the lectin pathway. The last one, known as the alternative pathway, activates the complement cascade by randomly depositing complement C3 molecules on the surface of the pathogen (Sarma and Ward, 2011).

It has been shown that *B. burgdorferi* s.l. has mechanisms to avoid the complement response, which are active at different time points during the infection cycle to achieve the ultimate protection against the damaging attack of the host's innate

immunity (Lin et al., 2020; Steinbrink et al., 2022). These include mainly surface-expressed proteins capable of binding directly to the components of the complement cascade pathways or complement regulatory factors. Among them are proteins such as CspA (Kraiczy et al., 2006), CspZ (Haupt et al., 2007), ErpP (Kraiczy et al., 2004b), ErpA (Kraiczy et al., 2004a), and ErpC (Brangulis et al., 2015b). All of them are capable to bind factor H, additionally CspA and CspZ interact with factor-H-like 1 protein, while ErpP, ErpC, and ErpA (OspE-releated protein) with complement factor H-related proteins (CFHRs) (Hallström et al., 2013). CspA has been shown to be down-regulated or completely turned off in the mammalian host environment. This indicates that CspA may protect *B. burgdorferi* s.l. from complement while the bacteria are still in the feeding tick and during transmission (Brooks et al., 2003; Kraiczy et al., 2004a; McDowell et al., 2006). Quite recently, BBK32 has also been shown to have a binding capacity C1r subunit of C1. Since the C1 complex is the initiating step of classical pathway, binding of BBK32 to C1r effectively blocking MAC formation (Garcia et al., 2016).

It seems very interesting that the genospecies of *B. burgdorferi* s.l. differ significantly in their ability to survive in the presence of complement from different vertebrates. This may explain why different representatives of *B. burgdorferi* s.l. complex show affinity to various hosts as reservoirs. Thus, *B. afzelii*, *B. mayonii*, and *B. bavariensis* are resistant to the complement of mammalian host, while *B. garinii* and *B. valaisiana* are not killed by bird sera. *B. burgdorferi* s.l. that are isolated from both avian and mammalian reservoirs show resistance to both types of complement (Kurtenbach et al., 2002; Steinbrink et al., 2022).

Proteins in tick saliva have immunomodulatory, antithrombotic, and vasodilating effects, enabling arachnids to feed to repletion. However, they also help pathogens transmit to a new host. Tick salivary lectin pathway inhibitor is the dominant complement inhibitor in tick saliva, significantly reducing pathogen lysis. However, complement inhibition is not the only way to suppress the host's immune response (Wagemakers et al., 2016). The salivary gland protein Salp15 binds to the CD4 co-receptor on CD4 T lymphocytes, decreasing the production of interleukin 2 (IL-2) and thus contributing to the attenuation of the T-cell response. Slap15 is also bound by OspC on the cell surface, protecting *B. burgdorferi* s.l. from the antibody response (Dai et al., 2009). However, by the action of other salivary proteins, pro-inflammatory cytokines such as IL-6, tumor necrosis factor α (TNFα) and γ (TNFγ) can also be down-regulated (Helble et al., 2021). *B. burgdorferi* s.l. also shows resistance to anti-systemic proteins and peptides produced in response to infection, i.e., lactoferrin, azurocidin, proteinase 3 and cathelicidin, and limited sensitivity to lysosomes (Sarkar et al., 2009). Resistance to lactoferrin, an iron-binding and transporting protein, is probably due to the fact that *B. burgdorferi* s.l.

does not require iron. Similarly, resistance to cathelicidin results in the absence of lipopolysaccharide in the outer cell membrane (Anderson and Brissette, 2021).

Activation of the primary immune response at the tick bite site also leads to the production of chemokines and pro-inflammatory cytokines (e.g., IL-1β, IL-6, TNFα, interferon γ) by host immune system cells (such as neutrophils, macrophages, and dendritic cells) which in turn results in the activation of further cells of the immune system and the development of a local inflammatory reaction (Cerar et al., 2016; Kraiczy et al., 2001; Strle et al., 2009). *B. burgdorferi* s.l., however, is also able to evade this type of response by inducing increased production of anti-inflammatory IL-10. This leads not only to a decrease in the level of pro-inflammatory interleukins, but also to the inhibition of macrophage phagocytosis and a decrease in the production of costimulatory molecules in antigen presenting cells. In addition, it also reduces the production of reactive oxygen species and nitric oxide by macrophages (Chung et al., 2013).

Another form of evasion of the innate immune response is the intracellular localization of *B. burgdorferi* s.l., although this is a rare occurrence. *B. burgdorferi* s.l. can infect endothelial cells, fibroblasts, nerve cells, glial cells, and macrophages. In addition, it allows *B. burgdorferi* s.l. to survive short-term antibiotic therapy, which may be the cause of chronic or reoccurring Lyme disease (Anderson and Brissette, 2021; Wu et al., 2011).

As the disease progresses, along with the spread of pathogens within the infected organism, a humoral immune response is triggered based on specific antibodies produced by plasma cells (B-cells). First, after about 2-3 weeks from infection, M class antibodies appear, reaching the highest level after 3-6 weeks, after which their titer decrease (Craft et al., 1984). However, in some patients high titer of IgM persists also in the later stages of the disease (Markowicz et al., 2021). Initially released IgM have a relatively low affinity for the antigen and are directed mainly against flagellin (p41) and the OspC proteins (Goettner et al., 2005; Lohr et al., 2018; Markowicz et al., 2021). Then, after about 3-6 weeks, IgG start to form, although sometimes they may appear with a certain delay (Craft et al., 1984). IgG are characterized by a high affinity for spirochete antigens and persist after *B. burgdorferi* s.l. infection, however, they do not provide long-term protective immunity. The reasons for this phenomenon may include the ability of the spirochete to downregulate gene expression of specific highly immunogenic proteins exposed on the surface, antigenic variation within the VlsE protein and a highly differentiated antigenic profile among genospecies of *B. burgdorferi* s.l. (Anderson and Brissette, 2021; Craft et al., 1984; Eiffert et al., 1996; Zhang et al., 1997).

Also, the transition of the spirochete to its other pleomorphic forms allows to confuse the response of the immune system, as the antigenic composition presented on

the RB and blebs is significantly reduced (Anderson and Brissette, 2021; Meriläinen et al., 2015). Moreover, highly immunogenic antigens such as OspC and DbpA are characterized by low sequence conservation within the *B. burgdorferi* s.l. complex, which may also result in reduced effectiveness of the humoral immune response when repeated infection with another genospecies occurs (Roberts et al., 1998; Theisen et al., 1993).

1.2.2. Lyme disease symptoms

B. burgdorferi s.l. does not produce classic toxins or other recognizable virulence factors that directly cause damage to the host tissues. Therefore, it seems that the multisystemic disorders known as Lyme disease are caused by too strong immune response to bacterial components (Stevenson et al., 2022). In the course of Lyme disease, 3 stages are distinguished (Figure 1.9):

a) early - lasting up to 8 weeks after infection;

b) early - disseminated - appearing 6-26 weeks after contact with a tick;

c) late - developing after 6 months from the infection (Hofmann et al., 2017; Krzyczmanik et al., 2012; Lohr et al., 2018).

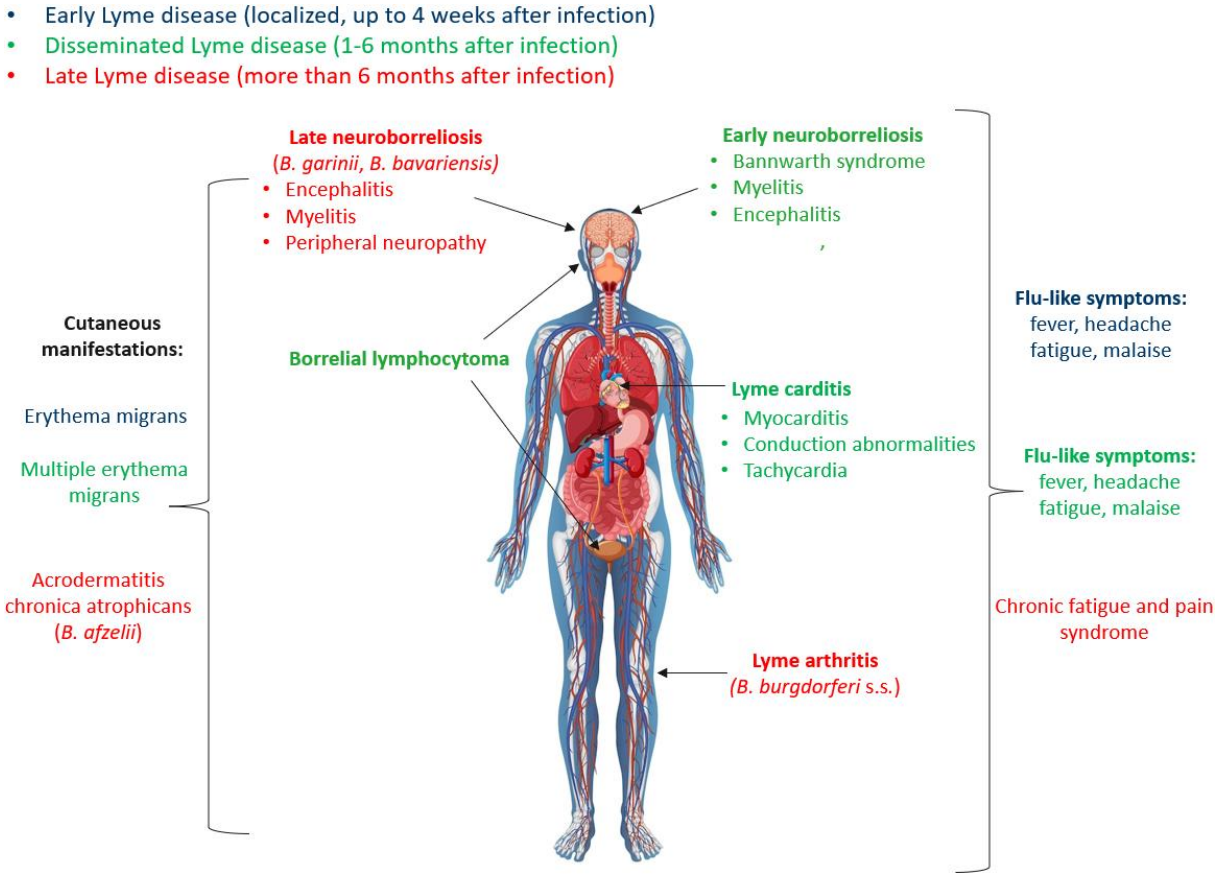

Figure 1. 9 Symptoms of Lyme disease.

The most characteristic manifestation of early Lyme disease is erythema migrans (EM) (Figure 1.10a), which appears in about 60-90% of those infected with *B. burgdorferi* s.l., about 3-30 days after the tick bite (Hofmann et al., 2017; Wang et al., 1999). This is a skin lesion, which the initial one has the form of a red stain, and expands over time, creating a characteristic pattern with the red circuit. At this stage, patients may not show other symptoms or experience flu-like symptoms (Shapiro, 2014; Stanek et al., 2012). Another cutaneous symptom of the early, local Lyme disease is the borrelial lymphocytoma (BL) (Figure 1.10b). This change occurs only in about 1-2% of patients. It is painless, mixed B and T lymphocytic infiltrates, occurs individually or multiple. Sometimes can appear simultaneously with EM or later (up to 10 months). BL is located in most cases on the earlobe, nipple, or scrotum. This untreated change disappears slowly - spontaneously within a few months to several years when it is treated - in a few weeks (Hofmann et al., 2017; Lohr et al., 2018).

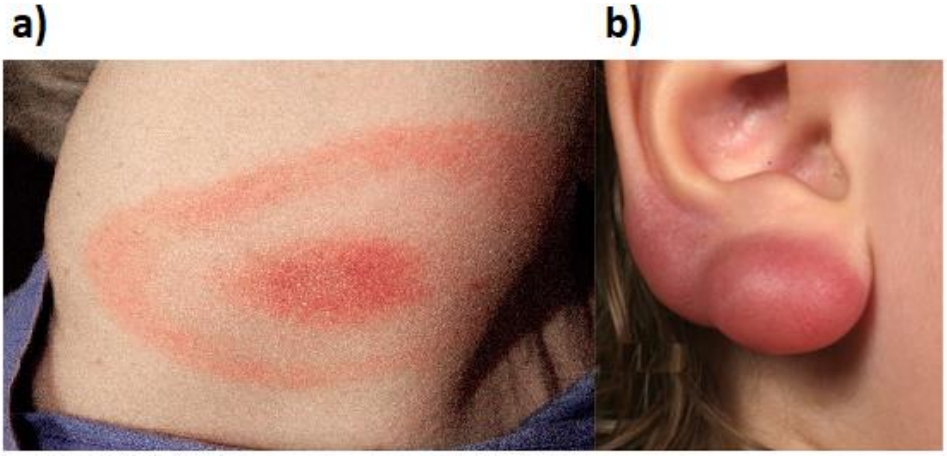

Figure 1. 10 Symptoms of early Lyme disease: a) erythema migrans, b) borrelial lymphocytoma (Hofmann et al., 2017).

If untreated, the infection can develop into an early disseminated phase after a few weeks or months. The dissemination of pathogens within the body occurs through the blood and lymph. Symptoms at this stage of the disease depend on the location of *B. burgdorferi* s.l. The most common disorders include uncharacteristic joint and/or muscle pain and synovitis. In the second stage of the disease, especially in children, early neuroborreliosis may also develop. It is manifested by cranial nerve palsy, lymphocytic meningitis and/or encephalitis, myelitis, radiculitis and neuritis. The coexistence of meningitis, cranial nerve palsy, and radicular syndrome is called Bannwarth syndrome (Hofmann et al., 2017; Krzyczmanik et al., 2012; Lohr et al., 2018).

One of the possible forms of the disease at this stage are also cardiac disorders occurring in about 5-10% of patients. These include myocarditis and/or pericarditis/endocarditis, conduction abnormalities, atrial fibrillation or tachycardia.

A small group of patients may also develop secondary erythema, which is smaller than the primary lesion and is uniformly colored (Aguero-Rosenfeld et al., 2005; Hofmann et al., 2017; Matyjasek and Zdrojewski, 2016).

The late phase of Lyme disease is a chronic infection that develops from one to several years after infection. Its course is largely dependent on the genospecies that caused the disease. Which is probably caused by different tissue tropisms of individual *B. burgdorferi* s.l. genospecies (Caine and Coburn, 2016). Therefore, some discrepancies in the course of the disease can be observed between Europe and North America and between different regions of Europe. *B. afzelii* is associated almost exclusively with acrodermatitis chronica atrophicans (ACA). *B. garinii* and *B. bavariensis* are often associated with neurological symptoms, and *B. burgdorferi* s.s. mainly causes Lyme arthritis. *B. spielmanii* has so far been isolated only from skin lesions (Fingerle et al., 2008; Stanek and Reiter, 2011; van Dam et al., 1993).

LA is one of the most common symptoms of late Lyme disease. It develops most often after 6 months (from 2 weeks to 2 years) from the onset of the first symptoms of *B. burgdorferi* s.l. infection. LA most often affects the large joints (knees, hips, elbows, and shoulders), and less often affects smaller joints, such as ankles, temporomandibular joints and hand joints. Usually, one joint is involved with accompanying edema of varying intensity and limited mobility. The course of LA is characterized by recurrent acute and irregular attacks and periods of remission. About 20% of patients with LA recover spontaneously, while the rest develop joint damage with associated impairment of joint function (Krzyczmanik et al., 2012; Lohr et al., 2018; Stanek et al., 2012).

ACA can show its first symptoms even several years after infection with *B. burgdorferi* s.l. ACA is characterized by extensive skin lesions where the dermis thins and becomes parchment-like. The skin is shiny in places affected by the disease, with increased or weakened pigmentation. Most often, the distal parts of the body are involved, but in some patients, the skin of the face and torso may also be affected. In many cases, these changes are preceded by the appearance of a red, inflammatory, edematous stage. In addition, it is accompanied by pain and itching, which can be caused by peripheral neuropathy (Hofmann et al., 2017; Krzyczmanik et al., 2012) .

Late neuroborreliosis develops very rarely, it occurs from 6 months to several years from the moment of infection. The most severe and serious forms of neuroborreliosis are encephalitis and myelitis, which can lead to spastic paresis of the limbs and damage to the cranial nerves. In addition, neuroborreliosis can lead to subacute memory disorders and polyneuropathy manifested by paraesthesias, radicular pain and hypersensitivity to pain stimuli (Flisiak et al., 2011; Krzyczmanik et al., 2012; Matyjasek and Zdrojewski, 2016).

About 10-20% of patients with Lyme disease, after a properly conducted treatment process, show a number of subjective symptoms, such as fatigue, headaches, muscle and joint pain, paraesthesia, irritability, and problems with memory and concentration. These symptoms, called post-Lyme syndrome (PLS), are characterized by variable intensity and a non-specific clinical picture. The pathomechanism of PLS remains unexplained, but it is believed that long-term infection with *B. burgdorferi* s.l. induces immunological or neurohormonal processes in the host brain, resulting in a number of disease symptoms that persist despite the elimination of the infectious agent. Particularly susceptible to the occurrence of these symptoms are patients who previously suffered from anxiety-depressive disorders (Marques, 2008; Steere et al., 2004).

1.3. Diagnosis of Lyme disease

Due to the varied course of Lyme disease, diagnosis based on clinical symptoms is very difficult. A correct diagnosis can be made only when the typical erythema migrans appear. Unfortunately, it is not always possible to diagnose Lyme disease on this basis, because it does not always appear in patients (up to 90%), and some of them, despite its occurrence, do not notice him. Moreover, EM sometimes takes non-specific forms. An additional difficulty in the correct diagnosis based on the occurrence of EM is allergens present in the tick's saliva. When introduced into the human body, they can cause a local inflammatory process of redness of various sizes, which does not indicate the course of Lyme disease. Therefore, it is necessary to consult an experienced physician who will be able to distinguish EM from inflammation reaction correctly (Eldin et al., 2019; Hofmann et al., 2017).

Other symptoms of Lyme disease are not specific enough to allow for a correct diagnosis, which is why laboratory methods play an essential role here. They are divided into two main groups: direct and indirect methods. Direct methods rely on the identification of the entire cell of the pathogen, its antigens, or genetic material in biological samples. Indirect methods are based on serological analysis (Lohr et al., 2018).

1.3.1. Culture of *B. burgdorferi* s.l.

The culture of *B. burgdorferi* s.l. in the Lyme disease diagnosis is not routinely performed due to the high growth requirements of spirochetes and their long division time (7-20 h). Therefore, this method is very time-consuming - a clearly negative test result can be found after few weeks of breeding. In addition, its sensitivity is also not too high and depends heavily on the type of sample taken. The sensitivity of this method for biopaths taken from the EM site ranges from 40-90%, while for samples taken from ACA

lesions, it is 20-60%. Much lower sensitivity (10-26%) is obtained for samples from the cerebrospinal fluid. For blood cultures, this rate is as low as 9% for European patients and increases to 40% using larger blood volumes from EM patients in the US. This method works the least when the starting material is synovial fluid, the test result in this case is almost never positive. For the reasons mentioned above, this approach is mainly used as a tool to complement the diagnostic process in patients with a malfunctioning immune system (Hofmann et al., 2017; Lohr et al., 2018; Wilske et al., 2007).

1.3.2. Molecular methods - polymerase chain reaction

The use of polymerase chain reaction (PCR) is most indicated in the early stages of the disease, when the organism has not yet produced specific antibodies. This allows for very early treatment, which prevents pathogens from spreading in the patient's body. In the late phase of the disease, this technique can support laboratory diagnostics, especially when serodiagnostic methods fail, for example in patients with immune defects. The following types of PCR reactions are used to diagnose Lyme disease: classic PCR, Real-Time PCR, nested-PCR, PCR/ESI-MS. When choosing the amplified *B. burgdorferi* s.l. DNA sequence, attention should be paid to the lack of homology with the DNA of other microorganisms and above all, with human genetic material. There are several recommended specific genome fragments of *B. burgdorferi* s.l., chromosomal: *fla*, *recA*, 16S rDNA, *p66*, *hbb*, *rpoB*, 5S-23S intergenic space, and plasmid: *ospA*, *ospB*, *ospC*, *vlsE* (Ružić-Sabljić and Cerar, 2017; Wilske et al., 2007).

Detection of *B. burgdorferi* s.l. DNA by PCR is possible in a variety of clinical materials, such as: skin bioptates, cerebrospinal fluid (CSF) and synovial fluid. The highest sensitivity of PCR-based diagnostic tests is obtained when examining synovial fluid, it is about 77.5%. These tests are also characterized by very high specificity, reaching 100%. However, when LA is suspected, the synovium may also be the starting material. This approach can lead to a significant increase in test sensitivity (even from 25% to 90%) (Jaulhac et al., 1996; Ružić-Sabljić and Cerar, 2017). In addition, it has been proven that the DNA of the spirochete persists longer in the synovial tissue than in the synovial fluid after antibiotic therapy (van Dam, 2011).

In the case of examining skin fragments taken from the EM, molecular diagnostics achieves a sensitivity of 80%, while specificity ranges from 98-100% (Nowakowski et al., 2002; Ružić-Sabljić and Cerar, 2017). However, since the mere presence of EM is sufficient to make a diagnosis, this approach may be used only to diagnose early Lyme borreliosis in patients with atypical forms of EM. A slightly lower sensitivity (75%) is obtained when examining skin biopsies taken from sites covered by ACA, additionally, this approach is also characterized by very high specificity. As with LA, ACA is also a

symptom of late Lyme disease, so patients at this stage of the disease almost always have a high circulating IgG titer (Stanek et al., 2012; van Dam, 2011).

Molecular diagnosis of neuroborreliosis is based on cerebrospinal fluid analysis. However, due to the small number of spirochetes in the CSF, the high affinity of the bacteria to the myelin sheath and the possibility of degradation of the genetic material, this approach has a rather low sensitivity (22.5%). The highest probability of detecting spirochete DNA in CSF occurs in early neuroborreliosis (Gąsiorowski et al., 2007; Mygland et al., 2010; Ružić-Sabljić and Cerar, 2017).

Blood samples, despite the ease of obtaining them, are not a good clinical material in the diagnosis of Lyme disease. This is due to the low number of spirochetes in the circulation, which is influenced by the strong tissue tropism of pathogens (joints, heart, nervous tissue). Blood PCR tests are only useful in the early phase of infection, when *B. burgdorferi* s.l. spreads from the tick injection site through the bloodstream to other organs. In addition, numerous PCR inhibitors (such as heparin, hemoglobin, host DNA) are present in the blood, which can lead to false negative results (Liveris et al., 2012; Lohr et al., 2018; Maraspin et al., 2011; Schmidt, 1997).

Urine is one of the most readily available clinical materials, which is why many scientists have studied its usefulness in the molecular diagnosis of Lyme disease. Initial literature reports were very promising. Bergmann et al. (2002) developed a PCR test detecting *B. burgdorferi* s.l. DNA in urine with a sensitivity of 85%. Unfortunately, after conducting research on a larger number of samples of Lyme patients, it turned out that the sensitivity and, in particular, the specificity of molecular tests using urine is not satisfactory. Currently, most European and American standards discourage using urine in PCR-based methods mainly due to the frequent occurrence of non-specific products and poor reproducibility of the results. These problems are probably due, as in the case of blood, to the low and transient presence of spirochetes and the presence of many PCR inhibitors in the urine (Aguero-Rosenfeld et al., 2005; Dunaj et al., 2013; Kondrusik et al., 2007; Lohr et al., 2018; Reed, 2002).

1.3.3. Serological diagnosis

Due to the large limitations of direct methods in the laboratory diagnosis of Lyme disease, resulting mainly from the presence of a very low number of *B. burgdorferi* s.l. in clinical samples and the difficulties in their cultivation, indirect tests based on the detection of class M and G antibodies are most often used (Schutzer et al., 2019).

In the current serological diagnosis, a two-tiered testing (TTT) approach is recommended (Figure 1.11), which was first introduced in 1993 in the USA (Centers for Disease Control and Prevention (CDC), 1995). The first step in this approach is a

sensitive enzyme-linked immunosorbent assay (ELISA). If the ELISA test is positive or equivocal, the Western blot (WB) is used as a confirmatory second-step test (Eldin et al., 2019).

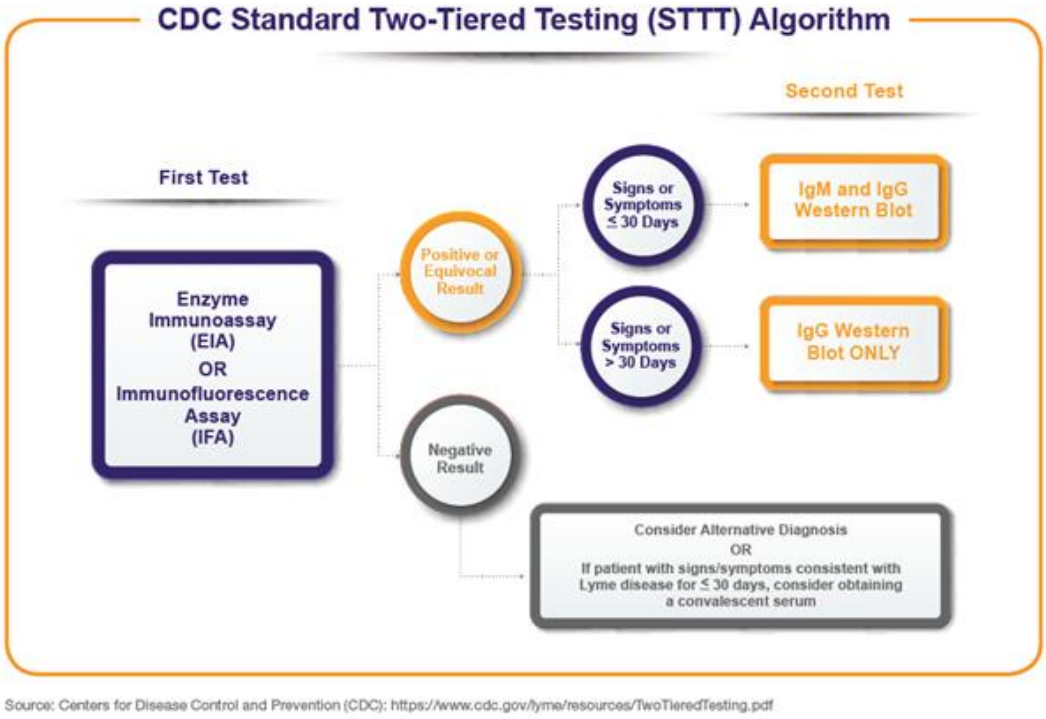

Figure 1. 11 Two-tiered algorithm used in Lyme disease serodiagnosis (www.cdc.gov).

ELISA, due to its high sensitivity, plays the screening test role. Initially, the ELISA used whole cell lysates (WCL) of *B. burgdorferi* s.l. as the source of antigens. Unfortunately, such antigen preparations did not have high specificity due to cross-reacting antigens in *B. burgdorferi* s.l. Therefore, since these tests were characterized by over-diagnosis of Lyme disease, it was necessary to introduce a second-stage test (Aguero-Rosenfeld et al., 2005; Bruckbauer et al., 1992).

The WB is used as a confirmatory test because it is characterized by much greater specificity due to the ability to distinguish individual protein bands. In order to achieve the best diagnostic utility, various guidelines have been proposed which differ between North America and Europe. It was recommended that in the USA for WB using *B. burgdorferi* s.s. 297 cell lysates. In IgM detection, the most sensitive and specific tests are those that take into account three antigen bands (p23 [OspC], p39 [BmpA], and p41 [FlaB]), such a test is interpreted as positive when at least two of them react (Engstrom et al., 1995). However, for the detection of IgG, the best specificity and sensitivity are obtained when considering 10 different antigens (p18-p17 [DbpA], p23 [OspC], p28 [OspD], p30 [OspA], p39 [BmpA], p41 [FlaB], p45, p58 [Hsp60 fragment], p66, and p93 proteins). The test is considered positive when at least 5 out of 10 expected bands

appear (Dressler et al., 1993) (Figure 1.12). In Europe, *B. afzelii* Pko is recommended as a source of antigens in WB, but *B. burgdorferi* s.s. 297 is also approved for use. IgM-WB should be considered positive when using the European *B. afzelii* Pko strain when at least one of the p41 (FlaB) and p17 [DbpA] bands appears. IgG-WB should be considered positive if there are at least two bands with p14, p17 [DbpA], p21, p23-25 [OspC], p30 [OspA], p39 [BmpA], p41[FlaB], p58 [fragment Hsp60] and p83/100. When using *B. burgdorferi* s.s 297, the recommendations are the same as for the USA (Dressler et al., 1993; Talagrand-Reboul et al., 2020).

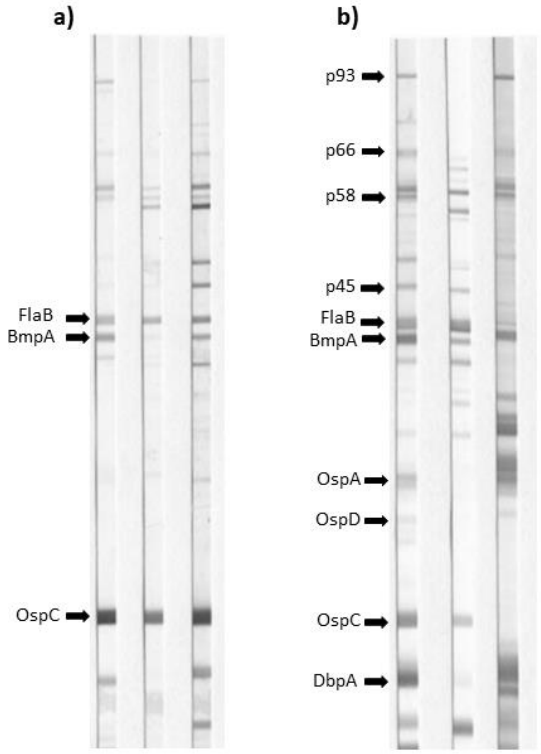

Figure 1. 12 Example of a positive Western blot: a) IgM detection; b) IgG detection (Aguero-Rosenfeld et al., 2005).

1.3.3.1. Limitation of serologic diagnosis of Lyme disease

1.3.3.1.1. Serologic window

The sensitivity of immunodiagnosis largely depends on the duration of the disease. IgM are produced in humans, approximately 2 weeks after infection, and the first to appear are antibodies against such antigens as OspC, BBK32, and flagellin (Aguero-Rosenfeld et al., 1993). However, the production of IgG usually begins after 3-6 weeks, and as the disease progresses, they replace IgM. The IgG response is directed against a broader spectrum of antigens starting with VlsE, OspC, BBK32, flagellin, and antibodies against DbpA, BmpA, and p58 proteins appear in later stages of infection (Aguero-Rosenfeld et al., 1993; Hauser and Wilske, 1997; Panelius et al., 2003). Due to the time required for the body to produce specific antibodies in the first stage of infection,

serological tests are often negative (R. A. Kalish et al., 2001; Theel, 2016). Only 10-50% of patients with early Lyme disease (EM less than 7 days) have detectable antibodies against *B. burgdorferi* s.l. As the infection progresses, the immune response gradually matures, resulting in an increased clinical sensitivity of serological tests during the later stages of the disease. In cases of the late phase of the disease, specific IgG are detected in almost all examined patients (Hansen et al., 1988; Hansen and Asbrink, 1989; Wilske et al., 2007).

1.3.3.1.2. Complex proteome

Another limitation is the different expression patterns of spirochaete genes in the tick and in the mammal (Gilmore et al., 2001). In addition, the diversity of surface proteins is increased by the phenomenon of antigenic variation, which is one way of evading the immune response by *B. burgdorferi* s.l. This means antibodies specific for one form of the antigen may not react with other variants (Norris, 2015). Problematic is also obtaining whole cell lysates containing all the most immunogenic antigens, as some are produced only *in vivo* (Gilmore et al., 2001; Schwan et al., 1995). In addition, gene expression of some proteins disappears due to the loss of plasmids encoding them. The factors mentioned above cause problems related to the standardization of antigen preparations, which significantly affects the repeatability of the results of diagnostic tests (Liang et al., 1999; Norris, 2015; Purser and Norris, 2000).

1.3.3.1.3. Genospecies diversity

The great genospecies diversity of *B. burgdorferi* s.l. and the low degree of conservation of amino acid sequences of proteins among them also have a negative impact on the effectiveness of Lyme disease serodiagnosis. This problem is particularly relevant in Europe, where there are as many as 5 genospecies pathogenic for humans. Most of the high immunogenic proteins are heterogeneous, and thus the use of WCL only one genospecies as antigen preparations in serodiagnostic assays carries the risk of obtaining a false-negative result (Jonsson et al., 1992; Lohr et al., 2018; Ohnishi et al., 2001; Roberts et al., 1998). Almost all available commercial diagnostic kits use combinations of recombinant antigens from different genospecies. They mainly contain proteins from the three most common pathogenic genospecies in Europe (*B. afzelii*, *B. garinii*, *B. burgdorferi* s.s.) and occasionally the less prevalent i.e., *B. bavariensis* and *B. spielmanii*. This allows for an increase in the effectiveness of immunoenzymatic assays but also significantly increases the cost of routine diagnosis (Goettner et al., 2005; Talagrand-Reboul et al., 2020).

1.3.3.1.4. Cross-reactions

B. burgdorferi s.l. produces many homologous proteins among microorganisms, which carries the risk of cross-reactions. The lack of specificity of diagnostic tests for Lyme disease prompted the introduction of a two-tiered testing strategy. The specificity of two-stage serology testing in scientific studies exceeded 99% when performed by high-performance reference laboratories. However, many reports indicate that in actual clinical practice, TTT shows much lower specificity (Branda et al., 2011; Centers for Disease Control and Prevention (CDC), 1995).

The problem of cross-reactions in the serodiagnosis of Lyme disease has been known for a long time. Already in the early 1990s, a study was carried out to identify cross-reactive antigens trying to increase the specificity of diagnostic tests. Many of the proteins that are the source of nonspecific reactions are probably undescribed, but the most immunogenic ones have been characterized quite well (Table 1.3) (Luther and Moskophidis, 1990). Several infections/diseases can be misdiagnosed as Lyme disease or vice versa. The most problematic are syphilis, relapsing fever, and viral infections caused by Epstein-Barr (EBV) and cytomegalovirus (CMV). Furthermore, people positive for rheumatoid factor (RF) are also often misdiagnosed with Lyme disease.

Relapsing fever *Borrelia* (RFB) are the bacteria closely related to *B. burgdorferi* s.l. This group includes such species as: *Borrelia hermsii, Borrelia miyamotoi*, *Borrelia hispanica Borrelia duttonii,* and *Borrelia recurrentis.* These bacteria can be divided into: lice-borne fever *Borrelia* (LBRF) and tick-borne relapsing fever *Borrelia* (TBRF). TBRF *Borrelia* are typically transmitted by soft ticks of the genus *Ornithodoros*, currently it seems that only *B. miyamotoi* is transmitted by hard-bodied ticks likewise *B. burgdorferi* s.l. LBRF is caused only by *B. recurrentis* (Jakab et al., 2022). TBRF *Borrelia* may be found on all continents except Australia and Antarctica and is a severe public health problem in some parts of the world. LBRF is reported mainly in Africa, and single cases in Europe occur mostly among refugees. During the development of relapsing fever, many non-specific symptoms may occur (e.g., headache, myalgia, chills, nausea, vomiting, arthralgia) and neurological disorders (e.g., meningitis, encephalitis, hemiplegia, facial palsy). Some of them are similar to Lyme disease symptoms, so the clinical differentiation of these two infections in most cases is impossible. It is worth remembering that EM does not appear during relapsing fever, one symptom that allows easy and undeniable differentiation of these diseases. In the past, *B. hermsii* WCL was used for relapsing fever diagnostics, however, too much antigen similarity between the two groups of bacteria caused many false positive results (Table 1.3). Nowadays, qPCR is mainly used to diagnose relapsing fever also,

serological tests based on the GlpQ protein, absent from *B. burgdorferi* s.l. have been developed (Talagrand-Reboul et al., 2020).

Syphilis is a sexually transmitted disease caused by spirochetes *T. pallidum*. Serological tests at all stages of infection remain the mainstay of diagnosis. Antibodies against *T. pallidum* antigens often react with *B. burgdorferi* s.l. proteins, particularly with ELISA when WCL is used as the source of antigens. This is due to the close phylogenetic relationship of the two pathogens, this cross-reactivity is strongly related to shared flagellar antigens (Magnarelli et al., 1990). In the IgM, cross-reactions occur with *B. burgdorferi* s.l. proteins such as: OspC, BBA64, BmpA, FlaB, OspF and OspC, BBA64, BmpA, FlaB, OspF in IgG (Table 1.3) (Magnarelli et al., 2002). So it may cause false-positive results of immunoenzymatic assays however, prior infection with *B. burgdorferi* s.l. does not appear to lead to a false-positive syphilis test (Patriquin et al., 2016). It has been proven that the cross-reactions between the antigens of *B. burgdorferi* s.l. and *T. pallidum* can be minimized by incubating the sera with *Reiter treponema* preparations. However, this procedure did not eliminate all non-specific interactions (Hunter et al., 1986; Raoult et al., 1989).

Human granulocytic anaplasmosis (HGA), formerly known as human granulocytic ehrlichiosis is caused by *Anaplasma phagocytophilum*, Gram-negative, intracellular bacteria. The main route of transmission of *A. phagocytophilum* is a bite of *Ixodes* ticks. Despite the ubiquitous presence of *A. phagocytophilum* in ticks and animal reservoirs, confirmed clinical cases of HGA in Europe are rare compared to the world state. It has been shown that sera collected from HGA patients show cross-reactions with *B. burgdorferi* s.l. proteins as OspC, BBA64, p37, FlaB, VlsE, OspA, OspC, OspF in the M class of antibodies and OspC, p37, FlaB, OspA, OspF in the IgG (Table 1.3). Interestingly, despite detecting these non-specific antigen-antibody reactions, ELISA tests performed on the WCL did not give false-positive results (Magnarelli et al., 2002). However, serum reactivity to both *B. burgdorferi* s.l. and *A. phagocytophilum* antigens is not always due to cross-reactions. People who live in *Ixodes* tick endemic areas and experience multiple tick bites are probably exposed to transmitting different pathogens. A patients with HGE infection may have been previously exposed to *B. burgdorferi* s.l. or vice versa and may produce antibodies to both pathogens. Furthermore, co-infections in humans and vectors have been confirmed (Obert et al., 2009; Schicht et al., 2011). Therefore, tests for other tick-borne diseases should be conducted when HGE, Lyme disease, or human babesiosis is suspected. Because EM is often absent, clinical manifestations of HGE, such as headache, fever, and fatigue, can be confused with those of Lyme disease and other infections. Laboratory analyses to identify disorders associated with abnormal blood cell counts (i.e., thrombocytopenia or leukopenia) and

to determine concentrations of serum hepatic transaminase can help separate HGE from borreliosis (Magnarelli et al., 1995; Obert et al., 2009).

People get infected with *Yersinia enterocolitica* and *Yersinia pseudotuberculosis* by ingesting contaminated food or water or by direct infection through blood transfusions. The infection may be asymptomatic, but in some cases, reactive arthritis similar to LA caused by *B. burgdorferi* s.l. may develop. The most commonly affected joints are the knees and ankles, but other joints, such as those of the toes, fingers, and wrists, may be involved. As in the case of Lyme disease, the diagnosis by cultures is not very sensitive, therefore serological tests detecting antibodies specific to *Yersinia* antigens may be helpful (Golkocheva-Markova et al., 2011; Rawlins et al., 2005). The newest yersiniosis tests focus on detecting antibodies against *Yersinia* outer proteins (YOPs) (Wielkoszynski et al., 2018). It has been reported that the cross-reactivity between *B. burgdorferi* s.l.-specific antibodies and the YOPs in Western blot. For anti-*B. burgdorferi* s.l. IgG, cross-reaction was detected with YopH, YopB, V-ag, YopD, YopN, YopP, and YopE, and for IgA with YopD (Golkocheva-Markova et al., 2011; Rawlins et al., 2005). All *B. burgdorferi* s.l. serum samples with the observed this cross-reactivity contained IgG against FlaB and IgG and IgM against OspC. It may prove antigenic similarity between OspC and FlaB antigens of *B. burgdorferi* s.l. and YopD of *Yersinia,* especially since two-way cross-reactivity is present. It has been showed that p60, FlaB, OspA and OspC *B. burgdorferi* s.l. antigens were highly cross-reactive with anti-*Yersinia* sera (Table 1.3) (Golkocheva-Markova et al., 2011; Rawlins et al., 2005). In this case, therefore, special care should be taken because it is possible to overdiagnosis both Lyme disease and yersiniosis.

Epstein-Barr virus is a gamma herpesvirus causing infection in humans worldwide. The prevalence of EBV is very high, about 90% of adults are infected with EBV. Most infections occur in young children and are asymptomatic or cause nonspecific symptoms (Nowalk and Green, 2016). It was observed that serum samples from patients with EBV infection cross-reacted with OspC protein (Table 1.3). In the studies conducted by Panelius et al. (2002), the percentage of patients with a positive EBV result in the OspC ELISA was initially as high as 73%, however, this cross-reactivity was limited by the addition of sodium thiocyanate and dropped to 46%. Unfortunately, the effect of decreasing non-specific reactions was not seen with sera specific for syphilis and rheumatoid factor (RF).

Cytomegalovirus belongs to viruses in the order *herpesvirales*. Usually, CMV infection is asymptomatic, but in people whose immune system is defective or immature (newborns, patients with AIDS, elderly) it can be a serious problem. The virus is highly distributed and the worldwide prevalence of CMV has been estimated at 83%

(66-90%) (Cannon et al. 2010). This means that most people worldwide (similar to EBV) have developed antibodies to CMV, which have been reported to cross-react with *B. burgdorferi* s.l. antigens (Goossens et al. 1999; Smismans et al. 2006b; Wojciechowska-Koszko et al. 2022). It was shown that anti-CMV IgG recognized such *B. burgdorferi* s.l. antigens as OspC, FlaB, BmpA and VlsE (Table 1.3) (Smismans et al., 2006; Wojciechowska-Koszko et al., 2022).

Parvovirus B19 (B19V) is a small single-stranded, non-enveloped DNA virus. In adults, it can cause joint pain or arthritis with pronounced morning stiffness what may imitate LA caused by *B. burgdorferi* s.l. (Vassilopoulos and Calabrese, 2008). Acute B19V infection can induce antibodies that are polyspecific and cross-react with a variety of bacterial antigens, especially for *B. burgdorferi* s.l and other unrelated pathogens such as *Salmonella* and *Campylobacter*. These antibodies can persist in the circulation for up to 3 months. False positive results for Lyme disease were obtained not only in the EIA but also in the more specific Western blot. Therefore, there is a possibility that an acute B19V infection could be misinterpreted as Lyme disease (Tuuminen et al., 2011). One of the likely explanations for this cross-reactivity is polyclonal stimulation. Another probable mechanism could be molecular mimicry. However, the lack of two-way cross-reactivity (*B. burgdorferi* s.l.-specific antibodies do not recognize B19V antigens) undermines this theory. Therefore, emphasis should be placed on a sensible interpretation of serological results for IgM and the exclusion of recent B19V infection of patients (Tuuminen et al., 2011).

One of the most common symptoms of late Lyme disease (especially in the US) is LA which shares common clinical features and synovial histology with rheumatoid arthritis, which makes the clinical symptoms often indistinguishable. Recommended serological tests might also lead to misdiagnosis due to the presence of rheumatoid factor, which is present in the serum of patients with arthritis (Hsieh et al., 2007) and other systematic diseases (Renaudineau et al., 2005). RF are antibodies with specificity directed against gamma globulin, are the most common auto-antibodies ever described in humans (Renaudineau et al., 2005). Research has shown that RF is reactive with many *B burgdorferi* s.l. antigens, including: LA7 (p22), BBA64, FlaA, BmpA, OppA2, VlsE, OspC (Table 1.3) (Magnarelli et al., 2000, 2002; Panelius et al., 2002; Tjernberg et al., 2007). Additionally, antibodies directed against OspA were detectable in the sera of some rheumatoid arthritis patients, so it also may be a source of false positive results of serological tests (Hsieh et al., 2007).

It seems interesting that in patients with oral infections, cross-reactions with *B. burgdorferi* s.l. antigens like FlaA, BmpA, OspF, OspC occur however, this phenomenon has not been fully understood (Magnarelli et al., 2000, 1996).

Table 1. 3 Cross-reactive proteins of *B. burgdorferi* s.l.

	LA7 (p22)	p60	FlaB (p41)	BBA65 (p35)	FlaA (p37)	BmpA (p39)	OppA2	VlsE/ C6	OspA (p30)	OspB	OspC	OspF	Ref.
Relapsing fever *Borrelia*		+	+	+	+	+		+	+	+	+	+	(Bruckbauer et al., 1992; Magnarelli et al., 2002)
Syphylis	+		+	+		+	+			+		+	(Luft et al., 1993; Magnarelli et al., 2002, 1996; Panelius et al., 2001)
Yersinia		+	+	+					+	+			(Golkocheva-Markova et al., 2011; Rawlins et al., 2005)
HGA	+		+	+	+			+	+		+	+	(Magnarelli et al., 2002)
EBV											+		(Panelius et al., 2002)
CMV			+			+		+			+		(Wojciechowska -Koszko et al., 2022)
B19V						+		+			+		(Tuuminen et al., 2011)
RF positive	+			+	+	+	+	+			+		(Magnarelli et al., 2000, 2002; Panelius et al., 2002; Tjernberg et al., 2007)
Oral infection					+	+					+	+	(Magnarelli et al., 2002, 1996)
Human tissue									+				(Ghosh et al., 2006; Steere et al., 2011)

HGA - human granulocytic anaplasmosis; EBV - Epstein-Barr virus; CMV – Cytomegalovirus; B19V - Parvovirus B19; RF - rheumatoid factor

1.3.3.1.5. Overdiagnosis of Lyme disease

Despite the many guidelines recommending testing for Lyme disease only in the presence of symptoms that indicate it and detecting IgM only if the patient's symptoms last shorter than 4 weeks, they are ignored. Therefore, the abuse of laboratory tests for *B. burgdorferi* s.l.-specific antibodies in situations where serological tests are not recommended is common, resulting in many false positives (Dessau et al., 2018; Hillerdal and Henningsson, 2021). There are also many problems with the correct interpretation of immunoassays results. Therefore, the abuse of laboratory tests for *B. burgdorferi* s.l.-specific antibodies in situations where serological tests are not recommended is common, resulting in many false positives (Lantos et al., 2016; Seriburi et al., 2012). The usefulness of serological tests is also influenced by the high prevalence of anti-*B. burgdorferi* s.l. antibodies, in some areas it reaches up to 20%, which means that a positive test result does not always mean that the disease is active (Hillerdal and Henningsson, 2021).

This is especially related to IgM because they are the first-line antibodies and have a lower concentration in the blood at its peak compared to IgG. Additionally, high levels of IgM are maintained in the blood for a very short time. Moreover, their affinity to antigens is lower because they are produced when the immune response is still immature. For the same reason, they are directed against a smaller spectrum of antigens, recognizing only those proteins and their fragments exposed in the early stages of infection. It has been shown that enzyme immunoassays for the detection of IgM more often lead to false positive results, which may be caused by their lower affinity (Hillerdal and Henningsson, 2021; Johnson et al., 1996; Keyt et al., 2020; Liu et al., 2019; Mäkelä et al., 1970). IgM should therefore, only be used in cases of suspicion of early Lyme disease, i.e., in cases of NB lasting < 6 weeks or Lyme carditis. Other clinical symptoms like LA and ACA are manifestations of late Lyme disease and appear after at least 6 weeks. Therefore in these cases, tests focused on the detection of more specific IgG should be carried out (Lantos et al., 2016).

It also turns out that false-positive results may be due to the long duration of the anti-*B. burgdorferi* s.l. immunoglobulins in the body. Kalish et. al. (2001) studied 79 patients diagnosed with Lyme disease 10-20 years earlier and now showed no signs of active disease. It was shown that up to 25% of the patients had specific IgG, while 10% had specific IgM. These reactivities were demonstrated using the recommended two-tiered diagnostic approach. The *B. burgdorferi* s.l. antigens that were mainly recognized by specific IgM many years after infection were OspC and FlaB. This means antibodies specific to proteins such as DbpA, BmpA, p45, p58, and p66 have disappeared over time. However, in the case of IgG in many cases, the pattern of recognized antigens did not change even after many years. The most recognizable proteins were DbpA, BmpA, FlaB, p58, and p93. Patients who developed LA

during the first diagnosis showed particular stability in the presence of antibodies, even 62% of them were still positive for IgG and 15% for IgM after at least 10 years (Kalish et al., 2001).

1.3.3.2. Recombinant proteins and synthetic peptides in Lyme disease serodiagnosis

Recombinant proteins, which are obtained with the use of genetic engineering methods, may be a potential solution to problems in Lyme disease serodiagnosis. They are produced in genetically modified hosts that ensure their efficient production. This form of protein very often differs from its native version by the presence of additional domains or mutations to increase its production and facilitate the purification process. At present, they are commonly used as antigens in commercial Western blots. ELISA is still based mainly on whole cell lysates, however, the addition to WCL of one or more recombinant proteins from different genospecies, such as VlsE or OspC, is quite common (EUROLINE Borrelia-RN-AT, EUROLINE Borrelia-RN-AT-ad) (Lohr et al., 2018). *B. burgdorferi* s.l. is difficult to cultivate, therefore, obtaining WCL requires considerable labor and costs (Hofmann et al., 2017; Lohr et al., 2018). Production of recombinant proteins is much more straightforward and cheaper, and allows for easy standardization of the composition of such protein preparations (Holec-Gąsior, 2013; Holec et al., 2008). Careful and thoughtful antigen selection can reduce cross-reactivity and allow test sensitivity independent of the *B. burgdorferi* s.l. genospecies that caused the infection, which will simplify the interpretation of diagnostic assays. For this purpose, antigens or their fragments are conserved within the *B. burgdorferi* s.l. group, as well as those that cause cross-reactivity, should be identified.

Undoubtedly, antigens of this type raise great hopes for developing an effective, one-stage diagnostic approach based solely on ELISA. This will limit the number of WB tests performed, which are more expensive and more difficult to interpret than ELISA, leading to large inter-laboratory discrepancies (Seriburi et al., 2012). For this reason, many scientists have focused their attention on trying to find or design highly diagnostically useful recombinant/chimeric *B. burgdorferi* s.l. antigens.

- VlsE

In a study by Bacon et al. (2003), the overall sensitivity (irrespective of the duration of infection) of IgG-ELISA based on VlsE antigen alone (IgG-ELISA-VlsE) was 65%. This result was not significantly different from those obtained using a standard two-tiered testing. When the phase of the disease was taken into account, the sensitivity of the IgG-ELISA-VlsE assay for patients with EM for one week was shown to be only 16%, but it increased significantly between 2 and 4 weeks post-infection, reaching 61%. In the late phase of the disease, the IgG-ELISA-VlsE was characterized by almost 100% sensitivity, and the specificity remained at the level of 98% (90-100% depending on the control group of patients). When IgM were detected by the ELISA-VlsE, the overall sensitivity of the assay dropped to 36%, it was also

lower for 2 to 4 weeks of disease (32%), and only 3% for the earliest phase of infection. The specificity of the IgM-ELISA-VlsE was 99%.

In another study, ELISA-VlsE showed high sensitivity in detecting IgG during the early phase of the disease, reaching even 80%, and its reactivity with IgM was at 40%. In addition, the specificity of such a tests was very high and reached 99% in both cases (Magnarelli et al., 2002). The WB showed that the reactivity of VlsE largely depends on the genospecies from which the antigen comes, and the sensitivity of the tests, depending on the VlsE variants, ranged from 61 to 89% (Goettner et al., 2005).

Since VlsE-based EIAs appear to be very sensitive and specific, it was proposed to be used as stand-alone tests, without the WB second-stage. However, two large studies have shown that next-generation FDA-approved tests based on full-length VlsE are less specific than standard two-tiered testing, reaching 98.1% and 99.5% respectively (Branda et al., 2017). Although differences in specificity are minor, they are statistically significant and can lead to profound differences in positive predictive value, depending on the prevalence of Lyme disease in the population. As a result, the introduction of unnecessary strong antibiotic therapy in many patients and the delay in correct diagnosis (Branda et al., 2011).

- C6 peptide

The usefulness of IgG and IgM ELISA based on synthetic 26 amino acid peptide from IR6 region (IgM/IgG-ELISA-C6) located within the *vlsE* gene was evaluated by Liang et al. (1999). The team tested sera from patients in the early phase of the disease, during antibiotic therapy, and in the chronic phase. The sensitivity of the IgM/IgG-ELISA-C6 in the early phase of the disease was 74%, in the late phase it increased to 100%, and for patients, during antibiotic therapy, it reached 90%. To evaluate the specificity of the IgM/IgG-ELISA C6, serum samples from patients with other spirochetal infections, chronic autoimmune or neurological conditions, and hospitalized individuals from non-Lyme endemic areas were tested. For these sera, the overall specificity of the ELISA was 99%. However, no cross-reactions with antibodies in the sera of patients with syphilis, relapsing fever, or rheumatoid factor positive have been observed. This is a very interesting observation because these are the three main sources of cross-reactivity in Lyme disease diagnosis. The only false-positive samples were from hospitalized patients with no known infections/disorders (Liang et al., 1999).

- OspC

One of the first antibodies appearing in the serum of infected *B. burgdorferi* s.l. are those directed against OspC. Literature data on the usefulness of the OspC protein in diagnosing early Lyme disease are wildly divergent. IgM against OspC have been observed in 25-80% of EM patients (Gerber et al., 1995; Magnarelli et al., 1996; Mathiesen et al., 1998; Padula et al., 1994) and in 48-72% of NB patients (Fung et al., 1994; Mathiesen et al., 1998).

Studies by Fung et al. (1994) show that up to 50% of patients develop an IgM response directed against the OspC antigen in the first week after infection, and during the early disseminated phase this percentage increases to 60%. After 2 months, the number of seropositive patients for IgM is about 60-70%. These high variances in the sensitivity of OspC-based assays are likely due to the exceptional heterogeneity of the OspC antigen among *B. burgdorferi* s.l. Antibodies can recognize protein epitopes with varying efficiency depending on the antigen variant was used in the test (Theisen et al., 1993).

• PepC10 and OspC1 peptides

To solve the problems with the high heterogeneity of the OspC antigen, scientists performed amino acid sequence analysis and isolated two conserved fragments located at both ends of the protein. Studies by Bacon et al. (2003) have shown that IgM-ELISA based on the 10 amino acid peptide C10 (pepC10) (IgM-ELISA-pepC10) is more effective in detecting the early phase of the disease than a two-tiered testing. The sensitivity of IgM-ELISA-pepC10 in patients with EM lasting less than a week reached 27%. As the disease progressed, the sensitivity of the tests increased to 55% for sera collected from patients within 2-4 weeks after the onset of EM (Bacon et al., 2003). In contrast, Arnaboldi et al. (2013) used in their studies of an N-terminal peptide OspC1 (20 amino acids). IgM-ELISA-OspC1 detected early Lyme disease with a sensitivity of 48.5% and a specificity of 100% (Arnaboldi et al., 2013). IgG-ELISA based on pepC10 and OspC1 were less sensitive than those directed to detecting IgM class antibodies. For the IgG-ELISA-OspC1, the sensitivity was around 25%, while for the IgG-ELISA-pepC10, it was only 15%. Based on these results, it is clear that the OspC1 and pepC10 peptides are characterized by better effectiveness in the serodiagnosis of early Lyme disease, similarly to full-length OspC (Arnaboldi et al., 2013; Bacon et al., 2003).

- DbpA

DbpA is a very immunogenic protein that has strongly attracted the attention of scientists focused on assessing the diagnostic utility of *B. burgdorferi* s.l. antigens (Salo et al., 2011). However, the disadvantage of DbpA is the high diversity of amino acid sequences between genospecies (Heikkilä et al., 2002b; Panelius et al., 2007; Schulte-Spechtel et al., 2006).

The sensitivity of the DbpA-based Immunoblots was up to 90% when the reactivity with several variants was added together. When only the reactivity of DbpA from one genospecies was considered, the sensitivity of the tests dropped significantly to around 50% for the best variant. However, the specificity of these tests was very high and reached even 100%, regardless of the DbpA variant (Heikkilä et al., 2002b; Schulte-Spechtel et al., 2006). The sensitivity of ELISA based on several variants of DbpA in the later stages of Lyme disease (NB

and LA) in the conducted studies was high and ranged from 79-100%. However, as in the case of WB, it decreased when only single protein variants were taken into account (Heikkilä et al., 2002b; Panelius et al., 2007, 2003). It is worth noting, however, that for patients with LA, i.e., a late manifestation of Lyme disease, the sensitivity for a single antigen was still high, reaching even 80% (Heikkilä et al., 2003, 2002b). These values for groups of patients in another stage of Lyme disease were already lower, for NB it was 50% and for sera collected from patients with EM only 13% (Heikkilä et al., 2002b). Differences in the reactivity of different DbpA variants with specific *B. burgdorferi* s.l. antibodies were seen in both ELISA and WB, indicating genospecies differences in both linear and conformational epitopes (Heikkilä et al., 2002b; Panelius et al., 2007; Schulte-Spechtel et al., 2006).

- BmpA

BmpA is an antigen whose band is taken into account when detecting both IgM and IgG using Western blot. This suggests that it is highly reactive and specific in detecting both classes of antibodies. However, in a study by Roessler et al. (1997), recombinant BmpA was not effectively recognized by anti-*Borrelia* antibodies in WB assays. Moreover, its reactivity was dependent on the *B. burgdorferi* s.l. genospecies from which the antigen was obtained. For the BmpA proteins of *B. afzelii* and *B. garinii,* the sensitivity of the IgG test regardless of the stage of the disease was 36.0 and 34.9%, respectively, as opposed to 13.9% for the BmpA of *B. burgdorferi* s.s. Also, IgM was not recognized BmpA very effectively, WB sensitivity was at most 8% (Roessler et al., 1997b). However, in a study by Goettner et. al (2005), the sensitivity of BmpA-based WB was higher, and reached already 50% for the most reactive variant derived from *B. garinii* (Goettner et al., 2005). The diagnostic value of BmpA appears to increase significantly in ELISA. During the detection of IgG in patients with EM, the ELISA-BmpA was characterized by a sensitivity of 45%, second only to the VlsE, it turned out to be more reactive than such antigens as DbpA, flagellin, and OspC (Magnarelli et al., 2002).

- BBK32

BBK32 seems to be a valuable tool in the diagnosis of different stages of Lyme disease, and its usefulness in the diagnosis LA, NB and EM has been demonstrated. The sensitivity of the IgG-ELISA-BBK32 for the most reactive variant of the antigen derived from *B. afzelii* in LA had ranged from 50%-100%. However, when detecting neuroborreliosis, enzyme immunoassays achieved a sensitivity of 93-100%. Also, patients in the early stage of Lyme disease (EM) developed IgG specific for BBK32, ELISA showed a sensitivity of 74% to 22% depending on the antigen variant used. Only 4-13% of the samples were positive when detecting IgM in sera from EM patients. The specificity of all tests was high, reaching the level of 89-96% (Heikkilä et al., 2003, 2002a; Panelius et al., 2003).

- Chimeric proteins

The team of Gomes-Solecki et al. (2000) was the first to attempt to assess the usefulness of chimeric proteins in the diagnosis of Lyme disease. They constructed 17 chimeric proteins composed of fragments of surface antigens such as: OspA, OspB, OspC, flagellin (FlaB), and p93 proteins derived from *B. burgdorferi* s.s. After the initial selection, the four most promising chimeric antigens were selected for further serological tests from all produced chimeric antigens by means of WB tests. These were: OspB-Fla (43 kDa), OspB-OspC-Fla (64 kDa), OspA-p93 (62 kDa) and OspA-p93 (97 kDa). The usefulness of the constructed chimeric proteins was assessed by performing IgM/IgG-ELISA. The OspB-OspC-Fla antigen was the most effective in detecting early Lyme disease (62%). It also achieved good results in detecting late-onset Lyme disease (87%), but the OspA-93 protein (89%) turned out to be slightly more sensitive in this respect. This experiment showed how important it is to select the right protein fragments to create chimeras. The proteins OspA-p93 (62 kDa) and OspA-p93 (97 kDa) differ significantly in their sensitivity in detecting early and late Lyme disease, although the only difference between them is the size of the p93 antigen fragment used to create the chimeric antigen. In order to determine the specificity of ELISA using the above-mentioned chimeric proteins, sera from people suffering from syphilis and autoimmune diseases (rheumatoid arthritis and systemic lupus erythematosus) and sera from healthy people from a non-endemic area were used. These antigens did not cross-react with sera obtained from healthy people living in the area where Lyme disease is not endemic, but false-positive results have been obtained in patients with syphilis, autoimmune diseases, and in people living in areas where *B. burgdorferi* s.l. occurrence (Gomes-Solecki et al., 2000).

Another example is the chimeric protein obtained by Bradshaw et al. (2017), consisting of the complete amino acid sequence of the DbpA protein fused to the C6 peptide derived from the VlsE antigen. A very high reactivity with IgG characterized the resulting chimeric protein. In the further part of the study, in order to also ensure the detection of IgM at a high level, ELISA using as an antigen the chimeric protein DbpA/C6 with the addition of OspC (ELISA-DbpA/C6-OspC), which are more sensitive than the WCL-based TTT for the detection of the early stage of Lyme disease, with a sensitivity of 78% and 29% for IgG and 64% and 51% for IgM, respectively. When sera from late-stage Lyme disease patients were tested, the ELISA-DbpA/C6-OspC still had a higher sensitivity to detect IgG (97% vs. 87%), however, TTT was more effective at detecting IgM (43% vs. 53% sensitivity) (Bradshaw et al., 2017).

1.3.4. Rational design of new diagnostic tools

The results obtained by the researchers indicate that recombinant proteins have the potential to improve the diagnosis of Lyme disease. They are already used in many commercially available serodiagnostic tests and displace native *B. burgdorferi* s.l. proteins

(Table 1.4). Although many of them show high diagnostic utility, a one-stage serodiagnostic test using recombinant proteins superior to the standard two-stage test has not yet been developed. Double testing significantly increases the costs of routine diagnosis of Lyme disease and extends the time necessary to make a final diagnosis. It seems that the most problematic in the current approach is Western blot, a second-stage test that is time-consuming and difficult to automate. In addition, its reading, as already mentioned, is subjective, which leads to significant discrepancies between laboratories. Unfortunately, this problem has not been solved even by using only recombinant proteins in WB (Dessau et al., 2018; Lantos et al., 2016; Lohr et al., 2018; Seriburi et al., 2012).

Table 1. 4 Recombinant *B. burgdorferi* s.l. proteins used in commercial assays

Recombinant protein	Characteristic	Commercial assays
VlsE	Surface lipoprotein	• Anti-Borrelia *EUROLINE*-RN-AT IgG/IgM (Euroimmun) • LIAISON® Borrelia IgG (DiaSorin) • recomLine Borrelia IgG/IgM (Microgen) • ZEUS ELISA Borrelia VlsE1/pepC10 IgG/IgM (ZEUS Scientific)
C6	Conserved fragment of VlsE	• C6 Lyme ELISA kit (Immunetics)
OspC	Surface lipoprotein, necessary for transimsion	• Anti-Borrelia *EUROLINE*-RN-AT IgG/IgM (Euroimmun) • Borrelia EliSpot (ArminLabs GmbH) • LIAISON® Borrelia IgG (DiaSorin) • recomLine Borrelia IgG/IgM (Microgen)
PepC10	Conserved fragment of OspC	• ZEUS ELISA Borrelia VlsE1/pepC10 IgG/IgM (ZEUS Scientific)
OspA	Surface lipoprotein	• Borrelia EliSpot (ArminLabs GmbH)
DbpA	Surface lipoprotein, adhesin	• Anti-Borrelia *EUROLINE*-RN-AT IgG/IgM (Euroimmun) • Borrelia EliSpot (ArminLabs GmbH) • recomLine Borrelia IgG/IgM (Microgen)
BmpA	Basic membrane protein	• Anti-Borrelia *EUROLINE*-RN-AT IgG/IgM (Euroimmun)
p83/100	Periplasmic protein	• Anti-Borrelia *EUROLINE*-RN-AT IgG/IgM (Euroimmun) • recomLine Borrelia IgG/IgM (Microgen)
p41	Flagella-building protein	• Anti-Borrelia *EUROLINE*-RN-AT IgG/IgM (Euroimmun) • recomLine Borrelia IgG/IgM (Microgen)

For these reasons, it seems that in order to simplify the diagnosis of Lyme disease and reduce its costs, new recombinant/chimeric proteins should be selected or designed. Due to the very complex proteome of *B. burgdorferi* s.l., this seems difficult, suffice it to say that in the

last 30 years, the diagnostic utility of a few recombinant/chimeric proteins of the spirochete has been established. In addition, they were practically only plasmid-encoded lipoproteins, which are highly immunogenic but poorly conserved within genospecies, which makes it very difficult to develop a universal diagnostic test for Europe. Problems in serodiagnosis of Lyme disease indicate that in order to obtain new recombinant proteins that can compete with those currently used, they must meet the following conditions:

- be an antigen (show immunogenicity and antigenicity)
- not have homologous sequences with proteins of other pathogens (not be a source of non-specific cross-reactions)
- be conserved within *B. burgdorferi* s.l.

An antigen is defined as a molecule characterized by immunogenicity, i.e., the ability to induce a specific immune response directed against itself, and antigenicity, i.e., the ability to specifically bind to immunoglobulins and receptors located on the surface of T lymphocytes (Zhang and Tao, 2015). Antigens can be a variety of molecules, including carbohydrates and lipids, but proteins are the most common and diverse antigens recognized by the immune system. Therefore, most research in the field of immunology focuses on them. One of the most challenging tasks in developing new diagnostic tools is the identification of antigens that stimulate the production of specific antibodies against the pathogen, especially when its genome/proteome is large. Therefore, also in the development of serodiagnosis of Lyme disease, it is necessary to initially identify the proteins recognized by antibodies contained in the sera of people infected with *B. burgdorferi* s.l., and then, based on the results obtained in this way, the antigens used in further stages of research are selected (Cobb and Kasper, 2005; De Libero and Mori, 2010; Rahman et al., 2019).

Two-dimensional electrophoresis combined with Western blot allows the detection of individual proteins in WCL recognized by specific antibodies in the sera. In addition, if combined with mass spectrometry and/or sequencing, it will allow precise identification of the antigens (Wittmann-Liebold et al., 2006). This approach is commonly used to search for novel pathogen antigens with diagnostic utility and has also been used to analyze the *B. burgdorferi* s.l. proteome (Dea-Ayuela and Bolás-Fernández, 2005; Nowalk et al., 2006). The proteome array is another method that allows the identification of many proteins inducing an immune response in one experiment. This method involves *in vivo* recombinant cloning of ORF genes and *in vitro* expression of their products, which allows for the rapid generation of complete proteomes of microorganisms. The unpurified protein can be printed directly into a microarray slide. However, an approach based on standard biotechnological protein production and purification is also acceptable, although it slows down the work and reduces the number of antigens tested. The profile of the humoral immune response of vaccinated or

infected animals and humans is then characterized on the basis of the reactivity of the individual proteins with the sera. This method has also been used to search for new diagnostic and vaccine targets to improve Lyme disease control (Barbour et al., 2008; Davies et al., 2005; Xu et al., 2008).

It should be remembered that the immune system does not recognize entire antigens that are too large, but only their fragments called epitopes (antigenic determinants). There are two types of epitopes recognized by different types of cells of the immune system, which include T-cell epitopes and B-cell epitopes. T lymphocytes are unable to recognize antigenic determinants in their native form, they need the help of antigen-presenting cells. These are cells that, after engulfing pathogens by phagocytosis, break down their proteins into short fragments and present them on their surface in the presence of molecules of the major histocompatibility complex (Bahrami et al., 2019). B-cell epitopes, on the other hand, are presented on the surface of the native antigen and interact directly with B-cell receptors, which, upon activation, initiate the production of specific antibodies. Therefore, they are mainly of interest when designing new diagnostic tools. B-cell epitopes are defined as surface-presented clusters of amino acids that are recognized by secreted antibodies or B-cell receptors. They can be divided into continuous (linear or sequential) and discontinuous (conformational) epitopes. Continuous epitopes form linear sequences of at least 6 amino acid residues, while non-contiguous epitopes form distant amino acid residues that are close together due to the three-dimensional structure of the antigen and make up the majority of B-cell epitopes identified so far (90%) (Bahrami et al., 2019).

B-cell epitope mapping may be the first step in the rational design of chimeric proteins. This enables detailed knowledge of the distribution of highly specific and reactive immunodominant fragments in antigen sequence and those that are the source of cross-reactions, which allows the selection of appropriate fragments for the construction of chimeric proteins. There are several methods for identifying both conformational and linear epitopes. Advances in genomics, proteomics, and computational methods have contributed significantly to the development of immunoinformatics. Computational methods predict the existence of potential epitopes based on such physicochemical properties as hydrophilicity, solvent accessibility, flexibility, turns, polarity, antigenicity, and surface exposure. In general, computational epitope prediction methods can be divided into two groups depending on whether the input is only the amino acid sequence of the antigen or its tertiary structure. These methods using the three-dimensional structure of the protein are characterized by greater regularity, unfortunately, it is not always possible to use them due to the fact that the spatial structure of many proteins is not known (Potocnakova et al., 2016). It has been shown that in order to increase the accuracy of prediction, it is worth compiling the results of several methods (Assis et al., 2014). However, even though *in silico* methods save time and money, they only

allow for the initial identification of potential antigenic determinant sequences. It is advisable to confirm the obtained results by experimental methods (Ahmad et al., 2016).

X-ray crystallography of antigen-antibody complexes is believed to be the most accurate method for structural epitope mapping. This technique guarantees precise identification of both continuous and discontinuous epitopes and provides information on binding strength. Despite its undeniable advantages, this method is not used routinely because it is complicated and expensive. It requires a large amount of highly purified protein-monoclonal antibody complexes and prior knowledge of the monoclonal antibody structure is necessary (Bahrami et al., 2019). Another technique that requires specialized equipment and advanced knowledge is nuclear magnetic resonance. In this approach, protons localized in epitope and paratope are subjected to a magnetic field and pulsed electromagnetic radiation to obtain an image of the protein complex in solution. However, this technique is only applicable to low molecular mass proteins. Furthermore, the structure of the antigen should be known, and the antigen-antibody complex should be highly pure and present at a relatively high concentration (Ahmad et al., 2016).

Linear B-cell epitopes seem to be much easier to identify. For their mapping, peptide microarrays consisting of many short peptides (15-20 aa) printed on a solid surface with overlapping amino acids are most often used (Figure 1.13). The complete antigen sequence is screened for fragments recognized by specific antibodies. This method enables the analysis of thousands of peptides simultaneously in a fast and cheap way, which is why it is currently the basis for many studies aimed at identifying new proteins with diagnostic or immunoprotective utility (Heiss et al., 2020). It is worth noting that the length of the applied peptides is not accidental. According to the Los Alamos National Laboratory immunological database, the average length of known linear peptides is 11, so peptides 15-20 in length are likely to contain the full sequence of most linear epitopes (Stephenson et al., 2015).

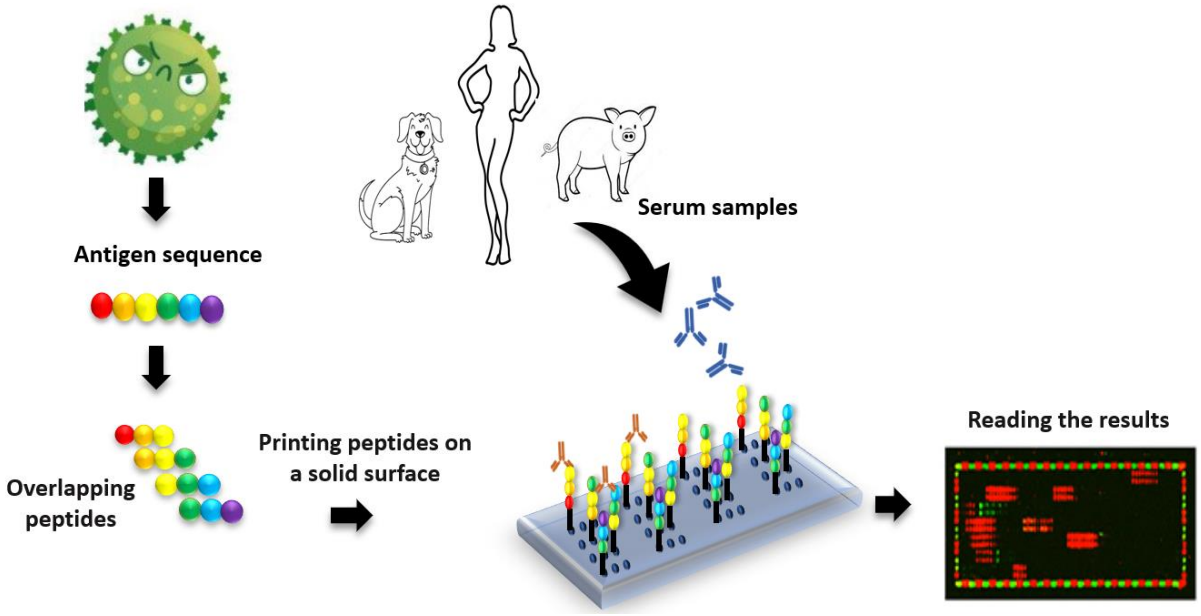

Figure 1. 13 General scheme of peptide microarray experiment.

There are now a large number of databases containing the amino acid sequences of many organisms. The most popular are UniProt (Bateman et al., 2021) and NCBI-Protein (Sharma et al., 2018), which contain millions of protein sequences in their collections. Among them are also protein sequences of various representatives of *B. burgdorferi* s.l. Together with bioinformatics tools (Protein Basic Local Alignment Search Tool (BLASTp), ClustalX), these data allow for a quick and easy determination of the degree of antigen conservation in the *B. burgdorferi* s.l. complex (Altschul et al., 1990; Larkin et al., 2007). This allows the preliminary selection of those that are worth laboratory testing because they may show high reactivity with antibodies directed against various genospecies, which, as has been mentioned many times, is very desirable in Europe (Goettner et al., 2005; Talagrand-Reboul et al., 2020). In addition, such an analysis allows for assessing the degree of sequence similarity with antigens found in other organisms, i.e., the likelihood of cross-reactions. This is very important as cross-reactivity significantly hinders the correct diagnosis of Lyme disease. Sequence analysis may be very helpful during the selection of fragments used for the construction of chimeric proteins due to the fact that it will allow the inclusion of only those fragments conserved within *B. burgdorferi* s.l. and eliminate those commonly found in antigens of other pathogens.

1.4. Biotechnological production of recombinant proteins

Proteins have been used in various industries for many years, e.g., pharmaceutical, food, and chemical. In the past, the only method of obtaining them was isolation from the tissues of living organisms. Unfortunately, methods for the isolation of wild-type proteins were usually characterized by high labor intensity and low efficiency. In addition, the mass production of pathogens in order to obtain their proteins useful in vaccinology and diagnostics

was a threat to the staff. The solution to the problem of the availability of proteins used in the industry came with the development of molecular biology and genetic engineering. This progress enabled the molecular cloning of genes and the biotechnological production of proteins involving the use of living biological systems. The basis of this technique is the introduction into the host cell of a heterologous gene encoding the desired protein by means of genetic transformation. As the host cells grow, the introduced gene is expressed.

Currently, many stable expression systems are on the market based on a wide range of organisms, from simple prokaryotes through yeast, insect cell, and mammalian cell, to transgenic plants and animals. It is up to the researcher on which of them he will base the production of the protein so as to preserve its spatial structure and properties, which is crucial for its usefulness. For industrial purposes, it is also important to achieve the highest protein production efficiency at moderate costs so that the entire process is profitable. It is generally difficult to decide which expression system is best for the production of heterologous proteins. This often depends on the target protein itself. Therefore, it is necessary to optimize each biotechnological process, which includes a number of stages, from the selection of the appropriate host to the selection of the optimal culture medium (Tables 1.5 and 1.6) (Chen, 2012; Desai et al., 2010; Karbalaei et al., 2020; Sahdev et al., 2008; Szmyt et al., 2015; Wang et al., 2013).

Table 1. 5 Stages of constructing and optimizing an efficient expression system (Chen, 2012; Correa and Oppezzo, 2015; Desai et al., 2010; Karbalaei et al., 2020; Sahdev et al., 2008; Szmyt et al., 2015; Wang et al., 2013)

No.	Description
1	Selection of the proper host, which ensures post-translational modification of protein (acetylation, glycosylation, phosphorylation).
2	Selection of an expression vector (episomal or integral) containing the appropriate: • promoter: ○ constitutive - usually used in the case of secretion of the synthesized protein into the periplasmic space or medium; ○ induced - useful for the production of proteins toxic to the host cell, allows strict control of protein production, chemical (e.g., IPTG) and physical (temperature) induction methods are used; • transcription terminator; • selection marker - which will enable the selection of cells that have accepted the vector e.g., antibiotic resistance genes, green fluorescent protein.
3	Optimization of codons in a gene encoding a protein due to the degeneracy of the genetic code. This problem can be solved by: changing rare codons by site-directed mutagenesis or *de novo* whole gene design; using special strains of bacteria that have more genes encoding rare tRNAs.
4	Gene fusion with a sequence facilitating protein purification or increasing its solubility (e.g., His-tag; S-tag).
5	Optional introduction of a signal sequence directing the protein to different cellular spaces or to the culture medium.
6	Proteolytic protection of the final product, e.g., using strains incapable of producing certain intracellular proteases.
7	Optimization of the medium composition (source of carbon and nitrogen, salinity, providing the required compounds to auxotrophs, conditions for possible induction) and growth parameters (temperature, oxygenation level, pH).

Bacterial expression systems are very attractive for the biotechnological production of protein due to their ability to grow quickly and high density on inexpensive medium, their well-known genome, and the ease of genetic manipulation. This made it possible to engineer a large number of vectors and mutated bacterial host strains that allow for flexible adaptation of the expression system to the needs. The most popular bacterial host used in the biotechnological production of proteins is *E. coli*, right after him are *Bacillus* (*B. megaterium*, *B. subtilis*, *B. subtilis*), and *Pseudomonas* species (*P. fluorescens*, *P. aeruginosa*, *P. putida*). Unfortunately, prokaryotic cells have a very limited possibility of introducing post-translational modifications, and their lack means that recombinant proteins are not able to perform their functions properly (Chen, 2012; Sahdev et al., 2008).

Expression systems based on yeast such as *Saccharomyces cerevisiae* and *Pichia pastoris* are very popular and provide efficient production of recombinant proteins. Their main advantages, as in the case of *E. coli*, are a simple cell structure, a small number of genes that allow easy genetic modifications, and quite rapid growth. In addition, they provide post-translational modification characteristics of eukaryotes. However, it should be remembered that these modifications are not always suitable for eukaryote higher cells, e.g., some of them occurring in therapeutic proteins may trigger immune reactions upon long-term administration in humans (Karbalaei et al., 2020; Khan et al., 2017).

Transgenic plants are extremely economical because the formation of biomass requires only solar energy, water, and mineral substrate. In addition, when using plants as bioreactors, it is possible to bypass the complex stage of protein purification because the protein can be accumulated in specific tissues. This is especially true of biopharmaceuticals which can be produced in the edible part of the plant and delivered by oral eliminating the need for downstream processes. Another advantage of plant expressive system is the possibility of obtaining biopharmaceuticals that will not contain pathogens harmful to people. In addition, plants can carry out most of the post-translational modifications required for protein stability and bioactivity (Desai et al., 2010).

Modern genetic engineering allows the production of transgenic animals that can be used as bioreactors. The gene constructs with which animal cells are modified in addition to the gene of target protein, also contain regulatory sequences that allow its expression only in specific tissues or/or stages of animals development. Expression systems are most often constructed so that the desired proteins are excreted with their milk or urine, which greatly facilitates the recovery and purification of the product. Rabbits, sheep, goats and cows are most often used for these purposes. An important advantage is the possibility of inheritance of transgenic genes, which would significantly reduce the time and financial effort in the engineering of transgenic animals (Kumar et al., 2015; Szmyt et al., 2015; Wang et al., 2013).

Table 1. 6 Advantages and disadvantages of expression systems (Chen, 2012; Desai et al., 2010; Karbalaei et al., 2020; Kumar et al., 2015; Sahdev et al., 2008; Szmyt et al., 2015; Wang et al., 2013)

Expression systems	Advantages	Disadvantages
Prokaryotic (*E. coli, Bacillus, Pseudomonas*)	• Ease of genetic transformation • Small, well-known genome • Fast growth on cheap medium • Very fast expression of a heterologous gene • Relatively low process costsprocess is not labour-intensive and time-consuming	• No post-translational modifications • Difficulty of obtaining proteins with disulfide bridges • Need for codon optimization - mainly for eukaryotic genes • Accumulation of target proteins as inclusion bodies • Possibility of contamination of the finished protein with host particles (e.g., bacterial endotoxin)
Yeast (*S. cerevisiae, P. pastoris)*	• Relatively low process costs • Ease of genetic modification • Post-translational modifications, correct protein folding • High performance	• Proteins may be glycosylated in a different way than the original host • Ethanol produced during sugar metabolism by *S. cerevisiae* has a negative effect on biomass production
Insect cells (*Spodoptera frugiperda, Drosophila melanogaster*)	• Post-translational modifications • High performance • Correct protein folding • Simultaneous expression of many genes	• Relatively high cost • Possibility of recombinant protein accumulation as inactive aggregates
Mammalian cells (HeLa, HEK, BHK)	• Post-translational modifications • Way of glycosylation very similar to human • Proper folding of proteins	• Possibility pollution by viral dna • High price • Long production time • Low efficiency
Transgenic plants (*Nicotiana tabacum, Daucus carota, Lectuca* sp.)	• Low costs • Low growth requirements • Easy or unnecessary protein purification • No threat from animal pathogens (including human)	• Difficulty in carrying out genetic modifications
Transgenic animals (*Pterophyllum* sp., *Salmo salar, Sus scrofa, Bos taurus, Ovis aries)*	• The possibility of secreting protein in milk, urine or animal seed • Post-translational modifications • Relatively easy protein purification • Reduction of costs and effort by inheriting the heterological gene by offspring	• Low transformation efficiency • Ethical problems • Production of protein in milk limited to the lactation period • Some proteins produced in milk in a high concentration have a negative effect on the animal • Threat from animal pathogens

2. THE AIM OF THE RESEARCH

The study aimed to construct prokaryotic expression systems enabling the production of monovalent and multivalent *B. burgdorferi* s.l. recombinant proteins and to perform a preliminary evaluation of their reactivity with antibodies present in human sera.

3. MATERIALS

3.1. Genetic material

- Genomic DNA from *B. burgdorferi* s.s. B31 (ATCC**;** #35210)
- Genomic DNA from *B. garinii* 20047 (DSM; #10534)
- Genomic DNA from *B. afzelii* PKo (DSM; #16073)
- Plasmid pET30 Ek/LIC (Novagen)
- Plasmid pET32a (Novagen)
- Plasmid pET42a (Novagen)
- Plasmid pUET1 constructed at the Department of Molecular Biotechnology and Microbiology of Gdańsk University of Technology (Dąbrowski and Kur, 1999)
- pUC57-BmpA-BBK32-G and pUC57-BmpA-BBK32-M constructed by GeneScript (Supplementary materials; Tables S1-S2, Figures S1-S2)

3.2. Bacterial strains

Table 3. 1 Used bacterial strains

Strain	Genotype	Origin
E. coli TOP10F'	F′ [*lac*I^q, *Tn*10(Tet^R)] *mcr*A Δ(*mrr-hsd*RMS-*mcr*BC) φ80*lac*ZΔM15 Δ*lac*X74 *rec*A1 *ara*D139 Δ(*ara leu*) 7697 *gal*U *gal*K *rps*L(Str^R) *end*A1 *nup*G	Invitrogen
E. coli BL21(DE3)pLysS	F$^-$ *omp*T *hsd*S$_B$ (r$_B^-$, m$_B^-$) *gal dcm* (DE3) pLysS(Cam^R)	Novagen
E. coli Rosetta(DE3)pLacI	F$^-$ *ompT hsdS*$_B$ (r$_B^-$ m$_B^-$) *gal dcm* (DE3) pLacIRARE2 (Cam^R)	Novagen
E. coli Rosetta(DE3)pLysS	F$^-$ *ompT hsdS*$_B$(r$_B^-$ m$_B^-$) *gal dcm* (DE3) pLysSRARE (Cam^R)	Novagen
E. coli Origami(DE3)™	*Δ(ara-leu)7697 ΔlacX74 ΔphoA Pvu*II *phoR araD139 ahpC galE galK rpsL* F′[*lac*$^+$ *lacI*^{q} *pro*] (DE3) *gor522*:Tn*10 trxB* (Kan^R, Tet^R)	Novagen
E. coli Stellar™	*F-, end*A1*, supE*44*, thi-1, rec*A1*, rel*A1*, gyr*A96*, phoA, Φ80d lacZΔ M15, Δ(lacZYA-argF) U169, Δ(mrr-hsdRMS-mcrBC), ΔmcrA, λ-*	TaKara

3.3. Culture media

- Luria Bertani medium (LB): tryptone 10 g; yeast extract 5 g; NaCl 10 g; distilled water up to 1000 ml
- Terrific Broth medium (TB): tryptone 12 g; yeast extract 24 g; glycerol 5 ml; KH_2PO_4 2.31 g; K_2HPO_4 12.54 g; distilled water up to 1000 ml
- Luria Bertani agar (LBA): tryptone 10 g; yeast extract 10 g; NaCl 10 g; agar 15 g; distilled water up to 1000 ml

3.4. Reagents and primers for polymerase chain reaction

3.4.1. Reagents

- PCR Mix Plus HGC (A&A Biotechnology; #2005-100G)
- Phusion High-Fidelity DNA Polymerase (Thermo Scientific; #F530S)
- 5X Phusion HF Buffer (Thermo Scientific; #F520L)
- 50 mM $MgCl_2$ (Thermo Scientific; #R0971)
- 10 mM dNTP (Thermo Scientific; #R0191)
- PCR templates - genomic DNA of *B. afzelii* PKo*, B. burgdorferi* s.s. B31, and *B. garinii* 20047
- Nucleases-free water (A&A Biotechnology)

3.4.2. Primers

Table 3. 2 Primers for amplification of *B. burgdorferi* s.l. genes for cloning using In-Fusion system (blue - sequence complementary to the MCS of plasmid pUET1; green - sequence complementary to the *B. burgdorferi* s.l. gene fragment, red - nucleotides inserted to shift the ORF)

Primer name	Primer sequence	Length [bp]	GC [%]	Tm [°C]
ForBB0108BG/BA/BB	5' – TGGACAGCCCAGATCCTCAAAATACTCCTGTTGCTATTATTAATCTATATAAAAATGAAA - 3'	60	32	66
RevBB0108BG/BB	5' – ATCGGTACCCAGATCTTTTAGACTAGAATCCAAGATTTGTATATTTGCAGACTTG - 3'	55	36	66
RevBB0108BA	5' – ATCGGTACCCAGATCTTTTAGACTAGAATCCAAAATTTGTATACTTGCAGACTTG - 3'	55	36	67
ForBB0126BB/BG	5' – TGGACAGCCCAGATCTTGTTGTTTTTTATAATTCTTTAGGCAAGGATTATGTAAAGAGT - 3'	60	32	66
ForBB0126BA	5' – TGGACAGCCCAGATCTTGTTGTTTTTTATAATTCTTTAAGTAAAGATTATGTAAAGAGTGGTGG - 3'	64	43	69
RevBB0126BA/BB/BG	5' – ATCGGTACCCAGATCATTTTGCTTAAGTTCTAAAATTTTATTATTTGCCATAT - 3'	55	36	66
ForBB0298BA	5' – TGGACAGCCCAGATCGTGGTAGCGAATCTAAAGAAAAATTGAATCTTGG - 3'	49	43	69
ForBB0298BB	5' – TGGACAGCCCAGATCGTGGCAATGAATCTAAAGAAAAATCAAATCTTGGT - 3'	50	40	69
ForBB0298BG	5' – TGGACAGCCCAGATCGTGGTAGTGAATCTAAAGAAAAATTGAATCTTGGG - 3'	50	42	69
RevBB0298BA/BB/BG	5' – ATCGGTACCCAGATCGATCCTAGAAACACCTTCTTTTTGCTCT - 3'	43	44	68
ForBB0323BA	5' – TGGACAGCCCAGATCTTAAAACGCCTCCGG - 3'	30	63	66
ForBB0323BB	5' – TGGACAGCCCAGATCATACGCCTCCAGAATCAAGAGAG - 3'	38	53	70
ForBB0323BG	5' – TGGACAGCCCAGATCATACAACGCCTCCAGAAGCAAG - 3'	37	54	71
RevBB0323BA	5' – ATCGGTACCCAGATCTTTAGCAGGAATTATTATTTTCCAGTTAGAAT - 3'	47	34	64
RevBB0323BB	5' – ATCGGTACCCAGATCTTTGGCAGGAATTATTATCTTCCAGTTAGAATGAATTAGA - 3'	55	36	67
RevBB0323BG	5' – ATCGGTACCCAGATCTTTAGCAGGAATTATTATCTTCCAGTTGGAATGAATCA - 3'	53	38	67
ForBB0689BA/BB/BG	5' – TGGACAGCCCAGATCGCGAAGATATGAAAATTCTATATTCAGAAAT - 3'	46	37	66
RevBB0689BA/BB/BG	5' – ATCGGTACCCAGATCTTTTCTTTTTCCAAAAAGAACTACAAATATATCTATATT - 3'	54	28	63

Tm - melting temperature

Table 3. 3 Primers for the construction of a chimeric gene containing fragments of the *bmpA* and *bba64* genes (green - sequence complementary to the *bmpA* of *B. burgdorferi* s.s. gene fragment, yellow - sequence complementary to the *bba64* of *B. burgdorferi* s.s. gene fragment, red - nucleotides inserted to shift the ORF, violet – restriction site, blue - overhangs)

Primer name	Primer sequence	RE	Length [bp]	GC [%]	Tm [°C]
Forward BmpABglII	5'- GTGACAGATCTCGAATTTAAAATTGAGCTTC - 3'	BglII	31	35.5	58
Reverse BmpA-BBA64	5'- GATAAAATTTGCCCAAGATTAATAAATTCTTTAAGAAAC - 3'	-	39	23.1	57
Forward BmpA-BBA64	5'- GTTTCTTAAAGAATTTATTAATCTTGGGCAAATTTTATC - 3'	-	39	23.1	57
Reverse BBA64XhoI	5'- CATAACTCGAGCTGAATTGGAGCAAG - 3'	XhoI	26	46.2	58

RE - restriction enzyme
Tm - melting temperature

Table 3. 4 Primers for the construction of a chimeric gene containing fragments of the *bmpA* and *bbk32* genes (green - sequence complementary to the *bmpA* of *B. burgdorferi* s.s. gene fragment, yellow - sequence complementary to the *bbk32* of *B. burgdorferi* s.s. gene fragment, red - nucleotides inserted to shift the ORF, violet – restriction site, blue - overhangs)

Primer name	Primer sequence	RE	Length [bp]	GC [%]	Tm [°C]
Forward BmpABglII	5'- GTGACAGATCTCGAATTTAAAATTGAGCTTC - 3'	BglII	31	35.5	58
Reverse BmpA-BBK32	5'- GATATCGATTGCTTAATCTAATAAATTCTTTAAGAAACTTC - 3'	-	41	53.4	59
Forward BmpA-BBK32	5'- GAAGTTTCTTAAAGAATTTATTAGATTAAGCAATCGATATC - 3'	-	41	53.4	59
Reverse BBK32XhoI	5'- CATAACTCGAGGTACCAAACGCCATTC - 3'	XhoI	26	46.2	60

RE - restriction enzyme
Tm - melting temperature

3.5. Restriction enzymes and buffers

Table 3. 5 Restriction enzymes

Restriction enzyme	Resriction site	Buffer	Reaction temperature
HinfI (Thermo Scientific; #ER0802)	5'- G/ANTC - 3'	**10x Buffer Red**: 0.1 M Tris-HCl (pH 8.5 at 37°C); 0.1 M $MgCl_2$; 1 M KCl; 1 mg/ml BSA	37°C
HindIII (Thermo Scientific; #ER0505)	5'- A/AGCTT - 3'	**10x Buffer Red**: 0.1 M Tris-HCl (pH 8.5 at 37°C); 0.1 M $MgCl_2$; 1 M KCl; 1 mg/ml BSA or **10x Buffer Tango:** 0.33 M Tris-CH_3COOH (pH 7.9 at 37°C); 0.1 M $Mg(CH_3COO)_2$; 0.66 M CH_3COOK; 1 mg/ml BSA	
XhoI (Thermo Scientific; #ER0691)	5'-C/TCGAG - 3'		
BglII (Thermo Scientific; #ER0081)	5'- A/GATCT - 3'	**10x Buffer Orange:** 0.5 M Tris-HCl (pH 7.5 at 37°C); 0.1 M $MgCl_2$; 1 M KCl; 1 mg/ml BSA or **10x Buffer Tango:** 0.33 M Tris-CH_3COOH (pH 7.9 at 37°C); 01 M $Mg(CH_3COO)_2$. 0.66 M CH_3COOK; 1 mg/ml BSA	
NdeI (Thermo Scientific; #ER0581)	5'- CA/TATG - 3'	**10x Buffer Orange:** 0.5 M Tris-HCl (pH 7.5 at 37°C); 0.1 M $MgCl_2$; 1 M KCl; 1 mg/ml BSA	
SacI (Thermo Scientific; #ER1131)	5'-GAGCT/C - 3'	**10x Buffer SacI:** 0.1 M Bis-Tris Propan-HCl (pH 6.5 at 37°C); 0.1 M $MgCl_2$; 1 mg/ml BSA	
XbaI (Thermo Scientific; #ER0682)	5'- T/CTAGA - 3'	**10x Buffer Tango:** 0.33 M Tris-CH_3COOH (pH 7.9 at 37°C); 0.1 M $Mg(CH_3COO)_2$; 0.66 M CH_3COOK; 1 mg/ml BSA	
EcoRV (Thermo Scientific; #ER0301)	5'-A/AGCTT-3'	**10x Buffer Red:** 0.1 M Tris-HCl (pH 8.5 at 37°C); 0.1 M $MgCl_2$; 1 M KCl; 1 mg/ml BSA	
ScaI (Thermo Scientific; #ER0431)	5' -A GT/ACT- 3'	**10x Buffer ScaI**: 0.1 M Bis-Tris Propane-HCl (pH 6.5 at 37°C); 0.1 M $MgCl_2$; 1M KCl; 0.1 mg/ml BSA	
SmaI (Thermo Scientific; #ER0662)	5'-CCC/GGG -3'	**10x Buffer Tango:** 0.33 M Tris-CH_3COOH (pH 7.9 at 37°C); 0.1 M $Mg(CH_3COO)_2$; 0.66 M CH_3COOK; 1 mg/ml BSA	30°C

3.6. Molecular cloning reagents

- DNA T4 ligase (Thermo Scientific; # EL0014)
- 10x T4 DNA Ligase buffer (Thermo Scientific; #B69)
- 10 mM ATP solution (Thermo Scientific; #PV3227)
- In-Fusion® HD Cloning Kit (Takara)
- Stellar™ Competent Cells (Takara; #636766)
- SOC medium (Takara; #ST0215)

3.7. Buffers and reagents for agarose electrophoresis

- Agarose (Prona; #RN100)
- 1xTris-acetate-EDTA buffer (TAE): 40 mM Tris, 20 mM acetic acid, 1 mM EDTA
- 6X Loading Dye (Thermo Scientific; #R0611)
- Ethidium bromide solution 5 mg/ml (Sigma; #1239-45-8)

3.8. Buffers and reagents for polyacrylamide electrophoresis

- Polyacrylamide gel components:
    - 30% Acrylamide/Bisacrylamide solution (29% acrylamide; 1% N,N'-Methylenebisacrylamide)
    - 1.5 M Tris-HCl (pH 8.8) (Sigma, #17-1321-01)
    - 1 M Tris-HCl (pH 6.8) (Sigma, #17-1321-01)
    - 10% ammonium persulfate (APS) (Sigma; #A3678)
    - 10% sodium dodecyl sulfate (SDS) (Sigma; #1.06022)
    - N,N,N′,N′-Tetramethylethylenediamine (TEMED) (Sigma; # 1.10732)
    - Distilled water

Table 3. 6 Composition 5% (stacking gel) polyacrylamide gel (final volume 3 ml)

Component	Volume [ml]
Water	2.1
30% Acrylamide/Bisacrylamide solution	0.5
1 M Tris-HCl (pH 6.8)	0.38
10% SDS	0.03
10% APS	0.03
TEMED	0.008

Table 3. 7 Composition 15% (separating gel) polyacrylamide gel (final volume 5 ml)

Component	Volume [ml]
Water	1.1
30% Acrylamide/Bisacrylamide solution	2.5
1 M Tris-HCl (pH 8.8)	1.3
10% SDS	0.05
10% APS	0.05
TEMED	0.004

Table 3. 8 Composition 12% (separating gel) polyacrylamide gel (final volume 5 ml)

Component	Volume [ml]
Water	1.6
30% Acrylamide/Bisacrylamide solution	2.0
1 M Tris-HCl (pH 8.8)	1.3
10% SDS	0.05
10% APS	0.05
TEMED	0.004

- SDS-PAGE loading buffer: 0.25% bromophenol blue; 10% glycerol; 10% SDS; 1 M β-mercaptoethanol; 1 M Tris (pH 6.8)
- Staining solution: 50% methanol; 10% acetic acid; 0.05% Coomasie Brilliant Blue R-250 (Sigma; #1.12553)
- Destaining solution: 40% methanol; 7% acetic acid
- 1xTris-glycine (pH 8.3): 25 mM Tris-Cl; 250 mM glycine; 0.1% SDS

3.9. Ladders

3.9.1. DNA ladders

- GeneRuler 50 bp Plus DNA Ladder (Thermo Scientific; #SM0371): 50; 100; 150; 200; 250; 300; 400; 500; 600; 700; 800; 900; 1000 bp
- GeneRuler 100 bp Plus DNA Ladder (Thermo Scientific; #SM0321): 100; 200; 300; 400; 500; 600; 700; 800; 900; 1000; 1200; 1500; 2000; 3000 bp
- GeneRuler 1 kb DNA Ladder (Thermo Scientific; #SM0311): 250; 500; 750; 1000; 1500; 2000; 2500; 3000; 3500; 4000; 5000; 6000; 8000; 10 000 pb

3.9.2. Protein ladders

- SigmaMarker™ (Sigma; #S8445): 6,5; 14,2; 20; 24; 29; 36; 45; 55; 66; 97; 116; 200 kDa
- PageRuler™ Prestained Protein Ladder (Thermo Scientific; #26619): 10; 15; 25; 35; 40; 55; 70; 100; 130; 250 kDa
- SuperSignal™ Molecular Weight Protein Ladder (Thermo Scientific; #84785): 20; 30; 40; 50; 60; 80; 100; 150 kDa

3.10. Buffers and kits for DNA isolation and purification

3.10.1. Buffers and columns for plasmid DNA isolation

- L1 buffer: 50 mM Tris, 10 mM EDTA; 100 mg/ml RNase H
- L2 buffer: 0.2 M NaOH; 1% SDS
- L3 solution: 3 M potassium acetate
- G solution: 8 M guanidine hydrochloride
- 96% etanol
- TE buffer: 10 mM Tris-HCl; 1 mM EDTA (pH 8)
- Silica minicolumns (A&A Biotechnology)

3.10.2. Kits for DNA purification after enzymatic reactions

- Clean-Up Concentrator (A&A Biotechnology; #021-250C)
- Gel-Out Concentrator (A&A Biotechnology; #023-250C)

3.11. Buffers and reagents for recombinant protein purification

3.11.1. Buffers for column regeneration

- 0.5 M $NiCl_2$ solution
- Regeneration buffer: 50 mM EDTA (pH 8.0); 1% SDS
- Distilled water

3.11.2. Buffers for protein purification

3.11.2.1. A buffers (standard buffers)

- A1 (binding buffer): 5 mM imidazole; 20 mM Tris; 0.5 M NaCl; 0.1% Triton X-100 (pH 7.9-9.5)
- A1M (binding buffer): 5 mM imidazole; 20 mM Tris; 0.5 M NaCl; 0.1% Triton X-100; 5 M urea (pH 7.9-9.5)
- A1M2 (binding buffer): 5 mM imidazole; 20 mM Tris; 0.5 M NaCl; 0.1% Triton X-100; 1 M urea (pH 7.9-9.5)
- A2 (washing buffer): 50 mM imidazole; 20 mM Tris; 0.5 M NaCl; 0.1% Triton X-100 (pH 7.9-9.5)
- A2M (washing buffer): 50 mM imidazole; 20 mM Tris; 0.5 M NaCl; 0.1% Triton X-100; 5 M urea (pH 7.9-9.5)
- A2M2 (washing buffer): 5 mM imidazole; 20 mM Tris; 0.5 M NaCl; 0.1% Triton X-100; 1 M urea (pH 7.9-9.5)

- A3 (washing buffer): 80 mM imidazole; 20 mM Tris; 0.5 M NaCl; 0.1% Triton X-100 (pH 7.9-9.5)
- A3M (washing buffer): 80 mM imidazole; 20 mM Tris; 0.5 M NaCl; 0.1% Triton X-100; 5 M urea (pH 7.9-9.5)
- A3M2 (washing buffer): 5 mM imidazole; 20 mM Tris; 0.5 M NaCl; 0.1% Triton X-100; 1 M urea (pH 7.9-9.5)
- A4 (elution buffer): 0.5 M imidazole; 20 mM Tris; 0.5 M NaCl; 0.1% Triton X-100 (pH 7.9-9.5)
- A4M (elution buffer): 0.5 M imidazole; 20 mM Tris; 0.5 M NaCl; 0.1% Triton X-100; 5 M urea (pH: 7.9-9.5)
- A4M2 (elution buffer): 0.5 M imidazole; 20 mM Tris; 0.5 M NaCl; 0.1% Triton X-100; 1 M urea (pH 7.9-9.5)

3.11.2.2. B buffers

- B1 (binding buffer): 5 mM imidazole; 25 mM Tris-HCl; 150 mM NaCl (pH 7.9-9.5)
- B1M (binding buffer): 5 mM imidazole; 25 mM Tris-HCl; 150 mM NaCl; 5 M urea (pH 7.9-9.5)
- B2 (washing buffer): 50 mM imidazole; 25 mM Tris-HCl; 150 mM NaCl (pH 7.9-9.5)
- B2M (washing buffer): 50 mM imidazole; 25 mM Tris-HCl; 150 mM NaCl; 5 M urea (pH 7.9-9.5)
- B3 (washing buffer): 80 mM imidazole; 25 mM Tris-HCl; 150 mM NaCl (pH 7.9-9.5)
- B3M (washing buffer): 80 mM imidazole; 25 mM Tris-HCl; 150 mM NaCl; 5 M urea (pH 7.9-9.5)
- B4 (elution buffer): 0.5 M imidazole; 25 mM Tris-HCl; 150 mM NaCl (pH 7.9-9.5)
- B4M (elution buffer): 0.5 M imidazole; 25 mM Tris-HCl; 150 mM NaCl; 5 M urea (pH 7.9-9.5)

3.11.2.3. C buffers

- C1 (binding buffer): 5 mM imidazole; 50 mM Na_3PO_4; 500 mM NaCl (pH 7.9-9.5)
- C1M (binding buffer): 5 mM imidazole; 50 mM Na_3PO_4; 500 mM NaCl; 5 M urea (pH 7.9-9.5)
- C2 (washing buffer): 50 mM imidazole; 50 mM Na_3PO_4; 500 mM NaCl (pH 7.9-9.5)
- C2M (washing buffer): 50 mM imidazole; 50 mM Na_3PO_4; 500 mM NaCl; 5 M urea (pH 7.9-9.5)

- C3 (washing buffer): 80 mM imidazole; 50 mM Na_3PO_4; 500 mM NaCl (pH 7.9-9.5)
- C3M (washing buffer): 80 mM imidazole; 50 mM Na_3PO_4; 500 mM NaCl; 5 M urea (pH 7.9-9.5)
- C4 (elution buffer): 0.5 M imidazole; 50 mM Na_3PO_4; 500 mM NaCl (pH 7.9-9.5)
- C4M (elution buffer): 0.5 M imidazole; 50 mM Na_3PO_4; 500 mM NaCl; 5 M urea (pH 7.9-9.5)

3.11.2.4. D buffers

- D1 (binding buffer): 5 mM imidazole; 20 mM Na_3PO_4; 250 mM NaCl (pH 7.9-9.5)
- D1M (binding buffer): 5 mM imidazole; 20 mM Na_3PO_4; 250 mM NaCl; 5 M urea (pH 7.9-9.5)
- D2 buffer: 50 mM imidazole; 20 mM Na_3PO_4; 250 mM NaCl (pH 7.9-9.5)
- D2M buffer: 50 mM imidazole; 20 mM Na_3PO_4; 250 mM NaCl; 5 M urea (pH 7.9-9.5)
- D3 (washing buffer): 80 mM imidazole; 20 mM Na_3PO_4; 250 mM NaCl (pH 7.9-9.5)
- D3M (washing buffer): 80 mM imidazole; 20 mM Na_3PO_4; 250 mM NaCl; 5 M urea (pH 7.9-9.5)
- D4 (elution buffer): 0.5 M imidazole; 20 mM Na_3PO_4; 250 mM NaCl (pH 7.9-9.5)
- D4M (elution buffer): 0.5 M imidazole; 20 mM Na_3PO_4; 250 mM NaCl; 5 M urea (pH 7.9-9.5)

3.11.2.5. E buffers (Phosphate-Buffered Saline - PBS)

- E1 (binding buffer): 5 mM imidazole; 137 mM NaCl; 2.7 mM KCl; 8 mM Na_2HPO_4; 2 mM KH_2PO_4 (pH 7.9-9.5)
- E1M (binding buffer): 5 mM imidazole; 137 mM NaCl; 2.7 mM KCl; 8 mM Na_2HPO_4; 2 mM KH_2PO_4; 5M urea (pH 7.9-9.5)
- E2 (washing buffer): 50 mM imidazole; 137 mM NaCl; 2.7mM KCl; 8 mM Na_2HPO_4; 2 mM KH_2PO_4 (pH 7.9-9.5)
- E2M (washing buffer): 50 mM imidazole; 137 mM NaCl; 2.7 mM KCl; 8 mM Na_2HPO_4; 2 mM KH_2PO_4; 5M urea (pH 7.9-9.5)
- E3 (washing buffer): 80 mM imidazole; 137 mM NaCl; 2.7 mM KCl; 8 mM Na_2HPO_4; 2 mM KH_2PO_4 (pH 7.9-9.5)
- E3M (washing buffer): 80 mM imidazole; 137 mM NaCl; 2.7 mM KCl; 8 mM Na_2HPO_4; 2 mM KH_2PO_4; 5M urea (pH 7.9-9.5)

- E4 (elution buffer): 0.5 M imidazole; 137 mM NaCl; 2.7 mM KCl; 8 mM Na_2HPO_4; 2 mM KH_2PO_4 (pH 7.9-9.5)
- E4M (elution buffer): 0.5 M imidazole; 137 mM NaCl; 2.7 mM KCl; 8 mM Na_2HPO_4; 2 mM KH_2PO_4; 5M urea (pH 7.9-9.5)

3.11.2.6. F buffers (Storage buffer)

- F1 (binding buffer): 5 mM imidazole; 50 mM Tris-HCl; 150 mM NaCl (pH 7.9-9.5)
- F1M (binding buffer): 5mM imidazole; 50 mM Tris-HCl; 150 mM NaCl; 5 M urea (pH 7.9-9.5)
- F2 (washing buffer): 50 mM imidazole; 50 mM Tris-HCl; 150 mM NaCl (pH 7.9-9.5)
- F2M (washing buffer): 50 mM imidazole; 50 mM Tris-HCl; 150 mM NaCl; 5 M urea (pH 7.9-9.5)
- F3 (washing buffer): 80 mM imidazole; 50 mM Tris-HCl; 150 mM NaCl (pH 7.9-9.5)
- F3M (washing buffer): 80 mM imidazole; 50 mM Tris-HCl; 150 mM NaCl; 5 M urea (pH 7.9-9.5)
- F4 (elution buffer): 0.5 M imidazole; 50 mM Tris-HCl; 150 mM NaCl (pH 7.9-9.5)
- F4M (elution buffer): 0.5 M imidazole; 50 mM Tris-HCl; 150 mM NaCl; 5 M urea (pH 7.9-9.5)

3.11.2.6. G buffers

- G1 (binding buffer): 5 mM imidazole; 40 mM Tris-HCl; 100 mM KCl; 12.5 mM β-mercaptoethanol; 10% glycerol (pH 7.9-9.5)
- G1M (binding buffer): 5 mM imidazole; 40 mM Tris-HCl; 100 mM KCl; 12.5 mM β-mercaptoethanol; 10% glycerol; 5 M urea (pH 7.9-9.5)
- G2 (washing buffer): 50 mM imidazole; 40 mM Tris-HCl; 100 mM KCl; 12.5 mM β-mercaptoethanol; 10% glycerol (pH 7.9-9.5)
- G2M (washing buffer): 50 mM imidazole; 40 mM Tris-HCl; 100 mM KCl; 12.5 mM β-mercaptoethanol; 10% glycerol; 5 M urea (pH 7.9-9.5)
- G3 (washing buffer): 80 mM imidazole; 40 mM Tris-HCl; 100 mM KCl; 12.5 mM β-mercaptoethanol; 10% glycerol (pH 7.9-9.5)
- G3M (washing buffer): 80 mM imidazole; 40 mM Tris-HCl; 100 mM KCl; 12.5 mM β-mercaptoethanol; 10% glycerol; 5 M urea (pH 7.9-9.5)
- G4 (elution buffer): 0.5 M imidazole; 40 mM Tris-HCl; 100 mM KCl; 12.5 mM β-mercaptoethanol; 10% glycerol (pH 7.9-9.5)

- G4M (elution buffer): 0.5 M imidazole; 40 mM Tris-HCl; 100 mM KCl; 12.5 mM β-mercaptoethanol; 10% glycerol (pH 7.9-9.5)

3.11.3. Others

- His•Bind® Resin (Novagen; #69670)
- Protease inhibitor - phenylmethylsulfonyl fluoride (Sigma; #52332)

3.12. Human serum samples

This study used 388 human sera (160 IgG positive, 48 IgM positive, 180 negative) obtained from the National Institute of Public Health NIH - National Research Institute (Warsaw, Poland) and Department of Tropical Medicine and Epidemiology, Medical University of Gdańsk (Gdynia, Poland). All were gained during routine borreliosis screening. Anonymized information about each sample included only the collection date and the titer of anti-*B. burgdorferi* s.l. antibodies. In the institutions of origin, they were tested with a two-tiered tesing algorithm. After receiving the sera IgG and IgM levels were re-determined using a commercial ELISA (Borrelia plus VlsE, Euroimmun and Borrelia Select: recombinant antigens with OspC, Euroimmun, Lübeck Germany). The presence of specific anti-*B. burgdorferi* s.l. IgG, and IgM was further confirmed using a commercial WB (EUROLINE WB Borrelia, Euroimmun, Lübeck, Germany).

3.13. Buffers and reagents for Western blot

- Transfer buffer: 12.5 mM Tris; 96 mM glycine; 10% methanol
- TBST (pH 7.5): 10 mM Tris; 150 mM NaCl; 0.1% Tween 20
- Blocking buffer: 10 mM Tris; 150 mM NaCl; 0.1% Tween 20; 5% non-fat milk
- Buffer for colorimetric detection: 0.5 mg/ml 3,3'-diaminobenzidine (Sigma; #32750); 5 mM Tris-HCl (pH 7.6); 0.75% H_2O_2
- Reagent for chemiluminescence detection: Luminata™ Crescendo Western HRP substrate (Merck Millipore; #WBLUR0500)
- Nitrocellulose membrane pore size 0.45 µm (Sigma; #N8392)
- Whatman paper 3 MM (Sigma)
- Monoclonal anti-polyhistidine antibodies labeled with horseradish peroxidase (Sigma; #A7058)
- Ponceau S solution (Sigma; #P7170)
- Horseradish peroxidase labeled antibodies against human IgG (Jackson ImmunoResearch; #109-035-003)

- Horseradish peroxidase labeled antibodies against human IgM (Jackson ImmunoResearch; #109-035-129)
- 30% H_2O_2
- Sterile distilled water
- Serum samples

3.14. Materials and reagents for linear epitope mapping

3.14.1. Peptide microarray

Peptide microarrays (PEPperCHIP® Immunoassay), with overlapping peptides encoding BmpA (GenBank: AAC66757.1) and BBK32 (GenBank: AAC66134.1) proteins of *B. burgdorferi* s.s. B31 were made by PEPperPRINT, (Heidelberg, Germany). Each protein was printed in five identical copies.

3.14.2. Human serum samples

For linear epitope mapping, 30 sera negative, 22 IgG positive, 14 IgM positive, and 8 positive for both IgM and IgG were used. Sera were considered positive when the antibody titer exceeded 22 IU. The antibody titres for the individual sera are shown in Tables 3.9 – 3.12.

Table 3. 9 Negative sera used for linear epitope mapping

Sera number	IgG titer	IgM titer	Sera number	IgG titer	IgM titer
1	4.9	6.9	**16**	2.6	3.4
2	3.4	4.4	**17**	8.4	1.2
3	2	2.9	**18**	14.9	7.1
4	2.7	7.1	**19**	7.6	3.1
5	2.6	1.4	**20**	3.5	8.0
6	7.4	3.1	**21**	3.8	1.7
7	7.3	3.1	**22**	12.4	7.8
8	6.3	6.5	**23**	4.3	5.9
9	9.9	6.7	**24**	8.6	2.8
10	2.8	15.9	**25**	1.2	2.4
11	6.2	5.2	**26**	2.0	2.9
12	10.8	4.9	**27**	5.8	3.7
13	5.2	3.1	**28**	2.5	4.1
14	3.6	2.7	**29**	5.1	12.5
15	8.4	2.0	**30**	5.9	2.4

Table 3. 10 IgG-positive sera used for linear epitope mapping

Sera number	IgG titer	IgM titer	Sera number	IgG titer	IgM titer
31	62.5	6.7	**42**	98.7	7.6
32	64.5	3.4	**43**	91.8	2.2
33	74.2	3.3	**44**	114.2	3.9
34	99.7	19.7	**45**	138.1	2.7
45	103.4	10.7	**46**	154	8.0
36	104.6	6.6	**47**	156.6	2.5
37	24.6	6.7	**48**	180.7	17.0
38	25.1	6.3	**49**	186.6	5.3
39	211.2	15.0	**50**	82.2	7.0
40	89.5	2.3	**51**	145	14.0
41	154.0	1.9	**52**	63.2	11.1

Table 3. 11 IgM-positive sera used for linear epitope mapping

Sera number	IgG titer	IgM titer	Sera number	IgG titer	IgM titer
53	4.5	29.9	**60**	3.7	29.9
54	10.9	77.9	**61**	9.8	44.1
55	7.9	49.3	**62**	13.2	50.3
56	3.2	35.7	**63**	15.1	44.5
57	10.4	104.0	**64**	9.2	64.1
58	2.9	92.1	**65**	11.	344.6
59	8.8	27.8	**66**	12.5	92.7

Table 3. 12 IgG and IgM-positive sera used for linear epitope mapping

Sera number	IgG titer	IgM titer	Sera number	IgG titer	IgM titer
67	128.5	56.8	**71**	161.0	100.1
68	132.8	23.2	**72**	244.2	32.4
69	59.7	27.0	**73**	104.3	54.6
70	84.1	40.0	**74**	62.7	40.9

3.14.3. Buffers and reagents for linear epitope mapping

- Blocking buffer: PBS (pH 7.4); 1% (w/v) bovine serum albumin (BSA); 0.005% (v/v) Tween-20
- Standard buffer: PBS (pH 7.4); 0.005% (v/v) Tween-20
- Staining buffer: PBS (pH 7.4); 0.005% (v/v) Tween-20; 10% blocking buffer
- Dipping buffer: 1 mM Tris-HCl (pH 7.4)
- Goat anti-human IgG antibodies labeled with DyLight549 antibodies (Sigma-Aldrich, St. Louis, MO, USA)
- Goat anti-human IgM antibodies labeled with DyLight650 (Sigma-Aldrich, St. Louis, MO, USA)

3.15. Buffers and reagents for ELISA

- Carbonate buffer (coating) (pH 9.6): 200 mM carbonate buffer; 0.001% phenol red (Sigma; #P3532)
- Washing buffer (pH 7.4): 50 mM Tris; 0.88% NaCl; 0.1% Tween 20 (Sigma; #P9416)
- Blocking buffer (pH 7.2): PBS; 3% non-fat milk; 0.05% Tween 20 (Sigma; #P9416)
- Substrate SIGMAFAST™ OPD (o-phenylenediamine dihydrochloride) (Sigma #P9187)
- Stop solution: 2 M H_2SO_4
- Human serum samples
- Purified *B. burgdorferi* s.l. monovalent and multivalent recombinant proteins
- Horseradish peroxidase labeled antibodies against human IgM (Jackson ImmunoResearch; #109-035-129)
- Horseradish peroxidase labeled antibodies against human IgG (Jackson ImmunoResearch; #109-035-003)
- ELISA microplates (NUNC – Immuno™ Plater, MaxiSorp; M9410)

3.16. Reagents for the determination of protein concentration by the Bradford method

The Quick Start™ Bradford Protein Assay (Bio-Rad; #5000202) was used to determine the protein concentration.

3.17. Antibiotics

- Ampicillin (stock solution: 100 mg/ml in H_2O) (Sigma; #A0166)
- Chloramphenicol (stock solution: 34 mg/ml in 70% ethanol) (Sigma; #C3175)
- Kanamycin (stock solution: 20 mg/ml in H_2O) (Sigma; #K1377)
- Tetracycline (stock solution: 12.5 mg/ml in 70% ethanol) (Sigma; #T8032)

3.18. Other

- FastAP Thermosensitive Alkaline Phosphatase (Thermo Scientific; #EF0651)
- Induction solution: 1 M IPTG (Sigma; #I6758)
- Solution for the preparation of competent *E. coli* cells: 100 mM $CaCl_2$
- Dialysis tubing cellulose membrane (Sigma; #D9527)

3.19. Equipment

- Agarose electrophoresis apparatus (Blirt S.A.)
- Polyacrylamide electrophoresis apparatus (Blirt S.A.)
- Electrotransfer apparatus (Fermentas)
- Autoclave Omega Media (Prestige Medical)
- Multiskan FC plate reader (Thermo scientific)
- GenePix personal 4100a microarray scanner (Molecular Devices)
- Microcentrifuge MPW-210 (Sigma)
- pH-meter pH 210 Microprocessor (Hanna Instruments)
- Thermocycler GeneAmp PCR System 2400 (Perkin Elmer)
- Thermoblock Thermomixer comfort (Eppendorf)
- Centrifuge 5810 R (Eppendorf)
- Gel imaging device ChemiDoc™ MP (Bio-Rad)
- Incubator New Brunswick™ Innova®42 (Eppendorf)
- Scale PLS510-3 (Kern)

4. METHODS

4.1. Analysis of the amino acid sequence of *B. burgdorferi* s.l. proteins

4.1.1. Degree of conservation of amino acid sequences

The amino acid sequences of proteins from 5 *B. burgdorferi* s.l. genospecies (*B. afzelii, B. garinii, B. bavariensis, B. burgdorferi* s.s., *B. spielmanii*) were obtained from the National Center for Biotechnology Information (NCBI) (accession numbers are presented in Table 4.1). With the use of SignalP-5.0 Server (Almagro Armenteros et al., 2019) and UniProt database (Bateman et al., 2021) signal peptides and transmembrane domains in the amino acid sequence were identified and removed. Mature protein sequences prepared in this way were subjected to global multiple sequence alignments using ClustalX 2.0 (Larkin et al., 2007) software to determine the degree of conservation. Afterwards, a search for homologous that could be the source of cross-reactions among organisms such as *B. miyamotoi, B. hispanica, B. hermsii, T. pallidum, E. coli, A. phagocytophilum, Y. enterocolitica*, *Y. pseudotuberculosis,* cytomegalovirus, Epstein-Barr virus, influenza virus was performed using the protein BLAST (Altschul et al., 1990). The degree of identity of the homologs with the *B. burgdorferi* s.l. proteins was determined using the ClustalX 2.0 software (Larkin et al., 2007).

Table 4. 1 Protein amino acid sequences NCBI accession numbers

	BB0108	**BB0126**	**BB0298**	**BB0323**	**BB0689**
B. afzelii					
PKo	ABH01372.1	ABH01391.1	ABH01565.1	ABH01589.1	ABH01964.1
K78	AJY72106.1	AJY72124.1	AJY72289.1	AJY72312.1	AJY72665.1
HLJ01	AFU74378.1	AFU74397.1	AFU74587.1	-	AFU74994.1
***B. burgdorferi* s.s.**					
B31	AAC66497.1	AAC66520.1	AAC66650.1	AAC66700.1	AAC67038.1
N40	ADQ29524.1	ADQ29705.1	ADQ29505.1	ADQ29536.1	ADQ29414.1
JD1	ADQ30867.1	ADQ31046.1	ADQ30912.1	ADQ30523.1	ADQ30827.1
ZS7	ACK75015.1	ACK75129.1	ACK74844.1	ACK75045.1	ACK74705.1
B. garinii					
SZ	AHZ74426.1	AHZ74408.1	AHZ74244.1	AHZ74222.1	AHZ73871.1
NMJW1	AFT83445.1	AFT83463.1	AFT83628.1	AFT83650.1	AFT84003.1
BgVir	AEW68448.1	AEW68466.1	AEW68638.1	AEW68660.1	AEW69023.1
20047	AZA27564.1	AZA27582.1	AZA27737.1	AZA27757.1	AZA28088.1
B. bavariensis					
PBi	AAU06967.1	AAU06986.1	AAU07155.1	AAU07177.1	AAU07540.1
B. spielmanii					
A14S	WP_006434043.1	-	WP_006433448.1	EEF84725.1	WP_006433755.1

4.1.2. Continuous B-cell epitope prediction

Potential linear B-cell epitopes were identified with the use of three different tools available on IEDB: BepiPred-2.0 Sequential B-Cell Epitope Predictor (Jespersen et al., 2017), Parker Hydrophilicity Prediction (Parker et al., 1986) and Emini Surface Accessibility Scale (Emini et al., 1985) with a threshold value of 0.535, 1.0 and 1.2 respectively. Linear fragments with a minimum length of 6 amino acids detected by at least 2 tools were recognized as potential epitopes (da Silva et al., 2023). Highly conserved epitopes were considered to be those with an identity of at least 75% and 85% for plasmid and chromosomally encoded proteins, respectively.

4.1.3. Conformational B-cell epitope prediction

Potential conformational B-cell epitopes were predicted using three tools ElliPro (Ponomarenko et al., 2008), Epitopia (Rubinstein et al., 2009), and DiscoTope 1.1 (Haste Andersen et al., 2006). The 3D structures of *B. burgdorferi* s.s. antigens were obtained from the UniProt database (BB0298: Q57105; BB0689: O51632) (Bateman et al., 2021). Conserved conformational epitopes were considered to be those predicted by at least 2 methods with a minimum sequence identity of 85%.

4.2. Bacterial growth media

All bacterial growth media were sterilized for 30 min. at 120°C.

4.2.1. Liquid media

E. coli [Materials 3.2] were grown in LB or TB medium [Materials 3.3] with the addition of appropriate antibiotics (1 µl of ampicillin/chloramphenicol/tetracycline stock solution [Materials 3.17] was added per 1 ml of medium). Antibiotics were added after sterilization when the bacterial growth media reached the appropriate temperature. *E. coli* was inoculated in the medium with a loop or by adding liquid culture. The bacteria were then cultivated for an appropriate time with vigorous shaking at 20°C, 25°C, 30°C or 37°C [Materials 3.19].

4.2.2. Solid media

E. coli cultures were carried out on LBA medium [Materials 3.3] with the addition of appropriate antibiotics (as above) [Materials 3.16]. After adding antibiotics still liquid LBA was poured onto sterile Petri dishes. Bacteria were plated with a loop or a cell spreader. The plates were then incubated overnight (12-18 h) at 37°C.

4.3. Polymerase chain reaction

4.3.1. Amplification of gene fragments

Phusion® High-Fidelity DNA polymerase [Materials 3.4] was used to amplify the *bb0108s, bb0126s, bb0298s, bb0323s, bb0689s* gene fragments. The compositions of the reaction mixture are presented in the Table 4.2. In Tables 4.3-4.9 the PCR temperature profile for amplification of individual genes is given.

Table 4. 2 Reaction mixture for the amplification of gene fragments of *B. burgdorferi* s.l. with the use Phusion® High-Fidelity DNA polymerase

Components	Volume [µl]
Buffer	8
10 mM dNTPs	0.8
Forward primer	1
Reverse primer	1
Polymerase	0.4
Template (*B. burgdorferi* s.l. genomic DNA diluted 1:1000 v/v)	1
Water	27.8
Total volume	40

Table 4. 3 PCR profile for the amplification of the *bb0108* gene fragments from *B. afzelii* PKo, *B. burgdorferi* s.s. B31, *B. garinii* 20047

Parameters / Step	Temperature [°C]	Time [s]	No. of cycles
Initial denaturation	98	30	1
Denaturation	98	10	7
Annealing	61	25	
Extension	72	20	
Denaturation	98	8	30
Annealing	63	20	
Extension	72	15	
Final extension	72	420	1
Cooling	4	∞	1

Table 4. 4 PCR profile for the amplification of the *bb0126* gene fragments from *B. burgdorferi* s.s. B31*, B. garinii* 20047

Parameters / Step	Temperature [°C]	Time [s]	No. of cycles
Initial denaturation	98	30	1
Denaturation	98	10	7
Annealing	65	25	
Extension	72	22	
Denaturation	98	8	30
Annealing	67	18	
Extension	72	18	
Final extension	72	420	1
Cooling	4	∞	1

Table 4. 5 PCR profile for the amplification of the *bb0126* gene fragment from *B. afzelii* PKo

Parameters / Step	Temperature [°C]	Time [s]	No. of cycles
Initial denaturation	98	30	1
Denaturation	98	10	7
Annealing	53	25	
Extension	72	22	
Denaturation	98	8	30
Annealing	55	18	
Extension	72	18	
Final extension	72	420	1
Cooling	4	∞	1

Table 4. 6 PCR profile for the amplification of the *bb0298* gene fragments from *B. afzelii* PKo, *B. garinii* 20047

Parameters / Step	Temperature [°C]	Time [s]	No. of cycles
Initial denaturation	98	30	1
Denaturation	98	10	7
Annealing	65	25	
Extension	72	22	
Denaturation	98	8	30
Annealing	67	18	
Extension	72	22	
Final extension	72	420	1
Cooling	4	∞	1

Table 4. 7 PCR profile for the amplification of the *bb0298* gene fragment from *B. burgdorferi* s.s. B31

Parameters / Step	Temperature [°C]	Time [s]	No. of cycles
Initial denaturation	98	30	1
Denaturation	98	10	7
Annealing	53	25	
Extension	72	22	
Denaturation	98	8	30
Annealing	55	18	
Extension	72	22	
Final extension	72	420	1
Cooling	4	∞	1

Table 4. 8 PCR profile for the amplification of the *bb0323* gene fragments from *B. afzelii* PKo, *B. burgdorferi* s.s. B31*, B. garinii* 20047

Parameters / Step	Temperature [°C]	Time [s]	No. of cycles
Initial denaturation	98	30	1
Denaturation	98	10	7
Annealing	55	25	
Extension	72	36	
Denaturation	98	8	30
Annealing	60	18	
Extension	72	32	
Final extension	72	420	1
Cooling	4	∞	1

Table 4. 9 PCR profile for the amplification of the *bb0689* gene fragments from *B. afzelii* PKo, *B. burgdorferi* s.s. B31, *B. garinii* 20047

Parameters / Step	Temperature [°C]	Time [s]	No. of cycles
Initial denaturation	98	30	1
Denaturation	98	10	7
Annealing	63	25	
Extension	72	20	
Denaturation	98	8	30
Annealing	65	20	
Extension	72	15	
Final extension	72	420	1
Cooling	4	∞	1

4.3.2. Construction of chimeric genes *bmpA-bba64* and *bmpA-bbk32*

4.3.2.1. Amplification of *bmpA*, *bba64* and *bbk32* genes fragments used for the construction of multivalent chimeric proteins

PCR Mix Plus HGC [Materials 3.4] was used to amplify the *bmpA, bba64* and *bbk32* genes fragments. The compositions of the reaction mixture are presented in Table 4.10. In Tables 4.11 and 4.12 the PCR temperature profile for DNA amplification is given.

Table 4. 10 Reaction mixture for the amplification of gene fragments of *B. burgdorferi* s.l. with the use PCR Mix Plus HGC

Reaction components	Volume [µl]
PCR Mix Plus HGC	12.5
Forward primer	1
Reverse primer	1
Template (*B. burgdorferi* s.s. B31 genomic DNA diluted 1:1000 v/v)	1
Water	9.5
Total volume	25

Table 4. 11 PCR profile for the amplification of the *bba64* and *bbk32* genes fragments from *B. burgdorferi* s.s. B31

Parameters / Step	Temperature [°C]	Time [s]	No. of cycles
Initial denaturation	94	300	1
Denaturation	94	30	35
Annealing	55	30	
Extension	72	30	
Final extension	72	420	1
Cooling	4	∞	1

Table 4. 12 PCR profile for the amplification of the *bmpA* genes fragments from *B. burgdorferi* s.s. B31

Parameters / Step	Temperature [°C]	Time [s]	No. of cycles
Initial denaturation	94	300	1
Denaturation	94	30	35
Annealing	54	30	
Extension	72	60	
Final extension	72	420	1
Cooling	4	∞	1

4.3.2.2 Chimeric gene assembly

A single-cycle PCR reaction was used to combine two different DNA fragments into a chimeric genes *bmpA-bba64* and *bmpA-bbk32*. The composition of the reaction mixture and the temperature profile are shown in Tables 4.13 and 4.14.

Table 4. 13 Reaction mixture for assembling chimeric genes

Components	Volume [µl]
Buffer	4
10 mM dNTPs	0,4
PCR fragment 1	1
PCR fragment 2	1
Polymerase (Phusion High-Fidelity)	0.2
Water	13.4
Total volume	20

Table 4. 14 PCR profile for assembling chimeric genes

Parameters / Step	Temperature [°C]	Time [s]	No. of cycles
Denaturation	98	30	1
Annealing	55	40	
Extension	72	60	
Cooling	4	∞	

4.3.2.3 Amplification of chimeric genes

Phusion® High-Fidelity DNA polymerase [Materials 3.4] was used to amplify the DNA fragment obtained by gene assembling. The composition of the PCR mixture and the temperature profile are presented in Tables 4.15 and 4.16.

Table 4. 15 Reaction mixture used to amplify the chimeric genes

Components	Volume [µl]
Buffer	10
10 mM dNTPs	1
Forward primer	2
Reverse primer	2
Polymerase	0.5
Template (obtained chimeric genes)	3
Water	31.5
Total volume	50

Table 4. 16 PCR profile for the amplification of the *bmpA-BBA64* and *bmpA-bbk32* chimeric genes

Parameters / Step	Temperature [°C]	Time [s]	No. of cycles
Initial denaturation	98	30	1
Denaturation	98	8	35
Annealing	55	20	
Extension	72	40	
Final extension	72	420	1
Cooling	4	∞	1

4.4. Isolation of plasmid DNA

Plasmid DNA was isolated by alkaline lysis using A&A Biotechnology silica columns [Materials 3.10.1], proceeding according to the following protocol:

1. 1.5-3 ml of an overnight *E. coli* culture was centrifuged in tubes. The supernatant was removed, the pellet was saved.
2. The pellet was resuspended in 150 µl of L1 buffer [Materials 3.10.1].
3. 150 µl of buffer L2 [Materials 3.10.1] was added, then mixed by inverting the tube several times and incubated for 3 min. at room temperature.
4. 150 µl of L3 buffer [Materials 3.10.1] was added, the content of the tube was mixed by inverting it several times, then centrifuged for 10 min. at 12 000 rpm.
5. The clear supernatant was transferred to a new tube, then 500 µl of solution G was added [Materials 3.10.1].
6. Supernatant has been applied to the column placed in a 2 ml collection tube, then centrifuged for 30 s at 12 000 rpm, the filtrate was removed.
7. 500 µl of 96% ethanol were applied to the column [Materials 3.10.1], then centrifuged for 1 min. at 12 000 rpm.
8. 300 µl of 96% ethanol were applied to the column [Materials 3.10.1], then centrifuged for 2 min. at 12 000 rpm.
9. The column was transferred to a new tube and 60 µl of TE buffer was added [Materials 3.10.1]. The column was incubated for 3 min. at room temperature, then centrifuged for 1 min. at 12 000 rpm.
10. The column was removed and the purified plasmid DNA was stored at -20°C.

4.5. Purification of DNA after an enzymatic reaction

Clean-Up Concentrator (A&A Biotechnology) or Gel-Out Concentrator (A&A Biotechnology) [Materials 3.10.2] kits were used for DNA purification, according to the manufacturer's instructions.

4.6. Restriction digestion of DNA

DNA digestion was performed using a suitable restriction enzyme and a buffer dedicated to it or the Tango buffer [Materials 3.5.]. During digestion, samples were incubated at 37°C for 1 h or 1.5 h. The composition of the reaction mixtures is presented in Tables 4.17 and 4.18.

Table 4. 17 Digestion mixture with the use dedicated buffer

Components	Volume [µl]	Volume [µl]
DNA	10	25
Dedicated buffer	2	5
Enzyme	0.25	0.5
Water	7.75	19.5
Total volume	20	50

.**Table 4. 18** Digestion mixture with the use Tango buffer

Components	Volume [µl]	Volume [µl]
DNA	10	25
Tango buffer	4	10
Enzyme	0.25	0.5
Water	5.75	14.5
Total volume	20	50

4.7. Dephosphorylation of vector

In order to dephosphorylate the vector, 1 µl of alkaline phosphatase [Materials 3.18] was added to the tube immediately after the digestion reaction, then the mixture was incubated for 10 min. at 37ºC.

4.8. Molecular cloning

4.8.1. Ligase T4 cloning

Molecular cloning was performed using T4 DNA ligase [Materials 3.6]. The composition of the reaction mixture is presented in Table 4.19.

Table 4. 19 Ligation mixture

Components	Volume [µl]
Linear vector	2
Insert	8
Buffer	2
10 mM ATP	5
Ligase T4	1
Water	2
Total volume	20

The sample was incubated for 10 min. at 22ºC and then used to transform *E. coli* TOP10F' competent cells.

4.8.2. In-Fusion® HD Cloning

Molecular cloning using the In-Fusion kit was performed according to the protocol described below (Table 4.20). In-Fusion molar ratio calculator (https://www.takarabio.com/learning-centers/cloning/primer-design-and-other-tools/in-fusion-molar-ratio-calculator) was used to determine the correct vector to insert ratio [Methods 4.18].

Table 4. 20 Ligation mixture for molecular cloning using the In-Fusion HD Cloning kit

Components	Volume [µl]
5X In-Fusion Enzyme Premix	2 µl
Linear vector	100ng
Insert	Molar ratio insert to vector 2:1
Total volume	10 µl

1. The reaction mixture was incubated at 50°C for 15 min.
2. Then, 5 µl or 2.5 µl of the reaction mixture was added to 50 µl of Stellar™ competent cells [Materials 3.6] and incubated on ice for 30 min.
3. The tube was then placed in a thermoblock at 42°C for 45 s then placed on ice for 2 min.

4. 500 µl of SOC medium [Materials 3.6] was added to the mixture and the tube was incubated for 1 h at 37°C with shaking.
5. Samples were plated on LBA plates supplemented with appropriate antibiotics.

4.9. Transformation of *E. coli* cells

1. A single colony of the selected *E. coli* strain [Materials 3.2] were inoculated in 20-30 ml of LB medium [Materials 3.3] supplemented with appropriate antibiotics [Materials 3.17].
2. The cells were grown with vigorous shaking for 18 h at 37°C.
3. A starter culture was inoculated at a 1:50 dilution into fresh media supplemented with antibiotics [Materials 3.14].
4. Sample was Incubated at 37°C with shaking until OD_{600}=0.2, then cells were centrifuged at 4°C at 4 000 rpm for 10 min.
5. The supernatant was discarded, the pellet was resuspended with 40-50 ml ice-cold 0.1 M $CaCl_2$ [Materials 3.18] and incubated on ice for 30–60 min.
6. Cells were centrifuged at 4°C at 4 000 rpm for 10 min.
7. The supernatant was discarded, The pellet was resuspended with 1 ml ice-cold 0.1 M $CaCl_2$ [Materials 3.18] and incubated on ice for 30 min.
8. 1-5 µl (10 pg-100 ng) of plasmid or 10 µl ligation mixture was added to 100 µl competent cells and incubated on ice for 30–60 min.
9. A heat shock was then performed, a sample was placed at 42°C for 90 s, then was transferred into ice for 2 min.
10. 1 ml of LB was added to the sample, then was incubated for 1 h at 37°C with shaking.
11. Cells were centrifuged at room temperature at 2 000 rpm for 10 min, then 1 ml of supernatant was removed
12. Pellet was resuspended in the remaining supernatant and plateded on the Petri dish.

4.10. Electrophoretic techniques

4.10.1. Agarose gel electrophoresis

Electrophoresis was carried out in a 1-2% agarose gel with the addition of ethidium bromide at a voltage of 95 V for about 40-60 min. 2-5 µl of a sample with 2 µl

loading dye was added to each well [Materials 3.7]. The gels were analyzed under UV light with a wavelength of 312 nm using the ChemiDoc™ MP apparatus [Materials 3.19].

4.10.2. SDS-PAGE

A 1 ml culture pellet was resuspended in 400 µl TE [Materials 3.15]. 5 µl of loading buffer [Materials 3.8] was added to 10 µl of the sample, then the tube was placed in a thermoblock at 98°C for 10 min. for denaturation. After centrifugation, the samples were ready to be loaded into the wells.

15 µl of the sample was placed in each well. Electrophoresis was carried out in 1xTris-glycine buffer at a voltage of 80 V (stacking gel) and 120 V (separating gel). Then the gels were stained [Materials 3.8] for 1 h and after this time transferred into a decolorizing solution [Materials 3.8] for 3-4 h. The gels were visualized using the ChemiDoc™ MP apparatus.

4.11. Linear epitopes mapping

4.11.1 Epitope mapping procedure

1. Peptide microarrays with printed peptides [Materials 3.13.1] was fixed in a tray.
2. 200 µl of standard buffer [Materials 3.14.3] were applied to the places where the peptides were printed and incubated for 15 min. at room temperature.
3. The standard buffer was carefully removed with a pipette and 200 µl of blocking buffer was added [Materials 3.14.3]. The microarrays were incubated for 30 min. at room temperature on a shaker at 140 rpm.
4. The blocking buffer was removed and the slide was washed with standard buffer 3x1 min. at room temperature on a shaker at 140 rpm.
5. 200 µl of staining buffer [Materials 3.14.3] were applied and incubated for 15 min. at room temperature.
6. The staining buffer has been removed. Then, 200 µl of human sera [Materials 3.14.2] diluted 1:100 in staining buffer [Materials 3.14.3] were added and the peptide microarray was incubated at 4°C overnight with shaking at 140 rpm.
7. Sera were carefully removed by pipetting and the slide was washed with standard buffer [Materials 3.14.3] 3x1 min. at room temperature on a shaker at 140 rpm.
8. 200 µl of the appropriate secondary antibodies [Materials 3.13.3] diluted 1:1 000 in staining buffer were added and the slide was incubated in the dark at room temperature for 45 min. with shaking 140 rpm.

9. Secondary antibodies [Materials 3.14.3] were carefully removed by pipetting and the plate was washed with standard buffer 3x1 min. at room temperature on a shaker at 140 rpm.
10. The slides were carefully removed from the rack and immersed 3 times completely in the immersion buffer [Materials 3.13.3]. The slides were then left to dry.
11. The microarrays were scanned using the GenePix personal 4100a microarray scanner [Materials 3.19]. The median fluorescent signal intensity of each spot was extracted using MAPIX software [Methods 4.18].

4.11.2 Data analysis

For data analysis, the intensity of raw fluorescence signal in each spot corresponded to the median signal intensity, and it was subtracted from the median background intensity, then averaged across duplicate spots (Lin et al.; 2017). The resulting signals were normalized with a Z-Score (Cheadle et al., 2003; Dennis et al.;2021), Z-Score=(intensityP - mean intensityP1…Pn)/SD P1…Pn, where P is any BBK32 or BmpA peptide on the microarray, and P1…Pn represent the aggregate measure of all peptides. Heatmaps of IgG, IgM and mixed antibodies bound to the peptides were visualized using a Z-Score heatmap (http://www.heatmapper.ca/expression/), where peptides that showed Z-scores>2 were considered significantly reactive. Z-ratios from each immunoglobulin isotype were used for comparisons between peptides from positive and negative serum groups and were calculated by taking the difference between the averages of the observed peptide Z-scores and dividing them by the SD of all the peptide Z-score differences. A Z-ratio of ± 1.96 was inferred as significant ($P<0.05$). Analysis was focused on epitopes with Z-ratio>1.96 when comparing the peptide reactivity in the positive serum sample group to the same peptide in the negative serum sample group.

4.12. Biotechnological production of recombinant proteins in *E. coli*

1. Single colony of the selected *E. coli* strain [Materials 3.2] were inoculated in 20-30 ml of LB medium [Materials 3.3] supplemented with appropriate antibiotics [Materials 3.17].
2. The cells were grown with vigorous shaking for 18 h at 37°C.
3. A starter culture was inoculated at a 1:50 dilution into fresh media containing antibiotics.

4. Incubated at 37°C with shaking until OD_{600}=0.4, then 1 M IPTG was added to a concentration of 1 mM [Materials 3.18] to induce gene expression.
5. From just before induction and at hourly intervals, 1 ml of culture was taken for SDS-PAGE analysis.
6. The culture was grown at 20°C, 25°C, 30°C or 37°C for 4-18 h.
7. The cultures were centrifuged at 4 000 rpm for 10 min., the pellet was stored at 20°C until further analysis.

4.13. Purification of monovalent and multivalent recombinant proteins

Gravity flow columns loaded with 5 ml His•Bind®Resin was used for purification of monovalent and multivalent recombinant proteins [Materials 3.11.3].

4.13.1. Resin regeneration

1. Regeneration buffer was loaded (5 bed volumes) [Materials 3.11.3].
2. The column was washed with sterile distilled water (10 bed volumes).
3. $NiCl_2$ solution was deposited (5 bed volumes) [Materials 3.11.3].
4. The column was washed with the appropriate binding buffer A1-G1 or A1M-G1M (when protein was insoluble) (5 bed volumes) [Materials 3.11.2].

4.13.2. Protein purification

1. A pellet of monovalent/multivalent recombinant protein-producing *E. coli* from 100-150 ml cultures was resuspended in 30-35 ml of the appropriate binding buffer: A1-G1 or A1M-G1M (when protein was insoluble) [Materials 3.11.2].
2. Performed cell disintegration by sonication.
3. The obtained lysates were centrifuged at 9 000 rpm for 30 min., subsequently the supernatant was loaded to the column.
4. The column was washed with appropriate binding buffer: A1-G1 or A1M-G1M (when protein was insoluble) (approx. 5 bed volumes) [Materials 3.11.2].
5. The column was washed with appropriate washing buffer: A2-G2 or A2M-G2M (when protein was insoluble) (approx. 20 bed volumes) [Materials 3.11.2].
6. The column was washed with appropriate washing buffer: A3-G3 or A3M-G3M (when protein was insoluble) (approx. 1 bed volumes) [Materials 3.11.2].

7. Monovalent/multivalent recombinant proteins were eluted with 4-6 ml aliquots of the appropriate elution buffer: A4-G4 or A4M-G4M (when protein was insoluble) [Materials 3.11.2].

4.14. Western blot

4.14.1. His-tag domain detection

1. SDS-PAGE of samples containing *E. coli* lysates or purified monovalent and multivalent recombinant protein proteins was performed [Methods 4.10.2].
2. Semi-dry electrotransfer was used to transfer the proteins from the gel to the nitrocellulose membrane. The blotting sandwich was prepared in the following order (from anodic pad to cathodic): Whatman paper soaked in transfer solution; membrane soaked in transfer solution; polyacrylamide gel; Whatman paper soaked in transfer solution [Materials 3.13]. Electrotransfer was performed at 0.8 mA per cm2 for 1 h.
3. After electrotransfer, the membrane was washed 1x5 min. in TBST buffer [Materials 3.13].
4. The membrane was placed in blocking buffer [Materials 3.13] and incubated for 1 h with shaking at room temperature.
5. After blocking the membrane was washed 3x5 min. in TBST [Materials 3.13].
6. The membrane was then incubated with anti-Hist-tag antibodies [Materials 3.13] at a dilution of 1:7 500 in blocking buffer [Materials 3.13] for 1 h with shaking at room temperature.
7. The membrane was washed 3x5 min. in TBST [Materials 3.13].
8. The membrane was then placed in the detection buffer [Materials 3.13] until brown bands appeared, the color reaction was stopped by the addition of sterile water.

4.14.2. Determination of reactivity of monovalent and multivalent recombinant proteins with specific antibodies

4.14.2.1. Procedure using a standard polyacrylamide gel

1. SDS-PAGE was carried out according to procedure described in Methods 4.10.2. Per one well 3.5 or 7 µg of target protein was added.

2. Semi-dry electrotransfer was used to transfer the proteins from the gel to the nitrocellulose membrane. The electrotransfer was carried out in the same way as described in point 4.14.1.
3. After electrotransfer, the membrane was washed 1x5 min. in TBST buffer [Materials 3.13].
4. Then, the membrane was placed in blocking buffer [Materials 3.13] and incubated overnight at 4°C.
5. After blocking the membrane was washed 3x5 min. in TBST [Materials 3.13].
6. The membrane was incubated with the sera [Material 3.13] at a 1:200 dilution in blocking buffer [Material 3.13] for 1-1.5 h, at room temperature with shaking.
7. The membrane was washed 3x10 min. in TBST [Materials 3.13].
8. The membrane was incubated with goat anti-human IgG or IgM antibodies [Materials 3.13] at a dilution of 1:100 000-1:50 000 in blocking buffer.
9. The membrane was washed 3x10 min. in TBST [Materials 3.13].
10. The membrane was then incubated for 5 min. with a chemiluminescent substrate [Materials 3.13]. After this time, the results were read using the ChemiDoc™ MP (Bio-Rad) gel imaging device [Materials 3.19].

4.14.2.2. Procedure using a polyacrylamide gel with modified wells

1. SDS-PAGE was carried out in gels prepared with modified combs so that they had one large well. 40 µg of monovalent or multivalent recombinant protein was added to each enlarged well, the rest of the procedure was unchanged [Methods 4.10.2].
2. Semi-dry electrotransfer was used to transfer the proteins from the gel to the nitrocellulose membrane. The electrotransfer was carried out in the same way as described in point 4.14.1.
3. After electrotransfer, the membrane was washed 1x5 min. in TBST buffer [Materials 3.13].
4. A transfer check was performed by staining the membrane with Ponceau S solution [Materials 3.13] and marked exactly where the separated proteins were.
5. Then, the membrane was placed in blocking buffer [Materials 3.13] and incubated overnight at 4°C.
6. After blocking the membrane was washed 3x5 min. in TBST [Materials 3.13].

7. The membrane was cut into 0.5 cm strips.
8. The strips were incubated with the sera [Material 3.13] at a 1:200 dilution in blocking buffer [Material 3.13] for 1-1.5 h, at room temperature with shaking.
9. The strips were washed 3x10 min. in TBST [Materials 3.13].
10. The strips were incubated with anti-human IgG or IgM antibodies at a dilution of 1:100 000 - 1:75 000 in blocking buffer.
11. The strips were washed 3x10 min. in TBST [Materials 3.13].
12. The strips were then incubated for 5 min. with a chemiluminescent substrate [Materials 3.13]. After this time, the results were read using the ChemiDoc™ MP (Bio-Rad) gel imaging device [Materials 3.19].

4.15. Determination of the toxicity of monovalent and multivalent recombinant proteins for *E. coli* cells

While determining the potential toxicity of the produced monovalent and multivalent recombinant proteins, the conditions of expression of heterologous genes were simulated. An overnight culture of the appropriate *E. coli* strain was re-growth in fresh LB or TB medium to OD_{600}=0.04, followed by cultivation under conditions adapted for optimal production of monovalent/multivalent recombinant proteins. Every hour, a sample of the cultures was taken, and its OD_{600} value was measured. After 3 h of experiment induction by adding IPTG [Materials 3.18] occurred. *E. coli* cells transformed with the pUET1 [Materials 3.1] were used as control. The ANOVA test was used to determine the existence of a statistically significant difference in cell growth.

4.16. Determination of protein concentration

Protein concentrations were determined by the Bradford method using BSA as a protein standard. In order to make a standard curve, 18 µl of BSA standard [Materials 3.16] or water (blank) was added to 900 µl of Bradford reagent [Materials 3.16]. However, when determining the concentration of monovalent/multivalent recombinant proteins, 18 µl of the protein sample or buffer in which the protein was suspended (blank) was added to 900 µl of Bradford reagent [Materials 3.11.2]. 250 µl of appropriate mixtures were placed in the microplate wells, and then the absorbance was measured at the wavelength of 595 nm. The protein concentration was determined by the equation obtained from the standard curve.

4.17. Evaluation of target protein content in *E. coli* whole cell lysates and densitometric purity of protein preparations

SDS-PAGE was performed to assess the target protein content in *E. coli* whole cell lysates and the densitometric purity of the protein preparation [Methods 4.10.2]. Then, the obtained polyacrylamide gel was analyzed using the ChemiDoc™ MP device (Bio-Rad) and ImageLab software [Materials 3.19].

4.18. Dialysis

4.18.1. Direct dialysis to a storage buffer

1. 500 µl of the protein preparation was placed into the dialysis membrane, closed at both ends [Materials 3.18].
2. Samples prepared in this way were placed in 800 ml of a new buffer (PBS [Materials 3.11.2.5] or a storage buffer [Materials 3.11.2.6]) and incubated at 4°C overnight.
3. The next day, the samples were transferred to fresh buffer, this process was repeated twice.
4. After three days of dialysis, samples were transferred to new tubes and stored at -20°C until the next use.

4.18.2. Gradual dialysis to a storage buffer

1. 500 µl of the protein preparation was placed into the dialysis membrane, closed at both ends [Materials 3.18].
2. Samples prepared in this way were placed in 800 ml of a new buffer (PBS [Materials 3.11.2.5] or storage buffer [Materials 3.11.2.6]) with addition 3 M urea and incubated at 4°C overnight.
3. The next day, the samples were transferred to fresh buffer with addition 2 M urea and incubated at 4°C overnight.
4. The next day, the samples were transferred to fresh buffer with addition 1 M urea and incubated at 4°C overnight.
5. The next day, the samples were transferred to fresh buffer without denaturing agent and incubated at 4°C overnight.
6. After three days of dialysis, samples were transferred to new tubes and stored at -20°C until the next use.

4.19. ELISA

1. Microtitre plates were coated with the different purified monovalent or multivalent recombinant proteins or purified *E. coli* lysates (1 µg/well) in 0.2 M carbonate buffer (pH 9.6) [Materials 3.15].
2. Plates were incubated at 4°C overnight.
3. The wells were washed with 3x300 µl washing buffer [Materials 3.15].
4. Plates were blocked for 1 h at 37°C with blocking buffer [Materials 3.15].
5. Washing was performed in the same way as in step 3.
6. 100 µl of human serum diluted 1:100 in blocking buffer [Materials 3.15] was added to the wells and the plates were incubated at 37°C for 1 h.
7. Washing was performed in the same way as in step 3.
8. 100 µl of secondary anti-human IgG or IgM antibodies labeled with horseradish peroxidase [Materials 3.15] diluted 1:8000-1:64000 in blocking buffer [Materials 3.15] were added to the wells and incubated for 1 h at 37°C.
9. Washing was performed in the same way as in step 3.
10. 100 µl of OPD solution [Materials 3.15] was added to the wells, then incubated in the dark for 45 min. at 37°C.
11. The reaction was stopped by the addition of 100 µl of 2 M H_2SO_4 [Materials 3.15].
12. Absorbance at 492 nm was measured using a Multiskan FC plate reader [Materials 3.19].

4.20. Statistical analysis

For all data manipulation, GraphPad Prism software was used (GraphPad Prism, Version 9, San Diego, CA, USA). The presence of a statistically significant difference in the absorbance obtained for the negative and positive sera was determined with the use of Student's t-test. Statistical significance was considered when the p-value was below 0.05. Receiver operating characteristic (ROC) was performed to obtain area under the curve (AUC), optimal cut-off and the sensitivity and specificity of the assays based on monovalent and multivalent recombinant proteins. The optimal cut-off was determined as the absorbance of the point on the ROC curve closest to (0,1) corner (Perkins and Schisterman, 2006).

4.21. Software

- BepiPred-2.0 (tools.iedb.org/bcell)
- ClustalX2 (www.clustal.org/clustal2)
- DiscoTope (http://tools.iedb.org/discotope)
- ElliPro (http://tools.iedb.org/ellipro)
- Emini surface accessibility scale (tools.iedb.org/bcell)
- Epiopia (epitopia.tau.ac.il)
- GeneDoc (NRBSC; nrbsc.org/gfx/genedoc)
- Genome compiler (www.genomecompiler.com)
- GraphPad Prism version 9.0.0 (GraphPad Software; www.graphpad.com)
- Heatmapper! (Wishart Research Group; heatmapper.ca)
- Image Lab (Bio-Rad Laboratories)
- In fusion molar ratio calculator (https://www.takarabio.com/learning-centers/cloning/primer-design-and-other-tools/in-fusion-molar-ratio-calculator)
- MAPIX software (Molecular Devices)
- Parker Hydrophilicity Prediction (tools.iedb.org/bcell)
- PepSlide® Analyzer 2.0 (SICASYS Software GmbH)
- PlasmaDNA (research.med.helsinki.fi/plasmadna)
- Protein BLAST (www.ncbi.nlm.nih.gov)
- SnapGene® software (Dotmatics; snapgene.com).
- VectorNTI (www.thermofisher.com/pl/en/home/life-science/cloning/vector-nti-software.html)

5. RESULTS

5.1. Amino acid sequence analysis of *B. burgdorferi* s.l. antigens with potential diagnostic utility

When selecting antigens for initial bioinformatic analysis, the following features were desirable: literature reports on their potential immunogenicity (protein microarrays, two-dimensional electrophoresis), increase in production during tick feeding or shortly after transmission in a mammalian host, and cell surface display. Based on these premises, 5 antigens were selected: BB0108, BB0126, BB0298, BB0323, BB0698. Their brief characteristics and reasons for their selection are presented in Table 5.1.

Table 5. 1 Characteristics of proteins selected for bioinformatics analysis

Protein	Characteristic	References
BB0108	• Production increases during tick-mammal transmission • Localized in cell-envelope • Specific antibodies found in both human and murine sera	(Barbour et al., 2008; Xu et al., 2008)
BB0126	• Production increases during tick-mammal transmission • Hypothetical outer membrane protein	(Brooks et al., 2006; Ojaimi et al., 2003)
BB0298	• Production increases in mammalian host • Localized in cell-envelope	(Brooks et al., 2003; Caimano et al., 2015)
BB0323	• Essential for the establishment of *B. burgdorferi* s.l. infection in ticks and mammalian hosts • Production increases during tick-mammal transmission • Presented on the cell surface	(Kariu et al., 2015; Zhang et al., 2009)
BB0689	• Lipoproteins located on the outer membrane surface • Production increases during tick feeding • Immunogenic – specific antibodies (bactericidal) are found in tick-infected baboons	(Brangulis et al., 2015a; Brooks et al., 2006)

For all of them, the degree of sequence conservation between five pathogenic genospecies of *B. burgdorferi* s.l., was determined and the occurrence of potential B-cell epitopes was predicted. There are many tools available for the prediction of linear and discontinuous B-cell epitopes (Graves et al., 2020), and several studies have proven *in silico* epitope mapping to be consistent with experimental results (Maksimov et al., 2012; Nair et al., 2011). However, there is no consensus as to which one is the best (Graves et al., 2020). Therefore, three different algorithms were used in this study to obtain more accurate epitope predictions, those identified by at least two methods were considered potential B-cell epitopes. This way, conserved linear B-cell epitopes were predicted for

all selected antigens and conformational B-cell epitopes for 2 antigens (BB0298, BB0689) for which 3D structures were available.

5.1.1. Degree of conservation of amino acid sequences

SignalP 5.0 software and the UniProt database were used to predict the presence of signal or transmembrane sequences in 5 proteins of unknown reactivity with anti-*B. burgdorferi* s.l. antibodies [Methods 4.1.1]. Only in BB0126 no such fragments were detected; therefore, the full sequences of this protein were used in further steps. Multiple sequence alignment of 13 amino acid sequences of each protein allowed for the determination of the degree of conservation of these potentially immunogenic proteins among the pathogenic to humans *B. burgdorferi* s.l. genospecies (Table 5.2; Figures 5.1-5.5). All proteins showed a significant degree of identity. The least conserved protein was BB0689 with a sequence identity of 77%. Two of the tested proteins (BB0108, BB0298) were highly conserved, and their degree of identity was over 90%.

BLASTp showed homology between the studied proteins and those found in RF *Borrelia*. Overall, the degree of amino acid sequence identity ranged from 51% to 78% (Table 5.2). No significant identity was found with proteins of other organisms including *T. pallidum, E. coli, A. phagocytophilum, Y. enterocolitica*, *Y. pseudotuberculosis*, cytomegalovirs, Epstein-Barr virus, influenza virus and humans [Methods 4.1.1].

Table 5. 2 Analysis of the amino acid sequence of *B. burgdorferi* s.l. proteins to estimate their diagnostic value

Protein name	Conservation among *Bb*sl (% aa identity)	Signal peptide/ transmembrane domain	Conservation among other organisms (% aa identity)
BB0108	92%	1-19	• *B. hermsii* – 77-78% • *B. miyamotoi* – 73% • *B. hispanica* – 74-75%
BB0126	83%	-	• *B. hermsii* – 54% • *B. miyamotoi* – 52-54% • *B. hispanica* – 53-52%
BB0298	92%	1-15	• *B. hermsii* – 72-73% • *B. miyamotoi* – 60-70% • *B. hispanica* – 69-70%
BB0323	85%	1-20	• *B. hermsii* – 66-68% • *B. miyamotoi* – 66-67% • *B. hispanica* – 68%
BB0689	77%	1-15	• *B. hermsii* – 57-58% • *B. miyamotoi* – 51-54% • *B. hispanica* – 57-58%

*Bb*sl – *Borrelia burgdorferi* sensu lato

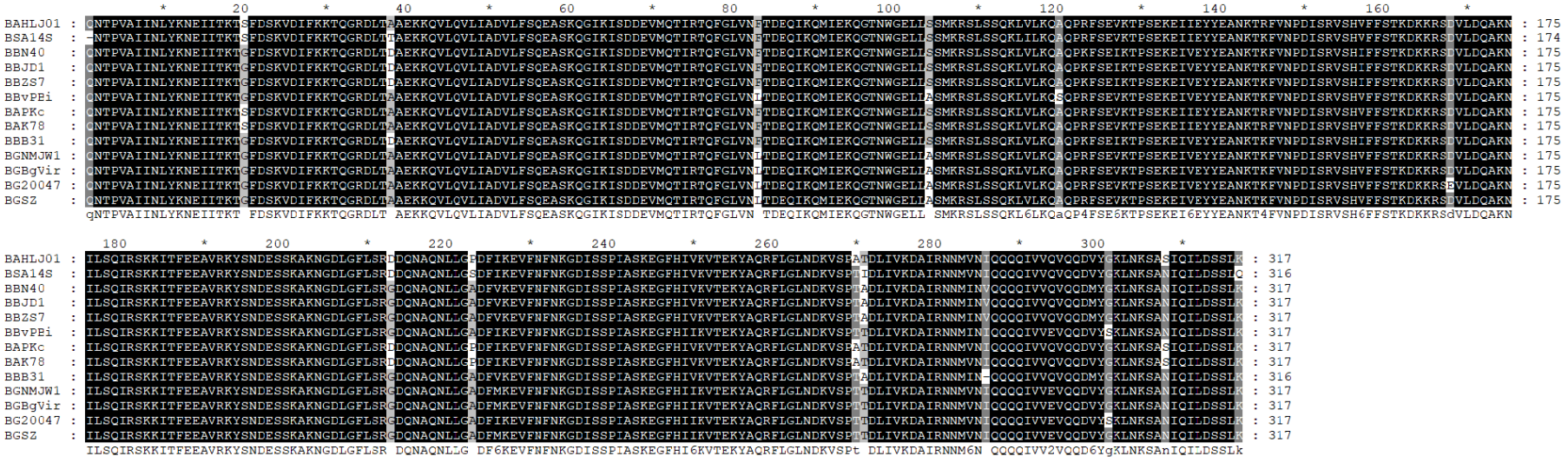

Figure 5. 1 Multiple amino acid sequence alignment of the BB0108 antigen of *B. burgdorferi* s.l. deposited in NCBI.

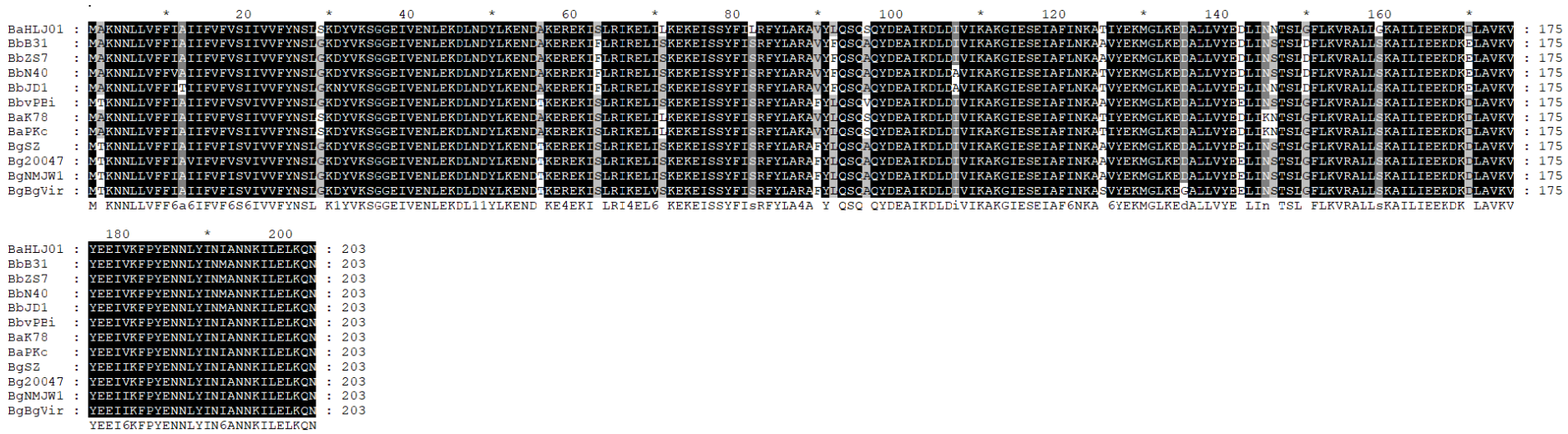

Figure 5. 2 Multiple amino acid sequence alignment of the BB0126 antigen of *B. burgdorferi* s.l. deposited in NCBI.

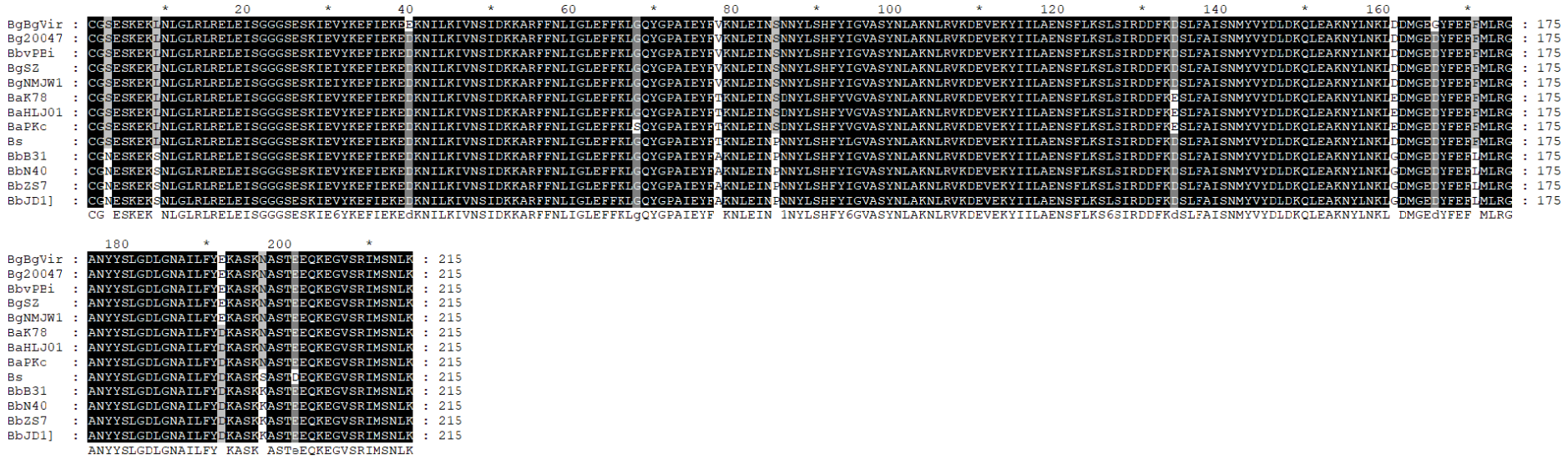

Figure 5. 3 Multiple amino acid sequence alignment of the BB0298 antigen of *B. burgdorferi* s.l. deposited in NCBI.

Figure 5. 4 Multiple amino acid sequence alignment of the BB0323 antigen of *B. burgdorferi* s.l. deposited in NCBI.

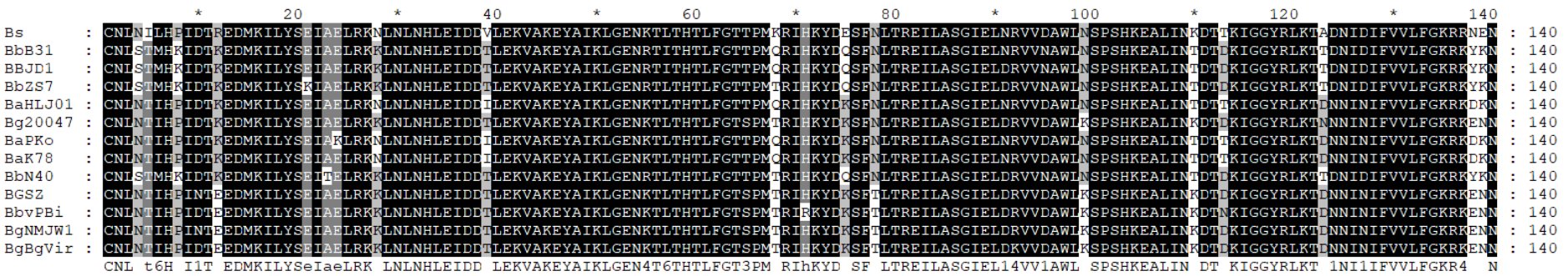

Figure 5. 5 Multiple amino acid sequence alignment of the BB0689 protein of *B. burgdorferi* s.l. deposited in NCBI.

5.1.2. Continuous B-cell epitope prediction

Based on the properties of the mature protein amino acid sequences, 19 highly conserved immunodominant fragments (IF) containing potential B-cell epitopes from 5 *B. burgdorferi* s.l. antigens were predicted (Table 5.3; Figures 5.8-5.12) [Methods 4.1.2]. For each antigen, charts showing the distribution of linear epitopes in their amino acid sequence were obtained, an example chart for BB0108 from *B. burgdorferi* s.s generated by the three bioinformatics tools used is shown in Figure 5.6.

The largest number of conserved immunodominant fragments was predicted for the BB0108 antigen. There were as many as 8 of them, 7 of which showed at least 90% identity among all tested *B. burgdorferi* s.l. sequences. The lowest number of linear epitopes was predicted for proteins BB0298s and BB0689s. There were two sequences for each of the antigens and the degree of identity was not more than 91%. 11 of the 19 identified potential B-cell epitopes were predicted by all three methods (Table 5.3).

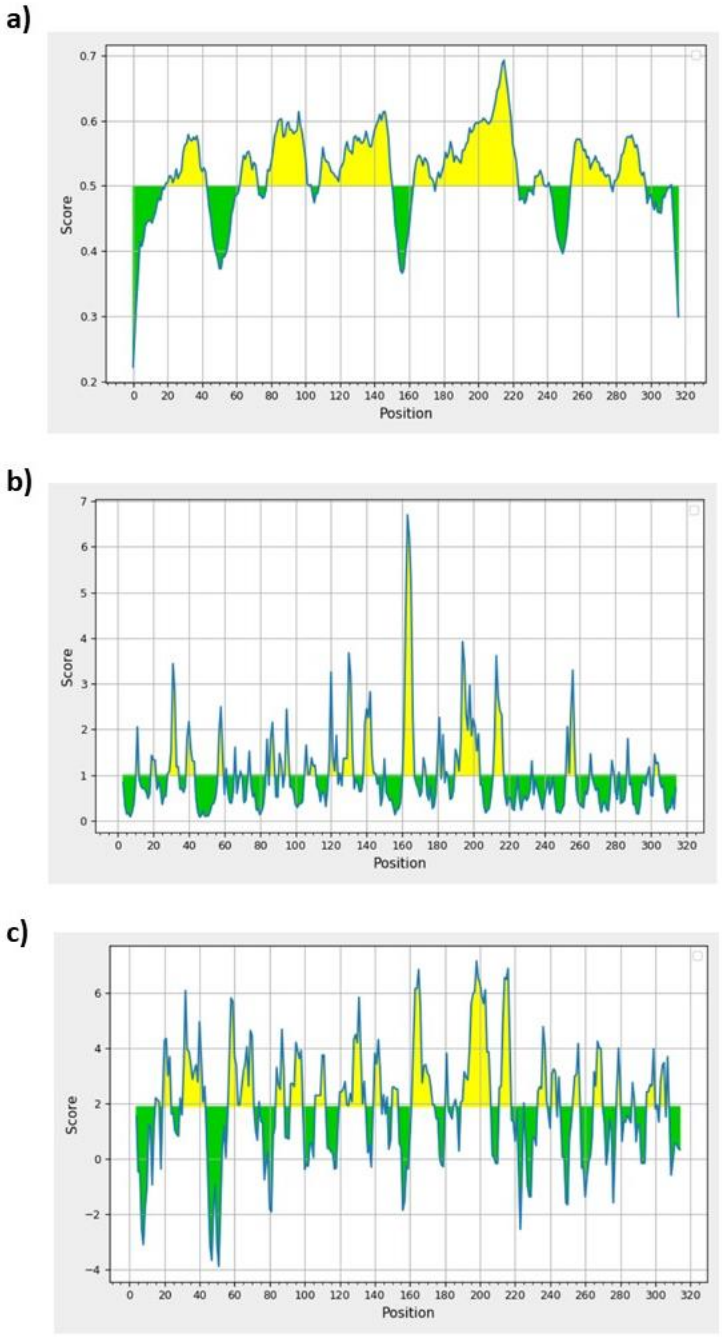

Figure 5. 6 Distribution of linear epitopes in BB0108 from *B. burgdorferi* s.s.: a) BepiPred-2.0; b) Emini Surface Accessibility Scale; c) Parker Hydrophilicity Prediction.

Table 5. 3 Predicted linear B-cell epitopes (non-conserved aa residues are marked in red, overlapping with conformational epitopes are shown in bold)

Protein name	Sequence of immundominant fragment	Conservation (% aa identity)	Prediction tools		
			BepiPred	Parker	Emini
BB0108	^{45}DIFKKTQGRDLTDAEKKQV^{63}	95%	✓	✓	✓
	^{74}SQEASKQGI^{82}	100%	x	✓	✓
	^{102}FTDEQIKQMIEKQGTNWGE^{120}	100%	✓	x	✓
	^{129}LSSQKLVLKQAQPKFSEIKTPSE KEIVEYYEANKTKFVNP^{168}	90%	✓	✓	✓
	^{177}FFSTKDKKRSDVLD^{190}	93%	✓	✓	✓
	^{196}SQIRSKKITFEEAVRKYSNDESS KAKNGDLGFLSRGDQNAQN^{238}	98%	✓	✓	✓
	^{251}FNKGDISSP^{259}	100%	✓	✓	x
	^{302}MINQQQQIVVQVQQDMYGKLNK SANIQIL^{330}	86%	✓	x	✓
BB0126	^{28}LGKDYVKSGGEIVE^{41}	86%	✓	x	✓
	^{93}QSQAQYDEAIKD^{104}	92%	✓	✓	✓
	^{163}LIEEKDKELAVKVYEEIIKFPYE^{185}	91%	✓	x	✓
BB0298	^{16}CGNESKEKSNLGLRLREL^{33}	89%	✓	✓	✓
	^{209}**ASKKASTEEQKEGVSR**^{224}	88%	✓	✓	✓
BB0323	^{116}NYLKENIEKYLNDAEANE^{133}	100%	✓	✓	✓
	^{276}FKTLELIERSRTLWEKGVEAK^{296}	90%	✓	✓	✓
	^{341}KLYNDPYLW^{349}	100%	✓	x	✓
	^{357}RQKIQNPDLIHSN^{369}	100%	✓	x	✓
BB0689	^{114}**SPSHKEALINTDTDKIGGYRLK T**^{137}	91%	✓	✓	✓
	^{143}IFVVLFGKRK^{152}	90%	✓	✓	✓

IF – immunodominant fragment

5.1.3. Conformational B-cell epitope prediction

Potential conserved conformational epitopes were identified for both analyzed proteins [Methods 4.1.3]. For BB0298 there were 3 such sequences, for BB0689 only one potentially conformational antigen determinant was identified (Table 5.4). All potential discontinuous epitopes were predicted by the three tools used. Figure 5.7 shows the distribution of epitopes on the surface of BB0298.

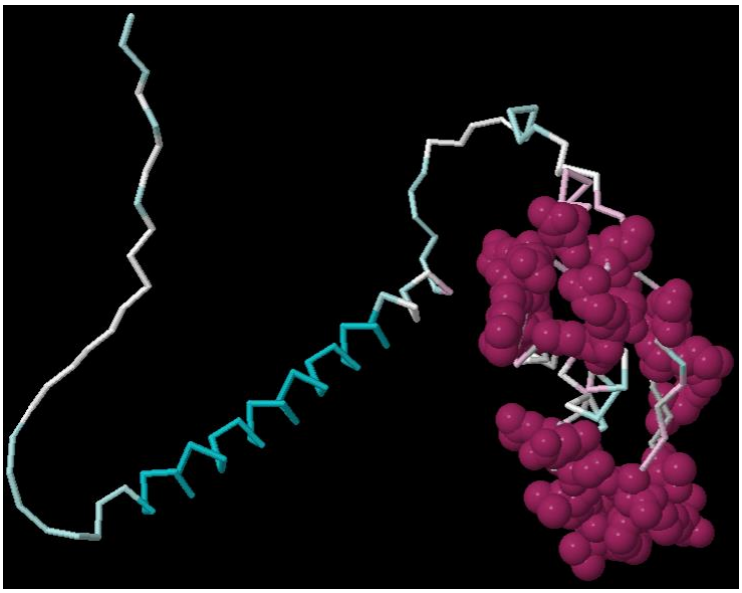

Figure 5. 7 Epitope distribution (red spheres) on the surface of BB0298 from *B. burgdorferi* s.s. B31 generated by the Epitopia software.

Table 5. 4 Predicted conformational B-cell epitopes (non-conserved aa residues are marked in red, overlapping with linear epitopes are shown in bold)

Protein name	Epitope sequence	Conservation (% aa identity)	Prediction tools		
			DiscoTope	ElliPro	Epitopia
BB0298	**A:C16, A:G17, A:N18, A:E19, A:S20, A:K21, A:E22, A:K23, A:N25, A:G27, A:L28, A:R29, A:L30, A:R31, A:E32, A:L33, A:E34, A:I35, A:S36, A:G37, A:G38, A:G39, A:S40, A:E41, A:S42, A:K43, A:I44, A:E45, A:V46, A:Y47, A:K48, A:E49**	94%	✓	✓	✓
	A:N119, A:L120, A:V122, A:K123, A:D124, A:E125, A:V126, A:E127, A:K128, A:Y129, A:I130	100%	✓	✓	✓
	A:L196, A:G197, A:D198, A:L199, A:G200, A:N201, A:I203, A:L204, A:D207, A:K208, A:A209, A:S210, A:K211, A:K212, A:A213, A:S214, A:T215, A:E216, A:E217, A:Q218, A:K219, A:E220, A:V222, A:S223, A:M226, A:S227, A:L229, A:K230	89%	✓	✓	✓
BB0689	A:T73, A:T75, A:L76, A:F77, A:G78, A:T79, A:Q83	86%	✓	✓	✓

5.1.4. Amino acid sequence analysis – summary

In total, 21 antigenic determinants were predicted in the amino acid sequence of the antigens, including both linear and conformational. Analysis of discontinuous epitopes was not performed for all antigens due to the unavailability of their 3D structures. Figures 5.8-5.12 show

the linear and conformational epitopes distribution in the amino acid sequences of the analyzed antigens.

```
  1-60 MKSFLFWVILGTVGISSFAQNTPVAIINLYKNEIITKTGFDSKVDIFKKTQGRDLTDAEK
 61-120 KQVLQVLIADVLFSQEASKQGIKISDDEVMQTIRTQFGLVNFTDEQIKQMIEKQGTNWGE
121-180 LLSSMKRSLSSQKLVLKQAQPKFSEIKTPSEKEIVEYYEANKTKFVNPDISRVSHIFFST
181-240 KDKKRSDVLDQAKNILSQIRSKKITFEEAVRKYSNDESSKAKNGDLGFLSRGDQNAQNLL
241-300 GADFVKEVFNFNKGDISSPIASKEGFHIVKVTEKYAQRFLGLNDKVSPTADLIVKDAIRN
301-336 NMINQQQQIVVQVQQDMYGKLNKSANIQILDSSLK
```

Figure 5. 8 Predicted B-cell epitopes for the BB0108 *B. burgdorferi* s.s. B31 antigen. Linear epitopes are in bold, non-conserved amino acids are marked in red, signal sequence is marked in gray.

```
  1-60 MAKNNLLVFFIAIIFVFVSIIVVFYNSLGKDYVKSGGEIVENLEKDLNDYLKENDAKERE
 61-120 KIFLRIRELISKEKEISSYFISRFYLARAVYFQSQAQYDEAIKDLDIVIKAKGIESEIAFL
121-180 NKAAVYEKMGLKEDALLVYEDLINSTSLDFLKVRALLSKAILIEEKDKELAVKVYEEIVKF
180-203 PYENNLYINMANNKILELKQN
```

Figure 5. 9 Predicted B-cell epitopes for the BB0126 *B. burgdorferi* s.s. B31 antigen. Linear epitopes are in bold, non-conserved amino acids are marked in red.

```
  1-60 MKILWLIILVNLFLSCGNESKEKSNLGLRLRELEISGGGSESKIEVYKEFIEKEDKNILK
 61-120 IVNSIDKKARFFNLIGLEFFKLGQYGPAIEYFAKNLEINPNNYLSHFYIGVASYNLAKNL
121-180 RVKDEVEKYIILAENSFLKSLSIRDDFKDSLFAISNMYVYDLDKQLEAKNYLNKLGDMGE
181-230 DYFEFLMLRGANYYSLGDLGNAILFYDKASKKASTEEQKEGVSRIMSNLK
```

Figure 5. 10 Predicted B-cell epitopes for the BB0298 *B. burgdorferi* s.s. B31 antigen. Linear epitopes are in bold, conformational epitopes are highlighted in color, non-conserved amino acids are marked in red, signal sequence is marked in gray.

```
  1-60 MNIKNKLISLLIVVAISFIACKTPPESRESKNAKIAQPDNKNFQLRDIKDIKNELIRERG
 61-120 HLFYSKEFNEAERLEEAMKQSFSKKKAIEGNEIALKVLERYKTIIRETREKKEKTNYLKE
121-180 NIEKYLNDAEANEAYIWIPLEIDEVNNLYFEATRKYKNYDLDNALDMYSKAFNRAQQAAK
181-240 NAKEAKALKETDERMYKQLKALEAASNLPIYSNNKLIKPSPWNGRAFIKERNSHLNLNKD
241-300 TYLLGEAEISIPIVLAYEEKVEIAKNSKPQEQFKTLELIERSRTLWEKGVEAKNVKNFRL
301-360 ANELFLESARYLEAYQSNASSELYVIKIGNTLWGISKKLYNDPYLWPKIWFANRQKIQNP
361-373 DLIHSNWKIIIPA
```

Figure 5. 11 Predicted B-cell epitopes for the BB0323 *B. burgdorferi* s.s. B31 antigen. Linear epitopes are in bold, non-conserved amino acids are marked in red, signal sequence is marked in gray.

```
  1-60 MKKLIIIFTLFLSQACNLSTMHKIDTKEDMKILYSEIAELRKKLNLNHLEIDDTLEKVAK
 61-120 EYAIKLGENRTITHTLFGTTPMQRIHKYDQSFNLTREILASGIELNRVVNAWLNSPSHKE
121-155 ALINTDTDKIGGYRLKTTDNIDIFVVLFGKRKYKN
```

Figure 5. 12 Predicted B-cell epitopes for the BB0689 *B. burgdorferi* s.s. B31 antigen. Linear epitopes are in bold, conformational epitopes are highlighted in color, non-conserved amino acids are marked in red, signal sequence is marked in gray.

5.2. Design of multivalent *B. burgdorferi* s.s. chimeric proteins

5.2.1. Multivalent chimeric protein design based on bioinformatics analysis

For the construction of multivalent chimeric proteins, antigens BmpA, BBK32, and BBA64 were selected, which were confirmed to induce the production of specific antibodies (Brandt et al., 2014; Li et al., 2006; Roessler et al., 1997b). It was decided to use the sequence of *B. burgdorferi* s.s. due to the fact that research conducted in Poland suggests that this genospecies may be dominant (Cisak et al., 2006; Strzelczyk et al., 2015).

In order to select fragments for the construction of chimeric proteins, a bioinformatic analysis of BmpA, BBK32, and BBA64 amino acid sequences was performed, which allowed the identification of conserved fragments and potential linear B-cell epitopes [Methods 4.1.1-4.1.2].

A signal peptide was identified in the sequences of the three antigens tested (Table 5.5) and it was removed for further analysis. BmpA was characterized by the highest degree of sequence conservation at 77%. The lowest identity was shown by BBA64 reaching 51%.

All of these antigens exhibit a sequence identity of 30% or more with at least one member of the relapsing fever *Borrelia*. Nonetheless, no significant identity with proteins from other organisms has been detected.

Table 5. 5 Analysis of the amino acid sequence of *B. burgdorferi* s.l. antigens to design multivalent chimeric proteins

Protein name	Conservation among *Bb*sl (% aa identity)	Signal peptide	Conservation among other organisms (% aa identity)
BmpA	77%	1-17	• *B. hermsii* – 38-60% • *B. miyamotoi* – 51-60% • *B. hispanica* – 38-58%
BBA64	51%	1-22	• *B. hermsii* – 24-35%
BBK32	61%	1-19	• *B. hispanica* – 26-51%

*Bb*sl – *Borrelia burgdorferi* sensu lato

Each of the analyzed proteins contained at least 5 immunodominant fragments with potential B-cell linear epitopes (Table 5.6, Figure 5.13-5.15).

Table 5. 6 Predicted linear B-cell epitopes (non-conserved aa residues are marked in red)

Protein name	Sequence of immundominant fragment	Conservation (%aa identity)	Prediction Tools		
			BepiPred	Parker	Emini
BmpA	^{65}LKESSSNSY^{73}	89%	✓	✓	✓
	^{177}KYANKDIKISTQ^{188}	75%	✓	✓	✓
	^{272}HLKTNTFEGGKL^{283}	67%			
	^{290}GVVGFVRNPKMISFELEKEIDNLSSKIIN^{319}	76%	✓	✓	✓
	^{324}VPSNKESYEKFL^{335}	83%	✓	X	✓
BBK32	^{25}RYEMKEESPGLFDKGNSILETSEESIKKPMNKKGKGKIARKKGKSKVSRKEPYIHSLKRDSANKSNFLQKN^{95}	44%	✓	✓	X
	^{110}EQSETRKEKIQKQQDEY^{126}	71%	X	✓	✓
	^{240}KLTQMYSTRLDNFAKAKAKEEAAKFTKEDLEKN^{272}	82%	✓	✓	X
	^{288}NFVYINDTHAKRKLENIEAEIKTL^{312}	50%	✓	✓	✓
	^{322}LYEAYKAIVTSILLMRDSLK^{341}	80%	✓	✓	X
	^{343}VQGIIDKNGVWY^{354}	42%	✓	✓	X
BBA64	^{28}KDSNESKKHKKEKRKG^{43}	38%	✓	✓	✓
	^{71}KASKQKNNP^{79}	33%	✓	✓	✓
	^{118}SRGEPN^{123}	50%	X	✓	✓
	^{148}SHEYTEERRM^{157}	50%	X	✓	✓
	^{214}VKDKLQQLNKPNLETLY^{228}	65%	✓	✓	X
	^{234}EKLTSLKEKWLKDTDDLIDEYNTNPDLQTDVSKL^{366}	47%	✓	✓	X
	^{270}TLRSKNSRAQFANI^{283}	29%	✓	✓	✓
	^{290}LVNTTTNIL^{298}	77%	✓	✓	✓

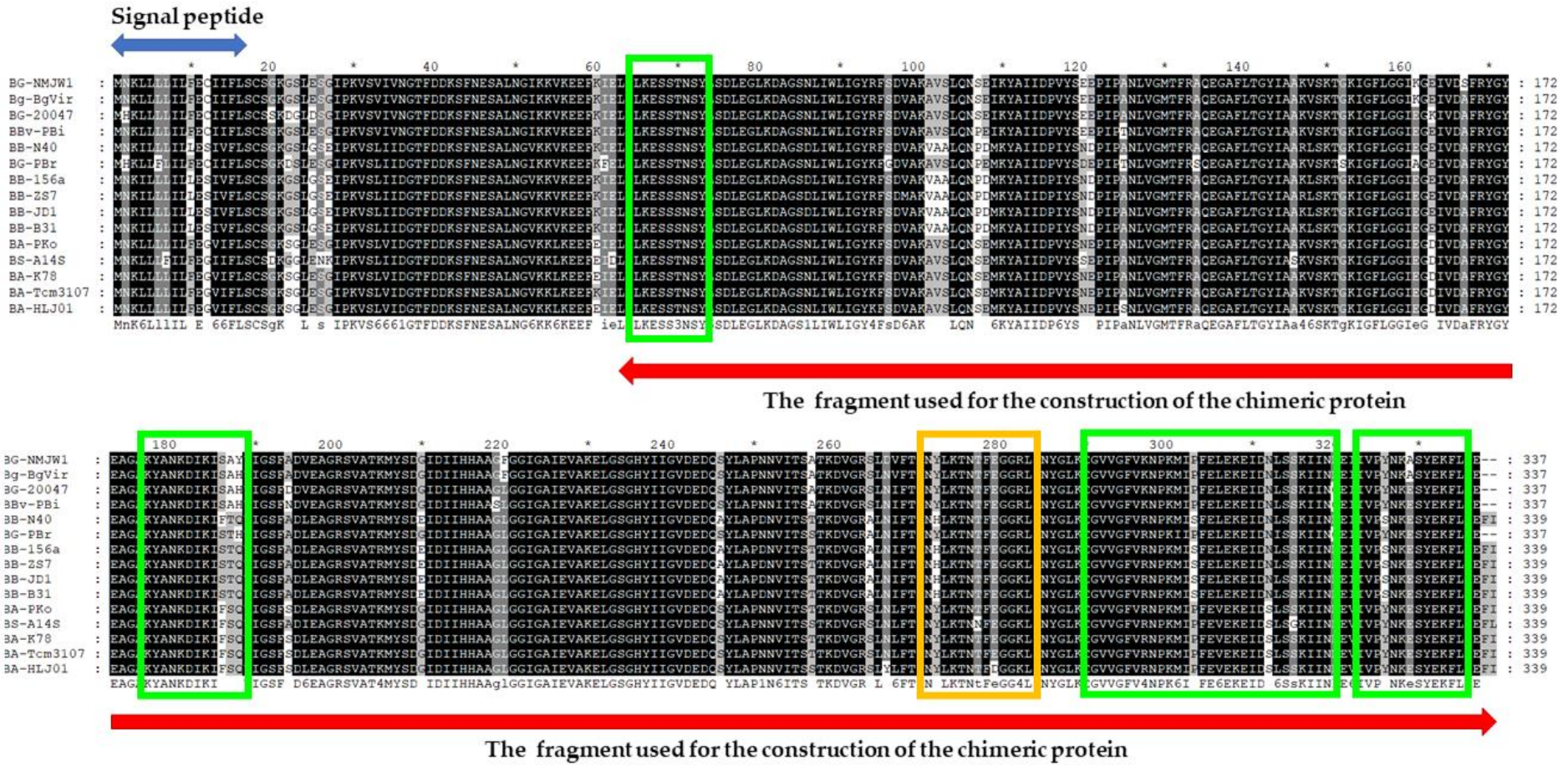

Figure 5. 13 Multiple amino acid sequence alignment of the BmpA protein of *B. burgdorferi* s.l. deposited in NCBI. Boxes mark potential B-cell linear epitopes. Green indicates at least 75% conservation of immunodominant fragment within *B. burgdorferi* s.l., orange less than 75%.

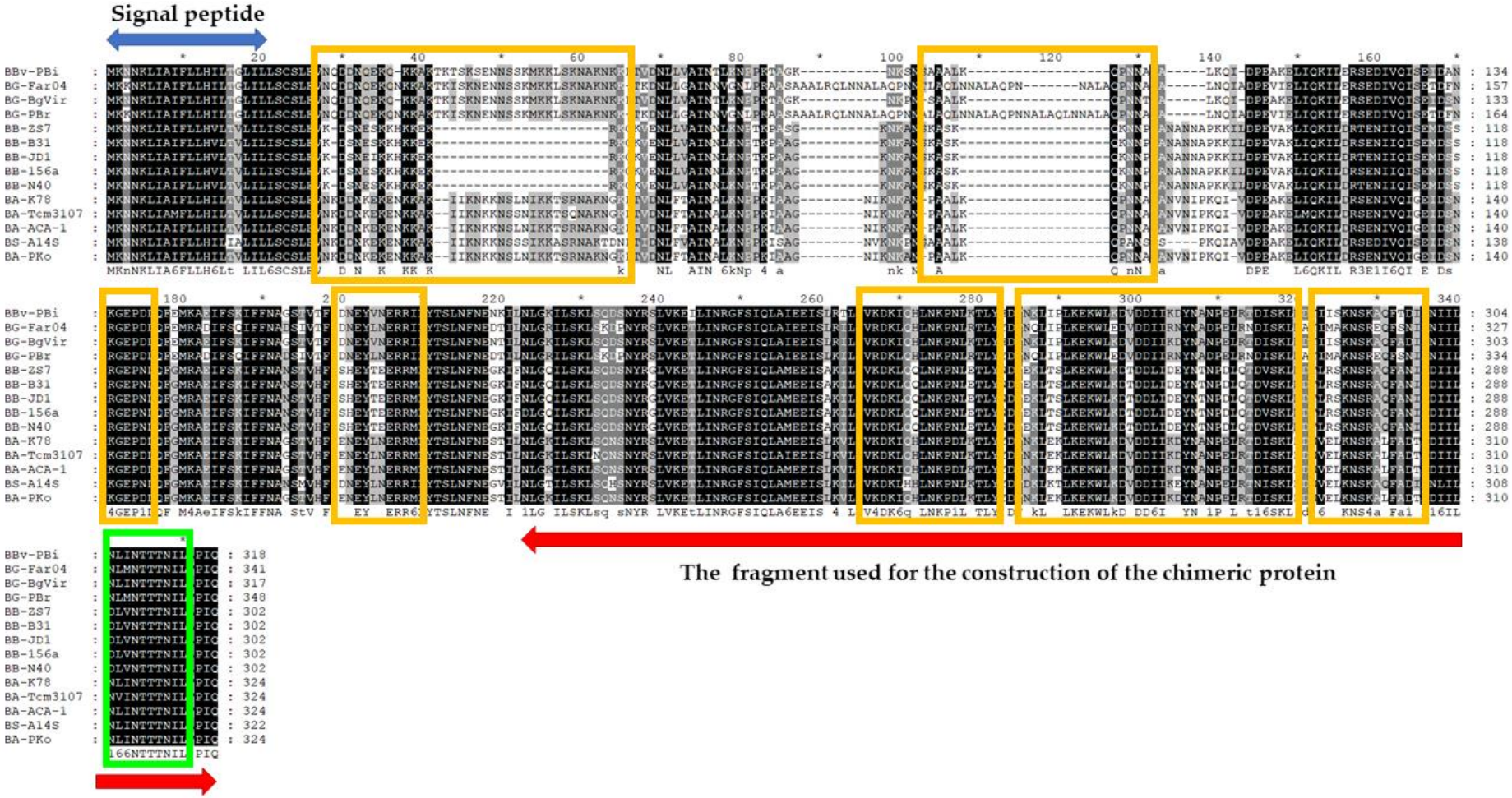

Figure 5. 14 Multiple amino acid sequence alignment of the BBA64 protein of *B. burgdorferi* s.l. deposited in NCBI. Boxes mark potential B-cell linear epitopes. Green indicates at least 75% conservation of immunodominant fragment within *B. burgdorferi* s.l., orange less than 75%.

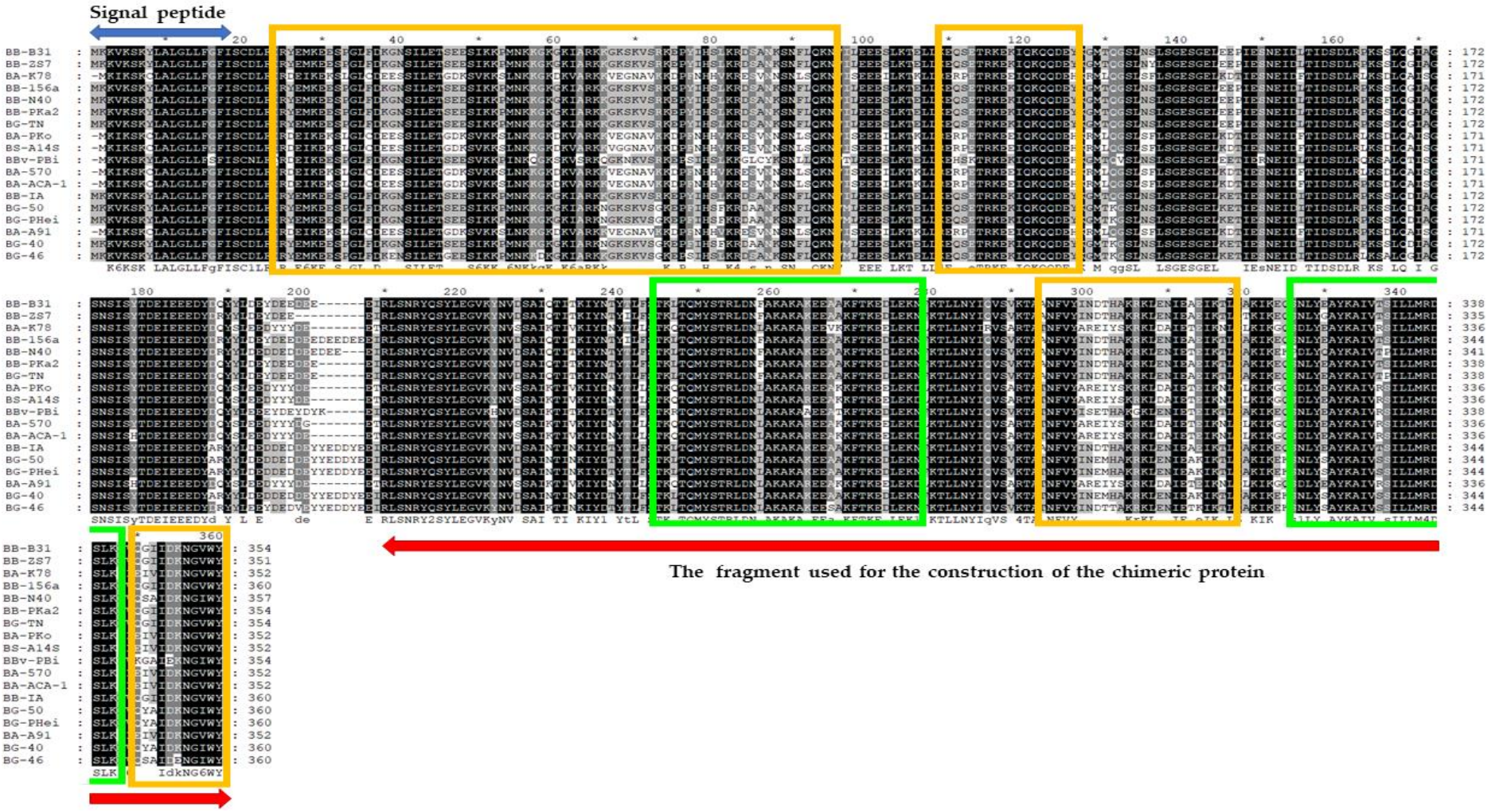

Figure 5. 15 Multiple amino acid sequence alignment of the BBK32 protein of *B. burgdorferi* s.l. deposited in NCBI. Boxes mark potential B-cell linear epitopes. Green indicates at least 75% conservation of immunodominant fragment within *B. burgdorferi* s.l., orange less than 75%.

While selecting the fragments for constructing chimeric proteins, efforts were made to choose those containing as many potential B-cell epitopes as possible with sequence conservation of at least 75%. Although the largest number of potential linear epitopes were identified in the BBA64 sequence, only one showed the expected 75% level of aa residues identity within *B. burgdorferi* s.l. complex (Table 5.6, Figures 5.13-5.15). Therefore, in this case, it was decided to lower this criterion. A fragment fringed by potential linear epitopes with a degree of sequence conservation of 65% and 75% was included in the construction of the chimeric protein. Based on these considerations, the following antigen fragments were selected for the construction of multivalent chimeric proteins:

- BmpA amino acid residues: 44-339
- BBA64 amino acid residues: 171-302
- BBK32 amino acid residues: 204-354

It was decided to design two multivalent chimeric proteins named BmpA-BBA64 and BmpA-BBK32. Each contained a highly conserved BmpA fragment at its N-terminus and at the C-terminus, there was a selected fragment of BBA64 or BBK32.

5.2.2. Multivalent chimeric protein design based on epitope mapping

5.2.2.1. Epitope mapping using peptide microarrays

For linear epitope mapping using peptide microarray BmpA and BBK32 were chosen. BBA64 was excluded due to its highest variability among *B. burgdorferi* s.l. Peptide microarrays with printed amino acid sequences were incubated with pooled serum samples positive for either IgG or IgM and sera positive for both immunoglobulin isotypes and negative controls (Figure 5.16) [Materials 3.14, Methods 4.11].

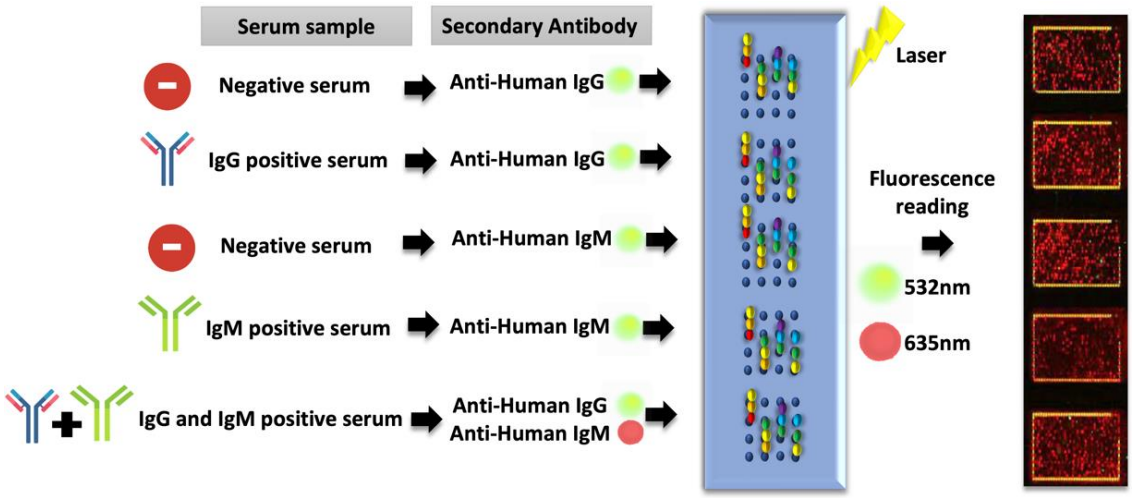

Figure 5. 16 Experimental design of the study. Four groups of sera were used: negative, positive for IgG, positive for IgM and positive for both IgM and IgG.

The results were visualized in a heatmap (Figure 5.17) where epitopes with Z-score>2 in different serum group were highlighted green or red, respectively [Methods 4.11, Methods 4.19]. A bright green arrow at the bottom of the heatmap corresponds to regions of highly reactive peptides recognized by IgG or IgM in positive serum samples, whereas a bright red arrow points to peptides recognized by immunoglobulins from negative serum samples. Some regions were reactive for immunoglobulins from both negative and positive serum samples which indicates cross-reactive peptide regions. For example, in BBK32 an extensive region of the protein (overlapping peptides no. 160 to 180) is recognized by IgG and IgM from positive and negative serum samples. This protein contains other isolated peptides reactive with both positive and negative sera, however Z-ratio> 1.96 is only found for positive samples. In BmpA this pattern of reaction is less frequent although some peptides such as no. 47, are recognized by IgG in positive and negative sera with a Z-score > 2, yet this peptide is also significantly more intensely recognized in samples from positive patients with a Z-ratio > 1.96. Peptides no. 97, 102, 103 are also recognized by IgM in positive and negative sera (Figure 5.17). Full Z- scores and Z-ratio values for all peptides are attached as an Excel file on the CD disc as Table S5.

Peptides significantly reactive for a single immunoglobulin isotype were observed in positive serum samples such as peptide no. 20 in BmpA which was reactive to IgG in the mixed (IgG+/IgM+) positive samples or peptide no. 26 which was only recognized by IgM from positive samples. In the same protein, a peptide region including the overlapping peptides no. 265-268 is reactive and recognized by IgM from IgG+/IgM+ samples (Figure 5.17, Table S3).

In BBK32, a peptide region with overlapping peptides from 38-45 was reactive only to IgM with a Z-ratio > 1.96 when compared with the control group (IgM in negative

samples). In addition, in this same protein the peptides no. 14, 88, 93, 112, 130 and 136 were reactive (Z-score > 2) and recognized only by IgG in the positive serum samples and showed a Z-ratio>1.96 when compared with control (IgG in negative samples) (Figure 5.17, Table S4).

In IgG+/IgM+ serum samples some peptides could significantly differentiate positive samples from negative samples for only one immunoglobulin type. This is observed in BmpA, as mentioned above, in peptide 20. Peptide overlapping region of peptides no. 142-146, 186 and 286 which were recognized by IgG, and peptides no. 25, 62, 64, 149, 173 and 220, recognized by IgM (Table S3). In protein BBK32, peptides such as no. 125, 127, 130, 185, 282 and 284 were recognized by IgM in IgG+/IgM+ serum samples while peptides recognized by IgG. in IgG+/IgM+ serum samples allowing for significant differentiation between IgG positive, and IgG negative samples were not found (Figure 5.17, Table S4).

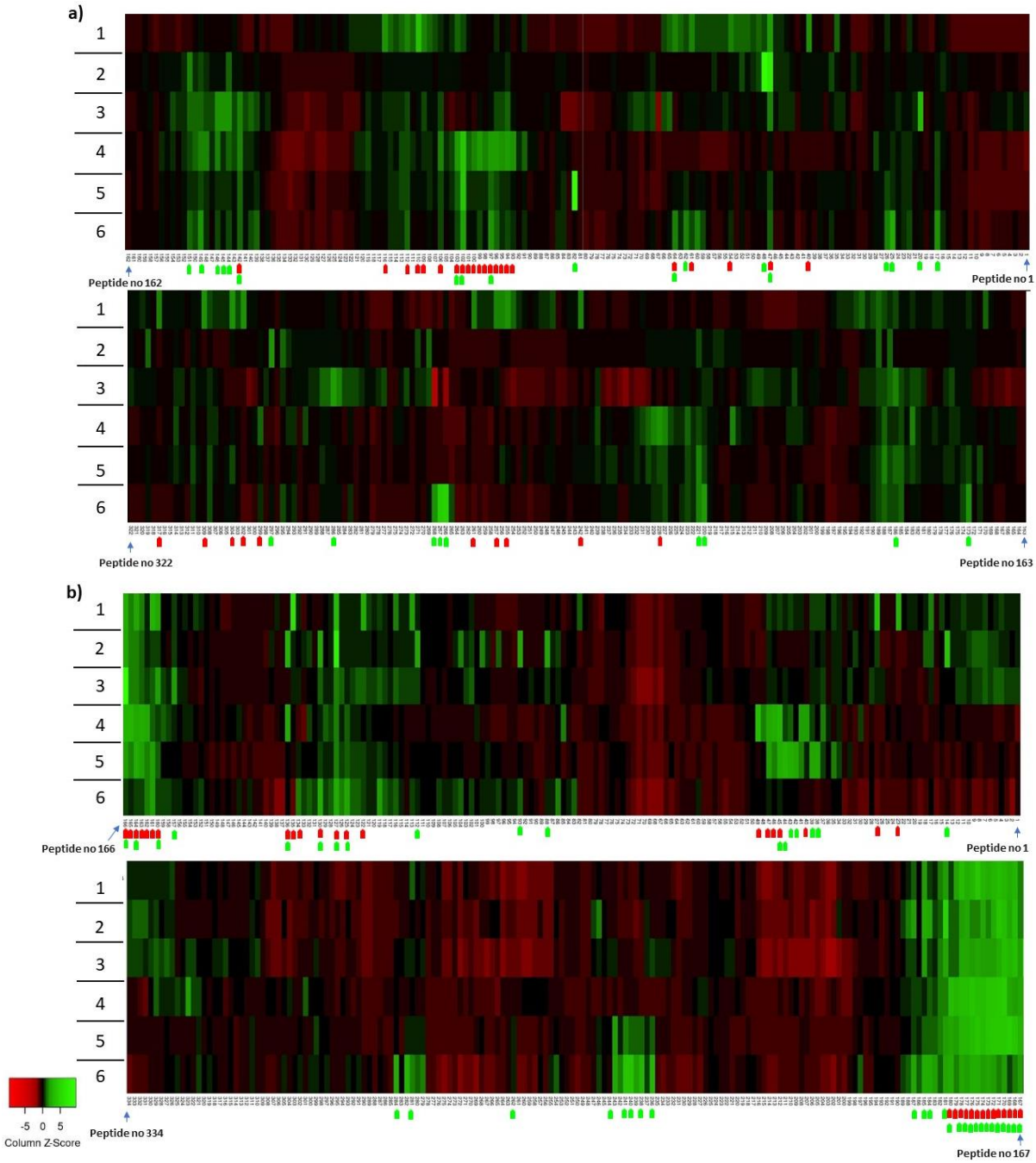

Figure 5. 17 Heatmap of the IgG and IgM reactive epitopes in positive IgG, positive IgM, positive IgG/IgM and negative serum samples in a) BmpA and b) BBK32 proteins. Reactivity against peptides is indicated with a Z-score and possible epitope regions are identified when Z-score>2. Green arrow shows significant reactivity with immunoglobulins from pooled positive sera, red arrows show peptides with significant reactivity with pooled sera from the control groups. **Legend:** 1 - IgG in negative sera; 2 - IgG in IgG positive sera; 3 - IgG in IgG and IgM positive sera; 4 - IgM in negative sera; 5 - IgM in IgM positive sera; 6 - IgM in IgG and IgM positive sera.

By analyzing the Z-score and Z-ratio values, immunodominant regions were identified that were recognized by IgM or IgG from positive serum samples and reacted with antibodies from negative serum samples. In the sequence of both proteins, 5 distinct immunodominant fragments recognized specifically by the antibodies contained in the positive sera were identified. Most often, they did not constitute a discreet fragment but

were separated by sequences reactive to negative sera. Only in the case of BBK32 can a domain containing three specific immunodominant fragments (IF3-IF5), containing no cross-reactive sequences, be identified. In the BmpA sequence, 6 non-specific immunodominant fragments distributed evenly throughout the antigen were isolated. In contrast, in the case of BBK32, 4 such fragments were identified and they were mainly located in the N-terminal part of the protein. The distribution of specific and cross-reacting immunodominant fragments in the BmpA and BBK32 antigen sequences is shown in Figure 5.18.

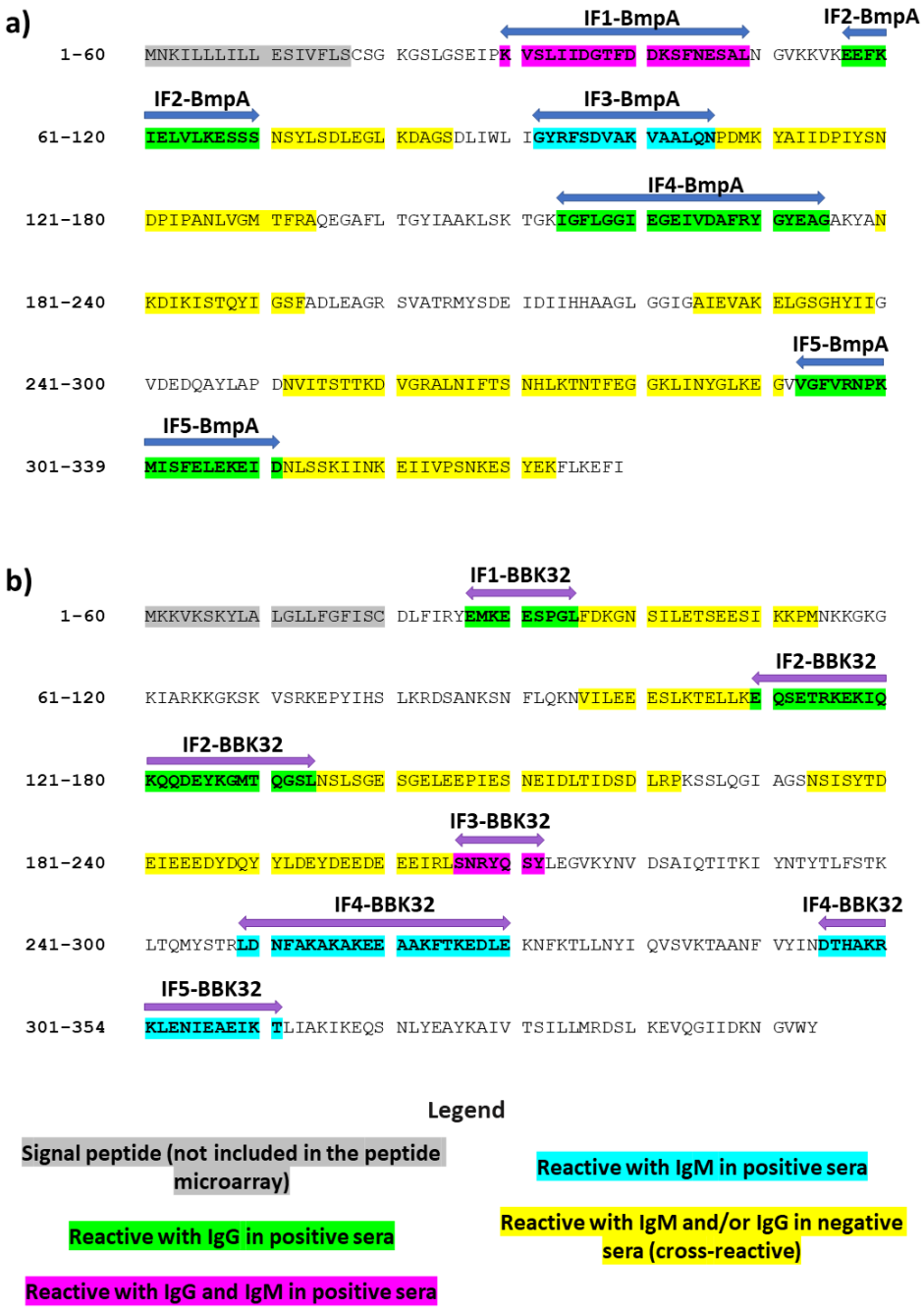

Figure 5. 18 Distribution of specific and cross-reactive immunodominant fragments: a) BmpA; b) BBK2. The arrows indicate the names of the fragments specifically recognized by the antibodies contained in the positive sera.

5.2.2.2. Analysis of the amino acid sequence of identified immunodominant fragments

Ten of identified immunodominant fragments (5 for both BmpA and BBK32) contained reactive epitopes recognized only by antibodies from positive serum samples (Z-ratio >1.96). Thus, it seems that they have the potential to differentiate positive and negative sera. Therefore, it was decided to take a closer look at the amino

acid sequence of these fragments and determine the degree of their conservation within *B. burgdorferi* s.l.

The amino acid sequence identity of BmpA specific immunodominant fragments (IF-BmpA) was high, ranging from 64% to 100% (Table 5.7). As the sequence used for epitope mapping was derived from *B. burgdorferi* s.s. B31, it was in this genospecies that the highest sequence identity was observed. The best-conserved immunodominant fragment was IF-4-BmpA, its identity was at least 95% in all genospecies. The IF3-BmpA peptide had the lowest sequence identity, reaching 64% for some *B. garinii* strains.

The amino acid sequence identity of BBK32 derived peptides was slightly lower, ranging from 67% to 100% (Table 5.8). Sequence differences between individual strains within genospecies were also more often observed. Again, the highest sequence identity was observed for *B. burgdorferi* s.s. It was clearly noticeable that the genospecies in which the selected immunodominant fragments were the most diverse was *B. spielmanii*. The degree of sequence identity for the IF2-BBK32 and IF4-BBK32 was 67%. However, for the rest of the genospecies, the degree of sequence identity was much higher and only fell below 80% for some strains of *B. afzelii.*

Table 5. 7 Degree of conservation of immunodominant fragments identified in BmpA within *B. burgdorferi* s.l. complex

No. IF	Sequence of immundominant fragments	Reactive Ab isotype	Length [aa]	Conservation (%aa identity)				
				***Bb* s.s.**[a]	***Ba***[b]	***Bg***[c]	***Bbv***[d]	***Bs***[e]
1	[29]KVSLIIDGTFDDKSFNESAL[48]	IgM/IgG	20	100%	95%	85%	85%	100%
2	[56]EEFKIELVLKESSS[69]	IgG	14	100%	86%	93%	93%	79%
3	[91]GYRFSDVAKVA[101]	IgM	11	100%	73%	64-100%	82%	91%
4	[153]IGFLGGIEGEIVDAFRYGYEAG[174]	IgG	22	100%	95%	95-100%	100%	95%
5	[292]VGFVRNPKMISFELEKEID[310]	IgG	19	100%	89%	89%	89%	95%

IF – immunodominant fragment; Ab - antibody
[a] *B. burgdorferi* s.s. (strains B31; JD1; 156a; N40)
[b] *B. afzelii* (strains: PKo; K78; ACA-1; A91)
[c] *B. garinii* (strains: 20047; 50; BgVir; 40)
[d] *B. bavariensis* (strain: PBi)
[e] *B. spielmanii* (strain: A14S)

Table 5. 8 Degree of conservation of immunodominant fragments identified in BBK32 within *B. burgdorferi* s.l. complex

No. IF	Sequence of immundominant fragments	Reactive Ab isotype	Length [aa]	Conservation (%aa identity)				
				***Bb* s.s.**[a]	***Ba***[b]	***Bg***[c]	***Bbv***[d]	***Bs***[e]
1	[27]EMKEESPGL[35]	IgG	9	100%	75-89%	89-100%	89%	67%
2	[110]EQSETRKEKIQKQQDEYKGMTQGSL[134]	IgG	25	96-100%	80-88%	96-100%	84%	76%
3	[206]SNRYQSY[212]	IgG/IgM	7	100%	86%	100%	100%	86%
4	[249]LDNFAKAKAKEEAAKFTKEDLE[270]	IgM	22	95-100%	82-86%	91-100%	86%	100%
5	[295]DTHAKRKLENIEAEIKT[311]	IgM	17	94-100%	78-89%	82%	82%	67%

IF – immunodominant fragment; Ab - antibody
[a] *B. burgdorferi* s.s. (strains B31; JD1; 156a; N40)
[b] *B. afzelii* (strains: PKo; K78; ACA-1; A91)
[c] *B. garinii* (strains: 20047; 50; BgVir; 40)
[d] *B. bavariensis* (strain: PBi)
[e] *B. spielmanii* (strain: A14S)

5.2.2.3. Design of multivalent chimeric proteins for IgG and IgM detection

Ten immunodominant fragments described in the previous section (IF1-IF5-BmpA and IF1-IF5-BBK32) were used to construct the multivalent chimeric proteins. They show a Z-score>2 and a Z-ratio>1.96 compared to negative samples. Therefore, they have potential diagnostic value as they distinguish between positive and negative sera and prevent cross-reactivity. These fragments were characterized by a fairly high degree of conservation of amino acid sequences within the *B. burgdorferi* s.l., which may contribute to the correct Lyme disease diagnosis, regardless of which genospecies caused the infection.

The identified immunodominant fragments were divided in terms of their reactivity with antibody isotypes and combined into two multivalent chimeric proteins: BmpA-BBK32-M (B/32-M) for detecting IgM and BmpA-BBK32-G (B/32-G) for IgG. In addition, non-reactive fragments were introduced into chimeric protein sequences to ensure a molecular weight of at least 20 kDa, which allows for efficient biotechnological production. Whereas introducing a flexible -GGG- sequence between individual peptides was intended to preserve the linear conformation of immunodominant fragments. Amino acid sequences of the designed multivalent chimeric proteins are shown in Figure 5.19.

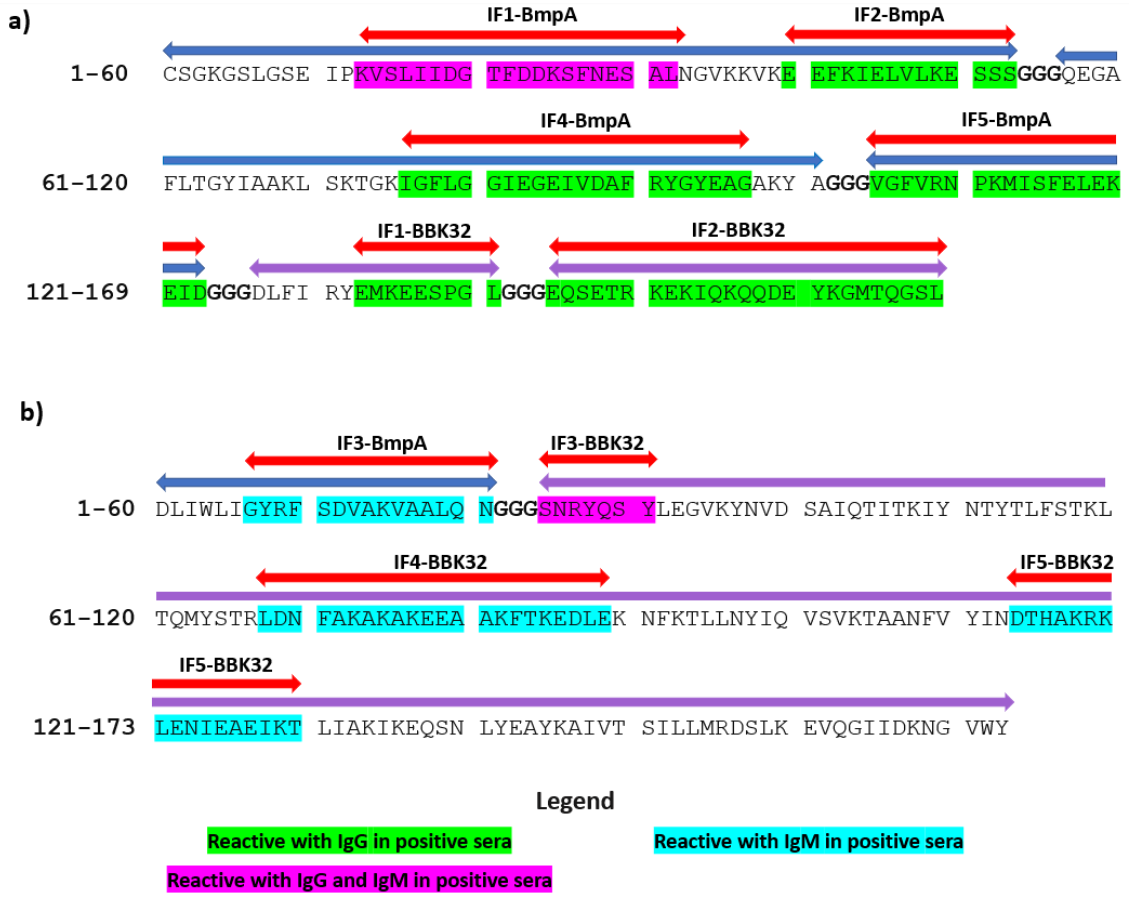

Figure 5. 19 Amino acid sequence of designed: a) BmpA-BBK32-G; b) BmpA-BBK32-M; red arrows indicate immunodominant fragments, blue arrows sequences derived from BmpA; purple arrows sequences derived from BBK32; -GGG- separating individual fragments are bolded.

5.3. Construction of recombinant plasmids

In order to produce *B. burgdorferi* s.l. proteins, recombinant plasmids carrying gene encoding selected antigens or their fragments were constructed. The nucleotide sequences encoding the signal peptides have been deleted from the genes to minimize the potential export signals that could have resulted in lower yields of recombinant protein in *E. coli*. Three different expression vectors were used as a backbone, i.e., pUET1, pET32a, pET42a [Materials 3.1]. Each vector allowed the introduction of additional S-Tag (1.7 kDa) domains at the N-terminus and an oligohistidine domain (His-tag; 1.1 kDa) at both the N- and C-terminus to the antigen sequence. The presence of S-tag and His-tag allows for rapid immune-identification of the recombinant protein. In addition, His-tag enables its efficient purification by metal affinity chromatography. Monovalent and multivalent recombinant proteins whose nucleotide sequences were cloned into pET32a or pET42a plasmid contained an additional thioredoxin 1 (TrxA; 11.8 kDa) or glutathione S-transferase (GST; 25.5 kDa) domain in their amino acid

sequence, respectively. Both of these domains improve the solubility and stability of proteins in an aqueous environment.

Molecular cloning was carried out by two methods, the first was the In-Fusion seamless system cloning enables directional cloning of any PCR fragment into any linearized vector (digested or PCR product). The only requirement was the presence at each end of the insert of 15 bp overlaps complementary to the vector sequence (Park et al., 2015). Another of them was the standard method of ligation of DNA fragments previously digested with appropriate restriction enzymes (Lessard, 2013) [Materials 3.6; Methods 4.8].

5.3.1. Construction of plasmids encoding monovalent recombinant proteins using the In-Fusion system

5.3.1.1. Amplification of genes fragments

Fragments of genes encoding selected antigens from three different *B. burgdorferi* s.l. genospecies (*B. afzelii*, *B. burgdorferi* s.s., *B. garinii*) were amplified by PCR [Methods 4.3.1] using DNA polymerase Phusion™ High-Fidelity [Materials 3.4.1]. The genomic DNA diluted 100 times was used as a template [Materials 3.1]. The PCR profile contained preliminary cycles in which the primers annealing temperature was used lower than the one at the later stages of amplification [Methods 4.3.1].

Primers have been designed to introduce at the ends of PCR products fragments complementary to multiple cloning site (MCS) of pUET1 vector, which were necessary for cloning using the In-Fusion system [Materials 3.4]. After the PCR, the obtained products were separated in 1.5% of agarose gel (Table 5.9; Figure 5.20) [Materials 3.7; Methods 4.10.1] and cleaned using the Gel-Out Concentrator kit [Materials 3.10.2; Methods 4.5].

Table 5. 9 PCR products encoding monovalent genes fragments

Gene	*B. burgdorferi* s.l. genospecies	PCR products size	Encoded native protein fragment (aa residues)
***bb0108*$_{BA}$**	*B. azfelii*	983 bp	20-336
***bb0108*$_{BB}$**	*B. burgdorferi* s.s.	983 bp	20-336
***bb0108*$_{BG}$**	*B. garinii*	983 bp	20-336
***bb0126*$_{BA}$**	*B. azfelii*	578 bp	22-203
***bb0126*$_{BB}$**	*B. burgdorferi* s.s.	578 bp	22-203
***bb0126*$_{BG}$**	*B. garinii*	578 bp	22-203
***bb0298*$_{BA}$**	*B. azfelii*	659 bp	17-225
***bb0298*$_{BB}$**	*B. burgdorferi* s.s.	659 bp	17-225
***bb0298*$_{BG}$**	*B. garinii*	659 bp	17-225
***bb0323*$_{BA}$**	*B. azfelii*	1103 bp	24-379
***bb0323*$_{BB}$**	*B. burgdorferi* s.s.	1097 bp	22-376
***bb0323*$_{BG}$**	*B. garinii*	1094 bp	23-376
***bb0689*$_{BA}$**	*B. azfelii*	407 bp	28-152
***bb0689*$_{BB}$**	*B. burgdorferi* s.s.	407 bp	28-152
***bb0689*$_{BG}$**	*B. garinii*	407 bp	28-152

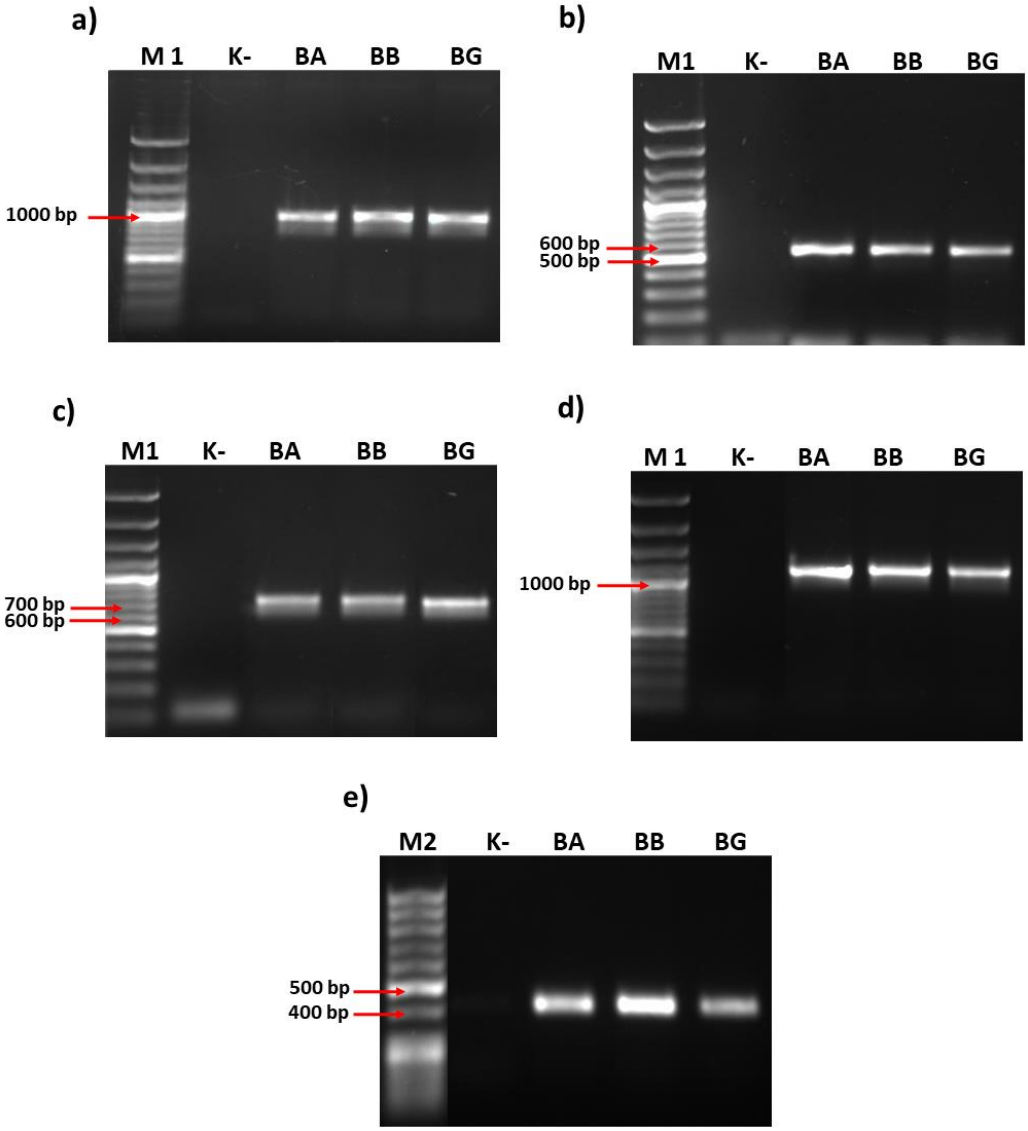

Figure 5. 20 PCR products encoding gene fragments: a) *bb0108*; b) *bb0126*; c) *bb0298*; d) *bb0323*; e) *bb0689.* **Lanes:** M1 - GeneRuler™ 100 bp Plus DNA Ladder; M2 - GeneRuler™ 50 bp Plus DNA Ladder; K- - negative control; BA - gene fragment obtained from *B. afzelii;* BB - gene fragment obtained from *B. burgdorferi* s.s.; BG - gene fragment obtained from *B. garinii*.

5.3.1.2. Molecular cloning using the In-Fusion system

Expression vector pUET1 with a size of 2856 bp was digested with BglII restriction enzyme [Materials 3.5; Methods 4.6], as a result of this process, a linear fragment of DNA was obtained. Then the reaction products were separated in 1.5% agarose gel and cleaned using the Gel-Out Concentrator kit [Materials 3.10.2; Methods 4.5; Materials 3.7; Methods 4.10.1]. The linear vector prepared this way was mixed with PCR products containing overlapping ends and assembled using the In-Fusion system [Methods 4.8.2]. Subsequently, the content of the reaction mixture was transformed into *E. coli* Stellar™ cells [Materials 3.2]. These reactions resulted in recombinant plasmids encoding antigens from three different genospecies of *B. burgdorferi* s.l. The scheme of

the molecular cloning using the In-Fusion system on the example of pUET1-BB0108BA is shown in the Figure 5.21.

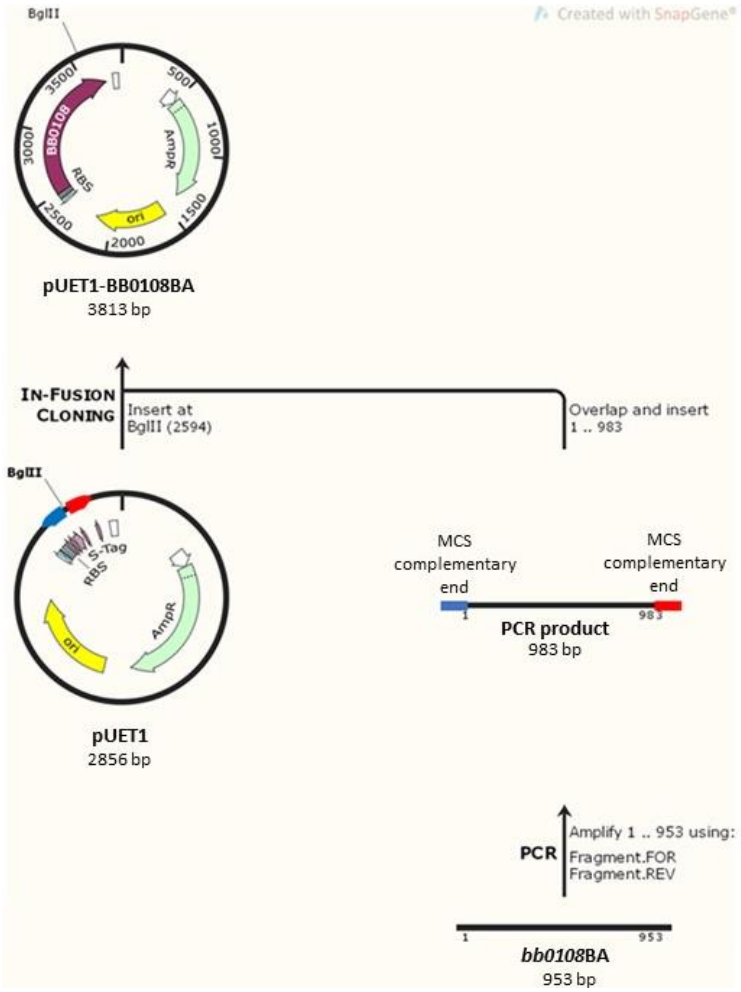

Figure 5. 21 Scheme of pUET1-BB0108BA construction using the In-Fusion system.

5.3.1.3. Identification of recombinant plasmids

As a result of the transformation, bacterial colonies were obtained. They were subcultured onto a LBA plate [Materials 3.3; Methods 4.2.2] and inoculated into LB medium [Materials 3.3; Methods 4.2.1]. Both media contained the addition of ampicillin as a selection marker [Materials 3.17]. Growth was carried out for 18 h. After this time, plasmid DNA isolation was performed [Methods 4.4]. The isolated plasmids were electrophoretically separated in a 1% agarose gel to evaluate the electrophoretic mobility in relation to the pUET1 containing no heterologous gene [Methods 4.10.1]. Then, to confirm the correctness of the obtained constructs, the slower migrating plasmid in the agarose gel was subjected to restriction analysis (RA). For this purpose, digestion reactions of vectors and potential recombinant plasmids with selected restriction enzymes were performed [Materials 3.5; Methods 4.6]. Then, to check whether the obtained DNA fragments correspond to those determined using the SnapGene software

[Methods 4.19] (Table 5.10), the digestion products were electrophoretically separated in a 1.5% agarose gel (Figure 5.22) [Methods 4.10.1]. In addition, plasmids forming the correct pattern during RA were also sequenced to confirm the successful cloning.

Table 5. 10 The expected size of DNA fragments generated during restriction analysis of recombinant plasmids encoding monovalent *B. burgdorferi* s.l. proteins (sizes of DNA fragments characteristic of recombinant plasmids are bolded)

Restriction enzymes	DNA fragments size [bp]
pUET1 (2868 bp)	
HinfI	**1742**; 517; 396; 75; 65; 61
NdeI	2369; **487**
pUET1-BB0108BA (3813 bp)	
HinfI	**1573**; 517; **502**; 396; **345**; **253**; 75; 65; 61; **26**
NdeI	2369; **1444**
pUET1-BB0108BB (3813 bp)	
HinfI	**1573;** 517; **528**; 396; **345**; **253**; 75; 65; 61
NdeI	2369; **1444**
pUET1-BB0108BG (3813 bp)	
HinfI	**1573**; 517; **502**; 396; **345**; **253**; 75; 65; 61; **26**
NdeI	2369; **1444**
pUET1-BB0126BA (3408 bp)	
HinfI	**2294**; 517; 396; 75; 65; 61
NdeI	2369; **1039**
pUET1-BB0126BB (3408 bp)	
HinfI	**2294**; 517; 396; 75; 65; 61
NdeI	2369; **595; 444**
pUET1-BB0126BG (3408 bp)	
HinfI	**2294**; 517; 396; 75; 65; 61
NdeI	2369; **1039**
pUET1-BB0298BA (3489 bp)	
HinfI	**1789**; 517; 396; 324; 196; 75; 65; 61; 49; 17
NdeI	2369; **1120**
pUET1-BB0298BB (3489 bp)	
HinfI	**1789**; 517; 396; 324; 196; 75; 65; 61; 49; 17
NdeI	2369; **1120**
pUET1-BB0298BG (3489 bp)	
HinfI	**1789**; 517; 396; 324; 196; 75; 65; 61; 49; 17
NdeI	2369; **1120**
pUET1-BB0323BA (3933 bp)	
HinfI	**1595**; **537**; 520; 517; 396; **167**; 75; 65; 61
NdeI	2369; **826; 738**
pUET1-BB0323BB (3927 bp)	
HinfI	**1762**; **852**; 517; 396; **199**; 75; 65; 61
NdeI	2369; **1109; 449**
pUET1-BB0323BG (3934 bp)	
HinfI	**1595**; **537**; 517; 511; 396; **167**; 75; 65; 61
NdeI	2369; **1555**
pUET1-BB689BA (3237 bp)	
HinfI	**1883**, 517, 396, 240; 75, 65, 61
NdeI	2369; **868**
pUET1-BB689BB (3237 bp)	
HinfI	**2123**, 517, 396, 75, 65, 61
NdeI	2369; **868**
pUET1-BB689BG (3237 bp)	
HinfI	**2123**, 517, 396, 75, 65, 61
NdeI	2369; **868**

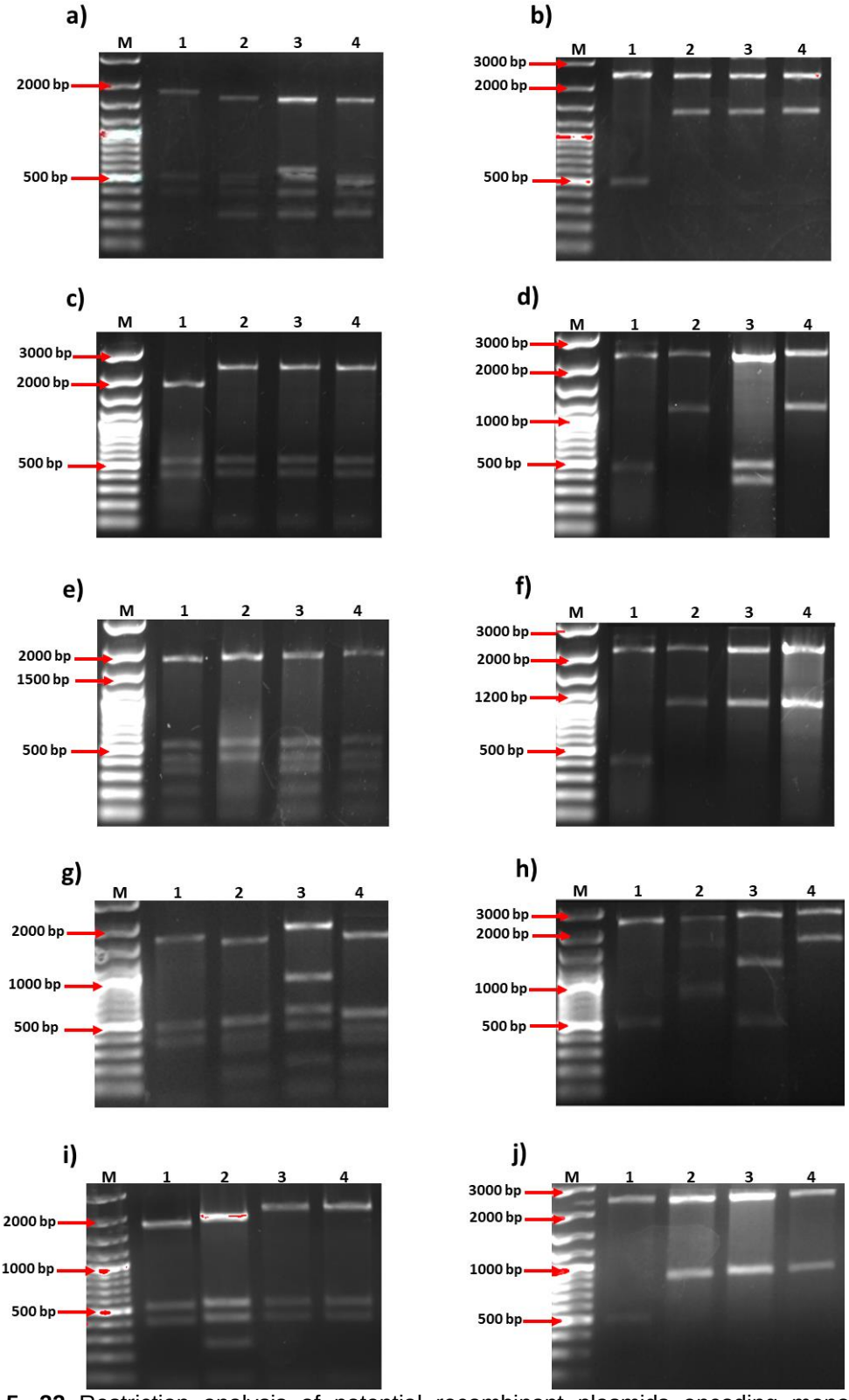

Figure 5. 22 Restriction analysis of potential recombinant plasmids encoding monovalent *B. burgdorferi* s.l. proteins: a) pUET1-BB0108s digested with HinfI; b) pUET1-BB0108s digested with NdeI; c) pUET1-BB0126s digested with HinfI; d) pUET1-BB0126s digested with NdeI; e) pUET1-BB0298s digested with HinfI; f) pUET1-BB0298s digested with NdeI; g) pUET1-BB0323s digested with HinfI; h) pUET1-BB0323s digested with NdeI; i) pUET1-BB0689s digested with HinfI; j) pUET1-BB0689s digested with NdeI. **Lanes:** M - GeneRuler 100 bp Plus DNA Ladder; 1 - pUET1 (control); 2 - gene variant derived from *B. afzelii*; 3 - gene variant derived from *B. burgdorferi* s.s.; 4 - gene variant derived from *B. garinii.*

Comparison of the migration rate of individual DNA fragments obtained during RA and the sequencing results allowed to conclude that recombinant plasmids encoding antigens BB0108s, BB0126s, BB0298s, BB0323s and BB0689s of *B. burgdorferi* s.l. were successfully constructed (Table 5.11).

Table 5. 11 Characteristics of constructed recombinant plasmids encoding monovalent *B. burgdorferi* s.l. recombinant proteins

Plasmid name	Plasmid size [bp]	Encoded monovalent protein	Encoded native protein fragment [aa]
pUET1-BB0108BA	3839	$BB0108_{BA}$	20-336
pUET1-BB0108BB	3839	$BB0108_{BB}$	20-336
pUET1-BB0108BG	3839	$BB0108_{BG}$	20-336
pUET1-BB0126BA	3408	$BB0126_{BA}$	22-203
pUET1-BB0126BB	3408	$BB0126_{BB}$	22-203
pUET1-BB0126BG	3408	$BB0126_{BG}$	22-203
pUET1-BB0298BA	3489	$BB0298_{BA}$	17-225
pUET1-BB0298BB	3489	$BB0298_{BB}$	17-225
pUET1-BB0298BG	3489	$BB0298_{BG}$	17-225
pUET1-BB0323BA	3933	$BB0323_{BA}$	24-379
pUET1-BB0323BB	3927	$BB0323_{BB}$	22-376
pUET1-BB0323BG	3924	$BB0323_{BG}$	23-376
pUET1-BB0689BA	3237	$BB0689_{BA}$	28-152
pUET1-BB0689BB	3237	$BB0689_{BB}$	28-152
pUET1-BB0689BG	3237	$BB0689_{BG}$	28-152

5.3.2. Construction of plasmids encoding multivalent chimeric proteins BmpA-BBA64 and BmpA-BBK32

5.3.2.1. Obtaining chimeric genes

The *bmpA-bba64* and *bmpA-bbk32* chimeric genes were obtained by assembling PCR products. It was necessary for each of the chimeric genes to obtain two PCR products containing overlapped sequences, enabling their combination into one DNA sequence encoding fragments from two different antigens (BmpA and BBA64 or BmpA and BBK32).

Two variants of the *bmpA* gene were obtained encoding amino acid residues 44-325 of the BmpA protein. One of them (*bmpA+bba64OL*) contained 20 nucleotides at the 3' end complementary to the *bba64* gene fragment, while the other (*bmpA+bbk32OL*) at the 3' end had 19 nucleotides complementary to *bbk32*. A fragment of the *bba64* gene encoding amino acid residues 171-302 of the BBA64 protein contained a 19-nucleotide sequence complementary to *bmpA* at its 5' end (*bba64+bmpAOL*). Similarly, PCR product encoding amino acid residues 204-254 of the

BBK32 protein also contained a fragment complementary to *bmpA* in its sequence (*bbk32+bmpAOL*). To the obtained DNA fragments restriction sites were also introduced. For *bmpA* it was sequence recognized by BglII and for *bba64* and *bbk32* XhoI restriction site (Figure 5.23; Table 5.12).

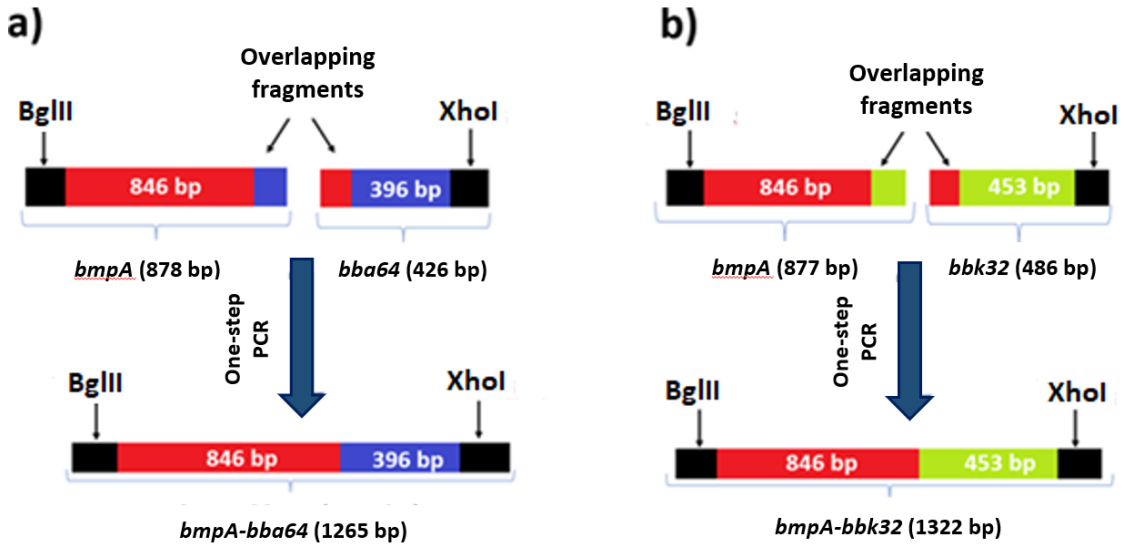

Figure 5. 23 Scheme of the construction of *bmpa-bba64* and *bmpA-bbk32* chimeric genes.

Table 5. 12 Characterization of PCR products used for the construction of chimeric genes

PCR product name	PCR product size [bp]	Overlapping to	RE site	Encoded native protein fragment [aa]
bmpA+bba64OL	878	*bba64* (20 bp)	BglII	• 44-339 BmpA
bba64+-bmpAOL	396	*bmpA* (19 bp)	XhoI	• 171-302 BBA64
bmpA-bba64 **(chimeric gene)**	1265	-	BglII, XhoI	• 44-339 BmpA • 171-302 BBA64
bmpA+bbk32OL	877	*bbk32* (19 bp)	BglII	• 44-339 BmpA
bbk32+bmpAOL	486	*bmpA* (22 bp)	XhoI	• 204-354 BBK32
bmpA-bbk32 **(chimeric gene)**	1322	-	BglII, XhoI	• 44-339 BmpA • 204-354 BBK32

RE site – restriction enzyme site

All DNA fragments were obtained by amplifying 100 times diluted genomic DNA of *B. burgdorferi* s.s. using PCR Mix Plus HGC [Materials 3.4.1; Methods 4.3.2.1]. After the PCR reaction, the obtained products were separated in a 1.5% agarose gel (Figure 5.24) and purified using the Gel-Out Concentrator kit [Materials 3.10.2; Methods 4.5; Materials 3.7; Methods 4.10.1].

In order to combine two partially complementary DNA fragments into one gene encoding a multivalent chimeric protein (BmpA-BBA64 or BmpA-BBK32), a modified one-step PCR reaction was performed [Methods 4.3.2.2]. Then, the amplified purified

products were used as a template in a standard PCR reaction to obtain an inserts for molecular cloning (Figure 5.24) [Methods 4. 3.2.3].

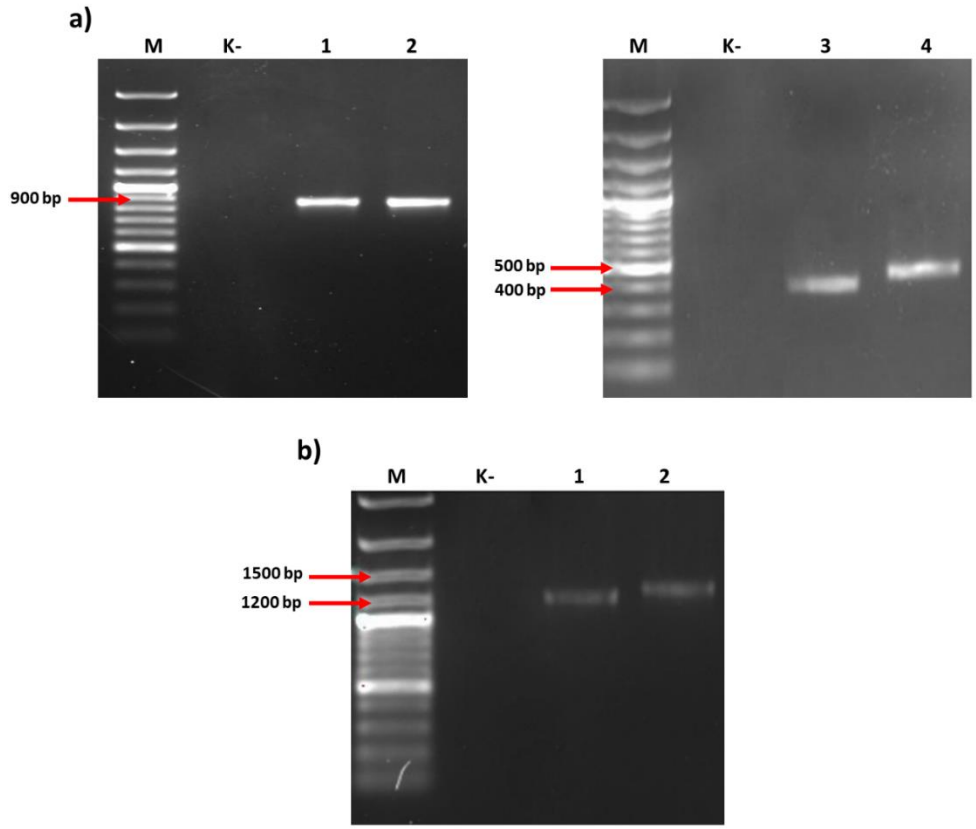

Figure 5. 24 Construction of chimeric genes: a) PCR products used to assemble chimeric genes. **Lanes**: M **-** GeneRuler 100 bp Plus DNA Ladder; K- - negative control; 1 - *bmpA+bba64OL*; 2 - *bmpA+bbk32OL*; 3 - *bba64+bmpAOL;* 4 - *bbk32+bmpAOL;* b) final PCR products encoding full sequence of *bmpA-bba64* and *bmpA-bbk32* chimeric genes. **Lanes:** M - GeneRuler 100 bp Plus DNA Ladder; K- - negative control; 1 - *bmpA-bba64* chimeric gene; 2 - *bmpA-bbk32* chimeric gene.

5.3.2.2. Molecular cloning

Expression vector pUET1 with a size of 2856 bp was digested with BglII and XhoI restriction enzymes simultaneously [Materials 3.5; Methods 4.6], as a result of this process a linear fragment of DNA with a length of 2756 bp was obtained. The next step was dephosphorylation of the vector using alkaline phosphatase FastAP [Methods 4.7]. Then the reaction products were separated in 1.5% agarose gel and purified using the Gel-Out Concentrator kit [Materials 3.10.2; Methods 4.5; Materials 3.7; Methods 4.10.1].

The *bmpA-bba64* and *bmpA-bbk32* chimeric genes were digested with BglII and XhoI. Digestion with two restriction enzymes was performed simultaneously with the use Tango buffer [Materials 3.5; Methods 4.6]. The digested inserts were separated in 1.5% agarose gel [Methods 4.9.1] and purified using the Gel-Out Concentrator kit [Materials 3.10.2; Methods 4.5; Materials 3.7; Methods 4.10.1].

Inserts and vector prepared this way were ligated (Figure 5.25). Subsequently, the content of the reaction mixture was transformed into *E. coli* TOP10F' competent cells [Materials 3.6; Methods 4.8.1; Methods 4.9].

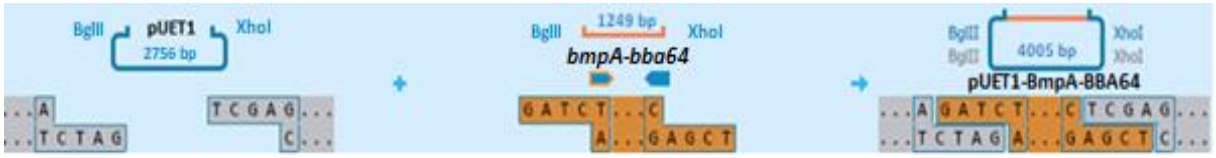

Figure 5. 25 Scheme of construction of pUET1-BmpA-BBA64 by standard molecular cloning.

5.3.2.3. Identification of recombinant plasmids

Identification of recombinant plasmids was carried out in the same way as described in section 5.3.1.3. (Table 5.13). The only difference was adding a second antibiotic to the growth media as *E. coli* TOP10F' carries a tetracycline resistance gene [Materials 3.2, Materials 3.17].

Table 5. 13 Expected size of DNA fragments generated by restriction analysis of pUET1-BmpA-BBA64 and pUET1-BmpA-BBK32 (sizes of DNA fragments characteristic of recombinant plasmids are bolded)

Restriction enzymes	DNA fragments size [bp]
pUET1 (2868 bp)	
HinfI	**1742**; 517; 396; 75; 65; 61
NdeI	2369; **487**
ScaI	Linear form
XbaI	Linear form
pUET1-BmpA-BBA64 (4005 bp)	
HinfI	**1510; 870**; 517; 396; **217**; 75; 65; 61
NdeI	2369; **1636**
ScaI	**3066; 939**
pUET1-BmpA-BBK32 (4062 bp)	
HinfI	**1510; 870**; 517; 396; **351**; **217**; 75; 65; 61
NdeI	2369; **1693**
XbaI	**3040; 1022**

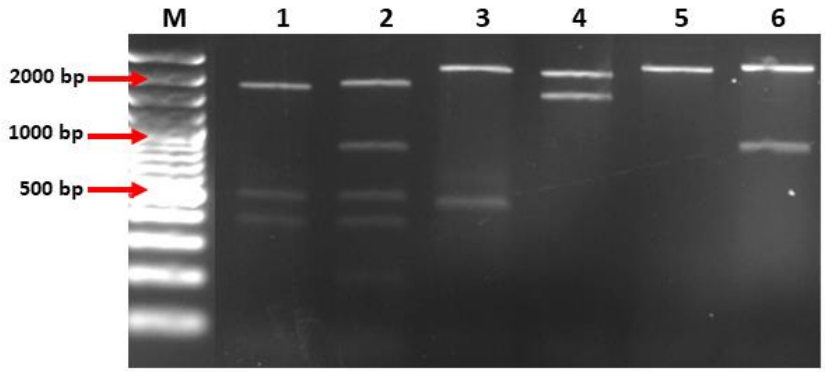

Figure 5. 26 Restriction analysis of potential recombinant plasmids pUET1-BmpA-BBA64. **Lanes:** M - GeneRuler 100 bp Plus DNA Ladder size marker; 1 - pUET1 digested with HinfI (control); 2 - pUET1-BmpA-BBA64 digested with HinfI; 3 - pUET1 digested with NdeI (control); 4 - pUET1-BmpA-BBA64 digested with NdeI; 5 - pUET1 digested with the SacI; 6 - pUET1-BmpA-BBA64 digested with SacI.

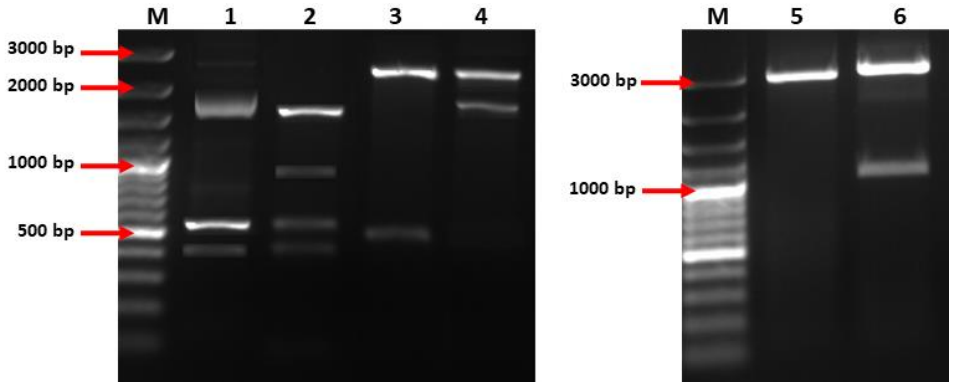

Figure 5. 27 Restriction analysis of potential recombinant plasmids pUET1-BmpA-BBK32. **Lanes:** M - GeneRuler 100 bp Plus DNA Ladder size marker; 1 - pUET1 digested with HinfI (control); 2 - pUET1-BmpA-BBK32 digested with HinfI; 3 - pUET1 digested with the NdeI (control); 4 - pUET1-BmpA-BBK32 digested with NdeI; 5 - pUET1 digested with the XbaI (control); 6 - pUET1-BmpA-BBK32 digested with XbaI.

Comparison of the migration of individual DNA fragments obtained during RA and the sequencing results allowed to conclude that recombinant plasmids encoding BmpA-BBA64 and BmpA-BBK32 multivalent chimeric proteins were successfully constructed (Figure 5.26-5.27; Table 5.14).

Table 5. 14 Characteristics of constructed recombinant plasmids encoding BmpA-BBA64 and BmpA-BBK32 *B. burgdorferi* s.s. chimeric proteins

Plasmid name	RE used in cloning	Plasmid size [bp]	Encoded multivalent protein	Encoded native protein fragment
pUET1-BmpA-BBA64	BglII XhoI	4005	BmpA-BBA64	• 44-325 BmpA • 171-302 BBA64
pUET1-BmpA-BBK32	BglII XhoI	4062	BmpA-BBK32	• 44-325 BmpA • 204-354 BBK32

RE - restriction enzyme

5.3.3. Construction of plasmids encoding multivalent chimeric proteins BmpA-BBK32-G and BmpA-BBK32-M

5.3.3.1. Molecular cloning

The recombinant plasmids pUET1-BmpA-BBK32-G and pUET1-BmpA-BBK32-M were obtained by standard molecular cloning using restriction enzymes and ligase. Genes encoding the BmpA-BBK32-G and BmpA-BBK32-M chimeric proteins have been synthesized by GeneScript (Rijswijk, Netherlands) and cloned into pUC57 plasmid between BamHI and HindIII restriction site constructing pUC57-BmpA-BBK32-G and pUC57-BmpA-BBK32-M recombinant plasmids [Materials 3.1].

pUET1 (2856 bp) was digested with restriction enzymes BglII and HindIII [Materials 3.1; Materials 3.5, Methods 4.6], obtaining linear DNA fragments. Reaction products were separated in a 1.5% agarose gel and purified using the Gel-Out

Concentrator kit [Materials 3.10.2; Methods 4.5; Materials 3.7; Methods 4.10.1]. The synthetic genes *bmpA-bbk32-G* and *bmpA-bbk32-M* were excised from plasmids pUC57-BmpA-BBK32-G and pUC57-BmpA-BBK32-M respectively with the enzymes BamHI and HindIII. This process resulted in linear DNA fragments of 514 bp (*bmpA-bbk32-G*) and 526 bp (*bmpA-bbk32-M*) (Figure 5.28), which were purified analogously as a vector. Plasmid pUC57 does not contain a BglII recognition site in its sequence. Therefore, it was necessary to excise the chimeric genes using BamHI. However, the restriction enzymes BamHI and BglII leave complementary sticky ends, so the enzyme change was not an obstacle in standard molecular cloning.

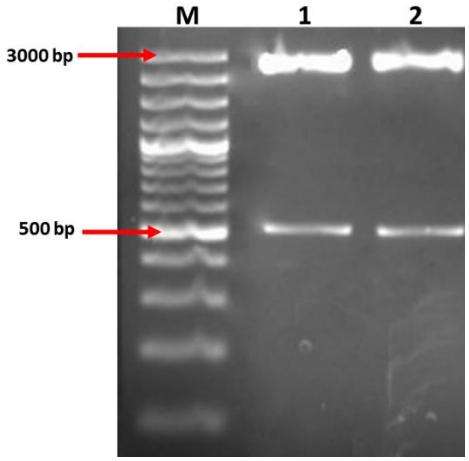

Figure 5. 28 Excision of the *bmpA-bbk32-G* and *bmpA-bbk32-M* synthetic genes from the pUC57 vector using BamHI and HindIII restriction enzymes. **Lanes:** M - GeneRuler 100 bp Plus DNA Ladder; 1 - pUC57-BmpA-BBK32-G; 2 - pUC57-BmpA-BBK32-M.

The DNA of the inserts and pUET1 prepared this way was ligated [Methods 4.8.1]. The ligation mixtures were then used to transform competent *E. coli* TOP10F' cells [Materials 3.2; Methods 4.9]. The cloning scheme is shown on the example of the construction of the plasmid pUET1-BmpA-BBK32-G in Figure 5.29.

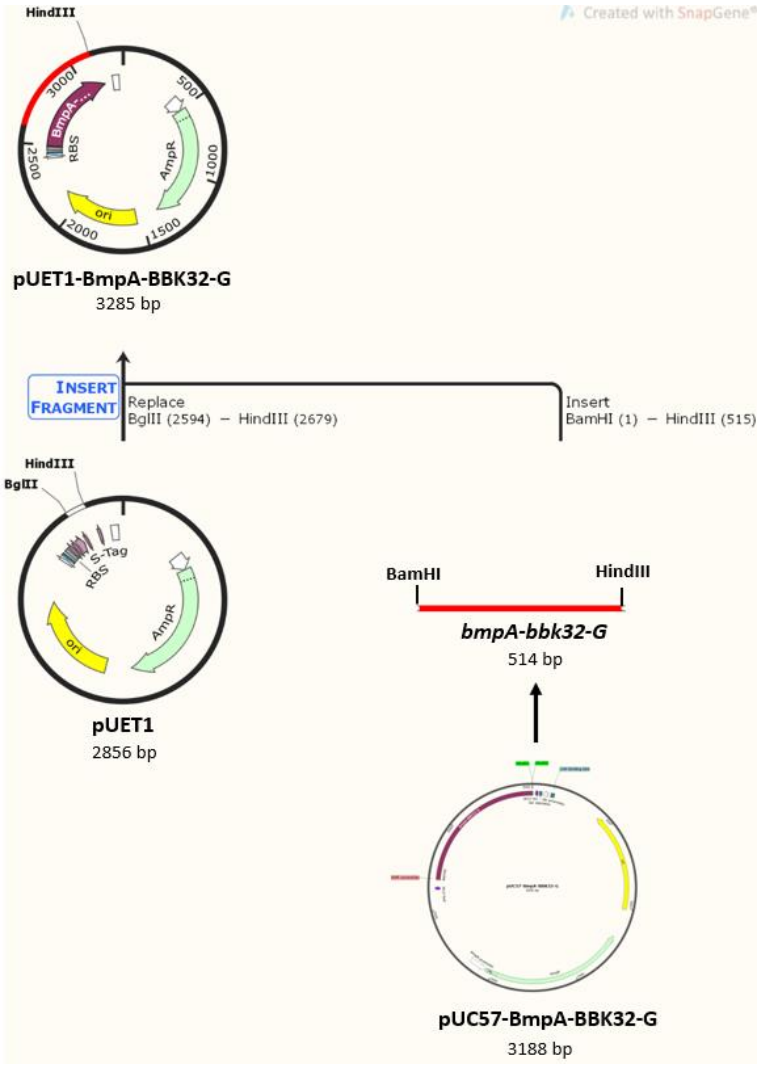

Figure 5. 29 Scheme of construction of pUET1-BmpA-BBK32-G.

5.3.3.2. Identification of recombinant plasmids

Identification of recombinant plasmids was carried out in the same way as described in section 5.3.2.3. (Table 5.15; Figure 5.30).

Table 5. 15 Expected size of DNA fragments generated by restriction analysis of pUET1-BmpA-BBK32-G and pUET1-BmpA-BBK32-M (sizes of DNA fragments characteristic to recombinant plasmids are bolded)

Restriction enzymes	DNA fragments size [bp]
pUET1 (2868 bp)	
HinfI	**1742**; 517; 396; 75; 65; 61
NdeI	2369; **487**
pUET1-BmpA-BBK32-G (3285 bp)	
HinfI	**2171**; 517; 396; 75; 65; 61
NdeI	2369; **916**
pUET1-BmpA-BBK32-M (3297 bp)	
HinfI	**2183**; 517; 396; 75; 65; 61
NdeI	2369; **928**

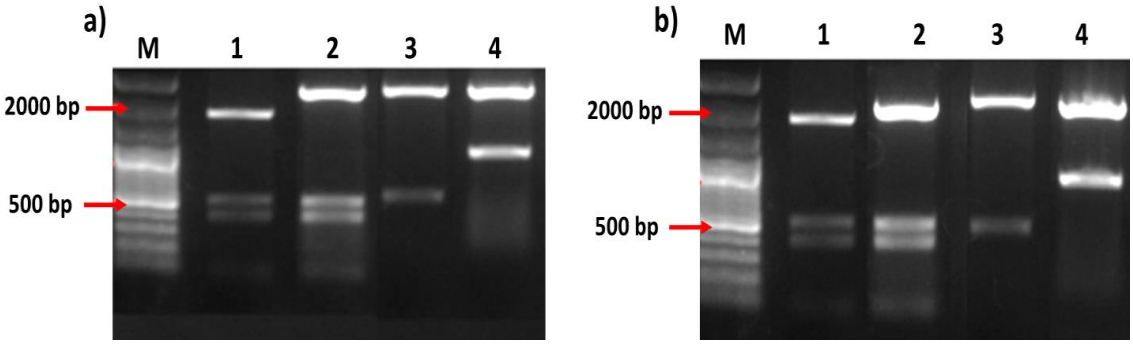

Figure 5. 30 Restriction analysis of potential recombinant plasmids: a) pUET1-BmpA-BBK32-G; b) pUET1-BmpA-BBK32-M. **Lanes:** M - GeneRuler 100 bp Plus DNA Ladder; 1 - pUET1 digested with HinfI (control); 2 - potential recombinant plasmids digested with HinfI; 3 - pUET1 digested with the NdeI (control); 4 - potential recombinant plasmids digested with NdeI.

Comparison of the migration of individual DNA fragments obtained during RA and the sequencing results allowed to conclude that recombinant plasmids encoding chimeric proteins BmpA-BBK32-G and BmpA-BBK32-M were successfully constructed (Figure 5.30; Table 5.16).

Table 5. 16 Characteristics of constructed recombinant plasmids encoding BmpA-BBK32-G and BmpA-BBK32-M multivalent chimeric proteins

Plasmid name	RE used in cloning	Plasmid size [bp]	Encoded multivalent protein	Encoded native antigen fragment [aa]
pUET1-BmpA-BBK32-G	BglII/BamHI HindIII	3285	BmpA-BBK32-G	• 18-70 BmpA • 135-179 BmpA • 293-311 BmpA • 21-35 BBK32 • 110-134 BBK32
pUET1-BmpA-BBK32-M	BglII/BamHI HindIII	3297	BmpA-BBK32-M	• 86-106 BmpA • 206-354 BBK32

RE - restriction enzyme

5.3.4. Construction of recombinant plasmids on pET32a and pET42a backbone

5.3.4.1. Molecular cloning

Vectors pET32a (5900 bp) and pET42a (5930 bp) [Materials 3.1] were digested with restriction enzymes BglII and XhoI [Materials 3.5; Methods 4.6] obtaining linear DNA fragments of 5817 bp and 5820 bp, respectively. Reaction products were separated in 1.5% agarose gel and purified using the Gel-Out Concentrator kit [Materials 3.10.2; Methods 4.5; Materials 3.7; Methods 4.10.1]. The inserts encoding the proper genes were excised from previously constructed plasmids pUET1-BB0126BA, pUET1-BmpA-BBA64, and pUET1-BmpA-BBK32 with the enzymes BglII and XhoI. This process resulted in linear DNA fragments of 652 bp (*bb0126BA*), 1249 bp (*bmpA-bba64*),

and 1306 bp (*bmpA-bbk32*) which were separated in agarose gels and purified [Materials 3.10.2; Methods 4.5; Materials 3.7; Methods 4.10.1].

The DNA of the inserts and pET32a and pET42a vectors prepared in this way was ligated [Materials 3.6; Methods 4.8.1]. The ligation mixtures were then used to transform competent *E. coli* TOP10F' cells which were plated on LBA medium with appropriate antibiotics [Materials 3.2; Methods 4.9]. For *E. coli* TOP10F' cells transformed with recombinant plasmids based on pET32a backbone, used tetracycline and ampicillin for pET42a [Materials 3.17].

The scheme of the construction of the recombinant plasmids on the example of pET42a-BB0126BA is shown in the Figure 5.31.

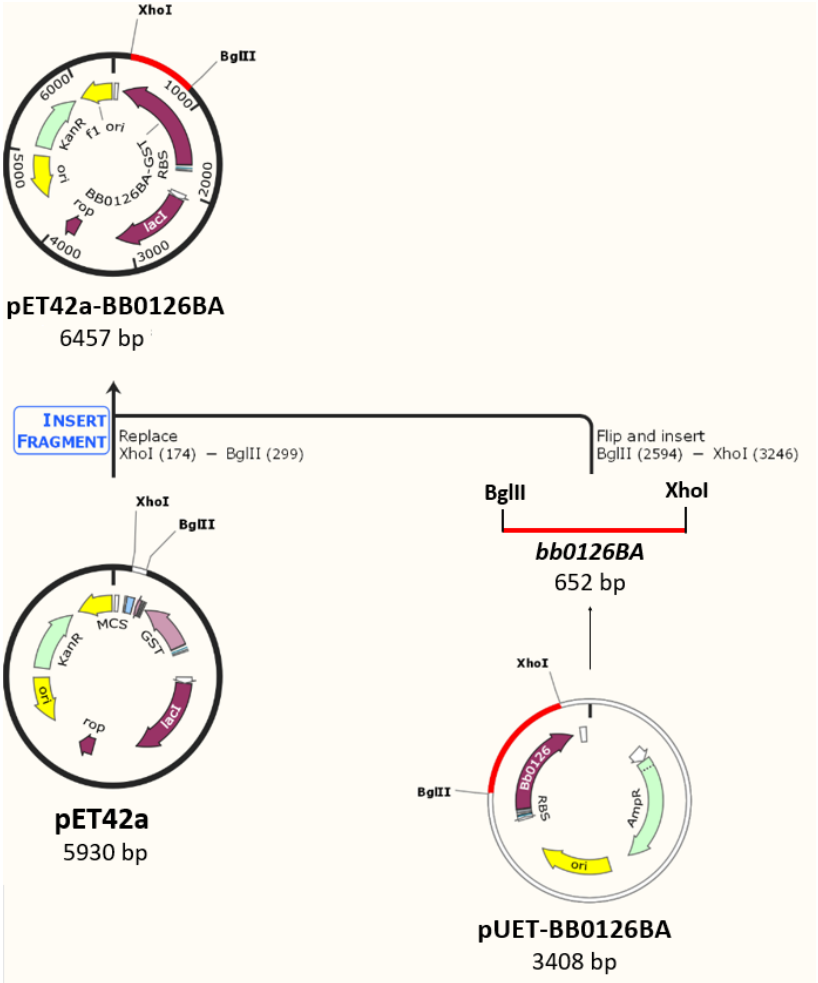

Figure 5. 31 Scheme of construction of pET42a-BB0126BA.

5.3.4.1. Identification of recombinant plasmids

Identification of recombinant plasmids was carried out in the same way as described in section 5.3.2.3. The only difference was using different antibiotics as selection markers depending on the backbone vector [Materials 3.1; Materials 3.17]. Tables 5.17 and 5.18 present the expected sizes of DNA fragments obtained during restriction analysis determined by SnapGene software. Figures 5.32-5.35 show

electrophoretic separations of products obtained during the digestion of potential recombinant plasmids with selected restriction enzymes.

Table 5. 17 The xpected size of DNA fragments generated by restriction analysis of recombinant plasmids based on pET32a backbone (sizes of DNA fragments characteristic to recombinant plasmids are bolded)

Restriction enzymes	DNA fragments size [bp]
pET32a (5900 bp)	
SacI	Linear form
XbaI	Linear form
NdeI	**5555**; 345
SmaI and XbaI	Linear form (no restriction site for SmaI)
pET32a-BB0126BA (6464 bp)	
SmaI and XbaI	**5401; 1068**
NdeI	**5529**; **595**; 345
pET32a-BmpA-BBA64 (7066 bp)	
SacI	**6127, 939**
XbaI	Linear form
pET32a-BmpA-BBK32 (7123 bp)	
SacI	Linear form
XbaI	**5756, 1367**

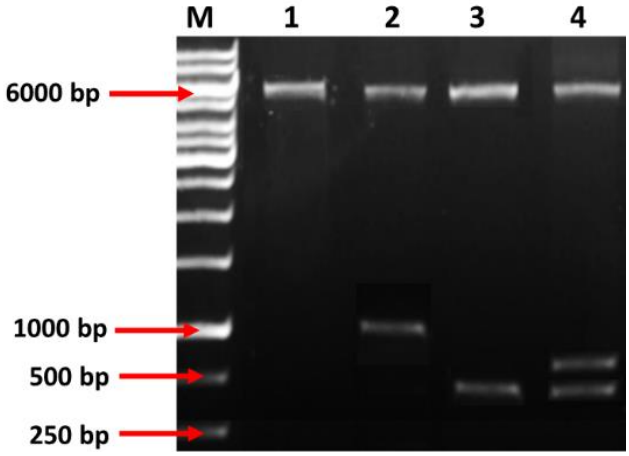

Figure 5. 32 Restriction analysis of potential recombinant plasmid pET32a-BB0126BA. **Lanes:** M - GeneRuler 1 kb DNA Ladder; 1 - pET32a digested with SmaI and XbaI (control); 2 - pET32a-BB0126BA digested with SmaI and XbaI; 3 - pET32a digested with NdeI (control); 4 - pET32a-BB0126BA digested with NdeI.

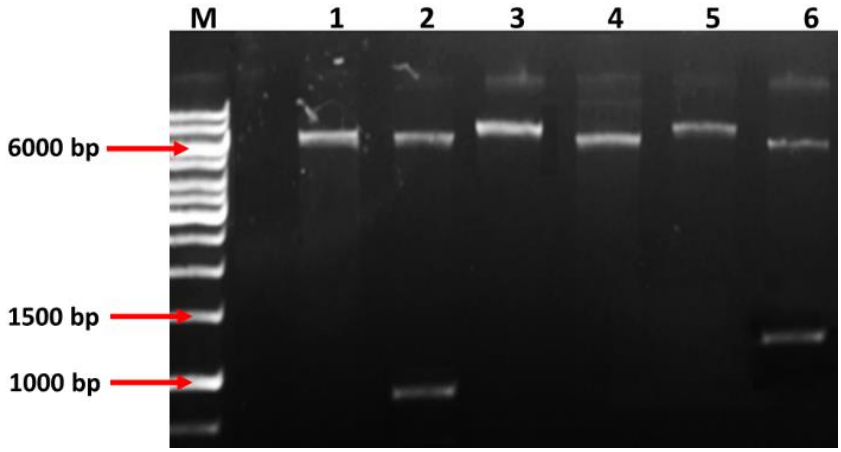

Figure 5. 33 Restriction analysis of potential recombinant plasmids pET32a-BmpA-BBA64 and pET32a-BmpA-BBK32. **Lanes:** M - GeneRuler 1 kb DNA Ladder; 1 - pET32a digested with SacI (control); 2 - pET32a-BmpA-BBA64 with SacI; 3 - pET32a-BmpA-BBK32 digested with SacI; 4 - pET32a digested with XbaI (control); 5 - pET32a-BmpA-BBA64 digested with XbaI; 6 - pET32a-BmpA-BBK32 digested with XbaI.

Table 5. 18 The expected size of DNA fragments generated by restriction analysis of recombinant plasmids based on pET42a backbone (sizes of DNA fragments characteristic to recombinant plasmids are bolded)

Restriction enzymes	DNA fragments size [bp]
pET42a (5930 pz)	
EcoRV	Linear form
XbaI	Linear form
NdeI and XhoI	5013; **917**
SmaI and XbaI	3732; **2198**
pET42a-BB0126BA (6457 bp)	
NdeI and XhoI	5013; **1282**
SmaI and XbaI	**3732**; **1410; 1315**
pET42a-BmpA-BBA64 (7054 bp)	
SmaI and XbaI	3732; **3322**
NdeI and XhoI	5013; **2041**
pET42a-BmpA-BBK32 (7111 bp)	
EcoRV	**6632**; **479**
XbaI	**5402**; **1709**

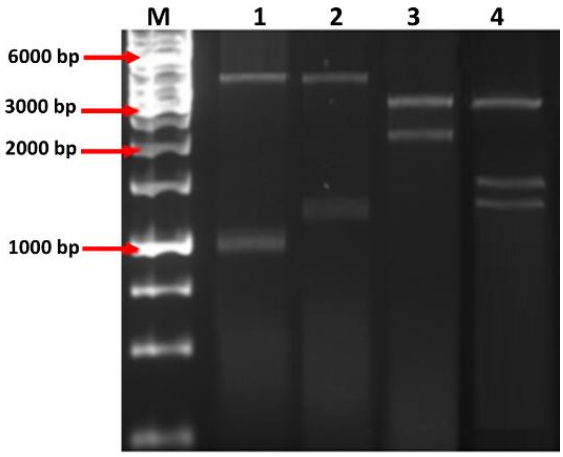

Figure 5. 34 Restriction analysis of potential recombinant plasmid pET42a-BB0126BA. **Lanes:** M - GeneRuler 1 kb DNA; 1 - pET42a digested with NdeI and XhoI (control); 2 - pET42a-BB0126BA digested with NdeI and XhoI; 3 - pET42a digested with SmaI and XbaI (control); 4 - pET42a-BB0126BA digested with SmaI and XbaI.

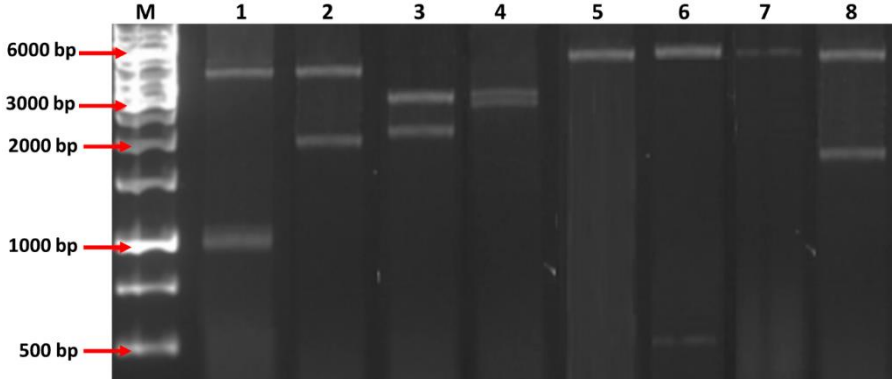

Figure 5. 35 Restriction analysis of potential recombinant plasmids pET42a-BmpA-BBA64 and pET42a-BmpA-BBK32. **Lanes:** M - GeneRuler 1 kb DNA Ladder; 1 - pET42a digested with NdeI and XhoI (control); 2 - pET42a-BmpA-BBA64 digested with NdeI and XhoI; 3 - pET42a digested with SmaI and XbaI (control); 4 - pET42a-BmpA-BBA64 digested with SmaI and XbaI; 5 - pET42a digested with EcoRV (control); 6 - pET42a-BmpA-BBK32 digested with EcoRV; 7 - pET42a digested with XbaI (control); 8 - pET42a - BmpA-BBK32 digested with XbaI.

Comparison of the migration rate of individual DNA fragments obtained during RA and the sequencing results allowed to conclude that recombinant plasmids pET32a-BB0126BA, pET32a-BmpA-BBA64, pET32a-BmpA-BBK32, pET42a-BB0126BA, pET42a-BmpA-BBA64 and pET42a-BmpA-BBK32 were successfully constructed (Table 5.19).

Table 5. 19 Characteristics of constructed recombinant plasmids based on pET32a and pET42a backbone

Plasmid name	RE used in cloning	Plasmid size [bp]	Encoded recombinant protein	Encoded native protein fragment [aa]
pET32a-BB0126BA	BglII XhoI	6469	BB0126BA-TrxA	• 22-203 BB0126BA
pET32a-BmpA-BBA64	BglII XhoI	7066	BmpA-BBA64-TrxA	• 44-325 BmpA • 171-302 BBA64
pET32a-BmpA-BBK32	BglII XhoI	7123	BmpA-BBK32-TrxA	• 44-325 BmpA • 204-354 BBK32
pET42a-BB0126BA	BglII XhoI	6457	BB0126BA-GST	• 22-203 BB0126BA
pET42a-BmpA-BBA64	BglII XhoI	7054	BmpA-BBA64-GST	• 44-325 BmpA • 171-302 BBA64
pET42a-BmpA-BBK32	BglII XhoI	7111	BmpA-BBK32-GST	• 44-325 BmpA • 204-354 BBK32

RE - restriction enzyme

5.4. Analysis of the amino acid sequence of monovalent and multivalent recombinant proteins encoded by the constructed plasmids

During this work, 19 recombinant plasmids based on pUET1 were obtained. 15 of them enabling the potential production of 5 monovalent *B. burgdorferi* s.l. recombinant proteins (BB0108, BB0126, BB0298, BB0323, BB0689) in three variants from the most widespread genospecies in Europe (*B. afzelii*, *B. burgdorferi* s.s., *B. garinii*). Whereas 4 of them encoded multivalent chimeric proteins BmpA-BBA64, BmpA-BBK32, BmpA-BBK32-G, and BmpA-BBK32-M. Moreover, the *bb0126BA*, *bmpA-bba64,* and *bmpA-bbk32* genes were cloned into pET32a and pET42a vectors to introduce additional fusion partners TrxA and GST, respectively.

A list of monovalent and multivalent recombinant proteins encoded by constructed plasmids, along with their characteristics, is presented in Tables 5.20-5.22. Molecular weights and isoelectric points were estimated by programs on the www.expasy.org [Methods 4.19]. The complete sequence of *B. burgdorferi* s.l. monovalent and multivalent recombinant proteins, including those with additional fusion domains, is shown in Figures 5.36-5.52 and 5.53-5.60, respectively.

Table 5. 20 Analysis of the amino acid sequence of monovalent recombinant proteins

Monovalent protein	Plasmid name	Protein length [aa]	Molecular mass [kDa]	pI	Domains
BB0108$_{BA}$	pUET1-BB0108BA	394	44.4	8.4	His-Tag, S-Tag
BB0108$_{BB}$	pUET1-BB0108BB	394	44.3	8.4	His-Tag, S-Tag
BB0108$_{BG}$	pUET1-BB0108BG	394	44.3	8.4	His-Tag, S-Tag
BB0126$_{BA}$	pUET1-BB0126BA	259	29.5	5.8	His-Tag, S-Tag
BB0126$_{BB}$	pUET1-BB0126BB	259	29.6	5.6	His-Tag, S-Tag
BB0126$_{BG}$	pUET1-BB0126BG	259	29.5	5.7	His-Tag, S-Tag
BB0298$_{BA}$	pUET1-BB0298BA	286	32.6	5.7	His-Tag, S-Tag
BB0298$_{BB}$	pUET1-BB0298BB	286	32.5	6.0	His-Tag, S-Tag
BB0298$_{BG}$	pUET1-BB0298BG	286	32.6	5.8	His-Tag, S-Tag
BB0323$_{BA}$	pUET1-BB0323BA	434	50.5	8.7	His-Tag, S-Tag
BB0323$_{BB}$	pUET1-BB0323BB	432	50.2	8.51	His-Tag, S-Tag
BB0323$_{BG}$	pUET1-BB0323G	431	50.1	8.8	His-Tag, S-Tag
BB0689$_{BA}$	pUET1-BB0689BA	202	22.9	7.0	His-Tag, S-Tag
BB0689$_{BB}$	pUET1-BB0689BB	202	22.9	6.5	His-Tag, S-Tag
BB0689$_{BG}$	pUET1-BB0689BG	202	22.9	7.0	His-Tag, S-Tag

Table 5. 21 Analysis of the amino acid sequence of multivalent chimeric proteins

Multivalent protein	Plasmid name	Protein length [aa]	Molecular mass [kDa]	pI	Domains
BmpA-BBA64	pUET1-BmpA-BBA64	458	51.0	5.8	His-Tag, S-Tag
BmpA-BBK32	pUET1- BmpA-BBK32	477	53.5	6.7	His-Tag, S-Tag
BmpA-BBK32-G	pUET1-BmpA-BBK32-G	218	23.6	6.4	His-Tag, S-Tag
BmpA-BBK32-M	pUET1-BmpA-BBK32-M	222	25.3	9.2	His-Tag, S-Tag

Table 5. 22 Analysis of the amino acid sequence of monovalent and multivalent recombinant proteins with additional domains

Recombinant protein	Plasmid name	Protein length [aa]	Molecular mass [kDa]	pI	Domains
BB0126$_{BA}$-TrxA	pET32a-BB0126BA	341	38.5	5.9	His-Tag, S-Tag, TrxA
BB0126$_{BA}$-GST	pET42a-BB0126BA	457	52.9	6.3	His-Tag, S-Tag, GST
BmpA-BBA64-TrxA	pET32a-BmpA-BBA64	573	63.3	5.6	His-Tag, S-Tag, TrxA
BmpA-BBA64-GST	pET42a-BmpA-BBA64	689	77.8	5.9	His-Tag, S-Tag, GST
BmpA-BBK32-TrxA	pET32a-BmpA-BBK32	592	65.7	6.2	His-Tag, S-Tag, TrxA
BmpA-BBK32-GST	pET42a-BmpA-BBK32	708	80.1	6.5	His-Tag, S-Tag, GST

```
  1-60 MHHHHHHSSG LVPRGSGMKE TAAAKFERQH MDSPDPQNTP VAIINLYKNE IITKTSFDSK
 61-120 VDIFKKTQGR DLTAAEKKQV LQVLIADVLF SQEASKQGIK ISDDEVMQTI RTQFGLVNFT
121-180 DEQIKQMIEK QGTNWGELLS SMKRSLSSQK LVLKQAQPRF SEVKTPSEKE IIEYYEANKT
181-240 RFVNPDISRV SHVFFSTKDK KRSDVLDQAK NILSQIRSKK ITFEEAVRKY SNDESSKAKN
241-300 GDLGFLSRDD QNAQNLLGPD FIKEVFNFNK GDISSPIASK EGFHIVKVTE KYAQRFLGLN
301-360 DKVSPATDLI VKDAIRNNMV NIQQQQIVVQ VQQDVYGKLN KSASIQILDS SLKDLGTDDD
361-394 DKSPGFSSTM AISDPNSSSV DKLAAALEHH HHHH
```

Figure 5. 36 Amino acid sequence of the BB0108$_{BA}$ monovalent recombinant protein. The sequence derived from the pUET1 vector is marked in black and the His-tag sequence within it is marked in green; the S-Tag domain in orange; fragment of the BB0108$_{BA}$ is marked in blue.

```
  1-60 MHHHHHHSSG LVPRGSGMKE TAAAKFERQH MDSPDPQNTP VAIINLYKNE IITKTSFDSK
 61-120 VDIFKKTQGR DLTAAEKKQV LQVLIADVLF SQEASKQGIK ISDDEVMQTI RTQFGLVNFT
121-180 DEQIKQMIEK QGTNWGELLS SMKRSLSSQK LVLKQAQPRF SEVKTPSEKE IIEYYEANKT
181-240 RFVNPDISRV SHVFFSTKDK KRSDVLDQAK NILSQIRSKK ITFEEAVRKY SNDESSKAKN
241-300 GDLGFLSRDD QNAQNLLGPD FIKEVFNFNK GDISSPIASK EGFHIVKVTE KYAQRFLGLN
301-360 DKVSPATDLI VKDAIRNNMV NIQQQQIVVQ VQQDVYGKLN KSASIQILDS SLKDLGTDDD
361-394 DKSPGFSSTM AISDPNSSSV DKLAAALEHH HHHH
```

Figure 5. 37 Amino acid sequence of the BB0108$_{BB}$ monovalent recombinant protein. The sequence derived from the pUET1 vector is marked in black and the His-tag sequence within it is marked in green; the S-Tag domain in orange; fragment of the BB0108$_{BB}$ is marked in blue.

```
  1-60  MHHHHHHSSG LVPRGSGMKE TAAAKFERQH MDSPDPQNTP VAIINLYKNE IITKTGFDSK
 61-120  VDIFKKTQGR DLTAAEKKQV LQVLIADVLF SQEASKQGIK ISDDEVMQTI RTQFGLVNLT
121-180  DEQIKQMIEK QGTNWGELLA SMKRSLSSQK LVLKQAQPRF SEVKTPSEKE IVEYYEANKT
181-240  KFVNPDISRV SHVFFSTKDK KRSEVLDQAK NILSQIRSKK ITFEEAVRKY SNDESSKAKN
241-300  GDLGFLSRGD QNAQNLLGAD FIKEVFNFNK GDISSPIASK EGFHIIKVTE KYAQRFLGLN
301-360  DKVSPTTDLI VKDAIRNNMV NIQQQQIVVE VQQDVYSKLN KSANIQILDS SLKDLGTDDD
361-394  DKSPGFSSTM AISDPNSSSV DKLAAALEHH HHHH
```

Figure 5. 38 Amino acid sequence of the BB0108$_{BG}$ monovalent recombinant protein. The sequence derived from the pUET1 vector is marked in black and the His-tag sequence within it is marked in green; the S-Tag domain in orange; fragment of the BB0108$_{BG}$ is marked in blue.

```
  1-60 MHHHHHHSSG LVPRGSGMKE TAAAKFERQH MDSPDLVVFY NSLSKDYVKS GGEIVENLEK
 61-120 DLNDYLKEND AKEREKISLR IKELILKEKE ISSYFISRFY LAKAVYLQSQ SQYDEAIKDL
121-180 DIVIKAKGIE SEIAFINKAT IYEKMGLKED ALLVYEDLIK NTSLGFLKVR ALLSKAILIE
181-240 EKDKDLAVKV YEEIVKFPYE NNLYINIANN KILELKQNDL GTDDDDKSPG FSSTMAISDP
241-259 NSSSVDKLAA ALEHHHHHH
```

Figure 5. 39 Amino acid sequence of the BB0126$_{BA}$ monovalent recombinant protein. The sequence derived from the pUET1 vector is marked in black and the His-tag sequence within it is marked in green; the S-Tag domain in orange; fragment of the BB0126$_{BA}$ is marked in blue.

```
  1-60 MHHHHHHSSG LVPRGSGMKE TAAAKFERQH MDSPDLVVFY NSLGKDYVKS GGEIVENLEK
 61-120 DLNDYLKEND AKEREKIFLR IRELISKEKE ISSYFISRFY LARAVYFQSQ AQYDEAIKDL
121-180 DIVIKAKGIE SEIAFLNKAA VYEKMGLKED ALLVYEDLIN STSLDFLKVR ALLSKAILIE
181-240 EKDKELAVKV YEEIVKFPYE NNLYINMANN KILELKQNDL GTDDDDKSPG FSSTMAISDP
241-259 NSSSVDKLAA ALEHHHHHH
```

Figure 5. 40 Amino acid sequence of the BB0126$_{BB}$ monovalent recombinant protein. The sequence derived from the pUET1 vector is marked in black and the His-tag sequence within it is marked in green; the S-Tag domain in orange; fragment of the BB0126$_{BB}$ is marked in blue.

```
  1-60 MHHHHHHSSG LVPRGSGMKE TAAAKFERQH MDSPDLVVFY NSLGKDYVKS GGEIVENLEK
 61-120 DLNDYLKEND TKEREKISLR IKELISKEKE ISSYFISRFY LARAFYLQSQ AQYDEAIKDL
121-180 DIVIKAKGIE SEIAFINKAA VYEKMGLKED ALLVYEELIN STSLGFLKVR ALLSKAILIE
181-240 EKDKDLAVKV YEEIVKFPYE NNLYINIANN KILELKQNDL GTDDDDKSPG FSSTMAISDP
241-259 NSSSVDKLAA ALEHHHHHH
```

Figure 5. 41 Amino acid sequence of the BB0126$_{BG}$ monovalent recombinant protein. The sequence derived from the pUET1 vector is marked in black and the His-tag sequence within it is marked in green; the S-Tag domain in orange; fragment of the BB0126$_{BG}$ is marked in blue.

```
  1-60 MHHHHHHSSG LVPRGSGMKE TAAAKFERQH MDSPDRGSES KEKLNLGLRL RELEISGGGS
 61-120 ESKIEVYKEF IEKEDKNILK IVNSIDKKAR FFNLIGLEFF KLSQYGPAIE YFTKNLEINS
121-180 DNYLSHFYVG VASYNLAKNL RVKDEVEKYI ILAENSFLKS LSIRDDFKES LFAISNMYVY
181-240 DLDKQLEAKN YLNKLEDMGE DYFEFFMLRG ANYYSLGDLG NAILFYDKAS KNASTEEQKE
241-286 GVSRIDLGTD DDDKSPGFSS TMAISDPNSS SVDKLAAALE HHHHHH
```

Figure 5. 42 Amino acid sequence of the BB0298$_{BA}$ monovalent recombinant protein. The sequence derived from the pUET1 vector is marked in black and the His-tag sequence within it is marked in green; the S-Tag domain in orange; fragment of the BB0298$_{BA}$ is marked in blue.

```
  1-60 MHHHHHHSSG LVPRGSGMKE TAAAKFERQH MDSPDRGNES KEKSNLGLRL RELEISGGGS
 61-120 ESKIEVYKEF IEKEDKNILK IVNSIDKKAR FFNLIGLEFF KLGQYGPAIE YFAKNLEINP
121-180 NNYLSHFYIG VASYNLAKNL RVKDEVEKYI ILAENSFLKS LSIRDDFKDS LFAISNMYVY
181-240 DLDKQLEAKN YLNKLGDMGE DYFEFLMLRG ANYYSLGDLG NAILFYDKAS KKASTEEQKE
241-286 GVSRIDLGTD DDDKSPGFSS TMAISDPNSS SVDKLAAALE HHHHHH
```

Figure 5. 43 Amino acid sequence of the BB0298$_{BB}$ monovalent recombinant protein. The sequence derived from the pUET1 vector is marked in black and the His-tag sequence within it is marked in green; the S-Tag domain in orange; fragment of the BB0298$_{BB}$ is marked in blue.

```
  1-60 MHHHHHHSSG LVPRGSGMKE TAAAKFERQH MDSPDRGSES KEKLNLGLRL RELEISGGGS
 61-120 ESKIEVYKEF IEKEDKNILK IVNSIDKKAR FFNLIGLEFF KLGQYGPAIE YFVKNLEINS
121-180 NNYLSHFYIG VASYNLAKNL RVKDEVEKYI ILAENSFLKS LSIRDDFKDS LFAISNMYVY
181-240 DLDKQLEAKN YLNKLDDMGE DYFEFFMLRG ANYYSLGDLG NAILFYEKAS KNASTEEQKE
241-286 GVSRIDLGTD DDDKSPGFSS TMAISDPNSS SVDKLAAALE HHHHHH
```

Figure 5. 44 Amino acid sequence of the BB0298$_{BG}$ monovalent recombinant protein. The sequence derived from the pUET1 vector is marked in black and the His-tag sequence within it is marked in green; the S-Tag domain in orange; fragment of the BB0298$_{BG}$ is marked in blue.

```
  1-60 MHHHHHHSSG LVPRGSGMKE TAAAKFERQH MDSPDRKTPP EARESKNAKI AQPNNEIFQL
 61-120 RDLKDIKNEL IRERGHLFYS KEFNEAERLE EAMKQNFSKK KAKEGNEIAL KVLERYKTII
121-180 KETKEKKEKT NYLKENIEKY LNDAEANEAY IWIPLEIDEV NNLYFEATRK YKNYDLDNAL
181-240 DMYSKAFNRA QQAAKNAKEA KALKETDERM YKQLKALEAA SNLPVYSNNK LIKPSPWNGR
241-300 AFIKERNGHL NLLNINAEDT YFLGETKTST PIVLAYEEKM EIAKTSNPQE QFKTLELIEQ
301-360 SRKLWEKGVE AKNVKNFRLA NELFLESARY LEAYQSNASS ELYVIKIGNT LWGISKKLYN
361-420 DPYLWPKIWF ANRQKIQNPD LIHSNWKIII PAKDLGTDDD DKSPGFSSTM AISDPNSSSV
421-434 DKLAAALEHH HHHH
```

Figure 5. 45 Amino acid sequence of the BB0323$_{BA}$ monovalent recombinant protein. The sequence derived from the pUET1 vector is marked in black and the His-tag sequence within it is marked in green; the S-Tag domain in orange; fragment of the BB0323$_{BA}$ is marked in blue.

```
  1-60 MHHHHHHSSG LVPRGSGMKE TAAAKFERQH MDSPDQTPPE SRESKNAKIA QPDNKNFQLR
 61-120 DIKDIKNELI RERGHLFYSK EFNEAERLEE AMKQSFSKKK AIEGNEIALK VLERYKTIIR
121-180 ETREKKEKTN YLKENIEKYL NDAEANEAYI WIPLEIDEVN NLYFEATRKY KNYDLDNALD
181-240 MYSKAFNRAQ QAAKNAKEAK ALKETDERMY KQLKALEAAS NLPIYSNNKL IKPSPWNGRA
241-300 FIKERNSHLN LLNTNKDTYL LGEAEISIPI VLAYEEKVEI AKNSKPQEQF KTLELIERSR
301-360 TLWEKGVEAK NVKNFRLANE LFLESARYLE AYQSNASSEL YVIKIGNTLW GISKKLYNDP
361-420 YLWPKIWFAN RQKIQNPDLI HSNWKIIIPA KDLGTDDDDK SPGFSSTMAI SDPNSSSVDK
421-432 LAAALEHHHH HH
```

Figure 5. 46 Amino acid sequence of the BB0323$_{BB}$ monovalent recombinant protein. The sequence derived from the pUET1 vector is marked in black and the His-tag sequence within it is marked in green; the S-Tag domain in orange; fragment of the BB0323$_{BB}$ is marked in blue.

```
  1-60 MHHHHHHSSG LVPRGSGMKE TAAAKFERQH MDSPDHTTPP EARENKNAKI AKLDTKSFEL
 61-120 RDIKDIKNEL IKERGHLFYS KEFNEAEKLE EAMKQNFSKK KAKEINEIAL KVIERYKTII
121-180 KETREKKEKV NYLKENIEKY LNDAEANEAY IWIPLEIDEV NNLYFEATRK YKNYDLDDAL
181-240 GMYSKAFNRA QQAAKNAKEA KALKETDERM YKQLKALEAA SNLPIYSNNK LIKPSPWNGR
241-300 AFIKERNSRL NLLNINEDTY LLGETETPIV LAYTEKLEIA KNSKPQEQFK TLELIERSRK
301-360 LWEKGVEAKH VKNFRLANEL FLESARYLEA YQSNASSELY VIKIGNTLWG ISKKLYNDPY
361-420 LWPKIWFANR QKIQNPDLIH SNWKIIIPAK DLGTDDDDKS PGFSSTMAIS DPNSSSVDKL
421-431 AAALEHHHHH H
```

Figure 5. 47 Amino acid sequence of the BB0323$_{BG}$ monovalent recombinant protein. The sequence derived from the pUET1 vector is marked in black and the His-tag sequence within it is marked in green; the S-Tag domain in orange; fragment of the BB0323$_{BG}$ is marked in blue.

```
  1-60 MHHHHHHSSG LVPRGSGMKE TAAAKFERQH MDSPDREDMK ILYSEIAKLR KNLNLNHLEI
 61-120 DDILEKVAKE YAIKLGENKT LTHTLFGTTP MQRIHKYDKS FNLTREILAS GIELNRVVDA
121-180 WLNSPSHKEA LINTDTTKIG GYRLKTDNNI NIFVVLFGKR KDLGTDDDDK SPGFSSTMAI
181-202 SDPNSSSVDK LAAALEHHHH HH
```

Figure 5. 48 Amino acid sequence of the BB0689$_{BA}$ monovalent recombinant protein. The sequence derived from the pUET1 vector is marked in black and the His-tag sequence within it is marked in green; the S-Tag domain in orange; fragment of the BB0689$_{BA}$ is marked in blue.

```
  1-60 MHHHHHHSSG LVPRGSGMKE TAAAKFERQH MDSPDREDMK ILYSEIAELR KKLNLNHLEI
 61-120 DDTLEKVAKE YAIKLGENRT ITHTLFGTTP MQRIHKYDQS FNLTREILAS GIELNRVVNA
121-180 WLNSPSHKEA LINTDTDKIG GYRLKTTDNI DIFVVLFGKR KDLGTDDDDK SPGFSSTMAI
181-202 SDPNSSSVDK LAAALEHHHH HH
```

Figure 5. 49 Amino acid sequence of the BB0689$_{BB}$ monovalent recombinant protein. The sequence derived from the pUET1 vector is marked in black and the His-tag sequence within it is marked in green; the S-Tag domain in orange; fragment of the BB0689$_{BB}$ is marked in blue.

```
  1-60 MHHHHHHSSG LVPRGSGMKE TAAAKFERQH MDSPDREDMK ILYSEIAELR KKLNLNHLEI
 61-120 DDTLEKVAKE YAIKLGENKT LTHTLFGTSP MTRIHKYDKS FNLTREILAS GIELDRVVDA
121-180 WLKSPSHKEA LINKDTDKIG GYRLKTNNNI NIFVVLFGKR KDLGTDDDDK SPGFSSTMAI
181-202 SDPNSSSVDK LAAALEHHHH HH
```

Figure 5. 50 Amino acid sequence of the BB0689$_{BG}$ monovalent recombinant protein. The sequence derived from the pUET1 vector is marked in black and the His-tag sequence within it is marked in green; the S-Tag domain in orange; fragment of the BB0689$_{BG}$ is marked in blue.

```
  1-60 MSDKIIHLTD DSFDTDVLKA DGAILVDFWA EWCGPCKMIA PILDEIADEY QGKLTVAKLN
 61-120 IDQNPGTAPK YGIRGIPTLL LFKNGEVAAT KVGALSKGQL KEFLDANLAG SGSGHMHHHH
121-180 HHSSGLVPRG SGMKETAAAK FERQHMDSPD LVVFYNSLSK DYVKSGGEIV ENLEKDLNDY
181-240 LKENDAKERE KISLRIKELI LKEKEISSYF ISRFYLAKAV YLQSQSQYDE AIKDLDIVIK
241-301 AKGIESEIAF INKATIYEKM GLKEDALLVY EDLIKNTSLG FLKVRALLSK AILIEEKDKD
301-341 LAVKVYEEIV KFPYENNLYI NIANNKILEL KQNLEHHHHH H
```

Figure 5. 51 Amino acid sequence of the BB0126$_{BA}$-TrxA monovalent recombinant protein. The sequence derived from the Pet32a vector is marked in black and the His-tag sequence within it is marked in green; the S-Tag domain in orange; TrxA domain in red; fragment of the BB0126$_{BA}$ is marked in blue.

```
  1-60 MSPILGYWKI KGLVQPTRLL LEYLEEKYEE HLYERDEGDK WRNKKFELGL EFPNLPYYID
 61-120 GDVKLTQSMA IIRYIADKHN MLGGCPKERA EISMLEGAVL DIRYGVSRIA YSKDFETLKV
121-180 DFLSKLPEML KMFEDRLCHK TYLNGDHVTH PDFMLYDALD VVLYMDPMCL DAFPKLVCFK
181-240 KRIEAIPQID KYLKSSKYIA WPLQGWQATF GGGDHPPKSD GSTSGSGHHH HHHSAGLVPR
241-300 GSTAIGMKET AAAKFERQHM DSPDLVVFYN SLSKDYVKSG GEIVENLEKD LNDYLKENDA
301-360 KEREKISLRI KELILKEKEI SSYFISRFYL AKAVYLQSQS QYDEAIKDLD IVIKAKGIES
361-420 EIAFINKATI YEKMGLKEDA LLVYEDLIKN TSLGFLKVRA LLSKAILIEE KDKDLAVKVY
421-457 EEIVKFPYEN NLYINIANNK ILELKQNLEH HHHHHHH
```

Figure 5. 52 Amino acid sequence of the BB0126$_{BA}$-GST monovalent recombinant protein. The sequence derived from the pET42a vector is marked in black and the His-tag sequence within it is marked in green; the S-Tag domain in orange and the GST domain in red; fragment of the BB0126$_{BA}$ is marked in blue.

```
  1-60 MHHHHHHSSG LVPRGSGMKE TAAAKFERQH MDSPDLEFKI ELVLKESSSN SYLSDLEGLK
 61-120 DAGSDLIWLI GYRFSDVAKV AALQNPDMKY AIIDPIYSND PIPANLVGMT FRAQEGAFLT
121-180 GYIAAKLSKT GKIGFLGGIE GEIVDAFRYG YEAGAKYANK DIKISTQYIG SFADLEAGRS
181-240 VATRMYSDEI DIIHHAAGLG GIGAIEVAKE LGSGHYIIGV DEDQAYLAPD NVITSTTKDV
241-300 GRALNIFTSN HLKTNTFEGG KLINYGLKEG VVGFVRNPKM ISFELEKEID NLSSKIINKE
301-360 IIVPSNKESY EKFLKEFINL GQILSKLSQD SNYRGLVKET LINRGFSIQL AMEEISAKIL
361-420 NVKDKLQQLN KPNLETLYND FEKLTSLKEK WLKDTDDLID EYNTNPDLQT DVSKLNDTLR
421-458 SKNSRAQFAN IHDIILDLVN TTTNILAPIQ LEHHHHHH
```

Figure 5. 53 Amino acid sequence of the BmpA-BBA64 multivalent chimeric protein. The sequence derived from the pUET1 vector is marked in black and the His-tag sequence within it is marked in green; the S-Tag domain in orange; the fragment from the BmpA antigen is marked in blue, and the fragment of the BBA64 protein is in violet.

```
  1-60 MHHHHHHSSG LVPRGSGMKE TAAAKFERQH MDSPDLEFKI ELVLKESSSN SYLSDLEGLK
 61-120 DAGSDLIWLI GYRFSDVAKV AALQNPDMKY AIIDPIYSND PIPANLVGMT FRAQEGAFLT
121-180 GYIAAKLSKT GKIGFLGGIE GEIVDAFRYG YEAGAKYANK DIKISTQYIG SFADLEAGRS
181-240 VATRMYSDEI DIIHHAAGLG GIGAIEVAKE LGSGHYIIGV DEDQAYLAPD NVITSTTKDV
241-300 GRALNIFTSN HLKTNTFEGG KLINYGLKEG VVGFVRNPKM ISFELEKEID NLSSKIINKE
301-360 IIVPSNKESY EKFLKEFIRL SNRYQSYLEG VKYNVDSAIQ TITKIYNTYT LFSTKLTQMY
361-420 STRLDNFAKA KAKEEAAKFT KEDLEKNFKT LLNYIQVSVK TAANFVYIND THAKRKLENI
421-477 EAEIKTLIAK IKEQSNLYEA YKAIVTSILL MRDSLKEVQG IIDKNGVWYL EHHHHHH
```

Figure 5. 54 Amino acid sequence of the BmpA-BBK32 multivalent chimeric protein. The sequence derived from the pUET1 vector is marked in black and the His-tag sequence within it is marked in green; the S-Tag domain in orange; the fragment from the BmpA antigen is marked in blue, and the fragment of the BBK32 protein is in violet.

```
  1-60 MHHHHHHSSG LVPRGSGMKE TAAAKFERQH MDSPDPCSGK GSLGSEIPKV SLIIDGTFDD
 61-120 KSFNESALNG VKKVKEEFKI ELVLKESSSG GGQEGAFLTG YIAAKLSKTG KIGFLGGIEG
121-180 EIVDAFRYGY EAGAKYAGGG VGFVRNPKMI SFELEKEIDG GGDLFIRYEM KEESPGLGGG
181-218 EQSETRKEKI QKQQDEYKGM TQGSLKLAAA LEHHHHHH
```

Figure 5. 55 Amino acid sequence of the BmpA-BBK32-G multivalent chimeric protein. The sequence derived from the pUET1 vector is marked in black and the His-tag sequence within it is marked in green; the S-Tag domain in orange; the fragment from the BmpA antigen is marked in blue, and the fragment of the BBK32 protein is in violet, glycine linkers are marked in red.

```
  1-60 MHHHHHHSSG LVPRGSGMKE TAAAKFERQH MDSPDPDLIW LIGYRFSDVA KVAALQNGGG
 61-120 SNRYQSYLEG VKYNVDSAIQ TITKIYNTYT LFSTKLTQMY STRLDNFAKA KAKEEAAKFT
121-180 KEDLEKNFKT LLNYIQVSVK TAANFVYIND THAKRKLENI EAEIKTLIAK IKEQSNLYEA
181-222 YKAIVTSILL MRDSLKEVQG IIDKNGVWYK LAAALEHHHH HH
```

Figure 5. 56 Amino acid sequence of the BmpA-BBK32-M multivalent chimeric protein. The sequence derived from the pUET1 vector is marked in black and the His-tag sequence within it is marked in green; the S-Tag domain in orange; the fragment from the BmpA antigen is marked in blue, and the fragment of the BBK32 protein is in violet, glycine linkers are marked in red.

```
  1-60 MSDKIIHLTD DSFDTDVLKA DGAILVDFWA EWCGPCKMIA PILDEIADEY QGKLTVAKLN
 61-120 IDQNPGTAPK YGIRGIPTLL LFKNGEVAAT KVGALSKGQL KEFLDANLAG SGSGHMHHHH
121-180 HHSSGLVPRG SGMKETAAAK FERQHMDSPD LEFKIELVLK ESSSNSYLSD LEGLKDAGSD
181-240 LIWLIGYRFS DVAKVAALQN PDMKYAIIDP IYSNDPIPAN LVGMTFRAQE GAFLTGYIAA
241-300 KLSKTGKIGF LGGIEGEIVD AFRYGYEAGA KYANKDIKIS TQYIGSFADL EAGRSVATRM
301-360 YSDEIDIIHH AAGLGGIGAI EVAKELGSGH YIIGVDEDQA YLAPDNVITS TTKDVGRALN
361-420 IFTSNHLKTN TFEGGKLINY GLKEGVVGFV RNPKMISFEL EKEIDNLSSK IINKEIIVPS
421-480 NKESYEKFLK EFINLGQILS KLSQDSNYRG LVKETLINRG FSIQLAMEEI SAKILNVKDK
481-540 LQQLNKPNLE TLYNDFEKLT SLKEKWLKDT DDLIDEYNTN PDLQTDVSKL NDTLRSKNSR
541-573 AQFANIHDII LDLVNTTTNI LAPIQLEHHH HHH
```

Figure 5. 57 Amino acid sequence of the BmpA-BBA64-TrxA multivalent chimeric protein. The sequence derived from the pET32a vector is marked in black and the His-tag sequence within it is marked in green; the S-Tag domain in orange; TrxA domain in red; the fragment from the BmpA antigen is marked in blue, and the fragment of the BBA64 protein is in violet.

```
  1-60 MSPILGYWKI KGLVQPTRLL LEYLEEKYEE HLYERDEGDK WRNKKFELGL EFPNLPYYID
 61-120 GDVKLTQSMA IIRYIADKHN MLGGCPKERA EISMLEGAVL DIRYGVSRIA YSKDFETLKV
121-180 DFLSKLPEML KMFEDRLCHK TYLNGDHVTH PDFMLYDALD VVLYMDPMCL DAFPKLVCFK
181-240 KRIEAIPQID KYLKSSKYIA WPLQGWQATF GGGDHPPKSD GSTSGSGHHH HHHSAGLVPR
241-300 GSTAIGMKET AAAKFERQHM DSPDLEFKIE LVLKESSSNS YLSDLEGLKD AGSDLIWLIG
301-360 YRFSDVAKVA ALQNPDMKYA IIDPIYSNDP IPANLVGMTF RAQEGAFLTG YIAAKLSKTG
361-420 KIGFLGGIEG EIVDAFRYGY EAGAKYANKD IKISTQYIGS FADLEAGRSV ATRMYSDEID
421-480 IIHHAAGLGG IGAIEVAKEL GSGHYIIGVD EDQAYLAPDN VITSTTKDVG RALNIFTSNH
481-540 LKTNTFEGGK LINYGLKEGV VGFVRNPKMI SFELEKEIDN LSSKIINKEI IVPSNKESYE
541-600 KFLKEFINLG QILSKLSQDS NYRGLVKETL INRGFSIQLA MEEISAKILN VKDKLQQLNK
601-660 PNLETLYNDF EKLTSLKEKW LKDTDDLIDE YNTNPDLQTD VSKLNDTLRS KNSRAQFANI
661-689 HDIILDLVNT TTNILAPIQL EHHHHHHHH
```

Figure 5. 58 Amino acid sequence of the BmpA-BBA64-GST multivalent chimeric protein. The sequence derived from the pET42a vector is marked in black and the His-tag sequence within it is marked in green; the S-Tag domain in orange; GST domain in red; the fragment from the BmpA antigen is marked in blue, and the fragment of the BBA64 protein is in violet.

```
  1-60 MSDKIIHLTD DSFDTDVLKA DGAILVDFWA EWCGPCKMIA PILDEIADEY QGKLTVAKLN
 61-120 IDQNPGTAPK YGIRGIPTLL LFKNGEVAAT KVGALSKGQL KEFLDANLAG SGSGHMHHHH
121-180 HHSSGLVPRG SGMKETAAAK FERQHMDSPD LEFKIELVLK ESSSNSYLSD LEGLKDAGSD
181-240 LIWLIGYRFS DVAKVAALQN PDMKYAIIDP IYSNDPIPAN LVGMTFRAQE GAFLTGYIAA
241-300 KLSKTGKIGF LGGIEGEIVD AFRYGYEAGA KYANKDIKIS TQYIGSFADL EAGRSVATRM
301-360 YSDEIDIIHH AAGLGGIGAI EVAKELGSGH YIIGVDEDQA YLAPDNVITS TTKDVGRALN
361-420 IFTSNHLKTN TFEGGKLINY GLKEGVVGFV RNPKMISFEL EKEIDNLSSK IINKEIIVPS
421-480 NKESYEKFLK EFIRLSNRYQ SYLEGVKYNV DSAIQTITKI YNTYTLFSTK LTQMYSTRLD
481-540 NFAKAKAKEE AAKFTKEDLE KNFKTLLNYI QVSVKTAANF VYINDTHAKR KLENIEAEIK
541-592 TLIAKIKEQS NLYEAYKAIV TSILLMRDSL KEVQGIIDKN GVWYLEHHHH HH
```

Figure 5. 59 Amino acid sequence of the BmpA-BBK32-TrxA multivalent chimeric protein. The sequence derived from the pET32a vector is marked in black and the His-tag sequence within it is marked in green; the S-Tag domain in orange; TrxA domain in red; the fragment from the BmpA antigen is marked in blue, and the fragment of the BBK32 protein is in violet.

```
  1-60 MSPILGYWKI KGLVQPTRLL LEYLEEKYEE HLYERDEGDK WRNKKFELGL EFPNLPYYID
 61-120 GDVKLTQSMA IIRYIADKHN MLGGCPKERA EISMLEGAVL DIRYGVSRIA YSKDFETLKV
121-180 DFLSKLPEML KMFEDRLCHK TYLNGDHVTH PDFMLYDALD VVLYMDPMCL DAFPKLVCFK
181-240 KRIEAIPQID KYLKSSKYIA WPLQGWQATF GGGDHPPKSD GSTSGSGHHH HHHSAGLVPR
241-300 GSTAIGMKET AAAKFERQHM DSPDLEFKIE LVLKESSSNS YLSDLEGLKD AGSDLIWLIG
301-360 YRFSDVAKVA ALQNPDMKYA IIDPIYSNDP IPANLVGMTF RAQEGAFLTG YIAAKLSKTG
361-420 KIGFLGGIEG EIVDAFRYGY EAGAKYANKD IKISTQYIGS FADLEAGRSV ATRMYSDEID
421-480 IIHHAAGLGG IGAIEVAKEL GSGHYIIGVD EDQAYLAPDN VITSTTKDVG RALNIFTSNH
481-540 LKTNTFEGGK LINYGLKEGV VGFVRNPKMI SFELEKEIDN LSSKIINKEI IVPSNKESYE
541-600 KFLKEFIRLS NRYQSYLEGV KYNVDSAIQT ITKIYNTYTL FSTKLTQMYS TRLDNFAKAK
601-660 AKEEAAKFTK EDLEKNFKTL LNYIQVSVKT AANFVYINDT HAKRKLENIE AEIKTLIAKI
661-708 KEQSNLYEAY KAIVTSILLM RDSLKEVQGI IDKNGVWYLE HHHHHHHH
```

Figure 5. 60 Amino acid sequence of the BmpA-BBK32-GST multivalent chimeric protein. The sequence derived from the pET42a vector is marked in black and the His-tag sequence within it is marked in green; the S-Tag domain in orange; GST domain in red; the fragment from the BmpA antigen is marked in blue, and the fragment of the BBK32 protein is in violet.

5.5. Production and purification of monovalent and multivalent recombinant proteins

All monovalent and multivalent *B. burgdorferi* s.l. recombinant proteins were produced using the Tabor-Studier prokaryotic system, based on genetically modified *E. coli* strains. They contain the gene encoding the T7 bacteriophage RNA polymerase

on their chromosome under the control of the *lacUV5* promoter, recognized by the *E. coli* RNA polymerase. The genes encoding the target recombinant proteins are introduced on expression plasmids under the control of the T7 promoter recognized by the bacteriophage T7 RNA polymerase, which enables induced by IPTG overproduction of the target protein.

E. coli of strains BL21(DE3)pLysS, Origami^{TM}(DE3), and Rosetta(DE3)pLacI, Rosetta(DE3)pLacI [Materials 3.2] were transformed with the DNA of the appropriate recombinant plasmids [Methods 4.9]. Grown bacterial colonies were individually inoculated in 20-30 ml of medium (LB, TB) [Materials 3.3] with the addition of antibiotics [Materials 3.17] and expressed according to the procedure described in Methods 4.12. In order to obtain the highest efficiency of target protein production, the optimization of gene expression conditions was carried out. During the experiments, samples of the bacterial culture were collected before induction of expression, at hourly intervals from that moment, and a sample from the culture after approx. 18 h from the moment of induction. Subsequently, the samples were separated by SDS-PAGE and used in Western blot to confirm the production of monovalent and multivalent recombinant proteins [Methods 4.10.1; Methods 4.14.1]. The proteins were then purified by single-step metal affinity chromatography [Methods 4.13].

5.5.1. Optimization of monovalent recombinant proteins production

In the first stage of expression optimization BL21(DE3)pLysS cells were used to produce monovalent *B. burgdorferi* s.l. recombinant proteins. Bacteria were cultivated in LB at 37°C, and induced by IPTG when OD_{600} reached 0.4 [Materials 3.18; Methods 4.12].

Electrophoretic separation of the obtained samples showed the effective production of all monovalent recombinant proteins in selected *E. coli* strain under the conditions used (Figure 5.61) [Methods 4.10.2].

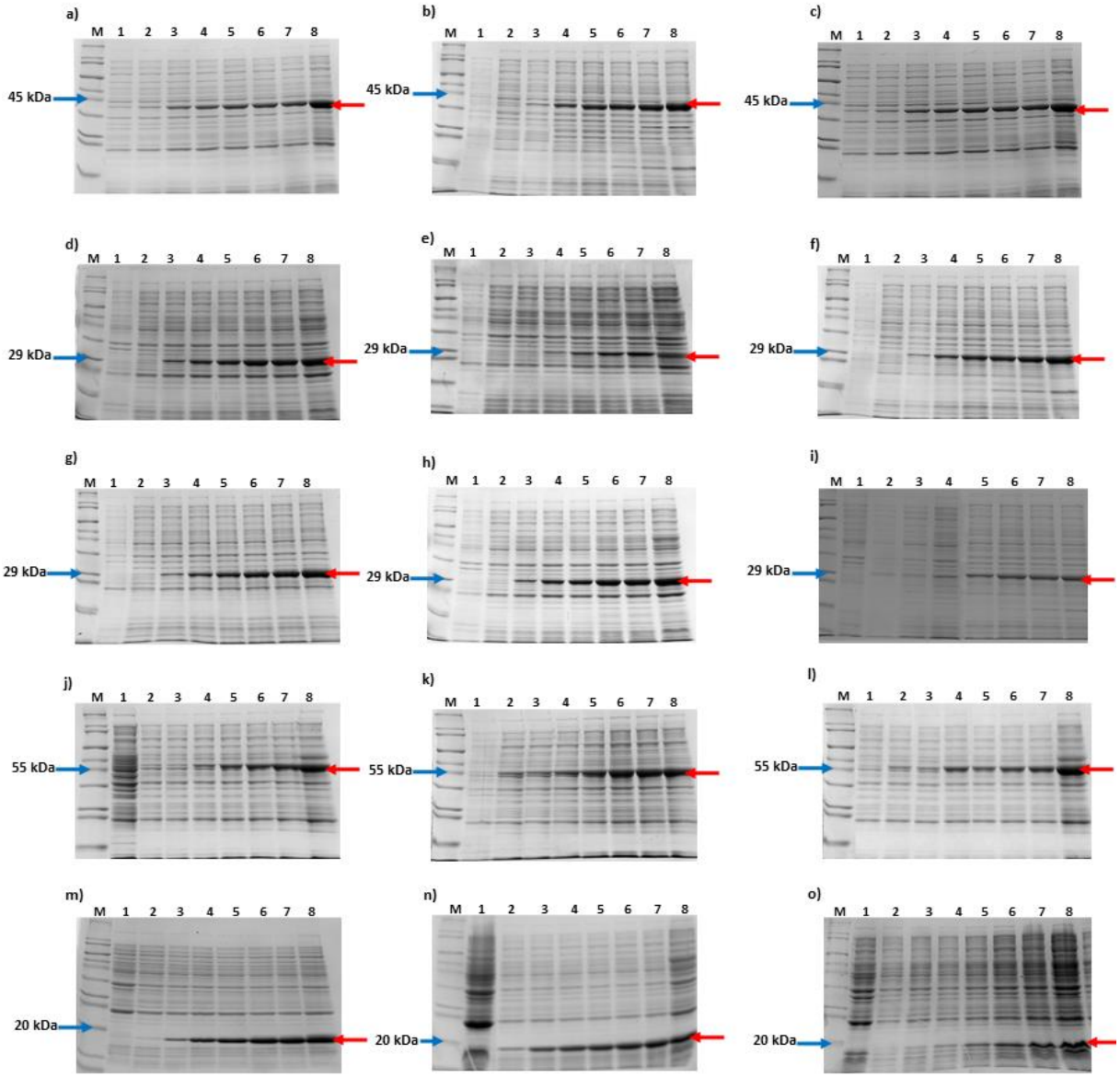

Figure 5. 61 Production of monovalent recombinant proteins. SDS-PAGE of proteins contained in *E. coli* BL21(DE3)pLysS whole cell lysates; (LB, 37°C). The bands corresponding to the putative recombinant proteins are marked with red arrows: a) $BB0108_{BA}$; b) $BB0108_{BB}$; c) $BB0108_{BG}$; d) $BB0126_{BA}$; e) $BB0126_{BB}$; f) $BB0126_{BG}$; g) $BB0298_{BA}$; h) $BB0298_{BB}$; i) $BB0298_{BG}$; j) $BB0323_{BA}$; k) $BB0323_{BB}$; l) $BB0323_{BG}$; m) $BB0689_{BA}$; n) $BB0689_{BB}$; o) $BB0689_{BG}$.

Lanes:

M - Protein marker, SigmaMarker™
1 - Negative control, *E. coli* BL21(DE3)pLysS + pUET1
2 - *E. coli* BL21(DE3)pLysS + appropriate recombinant plasmid, before induction
3 - *E. coli* BL21(DE3)pLysS + appropriate recombinant plasmid, 1 h after induction
4 - *E. coli* BL21(DE3)pLysS + appropriate recombinant plasmid, 2 h after induction
5 - *E. coli* BL21(DE3)pLysS + appropriate recombinant plasmid, 3 h after induction
6 - *E. coli* BL21(DE3)pLysS + appropriate recombinant plasmid, 4 h after induction
7 - *E. coli* BL21(DE3)pLysS + appropriate recombinant plasmid, 5 h after induction
8 - *E. coli* BL21(DE3)pLysS + appropriate recombinant plasmid, 18 h after induction

Subsequently, a Western blot was performed using anti-His-tag monoclonal antibodies [Methods 4.13.1]. This allowed the immune identification of recombinant proteins and made it possible to determine whether they were degraded (Figure 5.62).

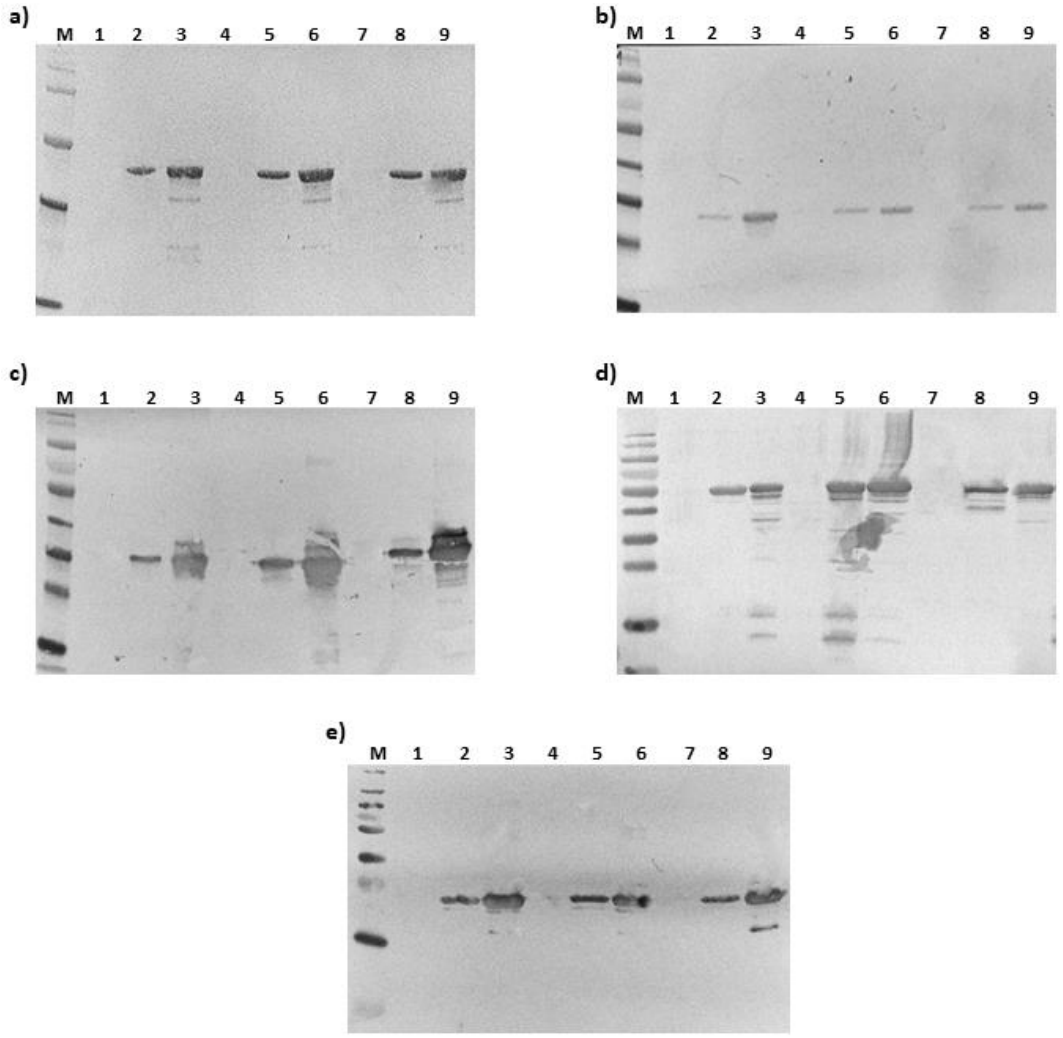

Figure 5. 62 Western blot using anti-His-tag antibodies (colorimetric detection). *E. coli* BL21(DE3)pLysS whole cell lysates (LB, 37°C): a) BB0108s; b) BB0128s; c) BB0298s, d)BB0323s, e) BB0689s.

Lanes:

M - Protein marker, PageRuler™ Prestained Protein Ladder

1 - *E. coli* BL21(DE3)pLysS + recombinant plasmid carrying heterologous gene from *B. afzelii*, before induction

2 - *E. coli* BL21(DE3)pLysS + recombinant plasmid carrying heterologous gene from *B. afzelii*, 4 h after induction

3 - *E. coli* BL21(DE3)pLysS + recombinant plasmid carrying heterologous gene from *B. afzelii*, 18 h after induction

4 - *E. coli* BL21(DE3)pLysS + recombinant plasmid carrying heterologous gene from *B. burgdorferi* s.s., before induction

5 - *E. coli* BL21(DE3)pLysS + recombinant plasmid carrying heterologous gene from *B. burgdorferi* s.s, 4 h after induction

6 - *E. coli* BL21(DE3)pLysS + recombinant plasmid carrying heterologous gene from *B. burgdorferi* s.s, 18 h after induction

7 - *E. coli* BL21(DE3)pLysS + recombinant plasmid carrying heterologous gene from *B. garinii*, before induction

8 - *E. coli* BL21(DE3)pLysS + recombinant plasmid carrying heterologous gene from *B. garinii*, 4 h after induction

9 - *E. coli* BL21(DE3)pLysS + recombinant plasmid carrying heterologous gene from *B. garinii*, 18 h after induction

Western blot analysis showed that none of the monovalent recombinant proteins were degraded to a high level, therefore it was decided not to change the original production conditions (LB, 37°C).

Polyacrylamide gels were also analyzed to estimate what part of the whole cell lysate from an overnight culture of *E. coli* BL21(DE3)pLysS transformed with recombinant plasmid is a target protein [Methods 4.21]. As these values differed depending on the gel for individual proteins, it was decided to calculate the average of three repetitions. For BB0108s, the percentages of part of WCL were in the range of 38-47%, for BB0126s it was 43-51%, BB0298s: 37-49%, BB0323s: 28-41%, while for BB0689 it was 45-55%. The complete results for each protein variant are shown in Table 5.23. Representative electropherograms for proteins derived from *B. afzelii* are shown in Figures 5.63-5.67.

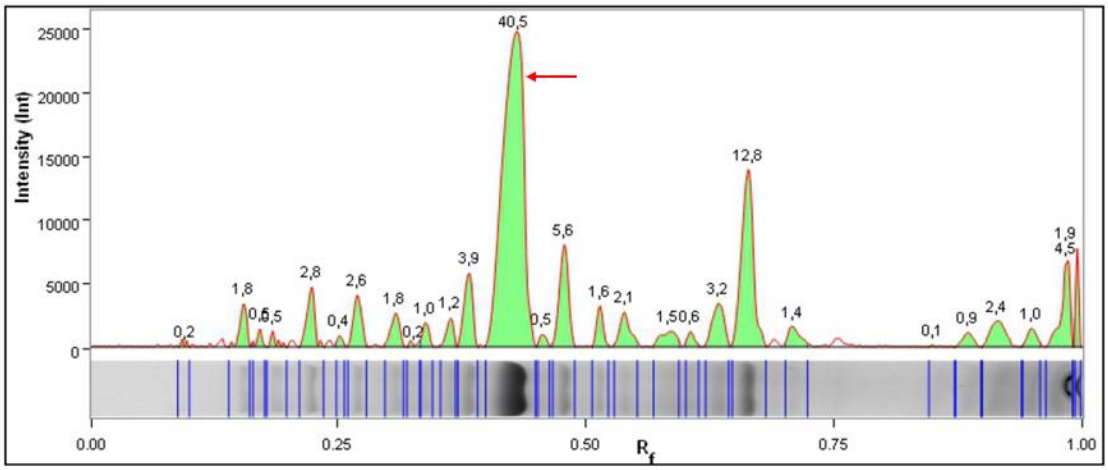

Figure 5. 63 Electropherogram showing the percentage of monovalent recombinant protein $BB0108_{BA}$ in *E. coli* BL21(DE3)pLysS + pUET1-BB0108BA whole cell lysate (LB, 37ºC). The red arrow indicates the peak corresponding to the recombinant protein.

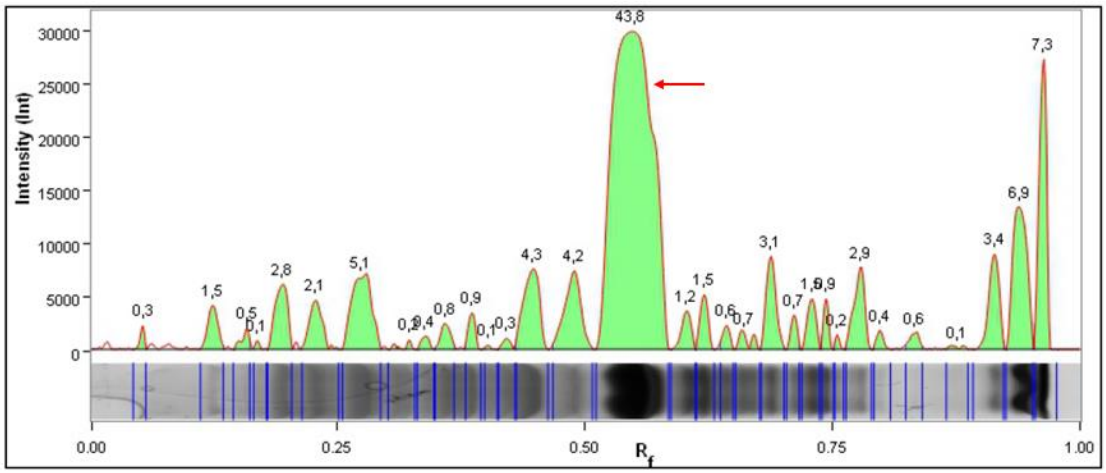

Figure 5. 64 Electropherogram showing the percentage of monovalent recombinant protein $BB0126_{BA}$ in *E. coli* BL21(DE3)pLysS + pUET1-BB0126BA whole cell lysate (LB, 37ºC). The red arrow indicates the peak corresponding to the recombinant protein.

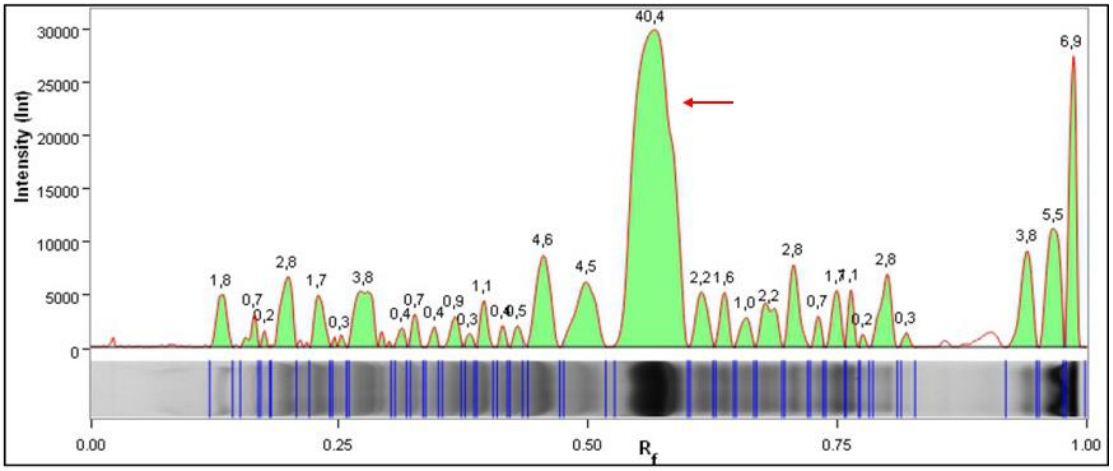

Figure 5. 65 Electropherogram showing the percentage of monovalent recombinant protein BB0298$_{BA}$ in *E. coli* BL21(DE3)pLysS + pUET1-BB0298BA whole cell lysate (LB, 37ºC). The red arrow indicates the peak corresponding to the recombinant protein.

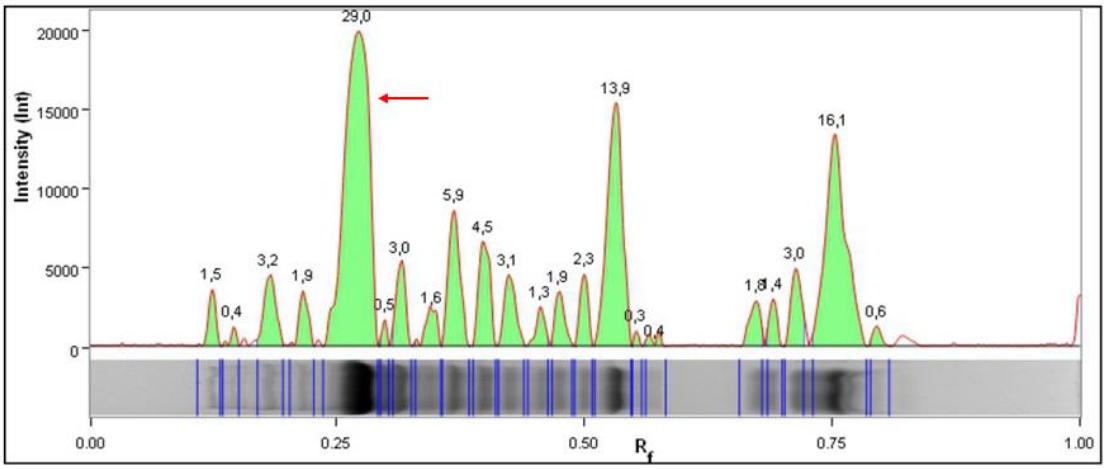

Figure 5. 66 Electropherogram showing the percentage of monovalent recombinant protein BB0323$_{BA}$ in *E. coli* BL21(DE3)pLysS + pUET1-BB0323BA whole cell lysate (LB, 37ºC). The red arrow indicates the peak corresponding to the recombinant protein.

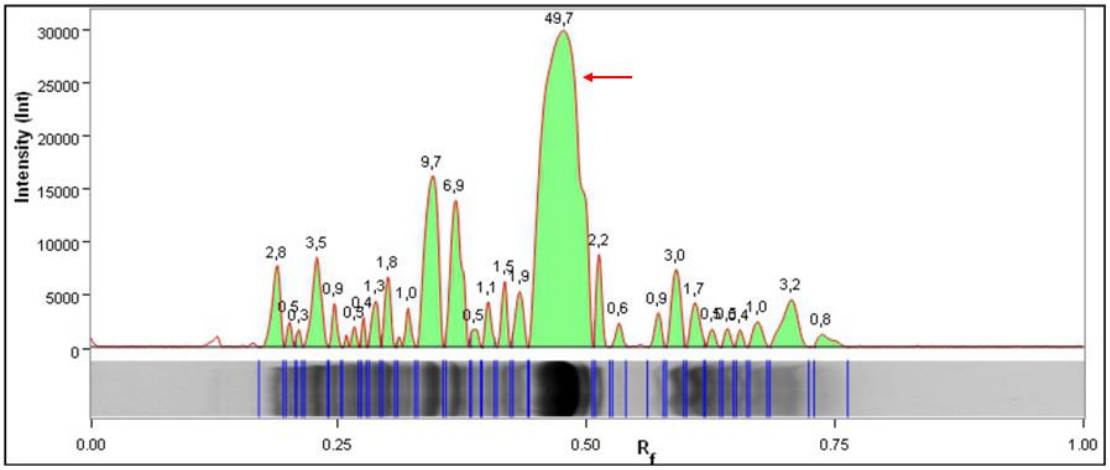

Figure 5. 67 Electropherogram showing the percentage of monovalent recombinant protein BB0689$_{BA}$ in *E. coli* BL21(DE3)pLysS + pUET1-BB0689BA whole cell lysate (LB, 37ºC). The red arrow indicates the peak corresponding to the recombinant protein.

5.5.2. Optimization of multivalent chimeric proteins production

Production optimization of the multivalent chimeric proteins BmpA-BBA64, BmpA-BBK32, BmpA-BBK32-M, and BmpA-BBK32-G, as in the case of monovalent recombinant proteins, began with the expression of genes in *E. coli* BL21(DE3)pLysS at 37ºC in LB. All chimeric proteins were produced in selected strains. However, BmpA-BBA64 and BmpA-BBK32 were heavily degraded what showed a Western blot (Figure 5.68) [Methods 4.14.1]. To reduce the degree of degradation, it was decided to use the lower temperature of 30ºC. To ensure efficient production of chimeric proteins despite the lack of an optimal temperature, *E. coli* was grown in TB, which allows for a higher cell mass than LB [Materials 3.3]. BmpA-BBK32-M and BmpA-BBK32-G were produced in *E. coli* BL21(DE3)pLysS at a very high level (Figure 5.69 and 5.70).

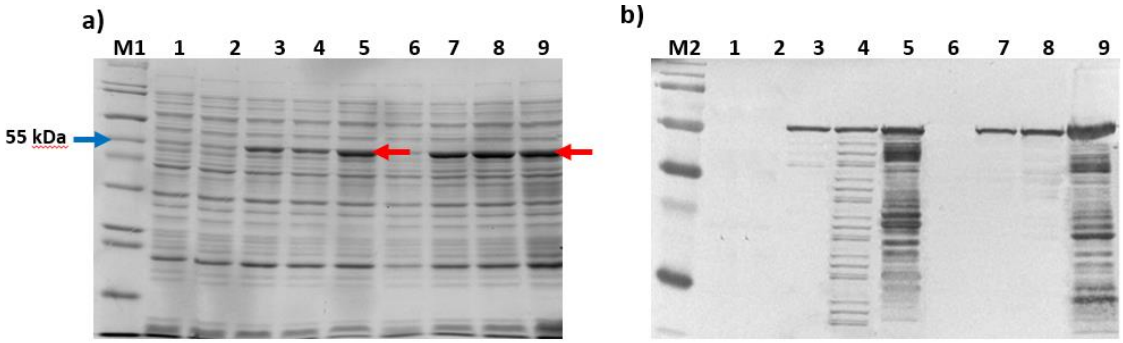

Figure 5. 68 Production of BmpA-BBK32 and BmpA-BBA64 multivalent chimeric proteins (LB, 37ºC): a) SDS-PAGE of proteins contained in *E. coli* BL21(DE3)pLysS whole cell lysate. The bands corresponding to the putative chimeric proteins are marked with red arrows; b) Western blot using anti-His-tag antibodies (colorimetric detection).

Lanes:

M1 - Protein marker, SigmaMarker™
M2 - Protein marker, PageRuler™ Prestained Protein Ladder
1 - Negative control, *E. coli* BL21(DE3)pLysS + pUET1
2 - *E. coli* BL21(DE3)pLysS + pUET1-BmpA-BBK32, before induction
3 - *E. coli* BL21(DE3 pLysS + pUET1-BmpA-BBK32, 3 h after induction
4 - *E. coli* BL21(DE3)pLysS + pUET1-BmpA-BBK32, 6 h after induction
5 - *E. coli* BL21(DE3)pLysS + pUET1-BmpA-BBK32, 18 h after induction
6 - *E. coli* BL21(DE3)pLysS + pUET1-BmpA-BBA64, before induction
7 - *E. coli* BL21(DE3)pLysS + pUET1-BmpA-BBA64, 3 h after induction
8 - *E. coli* BL21(DE3)pLysS + pUET1-BmpA-BBA64, 6 h after induction
9 - *E. coli* BL21(DE3)pLysS + pUET1-BmpA-BBA64, 18 h after induction

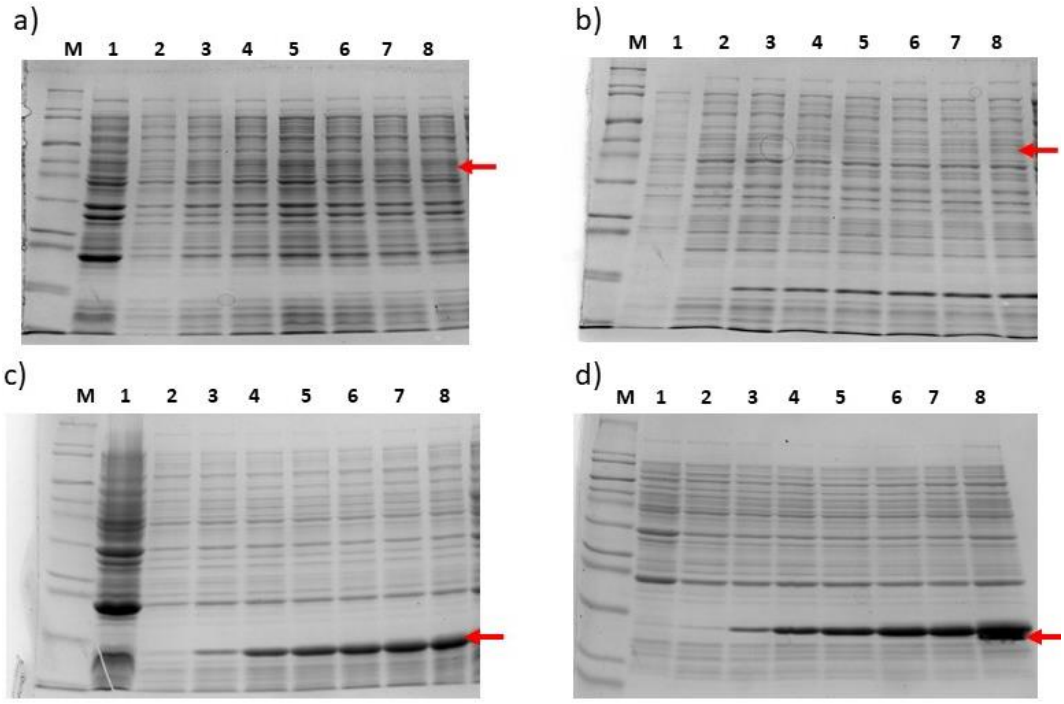

Figure 5. 69 Production of multivalent chimeric proteins under optimal conditions. SDS-PAGE of proteins contained in *E. coli* BL21(DE3)pLysS whole cell lysate. The bands corresponding to the putative chimeric proteins are marked with red arrow: a) BmpA-BBA64 (TB, 30ºC); b) BmpA-BBK32 (TB, 30ºC); c) BmpA-BBK32-M (LB, 37ºC); d) BmpABBK32-G (LB, 37ºC).

Lanes:

M - Protein marker, SigmaMarker™
1 - Negative control, *E. coli* BL21(DE3)pLysS + pUET1
2 - *E. coli* BL21(DE3)pLysS + appropriate recombinant plasmid, before induction
3 - *E. coli* BL21(DE3 pLysS + appropriate recombinant plasmid, 1 h after induction
4 - *E. coli* BL21(DE3)pLysS + appropriate recombinant plasmid, 2 h after induction
5 - *E. coli* BL21(DE3)pLysS + appropriate recombinant plasmid, 3 h after induction
6 - *E. coli* BL21(DE3)pLysS + appropriate recombinant plasmid, 4 h after induction
7 - *E. coli* BL21(DE3)pLysS + appropriate recombinant plasmid, 5 h after induction
8 - *E. coli* BL21(DE3)pLysS + appropriate recombinant plasmid, 18 h after induction

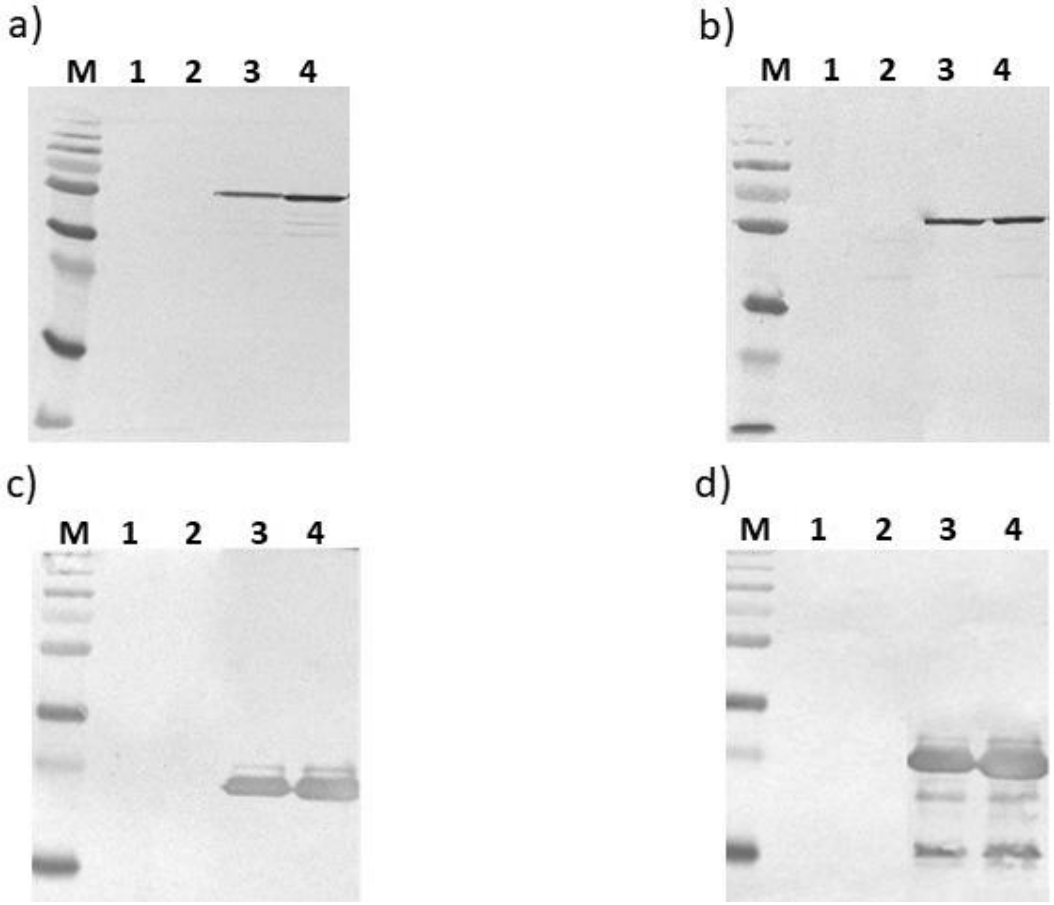

Figure 5. 70 Western blot using anti-His-tag antibodies (colorimetric detection): a) BmpA-BBA64 (TB, 30ºC); b) BmpA-BBK32 (TB, 30ºC); c) BmpA-BBK32-M (LB, 37ºC); d) BmpA-BBK32-G (LB, 37ºC).
Lanes:
M - Protein marker, PageRuler™ Prestained Protein Ladder
1 - Negative control, *E. coli* BL21(DE3)pLysS + pUET1
2 - *E. coli* BL21(DE3)pLysS + appropriate recombinant plasmid, before induction
3 - *E. coli* BL21(DE3)pLysS + appropriate recombinant plasmid, 4 h after induction
4 - *E. coli* BL21(DE3)pLysS + appropriate recombinant plasmid, 18 h after induction

Polyacrylamide gels were also analyzed to assess what part of the whole cell lysate of an approx. 18 h culture of *E. coli* BL21(DE3)pLysS transformed with appropriate recombinant plasmid is a target protein [Methods 4.21]. The results of the analysis are shown in Figures 5.71-5.74. BmpA-BBK32 and BmpA-BBA64 represented approx. 1% of all proteins separated in the lane. The situation is different in the case of chimeric proteins BmpA-BBK32-G and BmpA-BBK32-M, which *E. coli* cells strongly overproduces. Their content in the lysate is 44% for BmpA-BBK32-G and 37% for BmpA-BBK32-M. These values are the averages of the analysis of three gels.

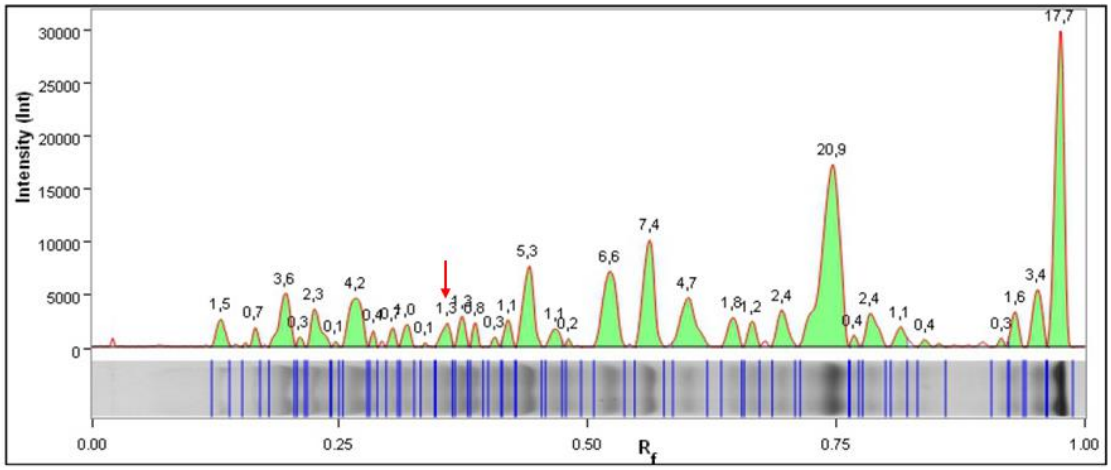

Figure 5. 71 Electropherogram showing the percentage of multivalent chimeric protein BmpA-BBA64 in *E. coli* BL21(DE3)pLysS + pUET1-BmpA-BBA64 whole cell lysate (TB, 30ºC). The red arrow indicates the peak corresponding to the recombinant protein.

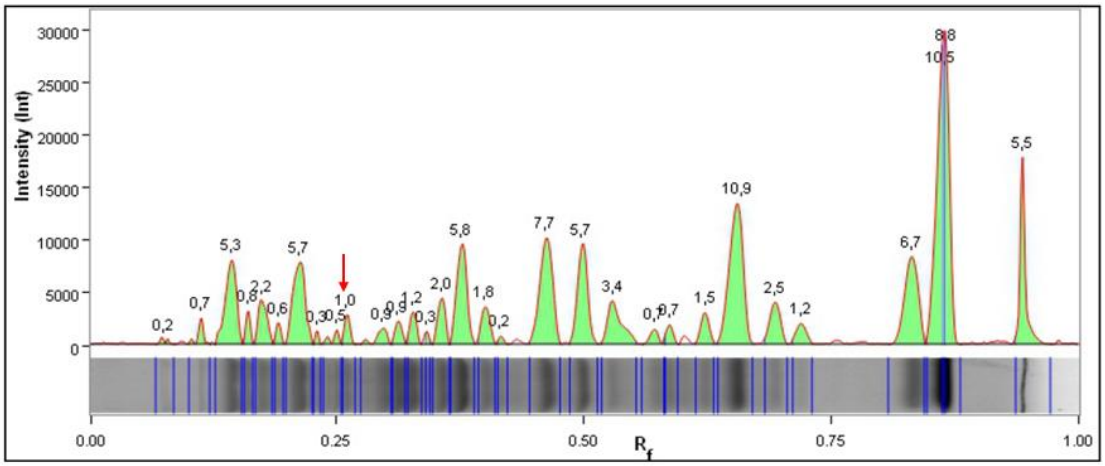

Figure 5. 72 Electropherogram showing the percentage of multivalent chimeric protein BmpA-BBK32 in *E. coli* BL21(DE3)pLysS + pUET1-BmpA-BBK32 whole cell lysate (TB, 30ºC). The red arrow indicates the peak corresponding to the recombinant protein.

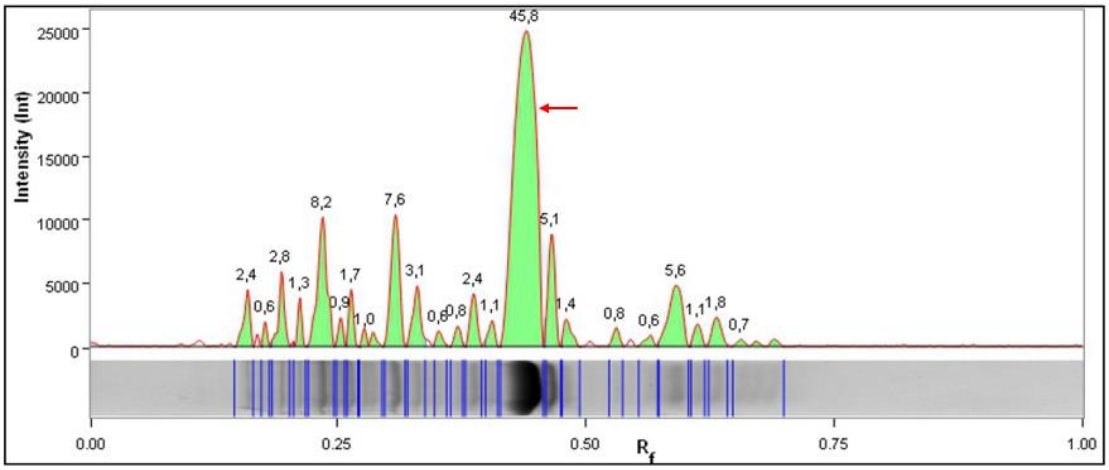

Figure 5. 73 Electropherogram showing the percentage of multivalent chimeric protein BmpA-BBK32-G in *E. coli* BL21(DE3)pLysS + pUET1-BmpA-BBK32-G whole cell lysate (LB, 37ºC). The red arrow indicates the peak corresponding to the recombinant protein.

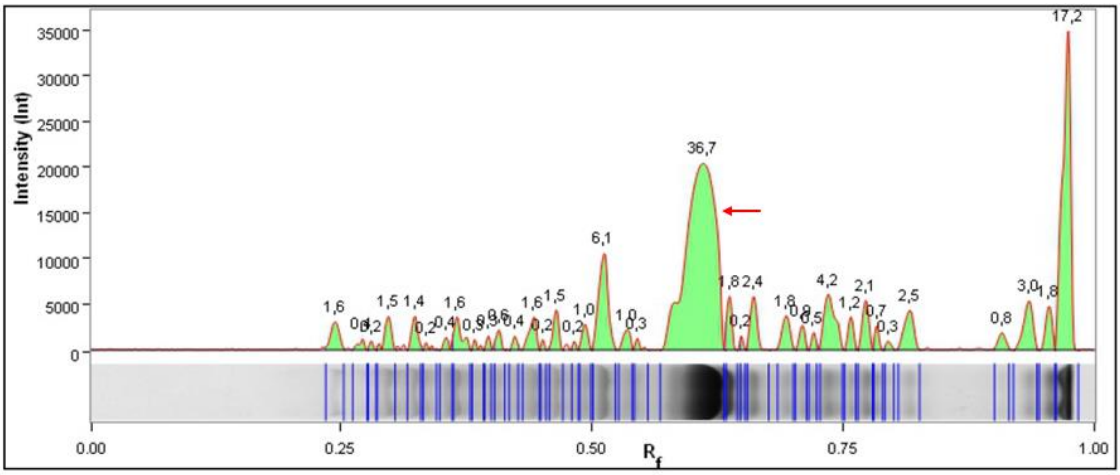

Figure 5. 74 Electropherogram showing the percentage of multivalent chimeric protein BmpA-BBK32-M in *E. coli* BL21(DE3)pLysS + pUET1-BmpA-BBK32-M whole cell lysate (LB, 37ºC). The red arrow indicates the peak corresponding to the recombinant protein.

5.5.3. Optimization of monovalent and multivalent recombinant proteins production – summary

During the production optimization, 5 monovalent recombinant proteins (BB0108s, BB0126s, BB0298s, BB0323s, BB0689s) coming from 3 different genospecies of *B. burgdorferi* s.l. and 4 multivalent chimeric proteins (BmpA-BBK32, BmpA-BBA64, BmpA-BBK32-M, BmpA-BBK32-G) were obtained. Optimized production conditions for individual proteins are shown in Table 5.23.

Table 5. 23 Optimized conditions for the production of monovalent and multivalent recombinant proteins

Recombinant protein	*E.coli* strain	Temperature	Culture medium	Gene expression time	% WCL
BB0108$_{BA}$	BL21(DE3)pLysS	37ºC	LB	18 h	43%
BB0108$_{BB}$			LB	18 h	47%
BB0108$_{BG}$			LB	18 h	38%
BB0126$_{BA}$	BL21(DE3)pLysS	37ºC	LB	18 h	43%
BB0126$_{BB}$			LB	18 h	45%
BB0126$_{BG}$			LB	18 h	51%
BB0298$_{BA}$	BL21(DE3)pLysS	37ºC	LB	18 h	37%
BB0298$_{BB}$			LB	18 h	49%
BB0298$_{BG}$			LB	18 h	47%
BB0323$_{BA}$	BL21(DE3)pLysS	37ºC	LB	18 h	31%
BB0323$_{BB}$			LB	18 h	41%
BB0323$_{BG}$			LB	18 h	35%
BB0689$_{BA}$	BL21(DE3)pLysS	37ºC	LB	18 h	45%
BB0689$_{BB}$			LB	18 h	50%
BB0689$_{BG}$			LB	18 h	55%
BmpA-BBA64	BL21(DE3)pLysS	30ºC	TB	18 h	1.1%
BmpA-BBK32	BL21(DE3)pLysS	30ºC	TB	18 h	1.3%
BmpA-BBK32-M	BL21(DE3)pLysS	37ºC	LB	18 h	44%
BmpA-BBK32-G	BL21(DE3)pLysS	37ºC	LB	18 h	37%

WCL - whole cell lysate

5.5.4. Determination of the toxicity of monovalent and multivalent recombinant proteins for *E. coli* cells

The potential toxicity of the produced monovalent and multivalent proteins to host cells was determined by measuring the growth dynamics of a bacterial culture carrying the pUET1 plasmid (control), compared to the growth of cells transformed with the appropriate plasmids encoding heterologous genes [Methods 4.15]. The results are shown in Figure 5.75.

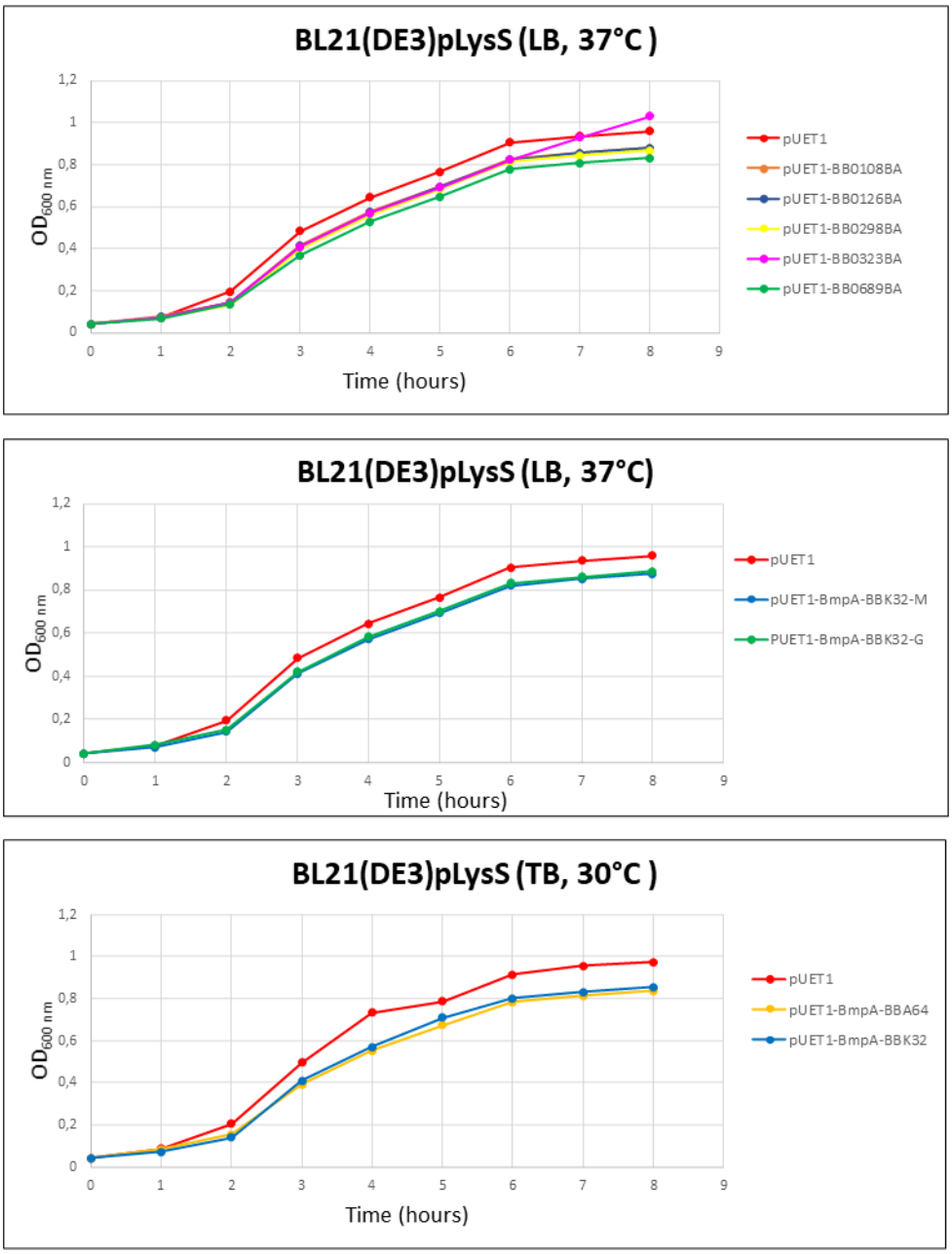

Figure 5. 75 Growth dynamics of *E. coli* BL21(DE3)pLysS during heterologous gene expression.

E. coli cells producing monovalent and multivalent *B. burgdorferi* s.l. recombinant proteins did not show statistically significant (P>0.05) inhibition of growth, suggesting that target proteins exhibit no host toxicity.

5.5.5. Purification of monovalent and multivalent recombinant proteins

The next step was to purify the produced monovalent and multivalent B. *burgdorferi* s.l. recombinant proteins. One-stage metal affinity chromatography on IDA resin, i.e., with iminodiacetic acid residues as active groups, was used for this purpose [Materials 3.11; Methods 4.13]. These residues have the ability to chelate transition metal ions, in this case Ni^{2+} was used. As histidine is an electron donor, His-tag (present at

both the N- and C-terminus of recombinant proteins) easily coordinates with immobilized nickel, binding to the affinity column while other proteins present in *E. coli* cell lysates are washed up. At this stage standard buffers (20 mM Tris-HCl; 500 mM NaCl; 0,1% Triton X- 100) with pH selected individually for the protein on the basis of its isoelectric point were used for purification [Materials 3.11.2.1]. The aim was to select the pH of the buffers used for antigen purification so that it was above the pI value of the target protein, which led to the histidine residues obtaining a negative charge.

The key step was to assess the degree of target protein content in the soluble and insoluble cytoplasmic fraction. Buffers with a high urea concentration were used to dissolve proteins in the form of inclusion bodies. In order to check in what form the recombinant *B. burgdorferi* s.l. proteins were produced by *E. coli*, two parallel purifications for all obtained proteins were performed - using buffers without and with 5 M urea [Methods 4.13.2].

The results of purification with both 5 M urea and non-urea buffers for selected monovalent and multivalent recombinant proteins are shown in Figures 5.76 and 5.77.

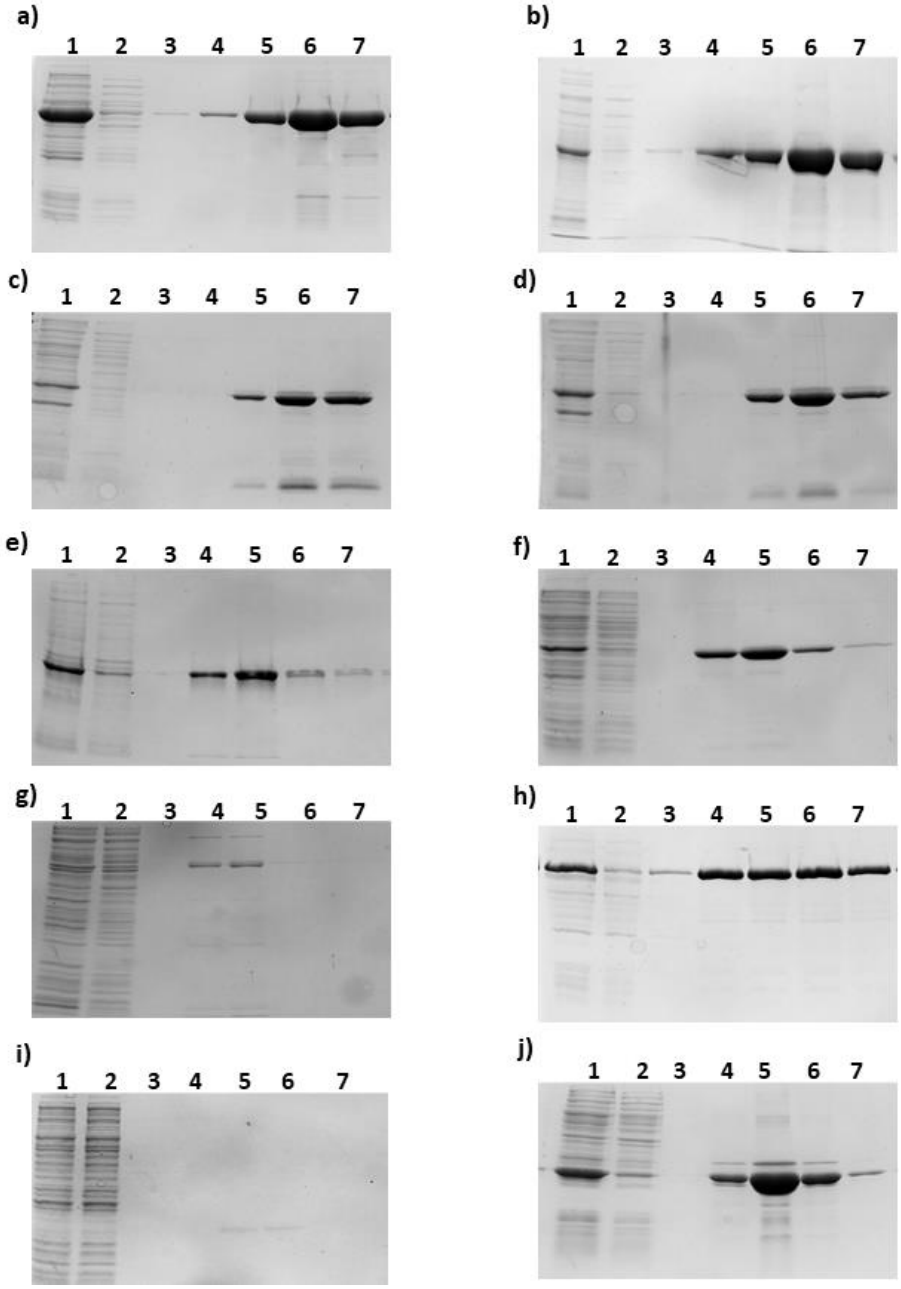

Figure 5. 76 Results of purification of monovalent recombinant proteins using standard buffers: a) BB0108$_{BA}$ (buffers without urea); b) BB0108$_{BA}$ (buffers with urea); c) BB0126$_{BA}$ (buffers without urea); d) BB0126$_{BA}$ (buffers with urea); e) BB0298$_{BA}$ (buffers without urea); f) BB0298$_{BA}$ (buffers with urea); g) BB0323$_{BA}$ (buffers without urea); h) BB0323$_{BA}$ (buffers with urea); i) BB0689$_{BA}$ (buffers without urea); j) BB0689$_{BA}$ (buffers with urea).

Lanes:

1 - *E. coli* BL21(DE3)pLysS lysate before loading into the affinity column
2 - *E. coli* BL21(DE3)pLysS lysate after passing through the affinity column
3 - First elution fraction
4 - Second elution fraction
5 - Third elution fraction
6 - Fourth elution fraction
7 - Fifth elution fraction

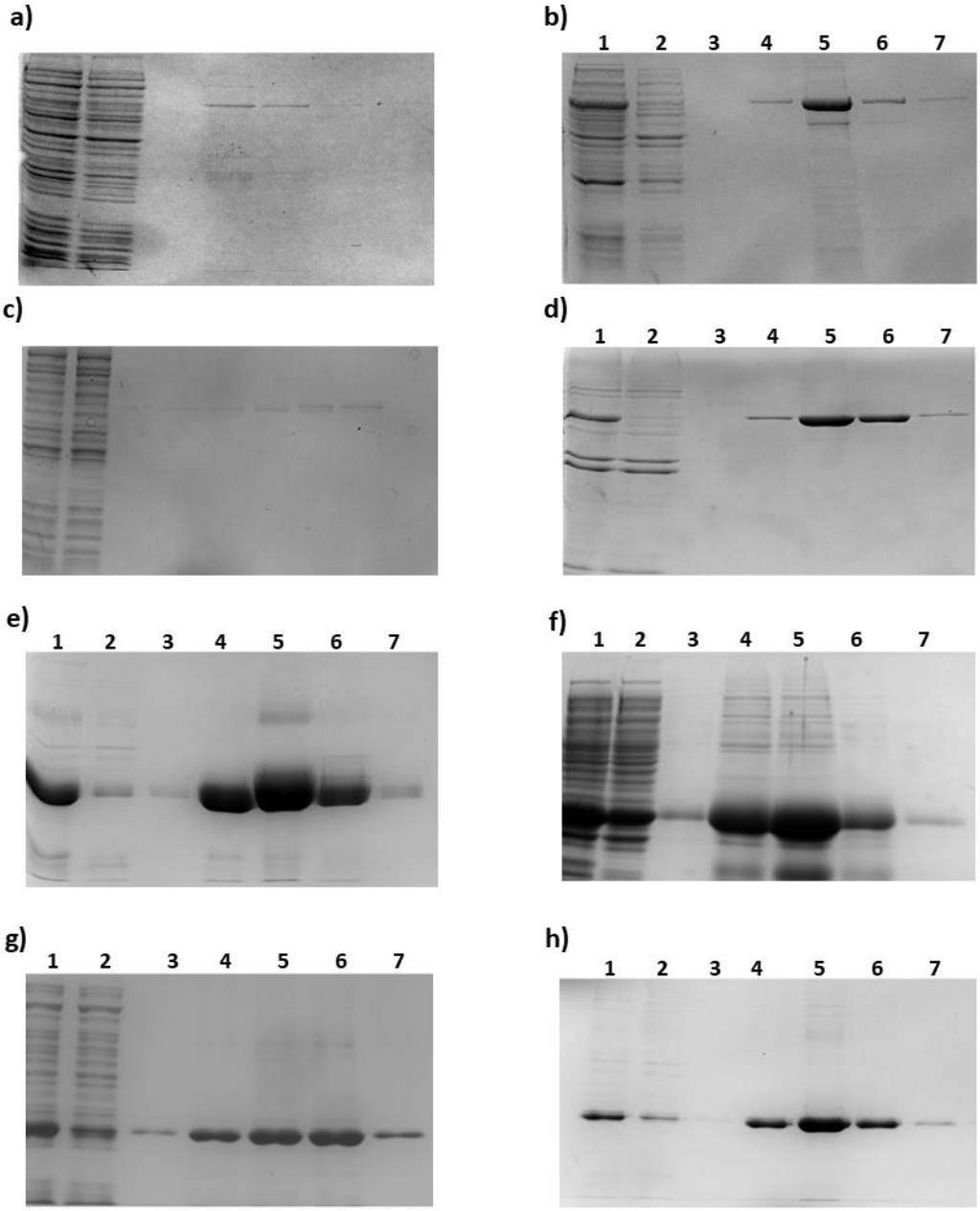

Figure 5. 77 Results of purification of multivalent chimeric proteins using standard buffers: a) BmpA-BBA64 (buffers without urea); b) BmpA-BBA64 (buffers with urea); c) BmpA-BBK32 (buffers without urea); d) BmpA-BBK32 (buffers with urea); e) BmpA-BBK32-G (buffers without urea); f) BmpA-BBK32-G (buffers with urea); g) BmpA-BBK32-M (buffers without urea); h) BmpA-BBK32-M (buffers with urea).

Lanes:

1 - *E. coli* BL21(DE3)pLysS lysate before loading into the affinity column
2 - *E. coli* BL21(DE3)pLysS lysate after passing through the affinity column
3 - First elution fraction
4 - Second elution fraction
5 - Third elution fraction
6 - Fourth elution fraction
7 - Fifth elution fraction

After the purification, the electrophoretic purity of the obtained protein preparations was assessed using ImageLab software [Methods 4.20]. An example

electropherogram obtained for $BB0108_{BA}$ is shown in Figure 5.78. Full results are included in Table 5.24.

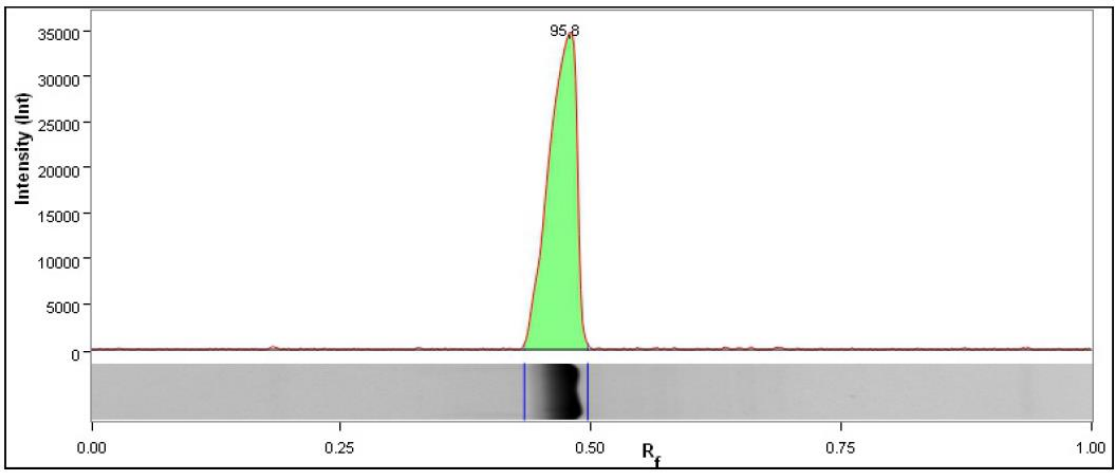

Figure 5. 78 Electropherogram showing the electrophoretic purity of the $BB0108_{BA}$ monovalent recombinant protein preparation in the elution fractions.

5.5.6. Purification of monovalent and multivalent recombinant proteins - summary

The obtained results indicate that BB0108s, BB0126s, BB0298s, BmpA-BBK32-G, and BmpA-BBK32-M were produced in a soluble form - there was no difference in purification efficiency depending on whether buffers with or without 5 M urea were used. In contrast, buffers containing 5 M urea had to be used to purify BB0323s, BB0689s, BmpA-BBK32, and BmpA-BBA64.

As a result of the applied procedure of one-stage purification of monovalent and multivalent recombinant proteins using metal affinity chromatography obtained antigens preparations with electrophoretic purity above 95%. Optimal purification conditions and the purity of the obtained protein preparations are shown in Table 5.24.

Table 5. 24 Optimal purification conditions for monovalent and multivalent recombinant proteins

Recombinant protein	Isoelectric point	Buffers pH	5 M urea	Purity
BB0108$_{BA}$	8.4	9.0	No	96%
BB0108$_{BB}$	8.4			97%
BB0108$_{BG}$	8.4			97%
BB0126$_{BA}$	8.4	7.9	No	97%
BB0126$_{BB}$	5.8			98%
BB0126$_{BG}$	5.6			98%
BB0298$_{BA}$	5.7	7.9	No	98%
BB0298$_{BB}$	5.7			97%
BB0298$_{BG}$	6.0			97%
BB0323$_{BA}$	5.8	9.5	Yes	95%
BB0323$_{BB}$	8.7			96%
BB0323$_{BG}$	8.5			96%
BB0689$_{BA}$	8.8	7.9	Yes	95%
BB0689$_{BB}$	7.0			98%
BB0689$_{BG}$	6.5			98%
BmpA-BBA64	5.8	7.9	Yes	99%
BmpA-BBK32	6.7	7.9	Yes	96%
BmpA-BBK32-M	9.2	9.7	No	97%
BmpA-BBK32-G	6.3	7.9	No	98%

After purification BB0108s, BB0323s, BmpA-BBK32-G, and BmpA-BBK32-M were dialyzed directly into the storage buffer [Materials 3.11.2.6; Methods 4.18.1], whereas an alternative gradually method was used for dialysis of BB0126s, BB0298s, BB0689s, BmpA-BBA64, and BmpA-BBK32 [Methods 4.18.2].

5.5.7. Increasing the solubility of monovalent and multivalent recombinant proteins

It was noticed that after the purification, the proteins precipitated intensively after removing the denaturing agent. This concerned both the BB0689s, BmpA-BBK32, and BmpA-BBA64, i.e., those produced in the form of inclusion bodies, and BB0126s, and BB0298s purified without the use of urea. In addition, BB0323s, despite being produced as inclusion bodies, remained soluble after elution and refolding in a storage buffer [Materials 3.11.2.6; Methods 4.18.1].

5.5.7.1. Purification of monovalent and multivalent recombinant proteins using alternative buffers

The precipitation process was so fast that it was impossible to dialyze the purified proteins into a new buffer [Methods 4.118.1]. Therefore it was decided to purify target proteins using buffers with different compositions [Materials 3.11.2, Methods 4.13]. Their components and concentrations were selected based on scientific articles describing the

production of other *B. burgdorferi* s.l. recombinant proteins. The basic composition of the buffers with references is presented in Table 5.25 [Materials 3.11.2]. They differed in imidazole content, pH, and the presence of a denaturing agent. In addition, purification of BB0126s and BB0298s was performed using standard buffer A with the addition of 1 M urea [Materials 3.11.2.1].

Table 5. 25 Composition of buffers used to purify monovalent and multivalent recombinant proteins

No.	Immutable buffers components	Variables	Comments/References
1	20 mM Tris-HCl; 500 mM NaCl; 0.1% Triton X-100	Imidazole range: 5-500 mM; addition of urea (without, 1M and 5M); pH	Standard buffer
2	25 mM Tris-HCl; 150 mM NaCl	Imidazole range: 5-500 mM; addition of 5 M urea; pH	(Bettina Wilske et al., 1993)
3	50 mM Na_3PO_4; 500 mM NaCl	Imidazole range: 5-500 mM; addition of 5 M urea; pH	(Roessler et al., 1997b)
4	20 mM Na_3PO_4, 250 mM NaCl	Imidazole range: 5-500 mM; addition of 5 M urea; pH	(Gomes-Solecki et al., 2000)
5	PBS (137 mM NaCl; 2.7 mM KCl; 8 mM Na_2HPO_4; 2 mM KH_2PO_4)	Imidazole range: 5-500 mM; addition of 5 M urea; pH	(Heikkilä et al., 2002b)
6	50mM Tris-HCl; 150mM NaCl	Imidazole range: 5-500 mM; addition of 5 M urea; pH	Storage buffer (Křupka et al., 2012)
7	40 mM Tris-HCl; 100 mM KCl; 12.5 mM β-mercaptoethanol; 10% glycerol	Imidazole range: 5-500 mM; addition of 5 M urea; pH	(Brooks et al., 2006)

All alternative buffers allowed effective purification of monovalent and multivalent recombinant proteins (results not shown). However, none of them contributed to stopping the precipitation of the obtained proteins after removing the denaturation agent.

5.5.7.2 Change of gene expression conditions

Although as many as 7 different buffers were used in the purification, this did not stop the precipitation of obtained proteins, which suggested that the reason for this problem is other than their inappropriate composition. Therefore, it was decided to change the conditions of heterologous gene expression.

The first step was to lower the temperature (20ºC, 25ºC, and 30ºC) still using *E. coli* BL21(DE3)pLysS [Materials 3.2; Methods 4.12]. However, this approach did not bring the expected results. Lowering temperature reduced the level of production of recombinant proteins (Figure 5.79) but did not affect their solubility.

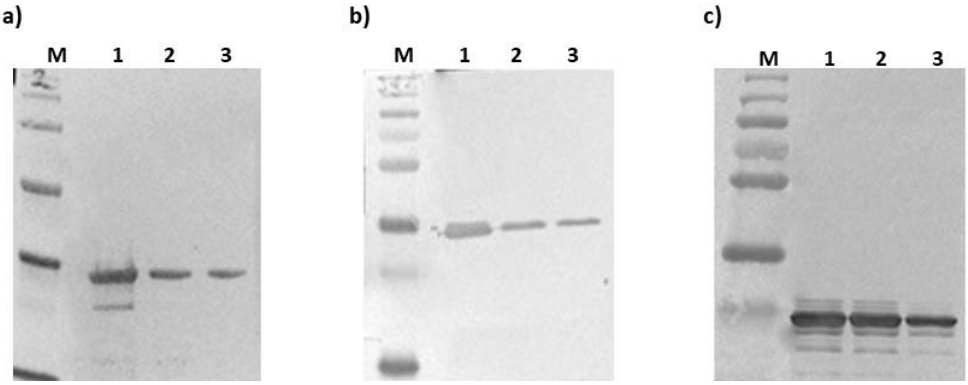

Figure 5. 79 Production of monovalent recombinant proteins in *E. coli* BL21(DE3)pLysS at different gene expression temperatures - Western blot using anti-His-tag antibodies (colorimetric detection): a) $BB0126_{BA}$ (LB); b) $BB0298_{BA}$ (LB); c) $BB0689_{BA}$ (LB).
Lanes:
M - Protein marker, PageRuler™ Prestained Protein Ladder
1 - Protein production at 37ºC (LB, 18 h after induction)
2 - Protein production at 30ºC (LB, 18 h after induction)
3 - Protein production at 20ºC (LB, 18 h after induction)

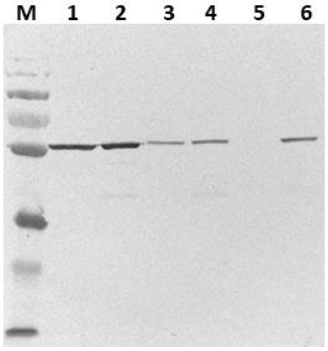

Figure 5. 80 Production of multivalent chimeric proteins BmpA-BBA64 and BmpA-BBK32 in *E. coli* BL21(DE3)pLysS at different gene expression temperatures - Western blot using anti-His-tag antibodies (colorimetric detection).
Lanes:
M - Protein marker, PageRuler™ Prestained Protein Ladder
1 - BmpA-BBA64 production at 30ºC (TB, 18 h after induction)
2 - BmpA-BBK32 production at 30ºC (TB, 18 h after induction)
3 - BmpA-BBA64 production at 25ºC (TB, 18 h after induction)
4 - BmpA-BBK32 production at 25ºC (TB, 18 h after induction)
5 - BmpA-BBA64 production at 20ºC (TB, 18 h after induction)
6 - BmpA-BBK32 production at 20ºC (TB, 18 h after induction)

Polyacrylamide gels were also analyzed to estimate what part of the whole cell lysates from an overnight culture of *E. coli* BL21(DE3)pLysS is target protein. Representative electropherograms for $BB0126_{BA}$, $BB0298_{BA}$, and $BB0689_{BA}$ are presented in Figures 5.81-5.83. The full results, which are the average of three measurements, are presented in Table 5.26. This analysis was not performed for BmpA-BBA64 and BmpA-BBK32 produced at lower temperatures because the visibility of the bands was so low that it was not possible to determine which of them corresponded to the target proteins.

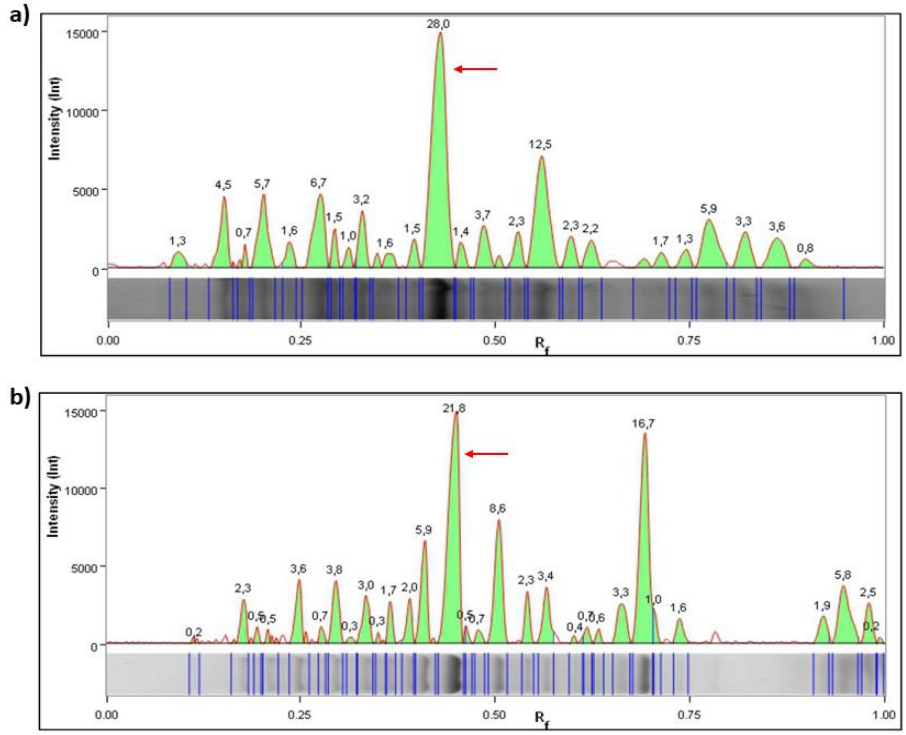

Figure 5. 81 Electropherogram showing the percentage of $BB0126_{BA}$ recombinant protein in *E. coli* BL21(DE3)pLysS + pUET1-BB0126BA whole cell lysates: a) LB, 30ºC; b) LB, 20ºC. The red arrow indicates the peak corresponding to the recombinant protein.

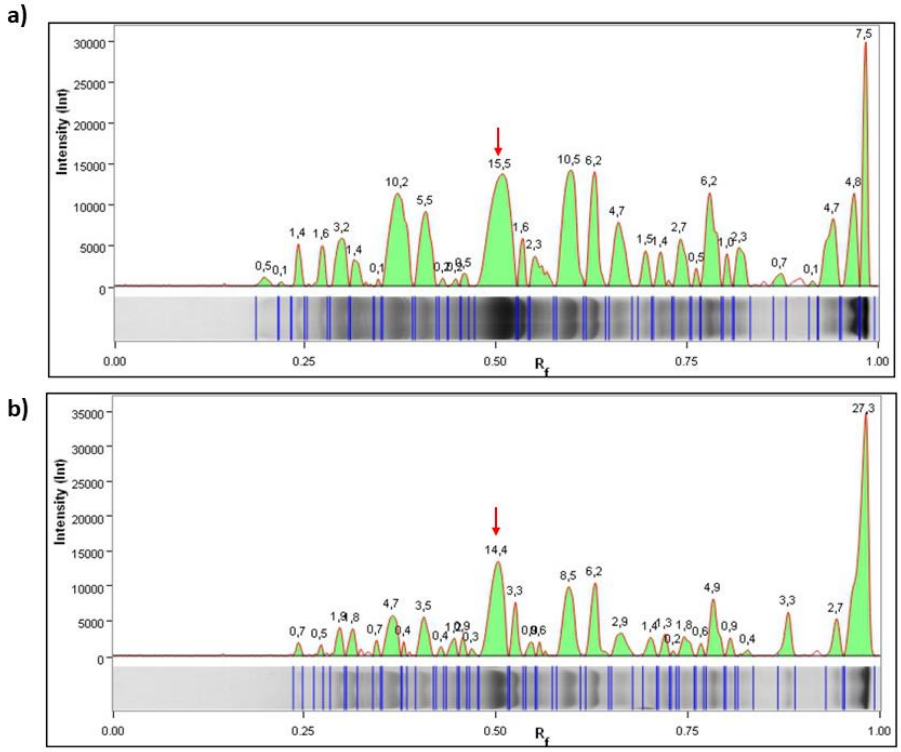

Figure 5. 82 Electropherogram showing the percentage of $BB0298_{BA}$ recombinant protein in *E. coli* BL21(DE3)pLysS + pUET1-BB0298BA whole cell lysates: a) LB, 30ºC; b) LB, 20ºC. The red arrow indicates the peak corresponding to the recombinant protein.

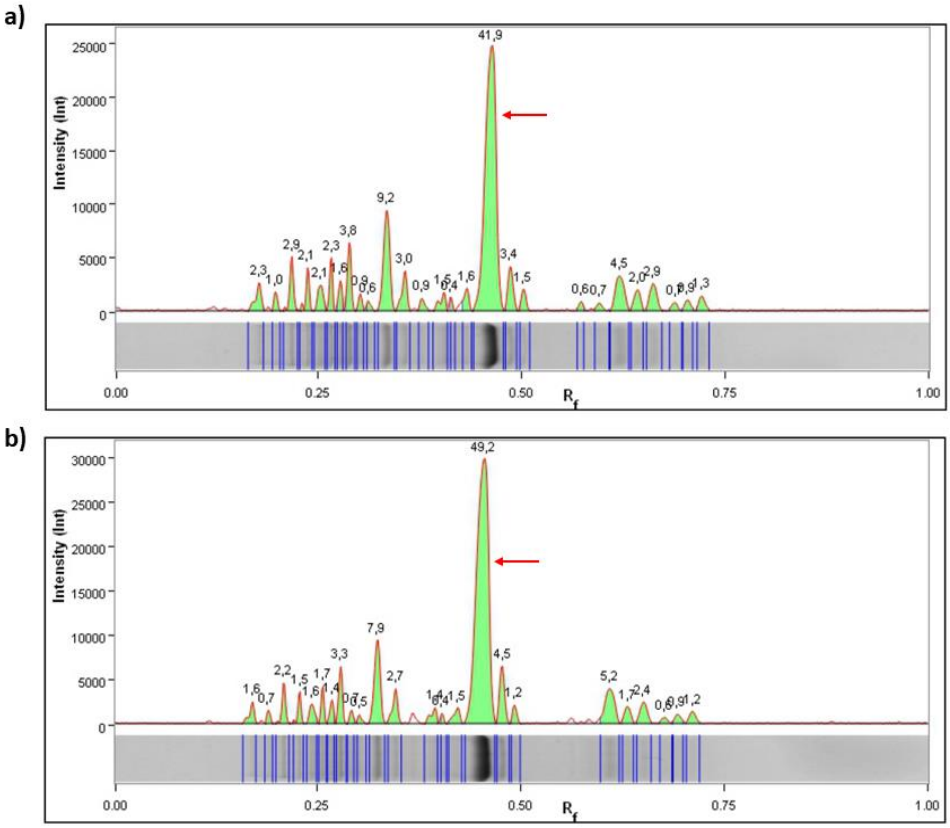

Figure 5. 83 Electropherogram showing the percentage of $BB0689_{BA}$ recombinant protein in *E. coli* BL21(DE3)pLysS + pUET1-BB0689BA whole cell lysates: a) LB, 30ºC; b) LB, 20ºC. The red arrow indicates the peak corresponding to the recombinant protein.

Table 5.26 shows the degree of overproduction of monovalent recombinant proteins at different temperatures.

Table 5. 26 The degree of overproduction of monovalent recombinant proteins at different gene expression temperatures

Monovalent protein	*E.coli* strain	Temperature	Culture medium	Gene expression time	% WCL
$BB0126_{BA}$	BL21(DE3)pLysS	37ºC	LB	18 h	43%
		30ºC			29%
		20ºC			24%
$BB0126_{BB}$	BL21(DE3)pLysS	37ºC	LB	18 h	45%
		30ºC			27%
		20ºC			25%
$BB0126_{BG}$	BL21(DE3)pLysS	37ºC	LB	18 h	51%
		30ºC			33%
		20ºC			22%
$BB0298_{BA}$	BL21(DE3)pLysS	37ºC	LB	18 h	37%
		30ºC			16%
		20ºC			12%
$BB0298_{BB}$	BL21(DE3)pLysS	37ºC	LB	18 h	49%
		30ºC			17%
		20ºC			17%
$BB0298_{BG}$	BL21(DE3)pLysS	37ºC	LB	18 h	47%
		30ºC			15%
		20ºC			16%
$BB0689_{BA}$	BL21(DE3)pLysS	37ºC	LB	18 h	45%
		30ºC			40%
		20ºC			41%
$BB0689_{BB}$	BL21(DE3)pLysS	37ºC	LB	18h	50%
		30ºC			42%
		20ºC			39%
$BB0689_{BG}$	BL21(DE3)pLysS	37ºC	LB	18h	55%
		30ºC			45%
		20ºC			44%

WCL - whole cell lysate

5.5.7.3. Change of *E. coli* strain

Because lowering the temperature did not increase monovalent and multivalent recombinant proteins' solubility, it was decided to use other strains of *E. coli* whose genetic features could contribute to obtaining recombinant proteins with the correct spatial structure (Mathieu et al., 2019). For this purpose strains Origami™(DE3), Rosetta(DE3)pLacI and Rosseta(DE3)pLysS were selected [Materials 3.2]. BB0126s, BB0298s, BB0689s, BmpA-BBA64 and BmpA-BBK32 were produced in *E. coli* Origami™(DE3). However, they were heavily degraded, which could be related to these proteins' higher expression level than BL21(DE3)pLysS (Figure 5.84). Whereas, not all target proteins were obtained using Rosset(DE3)pLacI or Rosset(DE3)pLysS (Table 5.27).

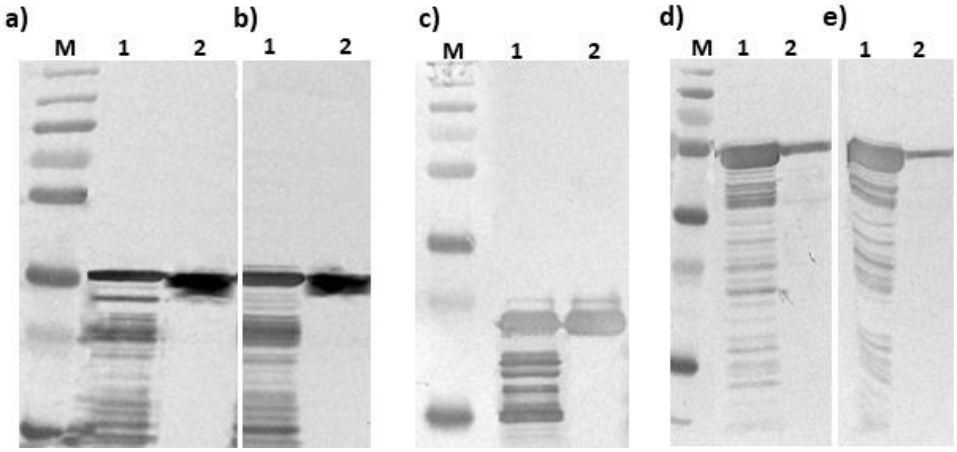

Figure 5. 84 The degree of degradation of monovalent and multivalent recombinant proteins depending on the *E. coli* strain - Western blot using anti-His-tag antibodies (colorimetric detection): a) $BB0126_{BA}$ (37ºC, LB); b) $BB0298_{BA}$ (37ºC, LB); c) $BB0689_{BA}$ (37ºC, LB); d) BmpA-BBA64 (30ºC, TB); e) BmpA-BBK32 (30ºC, TB).
Lanes:
M - Protein marker, PageRuler™ Prestained Protein Ladder
1 - Protein production in *E. coli* Origami™(DE3) (18 h after induction)
2 - Protein production in *E. coli* BL21(DE3)pLysS (18 h after induction)

Table 5. 27 Monovalent and multivalent recombinant production in different strains of *E. coli*

Recombinant protein	*E. coli* strain		
	Origami™(DE3)	Rosseta(DE3)pLacI	Rosseta(DE3)pLysS
$BB0126_{BA}$	Protein production	Protein production	Protein production
$BB0126_{BB}$	Protein production	Protein production	Protein production
$BB0126_{BG}$	Protein production	Protein production	Protein production
$BB0298_{BA}$	Protein production	No protein production	No protein production
$BB0298_{BB}$	Protein production	No protein production	No protein production
$BB0298_{BG}$	Protein production	No protein production	No protein production
$BB0689_{BA}$	Protein production	Protein production	Protein production
$BB0689_{BB}$	Protein production	Protein production	Protein production
$BB0689_{BG}$	Protein production	Protein production	Protein production
BmpA-BBA64	Protein production	Protein production	No protein production
BmpA-BBK32	Protein production	Protein production	No protein production

Despite the production of monovalent and multivalent recombinant proteins in other strains of *E. coli* and the use of various expression temperature, it was not possible to obtain them in a soluble form.

5.5.7.4 Addition of fusion partners

Another approach was to add domains that increase solubility to the sequences of monovalent and multivalent *B. burgdorferi* s.l. recombinant proteins. Many expression vectors have been engineered that enable the introduction of additional domains, the so-called fusion partners, that increase the solubility of the protein produced. In this study, the pET32a and pET42a vectors [Materials 3.1] encoding the TrxA and GST domains were selected and the genes *bb0126BA*, *bmpA-bbk32* and *bmpA-bba64* were

cloned into them. These proteins were chosen because of the ease of re-cloning the genes encoding them from previously constructed recombinant plasmids based on pUET1 backbone [Methods 4.8.1; Results 5.3.4].

5.5.7.4.1. Optimizing the production of monovalent and multivalent recombinant proteins with additional fusion partners

Optimization of the production of proteins with additional fusion partners (BB0126-TrxA, BB0126-GST, BmpA-BBK32-TrxA, BmpA-BBK32-GST, BmpA-BBA64-TrxA, BmpA-BBA64-GST) was carried out in the same way as described in Results 5.5.1 and 5.5.2 [Methods 4.12]. The expression of genes encoding these proteins took place in BL21(DE3)pLysS at 37°C in LB. However, some proteins were produced in small amounts (BB0126BA-GST), while others were heavily degraded (BmpA-BBA64-TrxA, BmpA-BBK32-TrxA, BmpA-BBA64-GST, BmpA-BBK32-GST), therefore for the production of some of them as the growth medium for *E. coli* was used TB and/or the temperature of the culture was lowered to 30ºC. Polyacrylamide gels and Western blots using samples from optimal conditions for the production of fusion proteins are shown in Figures 5.85 and 5.86 [Methods 4.10.2; Methods 4.14.1].

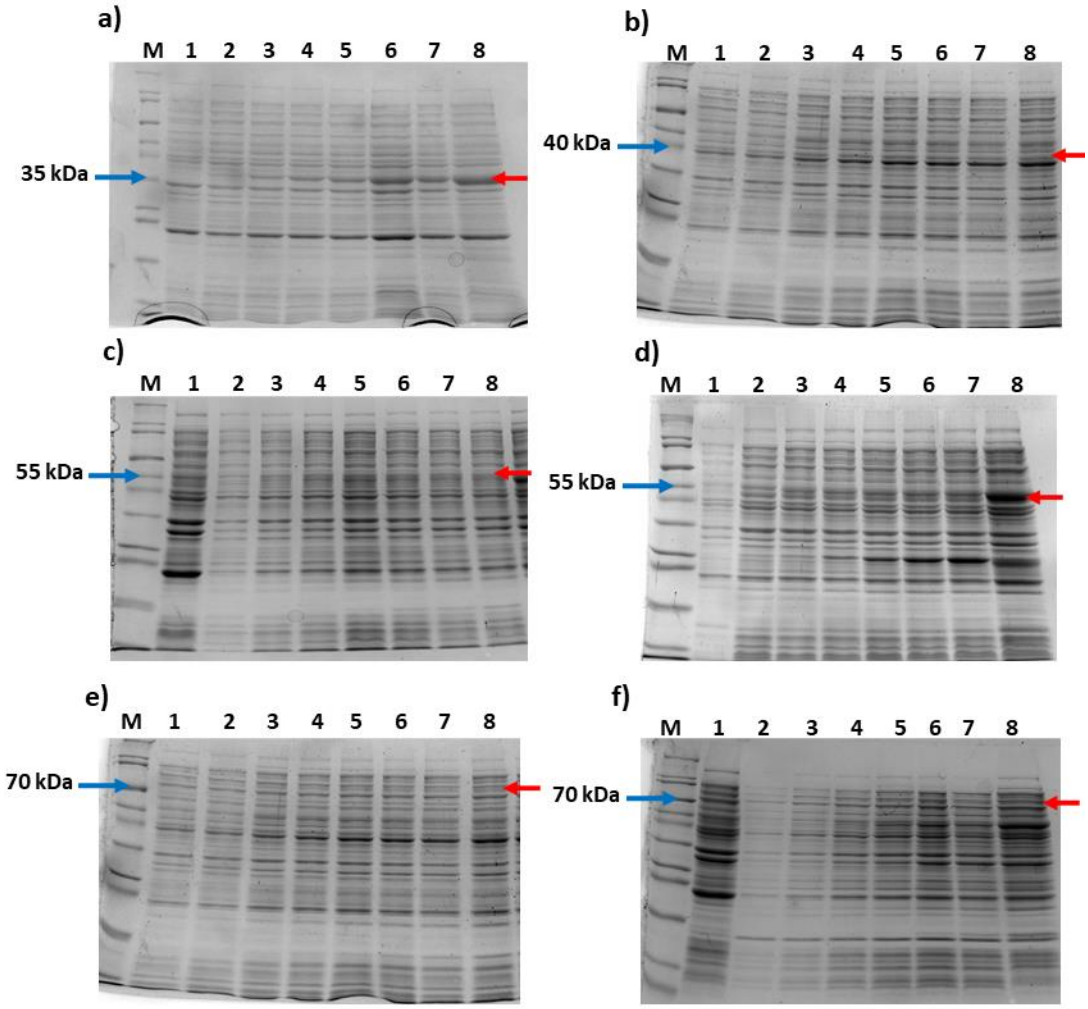

Figure 5. 85 SDS-PAGE of proteins contained in *E. coli* BL21(DE3)pLysS whole cell lysates. The bands corresponding to the putative recombinant proteins are marked with red arrows: a) BB0126$_{BA}$-TrxA (LB, 37°C); b) BB0126$_{BA}$- GST (TB, 37°C); c) BmpA- BBA64-TrxA (TB, 30ºC); d) BmpA-BBK32-TrxA (TB, 30ºC); e) BmpA-BBA64-GST (LB, 30ºC); f) BmpA-BBK32-GST (LB, 30ºC).

Lanes:

M - Protein marker, SigmaMarker™
1 - Negative control, *E. coli* BL21(DE3)pLysS + pUET1
2 - *E. coli* BL21(DE3)pLysS + appropriate recombinant plasmid, before induction
3 - *E. coli* BL21(DE3)pLysS + appropriate recombinant plasmid, 1 h after induction
4 - *E. coli* BL21(DE3)pLysS + appropriate recombinant plasmid, 2 h after induction
5 - *E. coli* BL21(DE3)pLysS + appropriate recombinant plasmid, 3 h after induction
6 - *E. coli* BL21(DE3)pLysS + appropriate recombinant plasmid, 4 h after induction
7 - *E. coli* BL21(DE3)pLysS + appropriate recombinant plasmid, 5 h after induction
8 - *E. coli* BL21(DE3)pLysS + appropriate recombinant plasmid, 18 h after induction

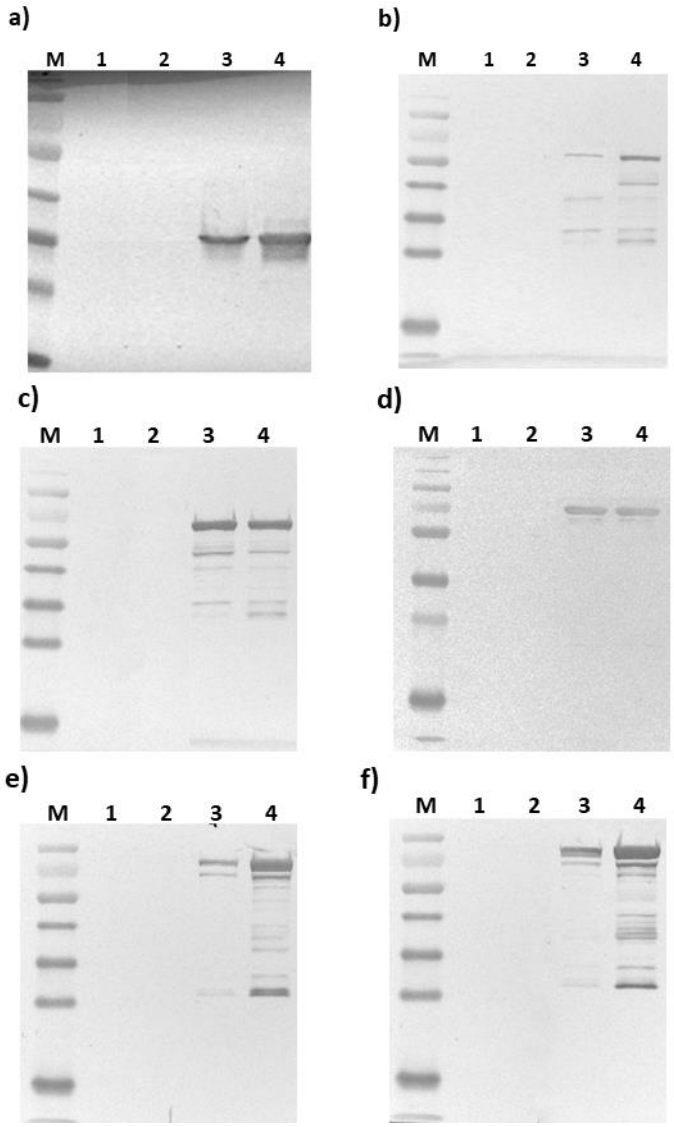

Figure 5. 86 Production of monovalent and multivalent recombinant proteins with additional fusion partners - Western blot using anti-His-tag antibodies (colorimetric detection). *E. coli* BL21(DE3)pLysS whole cell lysates: a) BB0126$_{BA}$-TrxA (LB, 37°C); b) BB0126$_{BA}$-GST (TB, 37°C); c) BmpA-BBA64-TrxA (TB, 30ºC); d) BmpA-BBK32-TrxA (TB, 30ºC); e) BmpA-BBA64-GST (LB, 30ºC); f) BmpA-BBK32-GST (LB, 30ºC).

Lanes:

M - Protein marker, PageRuler™ Prestained Protein Ladder
1 - Negative control, *E. coli* BL21(DE3)pLysS + pUET1
2 - *E. coli* BL21(DE3)pLysS + appropriate recombinant plasmid, before induction
3 - *E. coli* BL21(DE3)pLysS + appropriate recombinant plasmid, 4 h after induction
4 - *E. coli* BL21(DE3)pLysS + appropriate recombinant plasmid, 18 h after induction

The analysis of polyacrylamide gels [Methods 4.21] showed a varied content of target proteins in *E. coli* BL21(DE3)pLysS whole cell lysate (Figures 5.87 and 5.92). BB0126$_{BA}$-TrxA accounted more than 39% of the proteins visible in the lane, while for BB0126BA-GST it was only 1.1%. These values for different variants of the BmpA-BBA64 and BmpA-BBK32 chimeras were similar and ranged from 12% to 19% (Table 5.28).

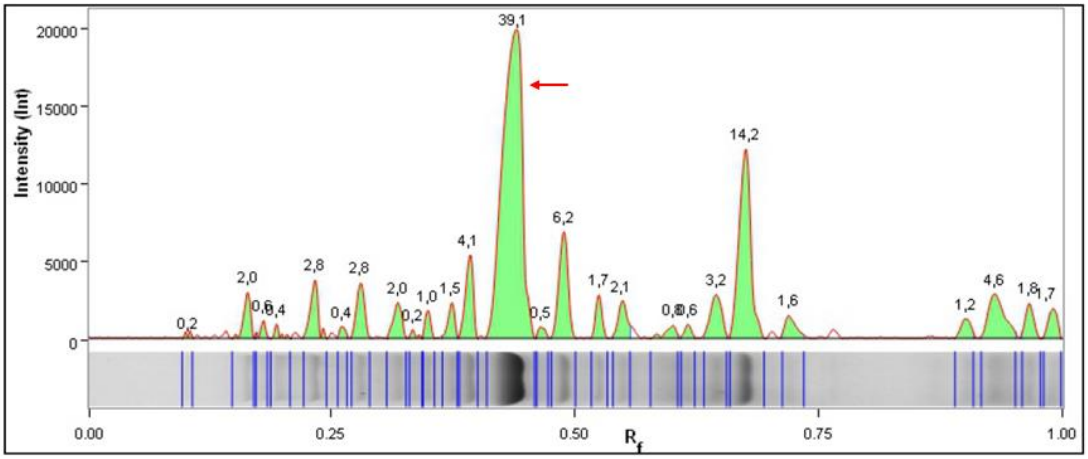

Figure 5. 87 Electropherogram showing the percentage of monovalent recombinant protein BB0126$_{BA}$-TrxA in *E. coli* BL21(DE3)pLysS + pET32a-BB0126BA whole cell lysates (LB, 37ºC). The red arrow indicates the peak corresponding to the recombinant protein.

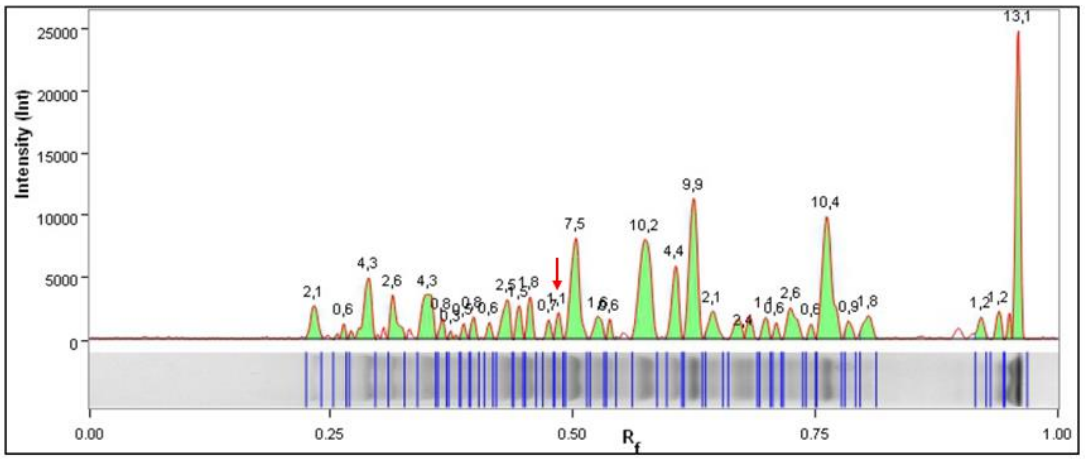

Figure 5. 88 Electropherogram showing the percentage of monovalent recombinant protein BB0126$_{BA}$-GST in *E. coli* BL21(DE3)pLysS + pET42a-BB0126BA whole cell lysates (TB, 37ºC). The red arrow indicates the peak corresponding to the recombinant protein.

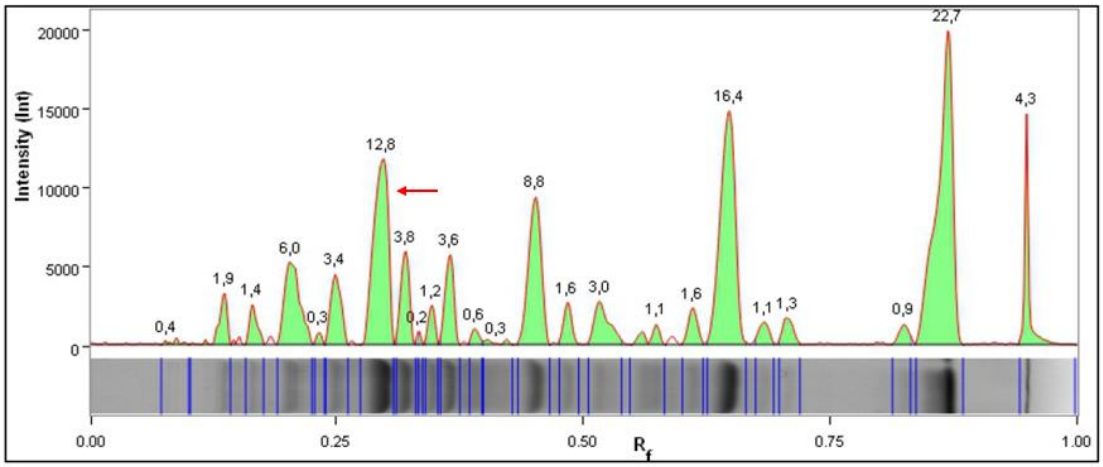

Figure 5. 89 Electropherogram showing the percentage of multivalent chimeric protein BmpA-BBA64-TrxA in *E. coli* BL21(DE3)pLysS + pET32a- BmpA-BBA64 whole cell lysates (TB, at 30ºC). The red arrow indicates the peak corresponding to the chimeric protein.

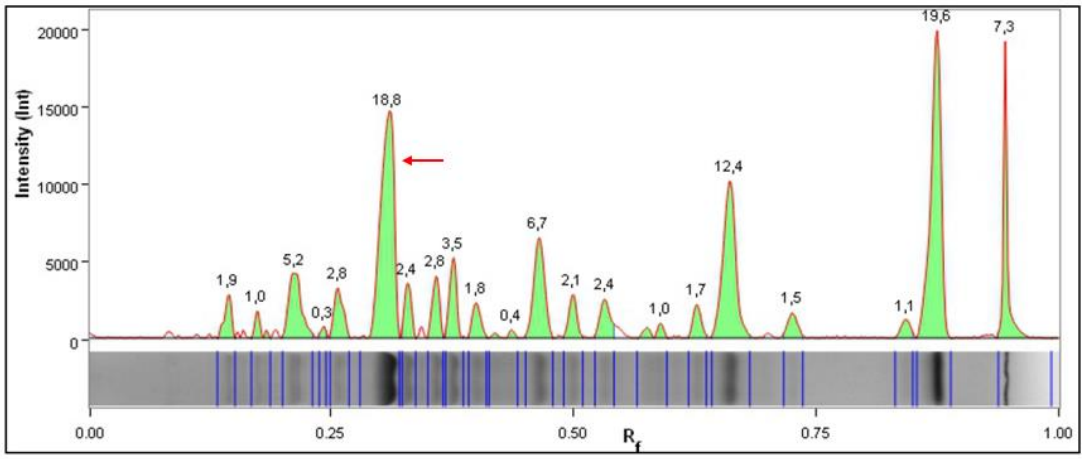

Figure 5. 90 Electropherogram showing the percentage of multivalent chimeric protein BmpA-BBK32-TrxA in *E. coli* BL21(DE3)pLysS + pET32a- BmpA-BBK32 whole cell lysates (TB, 30ºC). The red arrow indicates the peak corresponding to the chimeric protein.

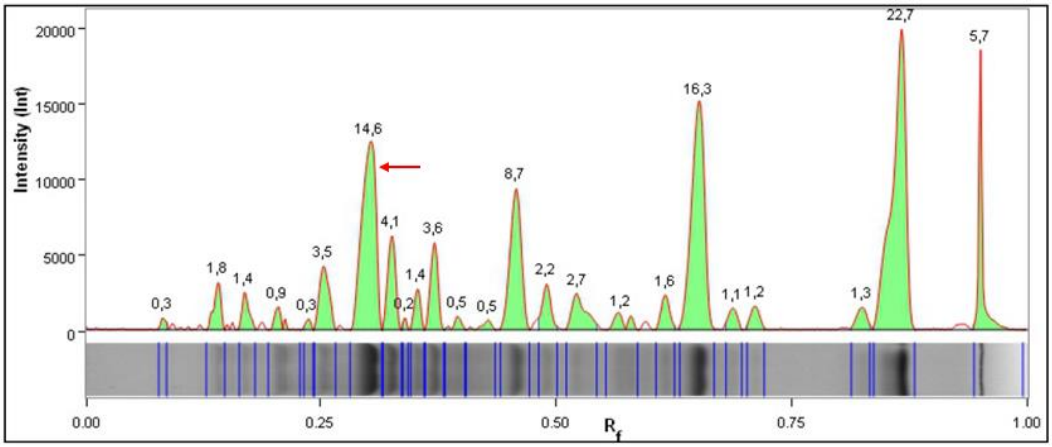

Figure 5. 91 Electropherogram showing the percentage of multivalent chimeric protein BmpA-BBA64-GST in *E. coli* BL21(DE3)pLysS + pET42a- BmpA-BBA64 whole cell lysates (LB, at 30ºC). The red arrow indicates the peak corresponding to the chimeric protein.

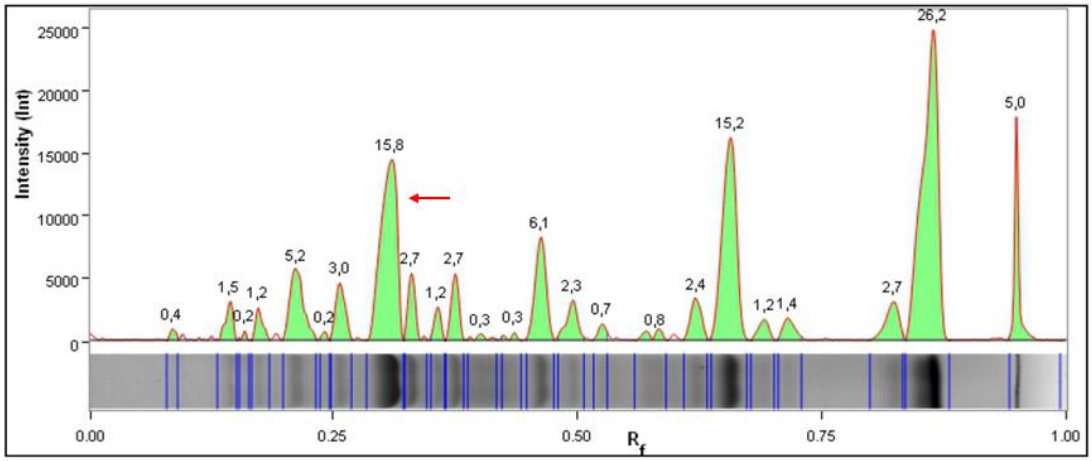

Figure 5. 92 Electropherogram showing the percentage of multivalent chimeric protein BmpA-BBK32-GST in *E. coli* BL21(DE3)pLysS + pET42a-BmpA-BBK32 whole cell lysates (LB, 30ºC). The red arrow indicates the peak corresponding to the chimeric protein.

5.5.7.4.2. Optimizing the production of monovalent and multivalent recombinant proteins with additional fusion partners - summary

During this stage of experiments obtained 3 monovalent/multivalent *B. burgdorferi* s.l. recombinant proteins ($BB0126_{BA}$, BmpA-BBK32, BmpA-BBA64) containing TrxA or GST fusion partners. Optimized production conditions for individual proteins with additional domains are shown in Table 5.28.

Table 5. 28 Optimized conditions for the production of monovalent and multivalent recombinant proteins with additional fusion partners

Recombinant protein	*E. coli* strain	Temperature	Culture medium	Expression time	% WCL
$BB0126_{BA}$-TrxA	BL21(DE3)pLysS	37°C	LB	18 h	41%
$BB0126_{BA}$-GST	BL21(DE3)pLysS	37°C	TB	18 h	1.1%
BmpA-BBA64-TrxA	BL21(DE3)pLysS	30ºC	TB	18 h	14%
BmpA-BBA64-GST	BL21(DE3)pLysS	30ºC	LB	18 h	15%
BmpA-BBK32-TrxA	BL21(DE3)pLysS	30ºC	TB	18 h	19%
BmpA-BBK32-GST	BL21(DE3)pLysS	30ºC	LB	18 h	17%

5.5.7.4.3. Purification of monovalent and multivalent recombinant proteins with additional fusion partner

Monovalent and multivalent recombinant proteins with additional fusion partners were purified in an analogous manner, as described in section 5.5.4. using standard buffers [Materials 3.11.2.1; Methods 4.14]. The first step was to determine whether heterologous proteins are produced by *E. coli* in a soluble form, for this purpose two parallel purifications were performed without and with the addition of 5 M urea to the buffers (Figure 5.93).

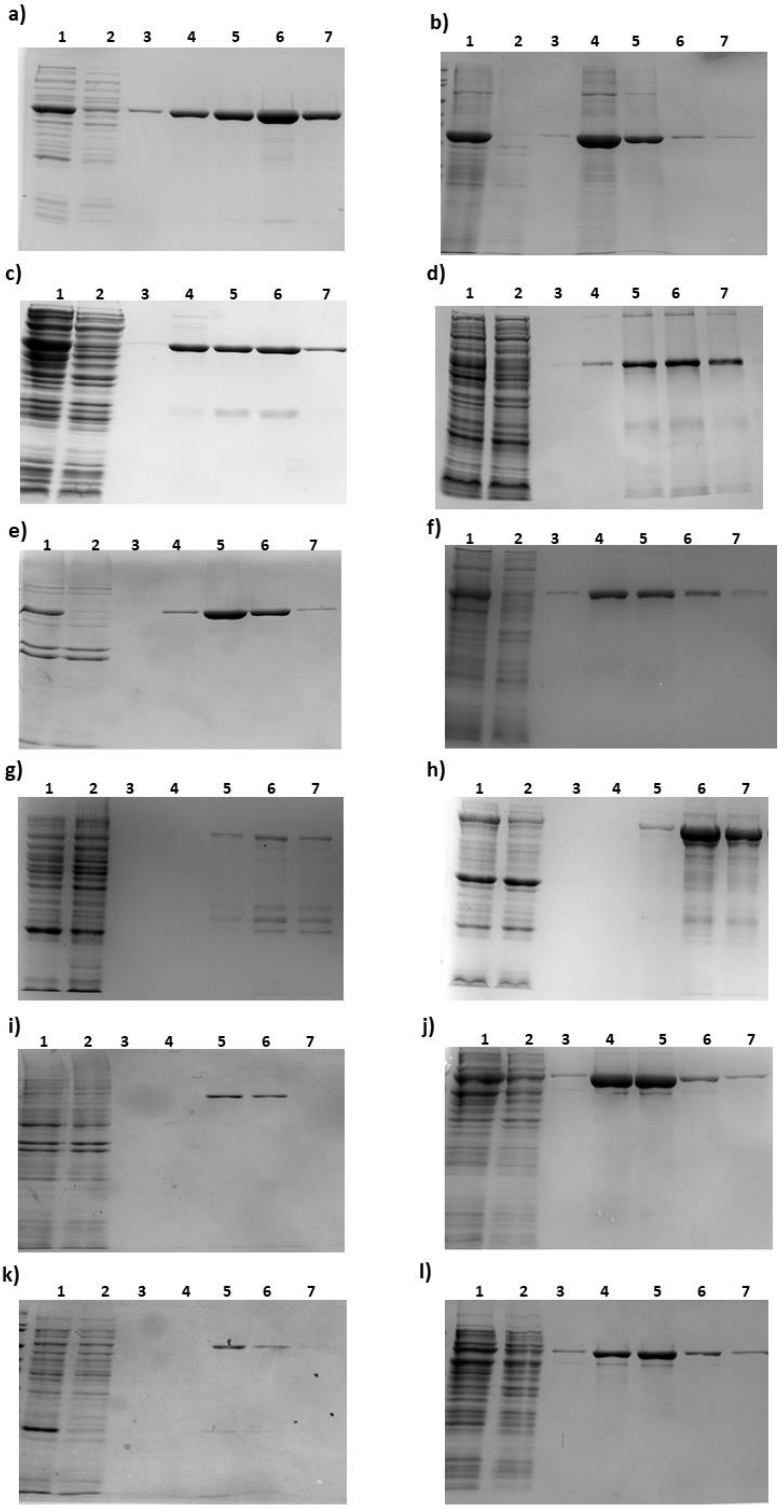

Figure 5. 93 Results of purification of monovalent/multivalent recombinant proteins with additional fusion partner using standard buffers: a) BB0126$_{BA}$-TrxA (buffers without urea); b) BB0126$_{BA}$-TrxA (buffers with urea); c) BB0126$_{BA}$-GST (buffers without urea); d) BB0126$_{BA}$-TrxA (buffers with urea); e) BmpA-BBA64-TrxA (buffers without urea); f) BmpA-BBA64-TrxA (buffers with urea); g) BmpA-BBA64-GST (buffers without urea); h) BmpA-BBA64-GST (buffers with urea); i) BmpA-BBK32-TrxA (buffers without urea); j) BmpA-BBK32-TrxA (buffers with urea); k) BmpA-BBK32-GST (buffers without urea); l) BmpA-BBK32-GST (buffers with urea).

Lanes:

1 - *E. coli* BL21(DE3)pLysS lysate before loading into the affinity column

2 - *E. coli* BL21(DE3)pLysS lysate after passing through the affinity column

3 - First elution fraction
4 - Second elution fraction
5 - Third elution fraction
6 - Fourth elution fraction
7 - Fifth elution fraction

After the purification, the electrophoretic purity of the obtained protein preparations was assessed using ImageLab [Methods 4.21].

5.5.7.4.4. Purification of monovalent and multivalent recombinant proteins with additional fusion partners - summary

The results indicate that BB0126BA-TrxA, BB0126BA-GST, and BmpA-BBA64-TrxA are produced by *E. coli* in a soluble form - it is unnecessary to use urea for their purification. On the other hand, BmpA-BBA64-GST, BmpA-BBK32-TrxA, and BmpA- BBK-GST are accumulated in the cell in the form of inclusion bodies, and it is necessary to use a denaturing agent to purify them.

As a result of the applied procedure of one-stage purification of recombinant antigens using metal affinity chromatography obtained protein preparations with electrophoretic purity in range 94-98%. Optimal purification conditions and the purity of the obtained recombinant and chimeric protein preparations are shown in Table 5.29.

Table 5. 29 Conditions for the purification of monovalent and multivalent *B. burgdorferi* s.l. recombinant proteins with additional domains

Recombinant protein	Isoelectric point	pH	5 M urea	Purity
$BB0126_{BA}$-TrxA	5.9	7.9	No	97%
$BB0126_{BA}$-GST	6.3	7.9	No	95%
BmpA-BBA64-TrxA	5.6	7.9	No	98%
BmpA-BBA64-GST	5.9	7.9	Yes	96%
BmpA-BBK32-TrxA	6.2	7.9	Yes	94%
BmpA-BBK32-GST	6.5	7.9	Yes	96%

However, despite the presence of domains with proven effectiveness in increasing the stability and solubility of recombinant proteins, it has not been possible to obtain the above antigens in a soluble form.

5.5.8. Determination of production efficiency of monovalent and multivalent recombinant proteins

The Bradford method determined the concentration of monovalent and multivalent recombinant proteins of *B. burgdorferi* s.l. in individual elution fractions [Methods 4.16]. Then, based on these data, the efficiency of the production of target proteins from 1 liter of bacterial culture of BL21(DE3)pLysS and Origami(DE3)™ was estimated. Calculations were made on the basis of protein concentration in preparations

obtained by purification using standard buffers A with 5 M or without urea [Materials 3.11.2.1]. The obtained results are summarized in Tables 5.30-5.32.

Table 5. 30 Efficiency of biotechnological production of monovalent recombinant proteins

Monovalent protein	*E. coli* strain	Culture medium	Temperature	Production efficiency [mg/l culture]
BB0108$_{BA}$	BL21(DE3)pLysS	LB	37ºC	59
BB0108$_{BB}$				61
BB0108$_{BG}$				63
BB0126$_{BA}$	BL21(DE3)pLysS	LB	37ºC	58
			30ºC	36
			20ºC	33
	Origami(DE3)™		37ºC	68
			30ºC	53
			20ºC	43
BB0126$_{BB}$	BL21(DE3)pLysS	LB	37ºC	47
			30ºC	40
			20ºC	32
	Origami(DE3)™		37ºC	69
			30ºC	50
			20ºC	37
BB0126$_{BG}$	BL21(DE3)pLysS	LB	37ºC	42
			30ºC	34
			20ºC	31
	Origami(DE3)™		37ºC	50
			30ºC	45
			20ºC	31
BB0298$_{BA}$	BL21(DE3)pLysS	LB	37ºC	55
			30ºC	47
			20ºC	38
	Origami(DE3)™		37ºC	67
			30ºC	52
			20ºC	36
BB0298$_{BB}$	BL21(DE3)pLysS	LB	37ºC	59
			30ºC	41
			20ºC	29
	Origami(DE3)™		37ºC	61
			30ºC	44
			20ºC	30
BB0298$_{BG}$	BL21(DE3)pLysS	LB	37ºC	61
			30ºC	47
			20ºC	25
	Origami(DE3)™		37ºC	68
			30ºC	30
			20ºC	24
BB0323$_{BA}$	BL21(DE3)pLysS	LB	37ºC	40
BB0323$_{BB}$				43
BB0323$_{BG}$				39
BB0689$_{BA}$	BL21(DE3)pLysS	LB	37ºC	78
			30ºC	68
			20ºC	50
	Origami(DE3)™		37ºC	86
			30ºC	72
			20ºC	56
BB0689$_{BB}$	BL21(DE3)pLysS	LB	37ºC	73
			30ºC	54

			20ºC	41
	Origami(DE3)™		37ºC	78
			30ºC	52
			20ºC	39
BB0689$_{BG}$	BL21(DE3)pLysS	LB	37ºC	71
			30ºC	62
			20ºC	33
	Origami(DE3)™		37ºC	75
			30ºC	57
			20ºC	30

Table 5. 31 Efficiency of biotechnological production of multivalent chimeric proteins

Multivalent protein	*E. coli* strain	Culture medium	Temperature	Production efficiency [mg/l culture]
BmpA-BBA64	BL21(DE3)pLysS	TB	30ºC	32
			25ºC	18
			20ºC	-
	Origami(DE3)™		30ºC	51
			25ºC	25
			20ºC	10
BmpA-BBK32	BL21(DE3)pLysS	TB	30ºC	19
			25ºC	20
			20ºC	13
	Origami(DE3)™		30ºC	53
			25ºC	25
			20ºC	11
BmpA-BBK32-M	BL21(DE3)pLysS	LB	37ºC	53
BmpA-BBK32-G	BL21(DE3)pLysS	LB	37ºC	93

Table 5. 32 Efficiency of biotechnological production of monovalent and multivalent recombinant proteins with additional fusion partners

Recombinant protein	*E. coli* strain	Culture medium	Temperature	Production efficiency [mg/l culture]
BB0126$_{BA}$-TrxA	BL21(DE3)pLysS	LB	37°C	33
BB0126$_{BA}$-GST	BL21(DE3)pLysS	TB	37°C	37
BmpA-BBA64-TrxA	BL21(DE3)pLysS	TB	30ºC	56
BmpA-BBA64-GST	BL21(DE3)pLysS	TB	30ºC	50
BmpA-BBK32-TrxA	BL21(DE3)pLysS	LB	30ºC	43
BmpA-BBK32-GST	BL21(DE3)pLysS	LB	30ºC	42

5.6. Evaluation of the reactivity of monovalent and multivalent recombinant proteins with specific antibodies

To estimate the reactivity of the obtained monovalent and multivalent recombinant proteins with specific anti-*B. burgdorferi* s.l. antibodies, two immunoenzymatic assays were used, i.e., Western blot and ELISA [Materials 3.13 and 3.15; Methods 4.14.2 and 4.19]. The assays were based on *B. burgdorferi* s.l. antigens produced in *E. coli* BL21(DE3)pLysS in LB or TB at 30ºC or 37ºC [Methods 4.12] and

purified using standard A buffers [Materials 3.11, Methods 4.13]. Monovalent and multivalent recombinant proteins with fusion partners were not used in the immunoenzymatic tests because the additional domains did not improve the solubility of target proteins and its presence could affect overall protein reactivity with antibodies.

5.6.1. Western blot

5.6.1.1. Determination of optimal Western blot conditions

A series of Western blots with chemiluminescence detection were performed to preliminary evaluate the reactivity of monovalent and multivalent recombinant proteins with specific anti-*B. burgdorferi* s.l. IgG and IgM in human serum [Materials 3.13, Methods 4.14.2.1]. The first stage was the selection of optimal assay conditions, i.e., dilution of sera and secondary antibodies, and the incubation time at each stage of the test.

In the case of monovalent recombinant proteins to limit the amount of used sera, two different antigens were applied to the same lane (Table 5.33). It should be noted that the recombinant proteins present in the mixture had to differ significantly in molecular mass so that during electrophoresis they formed two separated bands (Figure 5.94). BB0323s simirarly like BmpA-BBK32, BmpA-BBA64, BmpA-BBK32-G, and BmpA-BBK32-M were tested alone. Recombinant and chimeric proteins were loaded at 3.5 µg and 7 µg per lane, respectively.

Table 5. 33 Composition of monovalent recombinant protein antigen preparation used for the Western blot

Antigen preparation 1	Antigen preparation 2	Antigen preparation 3
BB0323s – 50 kDa	BB0108s – 44 kDa BB0126s – 30 kDa	BB0298s – 32 kDa BB0698s – 23 kDa

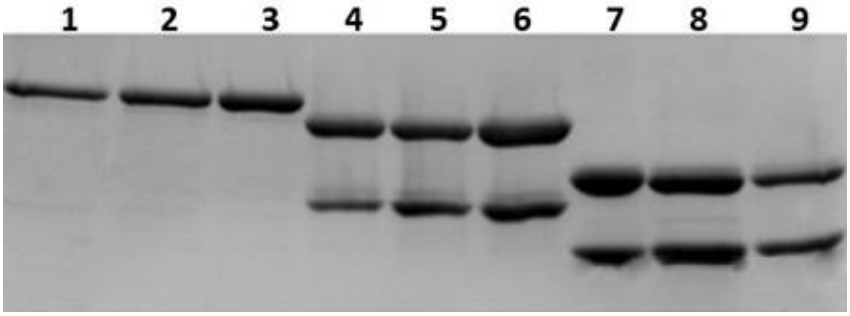

Figure 5. 94 SDS-PAGE of *B. burgdorferi* s.l. antigen preparations composed of monovalent recombinant proteins

Lanes:

1 - Antigen preparation 1BA - $BB0323_{BA}$
2 - Antigen preparation 1BB - $BB0323_{BB}$
3 - Antigen preparation 1BG - $BB0323_{BG}$
4 - Antigen preparation 2BA - $BB0108_{BA}$ and $BB0126_{BA}$
5 - Antigen preparation 2BB - $BB0108_{BB}$ and $BB0126_{BB}$
6 - Antigen preparation 2BG - $BB0108_{BG}$ and $BB0126_{BG}$
7 - Antigen preparation 3BA - $BB0298_{BA}$ and $BB0689_{BA}$

8 - Antigen preparation 3BB - $BB0298_{BB}$ and $BB0689_{BB}$
9 - Antigen preparation 3BG - $BB0298_{BG}$ and $BB0689_{BG}$

The obtained optimization results were satisfactory. It was possible to select such conditions that no signal was observed on the membranes incubated with negative sera, meaning no cross-reactions occurred. In contrast, a clear signal was seen on the membranes incubated with the positive sera (Figures 5.95-5.97). It was impossible to reduce the dilution of the sera or secondary antibodies to higher the sensitivity of Western blots because a signal was often obtained on the membranes incubated with the negative sera.

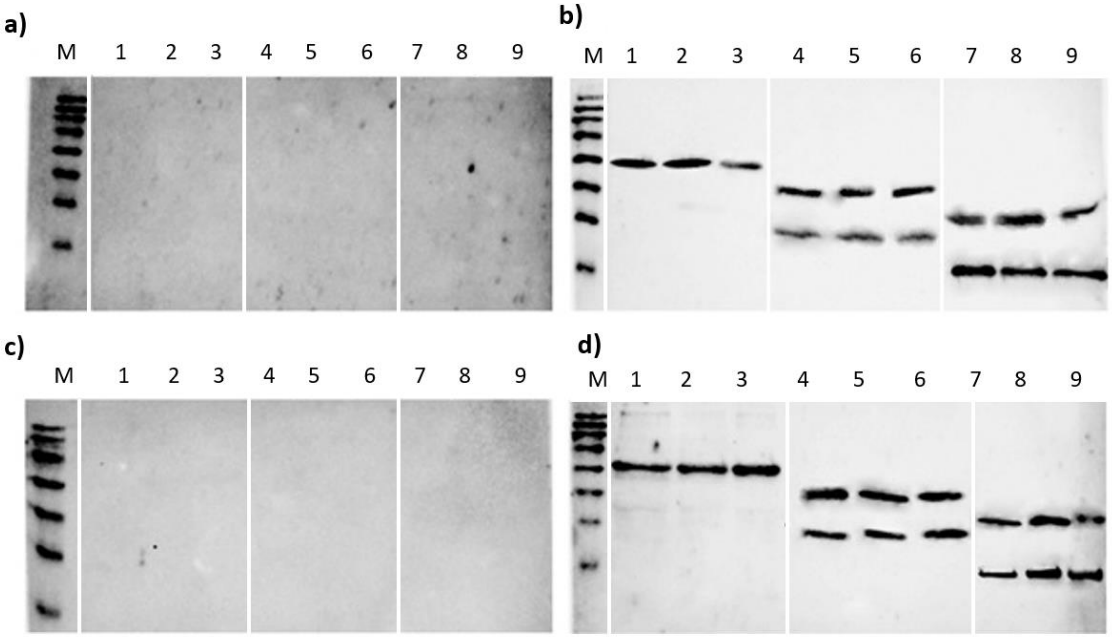

Figure 5. 95 Optimization of the Western blot based on monovalent recombinant proteins (chemiluminescence detection): a) membrane incubated with negative sera, IgM detection (serum sample dilution: 1:200; secondary antibodies dilution: 1:50 000); b) membrane incubated with positive sera, IgM detection (serum sample dilution: 1:200; secondary antibodies dilution: 1:50 000); c) membrane incubated with negative sera, IgG detection (serum sample dilution: 1:200; secondary antibodies dilution: 1:75 000); d) membrane incubated with positive sera, IgG detection (serum sample dilution: 1:200, secondary antibodies dilution: 1:75 000).
Lanes:
M - Protein marker, SuperSignal™
1 - Antigen preparation 1BA - $BB0323_{BA}$
2 - Antigen preparation 1BB - $BB0323_{BB}$
3 - Antigen preparation 1BG - $BB0323_{BG}$
4 - Antigen preparation 2BA - $BB0108_{BA}$ and $BB0126_{BA}$
5 - Antigen preparation 2BB - $BB0108_{BB}$ and $BB0126_{BB}$
6 - Antigen preparation 2BG - $BB0108_{BG}$ and $BB0126_{BG}$
7 - Antigen preparation 3BA - $BB0298_{BA}$ and $BB0689_{BA}$
8 - Antigen preparation 3BB - $BB0298_{BB}$ and $BB0689_{BB}$
9 - Antigen preparation 3BG - $BB0298_{BG}$ and $BB0689_{BG}$

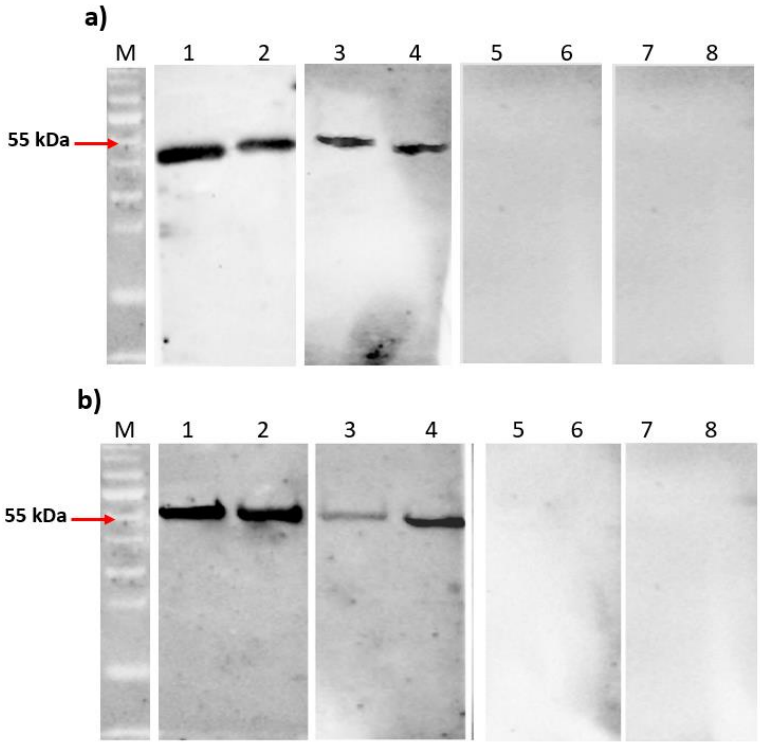

Figure 5. 96 Optimization of the Western blot based on BmpA-BBA64 and BmpA-BBK32 multivalent chimeric proteins: a) detection of specific IgM (serum sample dilution: 1:200; secondary antibodies dilution: 1:75 000); b) detection of specific IgG (serum sample dilution: 1:200; secondary antibodies dilution: 1:100 000) (chemiluminescence detection) .

Lanes:

M - Protein marker, PageRuler™ Prestained Protein Ladder
1 - BmpA-BBA64 incubated with positive sera I
2 - BmpA-BBK32 incubated with positive sera I
3 - BmpA-BBA64 incubated with positive sera II
4 - BmpA-BBK32 incubated with positive sera II
5 - BmpA-BBA64 incubated with negative sera I
6 - BmpA-BBK32 incubated with negative sera I
7 - BmpA-BBA64 incubated with negative sera II
8 - BmpA-BBK32 incubated with negative sera II

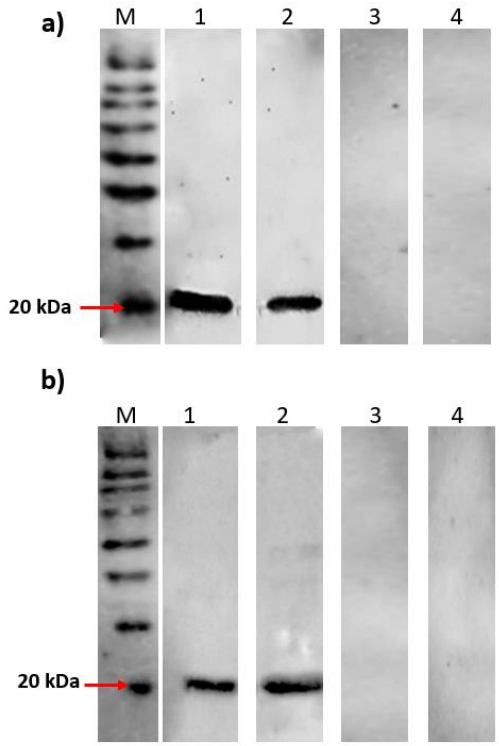

Figure 5. 97 Optimization of the Western blot based on: a) BmpA-BBK32-M (serum sample dilution: 1:200; anti-human IgM secondary antibodies dilution: 1:75 000); b) BmpA-BBK32-G (serum sample dilution: 1:200; anti-human IgG secondary antibodies dilution: 1:100 000) (chemiluminescence detection)
Lanes:
M - Protein marker, SuperSignal™
1 - chimeric protein incubated with positive sera I
2 - chimeric protein incubated with positive sera II
3 - chimeric protein incubated with negative sera I
4 - chimeric protein incubated with negative sera II

The best differentiation between the two groups of sera was obtained for the following conditions:

- monovalent recombinant proteins:
  - dilution of sera 1:200 (1.5 h incubation) and dilution of anti-human IgM secondary antibodies 1:50 000 (1 h incubation);
  - dilution of sera 1:200 (incubation 1 h) and dilution of anti-human IgM secondary antibodies 1:75 000 (incubation 1 h);
- multivalent chimeric proteins:
  - dilution of sera 1:200 (1 h incubation) and dilution of anti-human IgM secondary antibodies 1:75 000 (1 h incubation);
  - dilution of sera 1:200 (incubation 1 h) and dilution of anti-human IgG secondary antibodies 1:100 000 (incubation 1 h).

To estimate the reactivity of monovalent recombinant proteins with a large number of sera in a short time, it was decided to modify the Western blot procedure [Materials 3.13, Methods 4.14.2.2]. The structure of the gel combs was changed so that the prepared gels had one large lane (Figure 5.98). 40 µg of each protein was loaded into an enlarged well and standard electrophoretic separation and transfer to nitrocellulose membrane was performed. After transfer, the membrane was stained with Ponceau S reagent, and the exact location of separated proteins was marked. The membrane was then destained with a blocking buffer. After overnight blocking at 4°C, the membrane was cut into 5 mm wide strips. The further procedure was carried out identically to the standard WB [Materials 3.13; Methods 4.14.2.1].

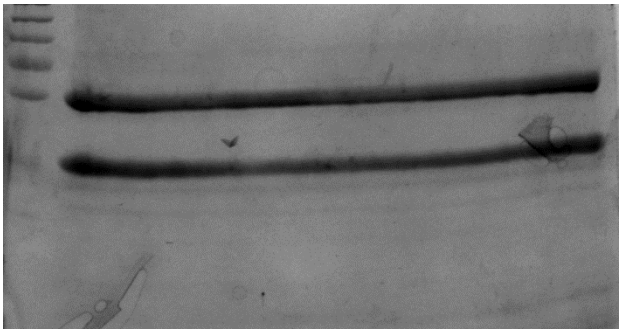

Figure 5. 98 SDS-PAGE of monovalent *B. burgdorferi* s.l recombinant proteins in polyacrylamide gel prepared with the use of modified combs.

5.6.1.2. Western blot based on monovalent recombinant proteins

Preliminary determination of reactivity of BB0108s, BB0126s, BB0298s, BB0323s and BB0689s recombinant proteins with IgG and IgM was performed with a of 75 human serum samples (25 negative, 25 IgM positive and 25 IgG positive).

Individual proteins showed varying reactivity with antibodies in human sera but were generally recognized by immunoglobulins with low efficiency. Slight differences in reactivity were seen between protein variants from different genospecies. It appears that in most cases, the *B. burgdorferi* s.s.derived protein were recognized by specific IgG less frequently than their *B. afzelii* and *B. garinii* equivalents (Table 5.34).

Table 5. 34 Results of IgG-Western blot based on monovalent recombinant proteins

Monovalent protein	Sensitivity (n=25)	Specificity (n=25)	PPV	NPV	Statistically significant (P<0.05)
BB0108$_{BA}$	48% (12/25)*	92% (2/25)*	86%	64%	Yes (P=0.0036)
BB0108$_{BB}$	40% (10/25)*	96% (1/25)*	91%	62%	Yes (P=0.0046)
BB0108$_{BG}$	44% (11/25)*	88% (3/25)*	79%	61%	Yes (P=0.0255)
BB0108$_{BA+BB+BG}$	48% (12/25)*	92% (2/25)*	86%	64%	Yes (P=0.0036)
BB0126$_{BA}$	24% (6/25)*	92% (2/25)*	75%	55%	No (P=0.2467)
BB0126$_{BB}$	20%(5/25)*	88% (3/25)*	63%	52%	No (P=0.7019)
BB0126$_{BG}$	16% (4/25)*	100% (0/25)*	100%	54%	No (P=0.1099)
BB0126$_{BA+BB+BG}$	24% (6/25)*	88% (3/25)*	67%	54%	No (P=0.4635)
BB0298$_{BA}$	24% (6/25)*	96% (1/25)*	86%	56%	No (P=0.0983)
BB0298$_{BB}$	20 % (5/25)*	100% (0/25)*	100%	56%	No (P=0.0502)
BB0298$_{BG}$	24% (6/25)*	100% (0/25)*	100%	57%	Yes (P=0.0223)
BB0298$_{BA+BB+BG}$	24% (6/25)*	96% (1/25)*	86%	56%	No (P=0.0983)
BB0323$_{BA}$	44% (11/25)*	88% (3/25)*	79%	61%	Yes (P=0.0255)
BB0323$_{BB}$	36% (9/25)*	92% (2/25)*	82%	59%	Yes (P=0.0374)
BB0323$_{BG}$	44% (11/25)*	92% (2/25)*	85%	62%	Yes (P=0.0083)
BB0323$_{BA+BB+BG}$	44% (11/25)*	88% (3/25)*	79%	61%	Yes (P=0.0255)
BB0689$_{BA}$	52% (13/25)*	72% (7/25)*	65%	60%	No (P=0.1482)
BB0689$_{BB}$	44% (11/25)*	76% (6/25)*	65%	58%	No (P=0.2321)
BB0689$_{BG}$	48% (12/25)*	72% (7/25)*	63%	58%	No (P=0.2436)
BB0689$_{BA+BB+BG}$	60% (15/25)*	64% (9/25)*	63%	62%	No (P= 0.1564)

* - number of positive sera/number of tested sera
PPV - positive predictive value
NPV – negative predictive value

The most frequently recognized by IgG contained in the positive sera were BB0108s and BB0689s and their reactivity never dropped below 40% reaching a maximum of 52% for BB0689$_{BA}$. BB0126s, and BB0298s were very weakly reactive, recognized only by antibodies contained in around 20% of tested sera. The specificity of antigen-antibody interactions was relatively high. It did not fall below 88%, except for BB0689s where the specificity dropped to 72%. The overall sensitivity and specificity of the tests when summing up the results for the three variants of a given antigen remained unchanged relative to the most reactive one, except for BB0689, where the sensitivity increased to 60% (15/25), but the specificity decreased to 64% (9/25).

A positive and negative predictive value (PPV, NPV) was also determined for Western blots based on all antigens. The highest PPV was obtained for BB0298s, which did not fall below 86%, and for variants, with *B. burgdorferi* s.s. and *B. garinii* it was 100%. The NPV only for BB0108 reached over 60% for all protein variants. Generally, PPV was relatively highly diversified and ranged from 63% to 100%. Whereas, the NPV was very homogeneous, in all cases was in the narrow range of 52-64% (Table 5.34).

In all cases, the monovalent recombinant proteins were more often recognized by antibodies contained in sera from individuals infected with *B. burgdorferi* s.l. However, after analyzed by Fisher's exact test and assuming *p*-value = 0.05, it was shown that a statistically significant difference in the reactivity of recombinant proteins with IgG contained in positive and negative sera occurs only for BB0108s (all variants), BB0323s (all variants) and $BB0298_{BG}$.

The Figures 5.99-5.101 shows representative IgG-WB results obtained for monovalent recombinant proteins derived from *B. afzelii*.

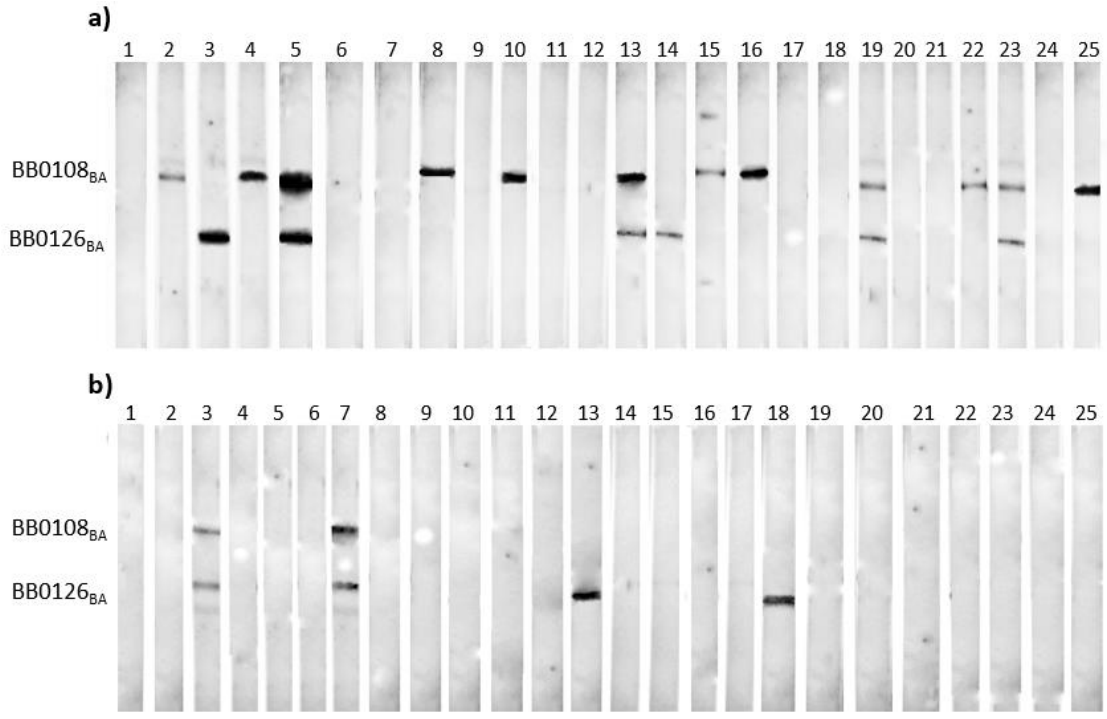

Figure 5. 99 IgG-Western blot results for $BB0108_{BA}$ and $BB0126_{BA}$ (chemiluminescence detection): a) incubation with 25 positive sera; b) incubation with 25 negative sera.

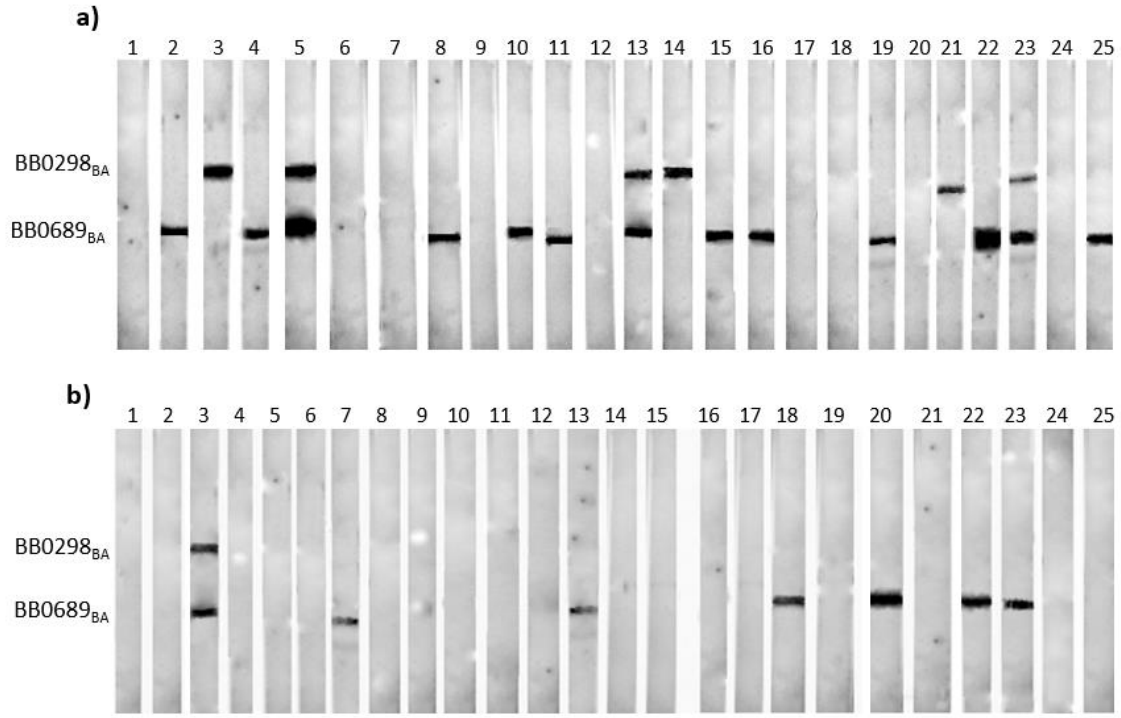

Figure 5. 100 IgG-Western blot results for $BB0298_{BA}$ and $BB0689_{BA}$ (chemiluminescence detection): a) incubation with 25 positive sera; b) incubation with 25 negative sera.

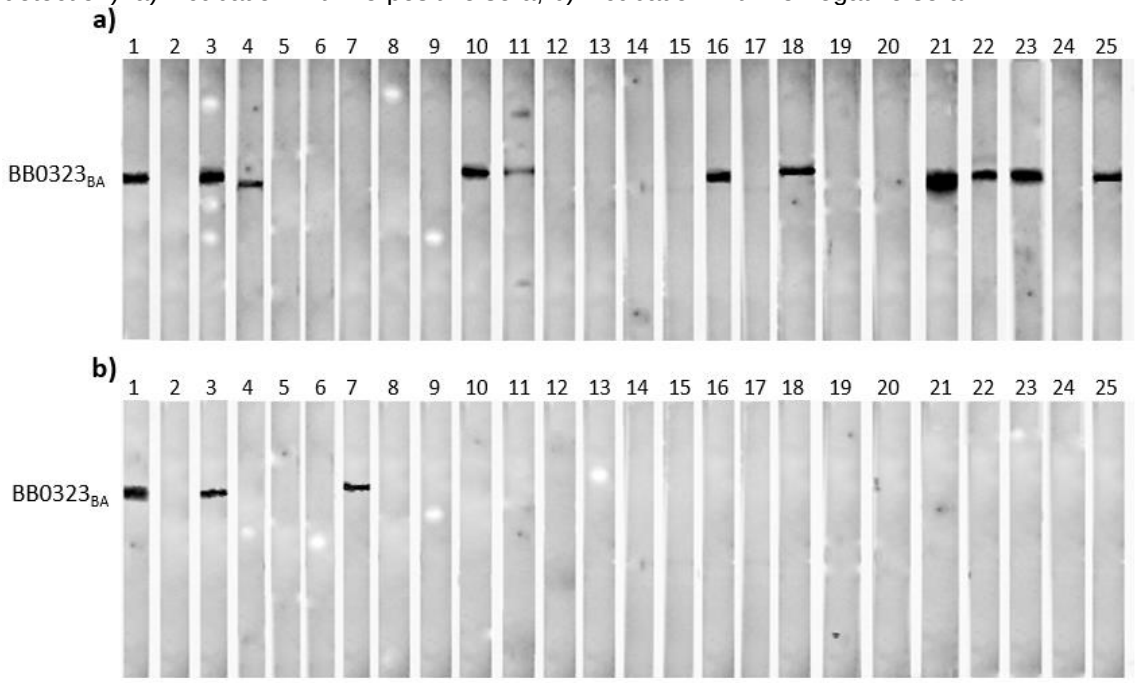

Figure 5. 101 IgG-Western blot results for $BB0323_{BA}$ (chemiluminescence detection): a) incubation with 25 positive sera; b) incubation with 25 negative sera.

All tested proteins were poorly recognized by IgM contained in serum samples (Table 5.35). The highest reactivity achieved for BB0108 from *B. afzelii* and *B. garinii* was 24%. Generally, antigens showed low cross-reactivity with IgM from the negative sera. The specificity of IgM-WB was over 90% in all cases.

Table 5. 35 Results of IgM-Western blot based on monovalent recombinant proteins

Monovalent protein	Sensitivity (n=25)	Specificity (n=25)	PPV	NPV	Statistically significant (P<0.05)
BB0108$_{BA}$	24% (6/25)*	96% (1/25)*	86%	56%	No (P=0.0983)
BB0108$_{BB}$	20% (5/25)*	96% (1/25)*	83%	55%	No (P=0.1895)
BB0108$_{BG}$	24% (6/25)*	96% (1/25)*	86%	56%	No (P=0.0983)
BB0108$_{BA+BB+BG}$	24% (6/25)*	96% (1/25)*	86%	56%	No (P=0.0983)
BB0126$_{BA}$	16% (4/25)*	92% (2/25)*	67%	52%	No (P=0.6671)
BB0126$_{BB}$	8% (2/25)*	92% (2/25)*	50%	50%	No (P>0.9999)
BB0126$_{BG}$	8% (2/25)*	92% (2/25)*	50%	50%	No (P>0.9999)
BB0126$_{BA+BB+BG}$	16% (4/25)*	92% (2/25)*	67%	52%	No (P=0.6671)
BB0298$_{BA}$	8% (2/25)*	96% (1/25)*	67%	51%	No (P>0.9999)
BB0298$_{BB}$	12% (3/25)*	92% (2/25)*	60%	51%	No (P>0.9999)
BB0298$_{BG}$	8% (2/25)*	96% (1/25)*	67%	51%	No (P>0.9999)
BB0298$_{BA+BB+BG}$	12% (3/25)*	92% (2/25)*	60%	51%	No (P>0.9999)
BB0323$_{BA}$	8% (2/25)*	96% (1/25)*	67%	51%	No (P>0.9999)
BB0323$_{BB}$	4% (1/25)*	96% (1/25)*	50%	50%	No (P>0.9999)
BB0323$_{BG}$	8% (2/25)*	92% (2/25)*	50%	50%	No (P>0.9999)
BB0323$_{BA+BB+BG}$	8% (2/25)*	92% (2/25)*	50%	50%	No (P>0.9999)
BB0689$_{BA}$	20% (5/25)*	96% (1/25)*	83%	55%	No (P=0.1895)
BB0689$_{BB}$	12% (3/25)*	96% (1/25)*	75%	52%	No (P=0.6092)
BB0689$_{BG}$	12% (3/25)*	92% (2/25)*	60%	51%	No (P>0.9999)
BB0689$_{BA+BB+BG}$	20% (5/25)*	92% (2/25)*	71%	53%	No (P=0.4174)

* - number of positive sera/number of tested sera
PPV - positive predictive value
NPV – negative predictive value

PPV and NPV were more uniform than for IgG-WB ranging from 50-86% and 49-56%, respectively. Both PPV and NPV reached the highest value for IgM-WB based on BB0108$_{BA}$ and BB0108$_{BG}$. Fisher's exact test showed no statistically significant differences in the reactivity of all tested antigens with the IgM contained in the negative and positive sera (Table 5.35).

5.6.1.3. Western blot based on multivalent chimeric proteins

The preliminary determination of the diagnostic utility of multivalent chimeric proteins with IgG and IgM was carried out using 40 seropositive sera with known specific antibody titers and 20 seronegative sera (20 IgG positive, 20 IgM positive, and 20 negative). The reactivity of BmpA-BBA64 and BmpA-BBK32 in Western blot with both

classes of antibodies was estimated, while in the case of BmpA-BBK32-M and BmpA-BBK32-G, only their utility for the detection of the antibody isotype for which they were designed was determined (Tables 5.36 and 5.37) [Methods 4.14.2.2].

Table 5. 36 Results of IgG-Western blot based on multivalent chimeric proteins

Multivalent protein	Sensitivity (n=20)	Specificity (n=20)	PPV	NPV	Statistically significant (P<0.05)
BmpA-BBA64	100% (20/20)*	100% (0/20)*	100%	100%	Yes
BmpA-BBK32	100% (20/20)*	100% (0/20)*	100%	100%	Yes
BmpA-BBK32-G	90% (18/20)*	100% (0/20)*	100%	91%	Yes

* - number of positive sera/number of tested sera
PPV - positive predictive value
NPV - negative predictive value

Table 5. 37 Results of IgM-Western blot based on multivalent chimeric proteins

Multivalent protein	Sensitivity (n=20)	Specificity (n=20)	PPV	NPV	Statistically significant (P<0.05)
BmpA-BBA64	65% (13/20)*	55% (9/20)*	59%	61%	No (P=0.3406)
BmpA-BBK32	65% (13/20)*	60% (8/20)*	62%	63%	No (P= 0.2049)
BmpA-BBK32-M	70% (14/20)*	80% (4/20)*	78%	73%	Yes

* - number of positive sera/number of tested sera
PPV - positive predictive value
NPV - negative predictive value

The results obtained for all tested multivalent chimeric proteins are shown in Figures 5.102-5.107.

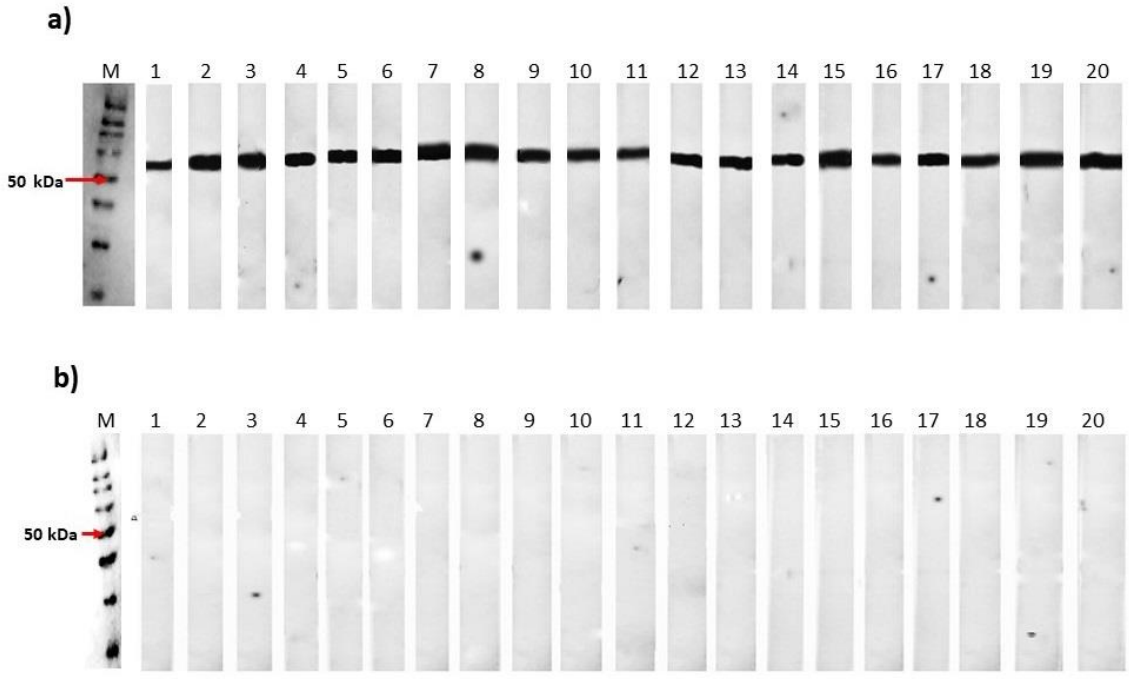

Figure 5. 102 IgG-Western blot results for BmpA-BBA64 (chemiluminescent detection): a) incubation with 20 positive sera; b) incubation with 20 negative sera; M - Protein marker, SuperSignal™.

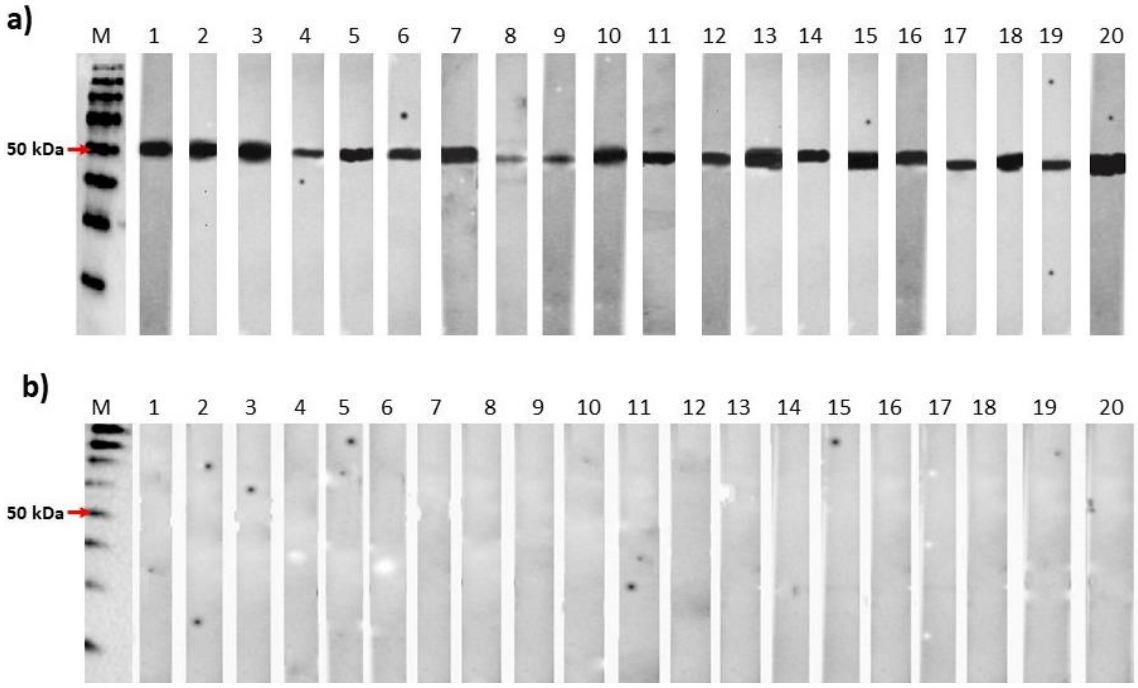

Figure 5. 103 IgG-Western blot results for BmpA-BBK32 (chemiluminescent detection): a) incubation with 20 positive sera; b) incubation with 20 negative sera; M - Protein marker, SuperSignal™.

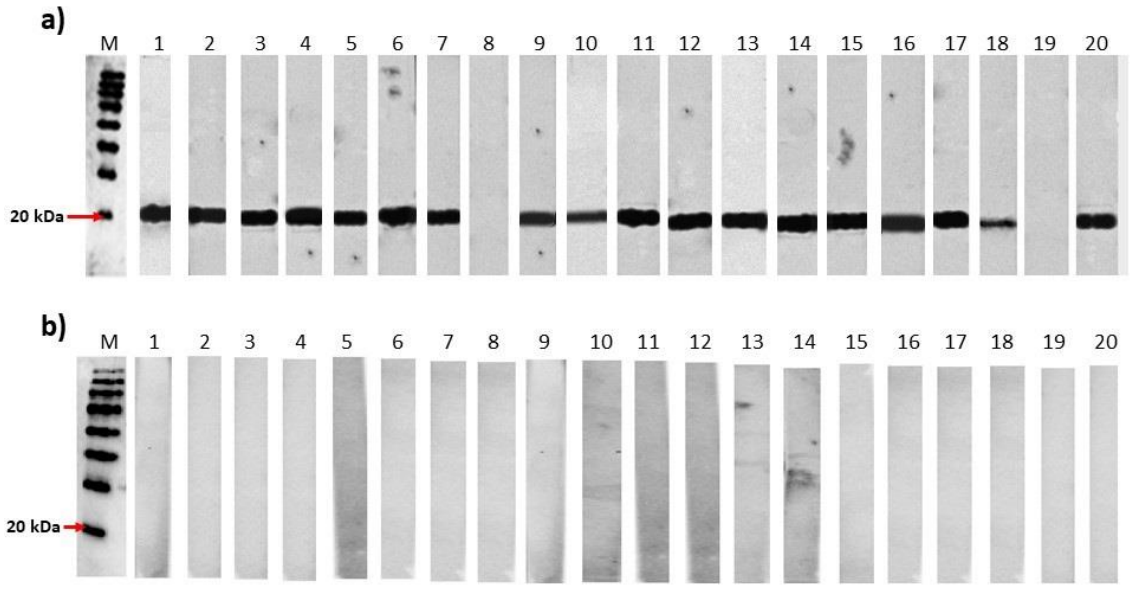

Figure 5. 104 IgG-Western blot results for BmpA-BBK32-G (chemiluminescent detection): a) incubation with 20 positive sera; b) incubation with 20 negative sera; M - Protein marker, SuperSignal™.

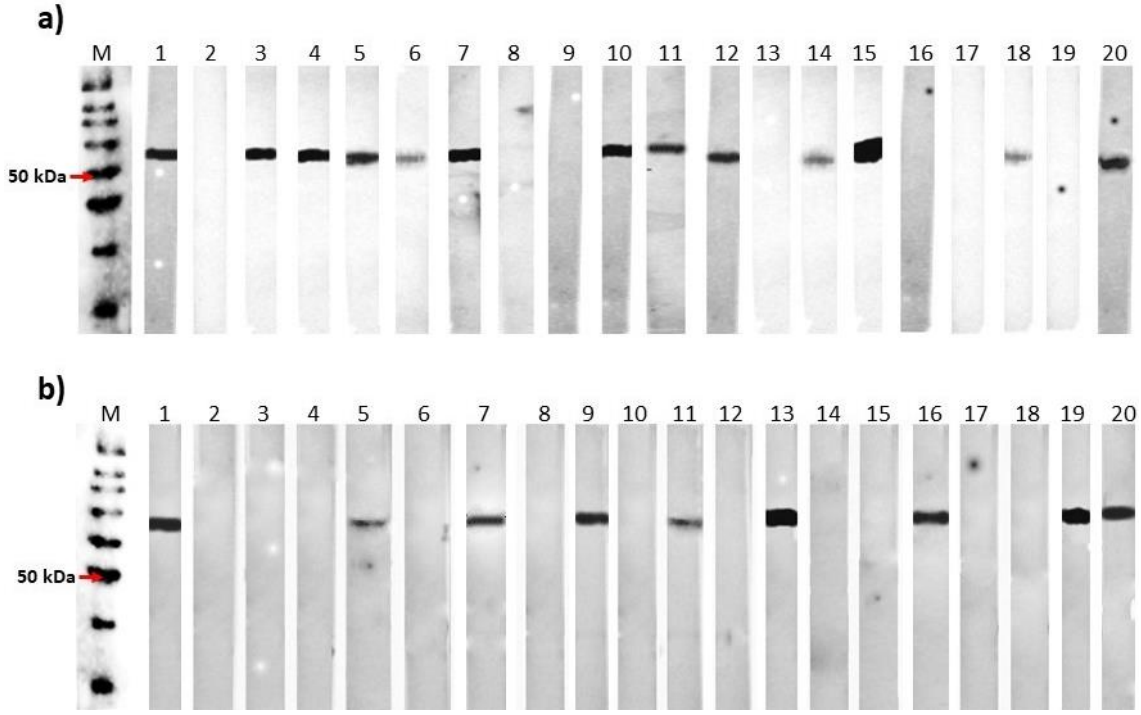

Figure 5. 105 IgM-Western blot results for BmpA-BBA64 (chemiluminescent detection): a) incubation with 20 positive sera; b) incubation with 20 negative sera; M - Protein marker, SuperSignal™.

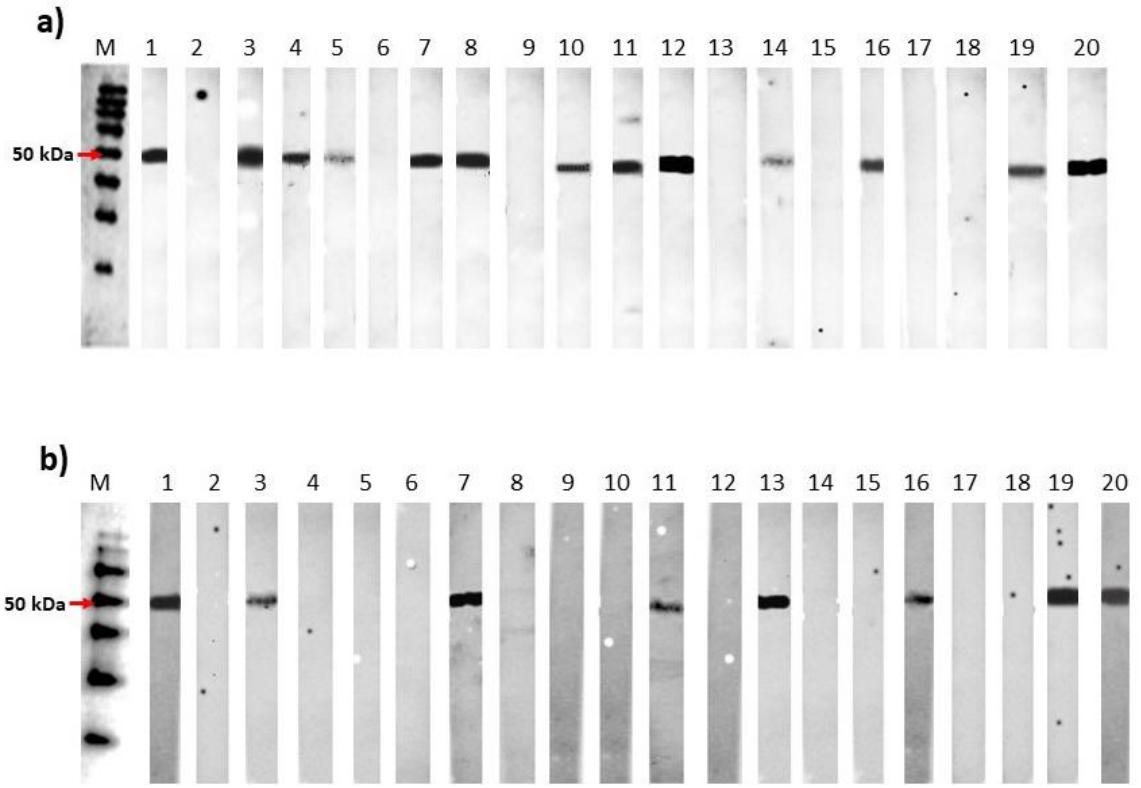

Figure 5. 106 IgM-Western blot results for BmpA-BBK32 (chemiluminescent detection): a) incubation with 20 positive sera; b) incubation with 20 negative sera; M - Protein marker, SuperSignal™.

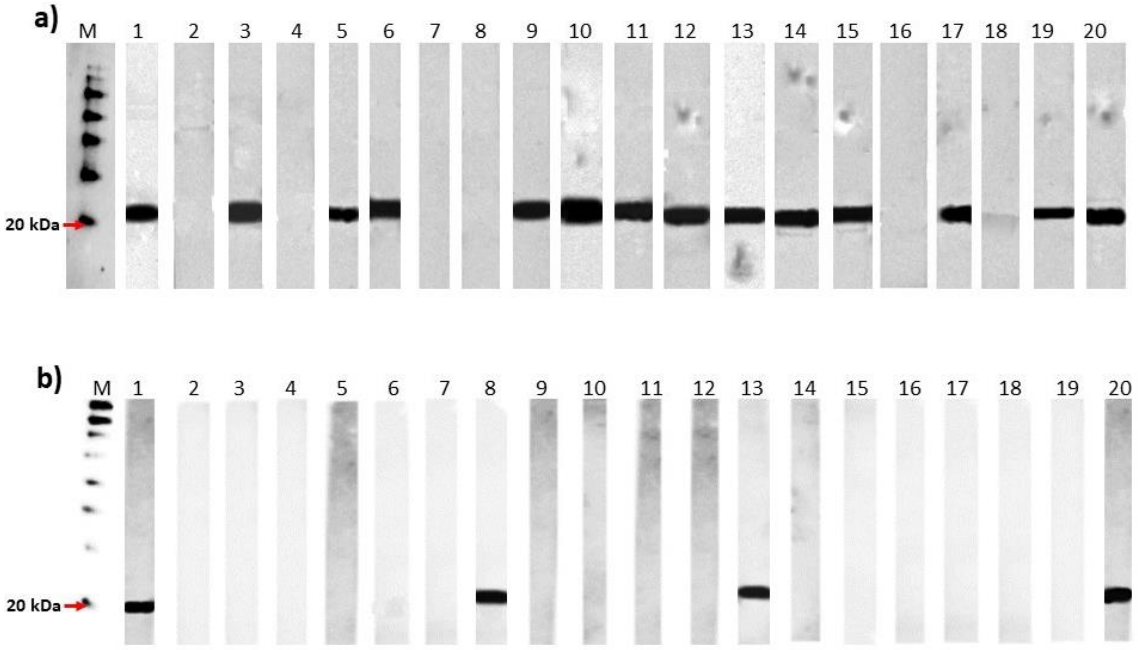

Figure 5. 107 IgM-Western blot results for BmpA-BBK32-M (chemiluminescent detection): a) incubation with 20 positive sera; b) incubation with 20 negative sera; M - Protein marker, SuperSignal™.

BmpA-BBA64, BmpA-BBK32, and BmpA-BBK32-G showed high reactivity with IgG in Western blot. When considering the bands of lower intensity Western blot based on BmpA-BBA64 and BmpA-BBK32 showed 100% sensitivity, this result was slightly lower for IgG-WB-BmpA-BBK32-G and amounted to 90%. Furthermore, no immunoreactivity of either chimeric protein was observed with serum samples from healthy patients (100% specificity). The PPV in all cases was 100%, while the NPV only for BmpA-BBK32-G decreased to 91%. Fisher's exact test showed a statistically significant difference in the reactivity of all chimeric proteins with IgG contained in both groups of sera (Table 5.36).

In the case of IgM detection using BmpA-BBA64, BmpA-BBK32, and BmpA-BBK32-M, the results were not so satisfactory. The sensitivity of the Western blot was similar for all antigens. For WB based on BmpA-BBA64, BmpA-BBK32 it was 55%, while for BmpA-BBK32-M it increased to 60%. The specificity of IgM-WB was 55%, 60% and 80% for BmpA-BBA64, BmpA-BBK32, and BmpA-BBK32-M, respectively. Fisher's exact test showed that only IgM-WB-BmpA-BBK32-M had statistically significant differences in reactivity with IgM in the negative and positive sera (Table 5.37).

5.6.2 ELISA

5.6.2.1. Determining the optimal conditions

In order to determine the conditions providing the highest efficiency for ELISA, optimization of the concentration of individual antigens, serum dilutions, and dilutions of

secondary antibodies labeled with horseradish peroxidase was carried out. Plates were coated with antigen or purified *E. coli* BL21(DE3)pLysS transformed with pUET1 lysate at 0.1 µg, 0.25 µg, 0.5 µg, 1 µg, and 2 µg per well. ELISA was performed using positive and negative sera diluted 1:100 and 1:200. The plates were then incubated with various dilutions of anti-human IgG or IgM antibodies (from 1:2 000 to 1:128 000).

Based on the results obtained for BB0108s, BB0323s, BmpA-BBK32-M, and BmpA-BBK32-G, it was found that the best differentiation between negative and positive sera was obtained in the assay where the plates were coated with 1 µg antigen per well. In ELISA based on the protein mix, the wells were coated with 0.33 µg of each antigen, thus the total antigen content remained unchanged. The dilution of the sera was 1:100, and the dilution of secondary antibodies was 1:16 000 and 1:32 000 for IgM and IgG, respectively (Figure 5.108).

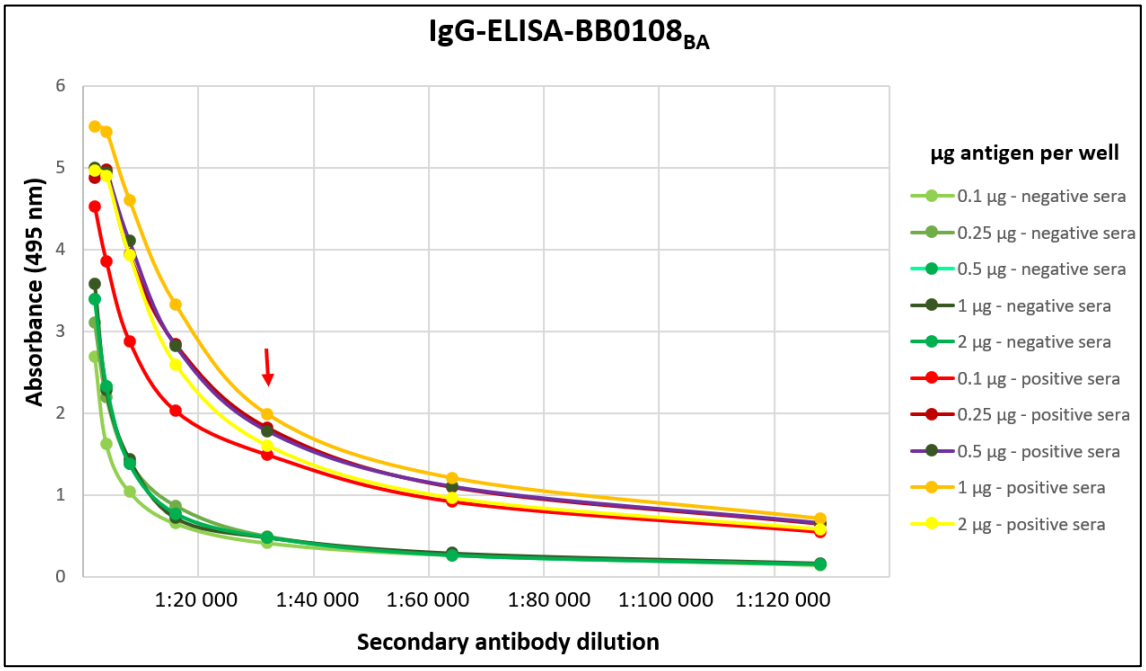

Figure 5. 108 Optimization of ELISA conditions on the example of $BB0108_{BA}$. The red arrow indicates the conditions that provide the best differentiation between negative and positive sera.

During optimization, BB0126s, BB0298s, BB0689s, BmpA-BBK32, and BmpA-BBA64 showed no reactivity with IgM and IgG in ELISA under any conditions. The obtained signal after incubation with positive sera for these proteins was so low that it did not differ from that obtained for the control, which was the purified *E. coli* lysate BL21(DE3)pLysS + pUET1 (Figure 5.109). Therefore, it was decided to exclude these proteins from further ELISA on a large pool of sera.

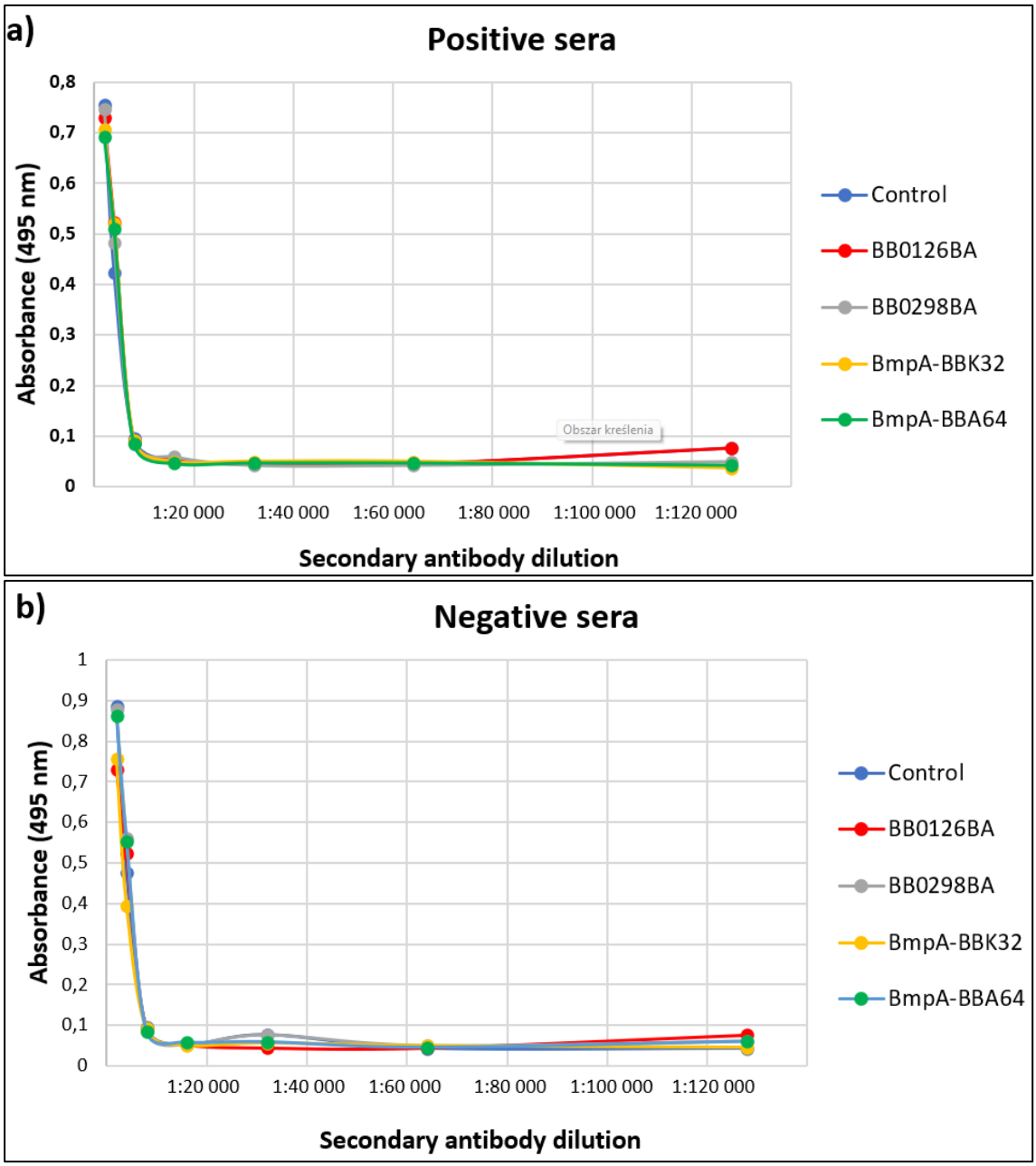

Figure 5. 109 Optimization of ELISA conditions for BB0126s, BB0298s, BB0689s, BmpA-BBK32, and BmpA-BBA64 antigens. Plates were coated with 1 µg antigen per well, secondary antibody dilution range 1:2 000 to 1:128 000: a) results for IgG positive sera; b) results for negative sera.

5.1.4.3. ELISA based on monovalent recombinant proteins

The sensitivity and specificity of ELISA based on BB0108s and BB0323s in detecting anti-*B. burgdorferi* s.l. IgG and IgM were determined using cut-off values obtained by ROC analysis.

The sensitivity of the IgG-ELISA based on BB0108s (IgG-ELISA-BB0108s) ranged from 74% to 82%, with the highest value obtained for $BB0108_{BA}$ (Table 5.38). The specificity of all IgG-ELISA-BB0108s was 82%. The area

under the curve value ranged from 0.807-0.877; again, the highest value was achieved with BB0108BA (Figures 5.110 and 5.111).

The sensitivity of the IgG-ELISA-BB0323s was the highest for $BB0323_{BA}$ and the lowest for $BB0323_{BB}$, reaching 72% and 62%, respectively (Table 5.38). The specificity for all variants of the antigen was around 90%, while the AUC reached the range of 0.805-0.840 (Figure 5.112-5.113).

The use of the BB0108s mixture in IgG-ELISA significantly increased the specificity (91%) of the assay and led to an increase in AUC (0.920), while in the case of BB0323s, this had no positive effect on any of the assay parameters.

Table 5. 38 IgG-ELISA based on BB0108s and BB0323s

Monovalent protein	Optimal cut-off	Sensitivity [%]	Specificity [%]	AUC	Mean absorbance	Median absorbance
$BB0108_{BA}$	0.193	82% (82/100)*	82% (18/100)*	0.877	P^a: 0.340 N^b: 0.153	P^a:0.317 N^b: 0.128
$BB0108_{BB}$	0.196	71% (71/100)*	82% (18/100)*	0.807	P^a: 0.323 N^b: 0.155	P^a: 0.297 N^b: 0.130
$BB0108_{BG}$	0.199	74% (74/100)*	82% (18/100)*	0.813	P^a: 0.355 N^b: 0.157	P^a: 0.314 N^b: 0.132
$BB0108_{Mix}$	0.254	80% (80/100)*	91% (9/100)*	0.920	P^a: 0.391 N^b: 0.166	P^a: 0.355 N^b: 0.141
$BB0323_{BA}$	0.363	72% (72/100)*	88% (12/100)*	0.840	P^a: 0.473 N^b: 0.326	P^a: 0.433 N^b: 0.309
$BB0323_{BB}$	0.372	62% (62/100)*	90% (10/100)*	0.805	P^a: 0.436 N^b: 0.321	P^a: 0.416 N^b: 0.299
$BB0323_{BG}$	0.362	64% (64/100)*	90% (10/100)*	0.832	P^a: 0.450 N^b: 0.307	P^a: 0.413 N^b: 0.285
$BB0323_{Mix}$	0.401	67% (67/100)*	90% (10/100)*	0.826	P^a: 0.492 N^b: 0.350	P^a: 0.452 N^b: 0.331

*- number of seropositive sera/number of tested sera
AUC - area under the curve
[a] - positive sera
[b] - negative sera

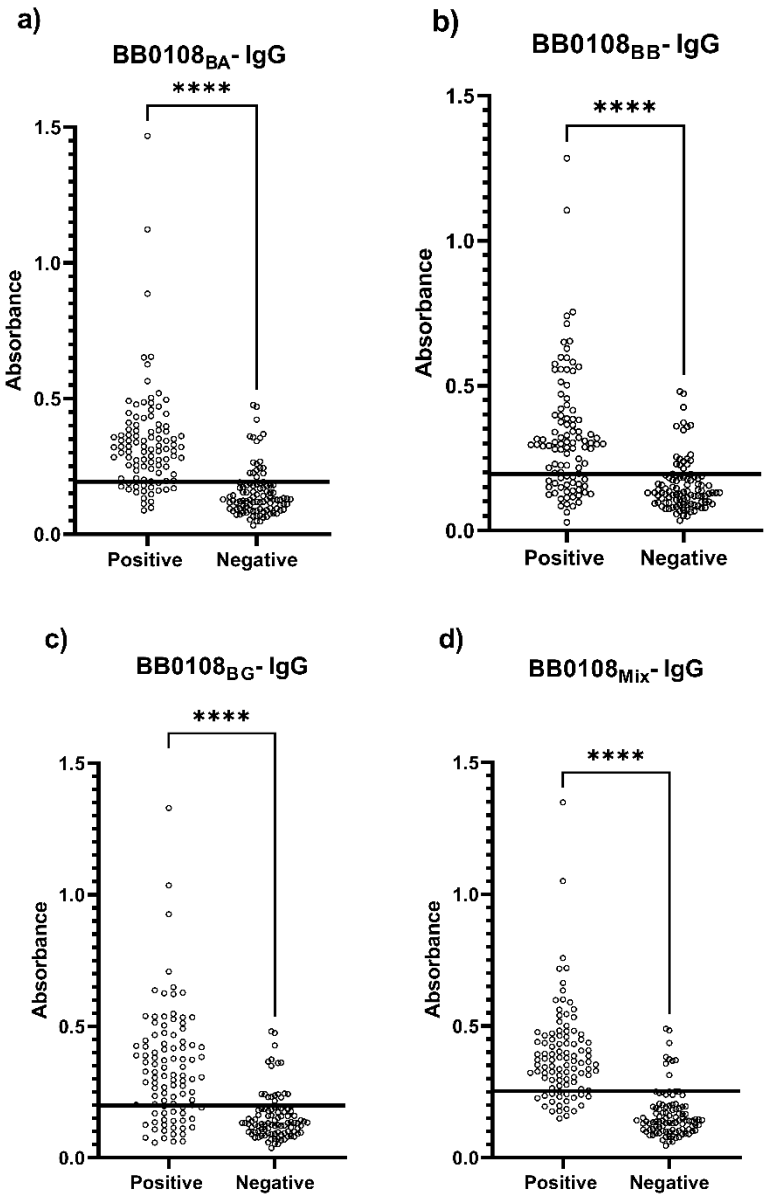

Figure 5. 110 Absorbance for negative and positive sera: a) IgG-ELISA-BB0108$_{BA}$; b) IgG-ELISA-BB0108$_{BB}$; c) IgG-ELISA-BB0108$_{BG}$; d) IgG-ELISA-BB0108$_{Mix}$. The horizontal line marks the cut-off.

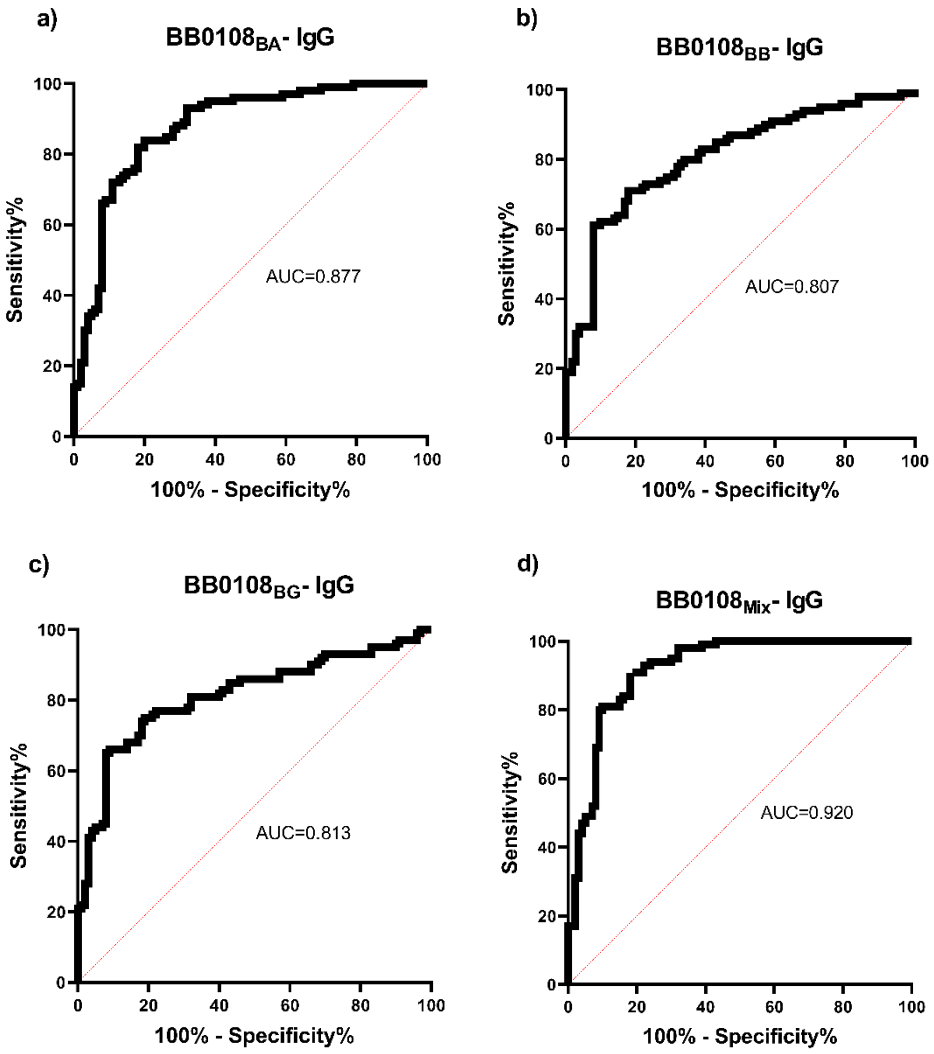

Figure 5. 111 ROC analysis and AUC: a) IgG-ELISA-BB0108$_{BA}$; b) IgG-ELISA-BB0108$_{BB}$; c) IgG-ELISA-BB0108$_{BG}$; d) IgG-ELISA-BB0108$_{MIX}$.

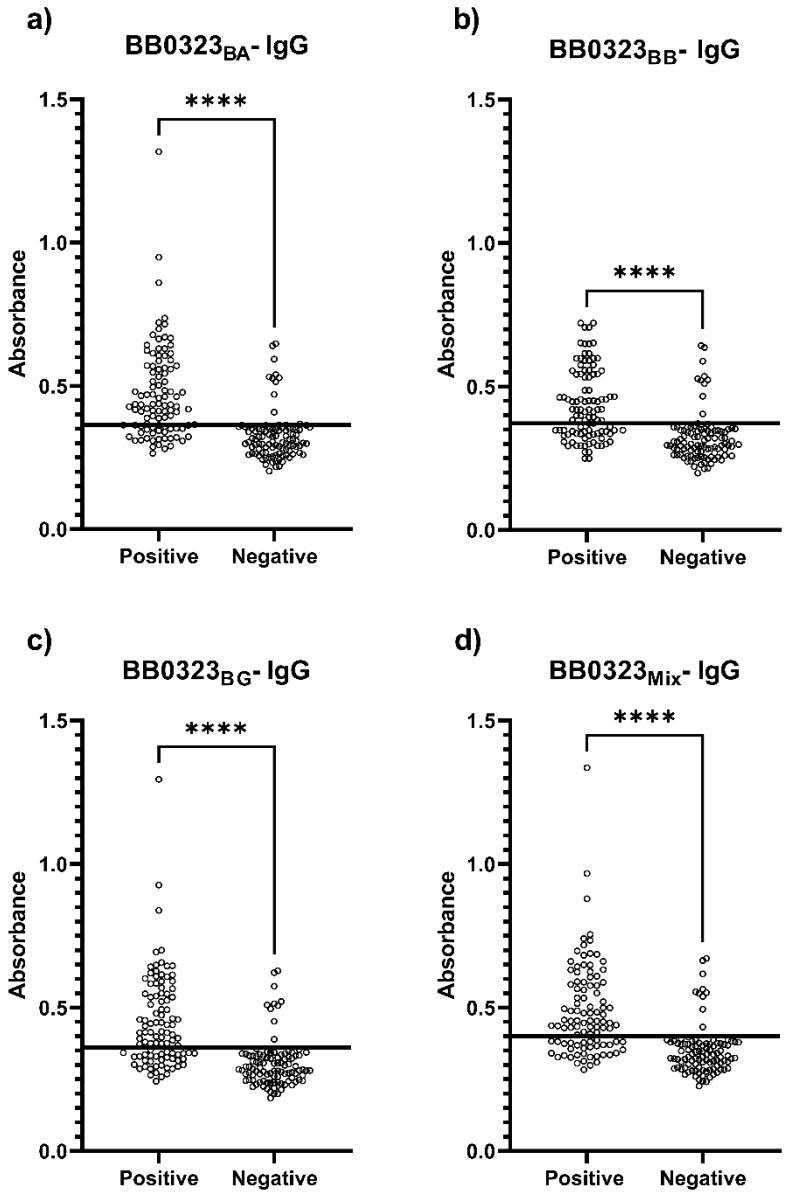

Figure 5. 112 Absorbance for negative and positive sera: a) IgG-ELISA-BB0323$_{BA}$; b) IgG-ELISA-BB0323$_{BB}$; c) IgG-ELISA-BB0323$_{BG}$; d) IgG-ELISA-BB0323$_{MIX}$. The horizontal line marks the cut-off.

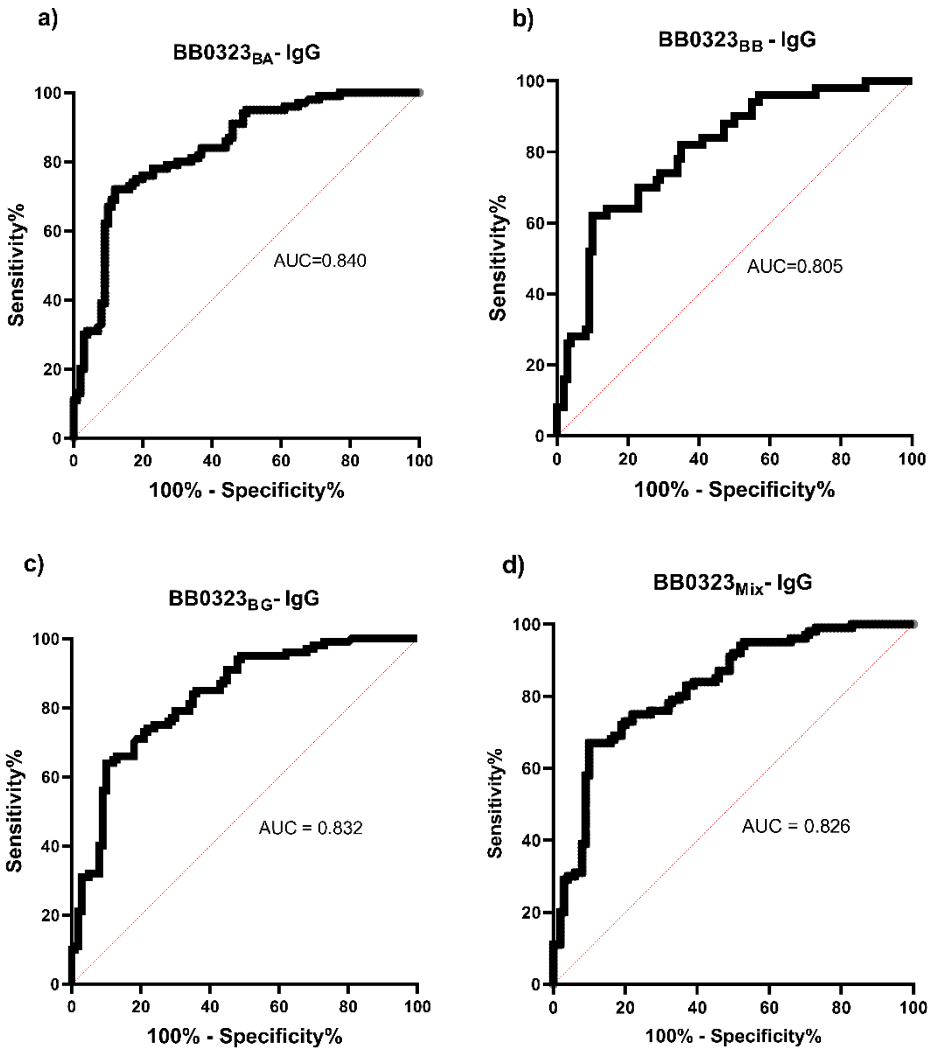

Figure 5. 113 ROC analysis and AUC: a) IgG-ELISA-BB0323$_{BA}$; b) IgG-ELISA-BB0323$_{BB}$; c) IgG-ELISA-BB0323$_{BG}$; d) IgG-ELISA-BB0323$_{Mix}$.

Sensitivity of IgM-ELISA based on three BB0108 variants, ranging from 52% to 63% (Table 5.39, Figure 5.114). However, unlike the IgG-ELISA here, BB0108$_{BB}$ provided the highest sensitivity. AUC also decreased to 0.724-0.736 (Figure 5.115). A slightly higher specificity of these tests was observed for BB0108$_{BG}$ (91%). The use of a mixture of antigens did not significantly affect sensitivity and specificity but resulted in an inconsiderable increase in AUC.

The Student's t-test showed no statistically significant differences in the absorbance of negative and positive sera in IgM-ELISA based on single BB0323 antigens (P>0.05) (Table 5.39; Figure 5.116). Also, the obtained AUC values in the range of 0.526-572 indicate that it was not possible to distinguish between these two groups of sera with IgM-ELISA (Figure 5.117). In the IgM-ELISA based on three variants of BB0323, a statistically significant difference was obtained in the absorbance level for the

two sera groups. However, the sensitivity and specificity did not reach satisfactory values, 60% and 71%, respectively.

Table 5. 39 IgM-ELISA based on BB0108s and BB0323s

Monovalent protein	Optimal cut-off	Sensitivity [%]	Specificity [%]	AUC	Mean absorbance	Median absorbance
$BB0108_{BA}$	0.219	56% (27/48)*	86% (9/65)*	0.724	P^a: 0.277 N^b: 0.171	P^a: 0.259 N^b: 0.145
$BB0108_{BB}$	0.234	63% (30/48)*	83% (12/65)*	0.736	P^a: 0.259 N^b: 0.183	P^a: 0.263 N^b: 0.159
$BB0108_{BG}$	0.234	52% (25/48)*	91% (6/65)*	0.729	P^a: 0.264 N^b: 0.157	P^a: 0.269 N^b: 0.144
$BB0108_{Mix}$	0.228	56% (27/48)*	86% (9/65)*	0.765	P^a: 0.287 N^b: 0.168	P^a: 0.246 N^b: 0.133
$BB0323_{BA}$	No statistical difference in absorbance for positive and negative sera (P=0.575)			0.533	P^a: 0.262 N^b: 0.250	P^a: 0.252 N^b: 0.232
$BB0323_{BB}$	No statistical difference in absorbance for positive and negative sera (P=0.052)			0.572	P^a: 0.294 N^b: 0.246	P^a: 0.273 N^b: 0.233
$BB0323_{BG}$	No statistical difference in absorbance for positive and negative sera (P=0.319)			0.526	P^a: 0.325 N^b: 0.301	P^a: 0.304 N^b: 0.284
$BB0323_{Mix}$	0.248	60% (29/48)*	71% (29/65)*	0.686	P^a: 0.333 N^b: 0.261	P^a: 0.323 N^b: 0.243

*- number of seropositive sera/number of tested sera
AUC - area under the curve
[a] - positive sera
[b] - negative sera

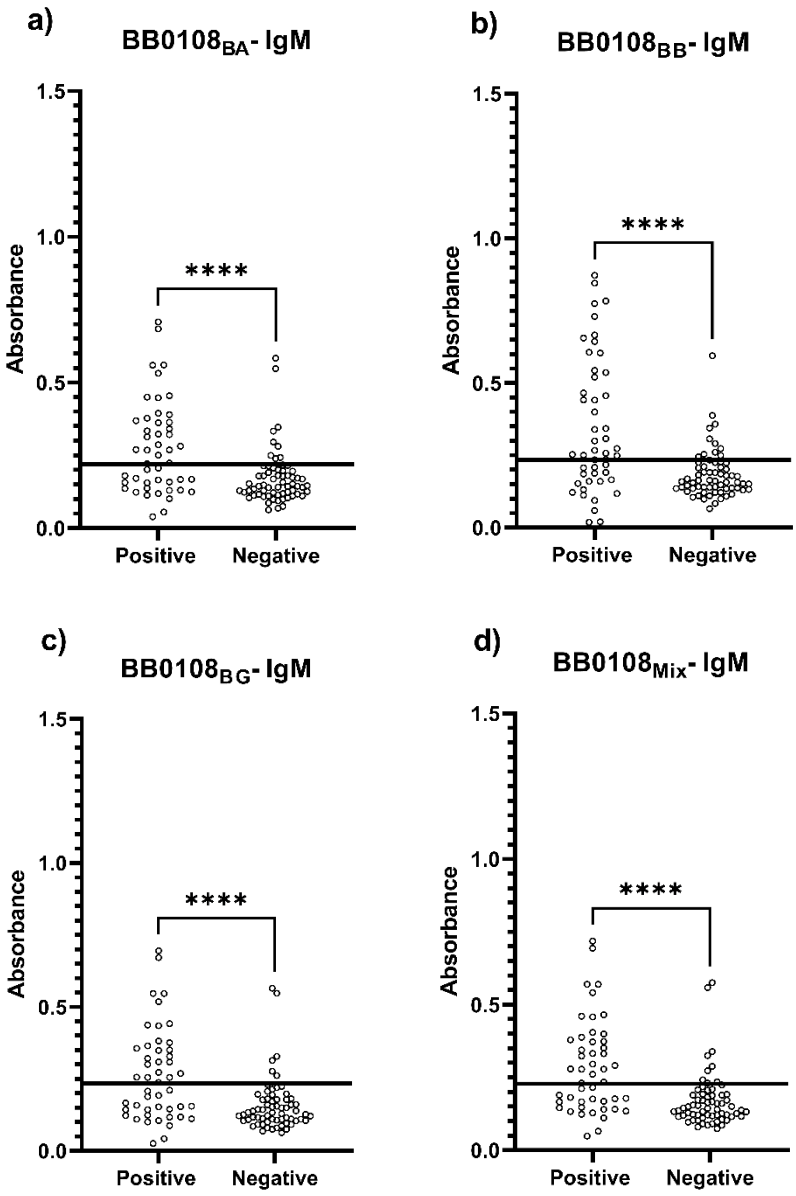

Figure 5. 114 Absorbance for negative and positive sera: a) IgM-ELISA-BB0108$_{BA}$; b) IgM-ELISA-BB0108$_{BB}$; c) IgM-ELISA- BB0108$_{BG}$; d) IgM-ELISA-BB0108$_{Mix}$. The horizontal line marks the cut-off.

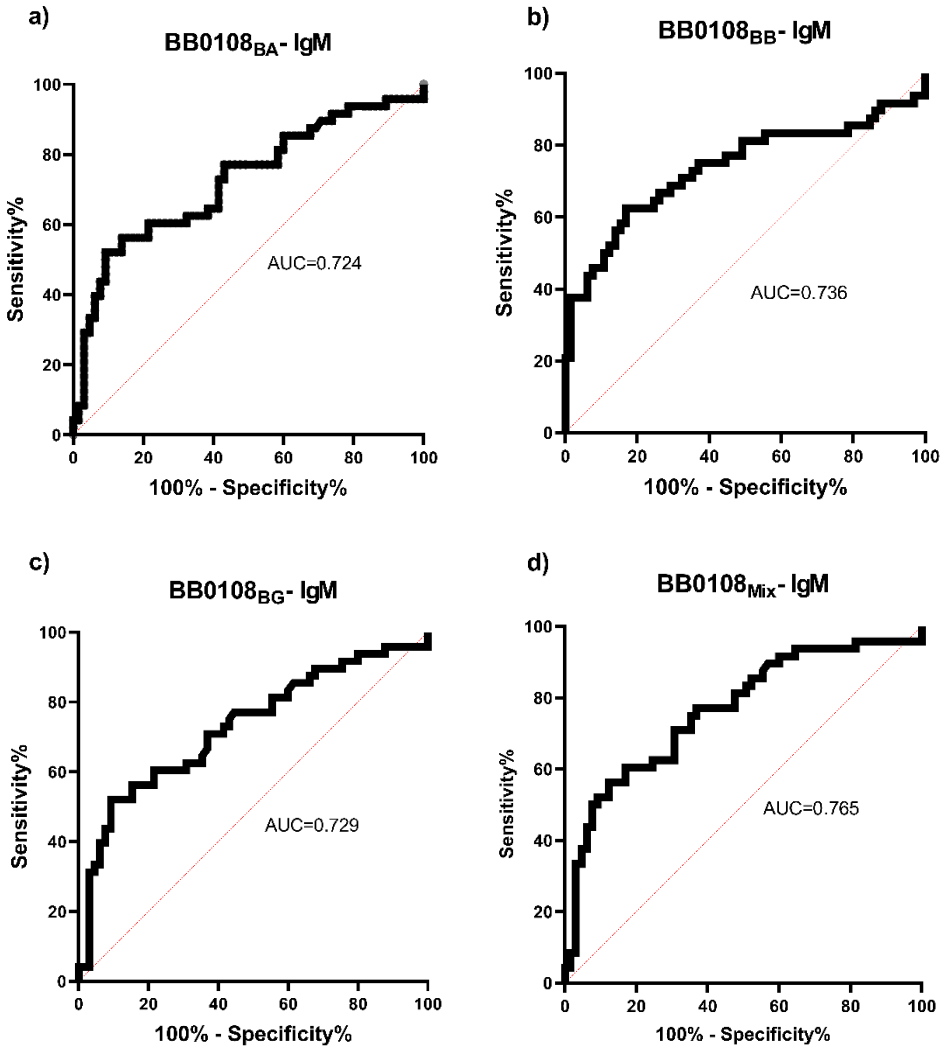

Figure 5. 115 ROC analysis and AUC: a) IgM-ELISA-BB0108$_{BA}$; b) IgM-ELISA-BB0108$_{BB}$; c) IgM-ELISA-BB0108$_{BG}$; d) IgM-ELISA-BB0108$_{MIX}$.

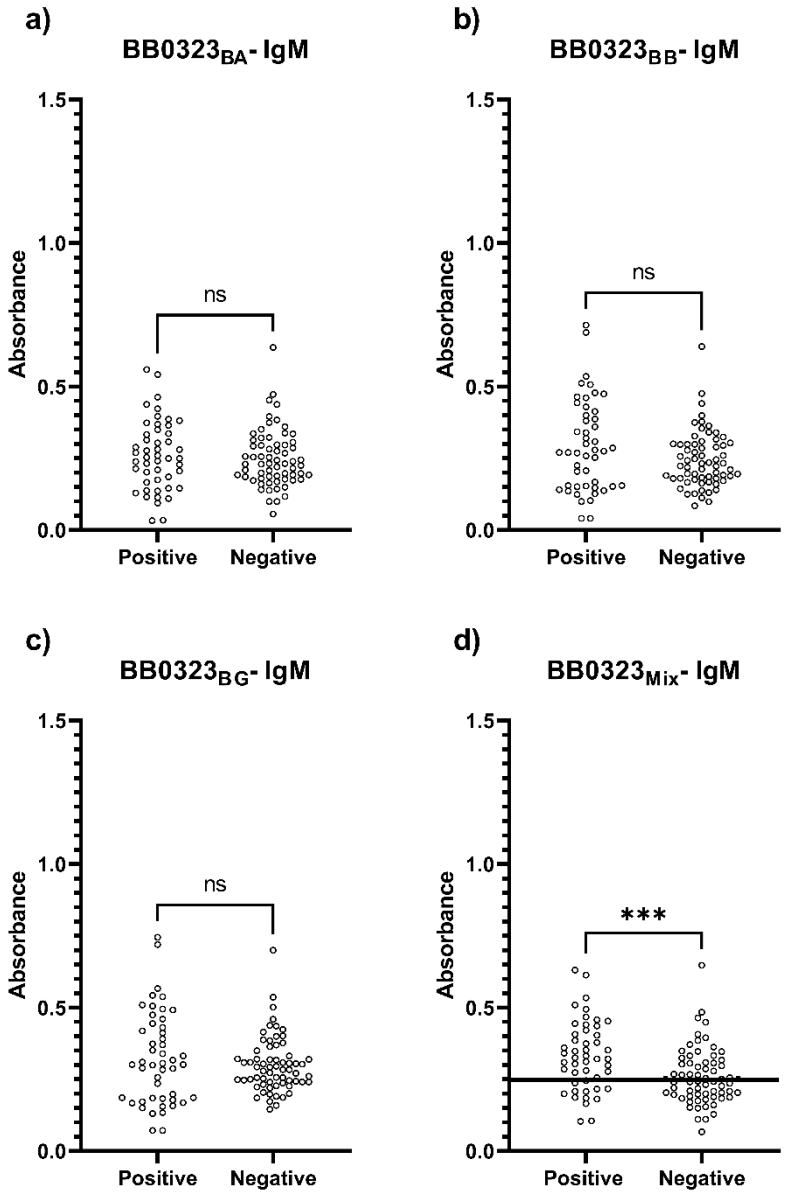

Figure 5. 116 Absorbance for negative and positive sera: a) IgM-ELISA-BB0323$_{BA}$; b) IgM-ELISA-BB0323$_{BB}$; c) IgM-ELISA- BB0323$_{BG}$; d) IgM-ELISA-BB0323$_{Mix}$. The horizontal line marks the cut-off.

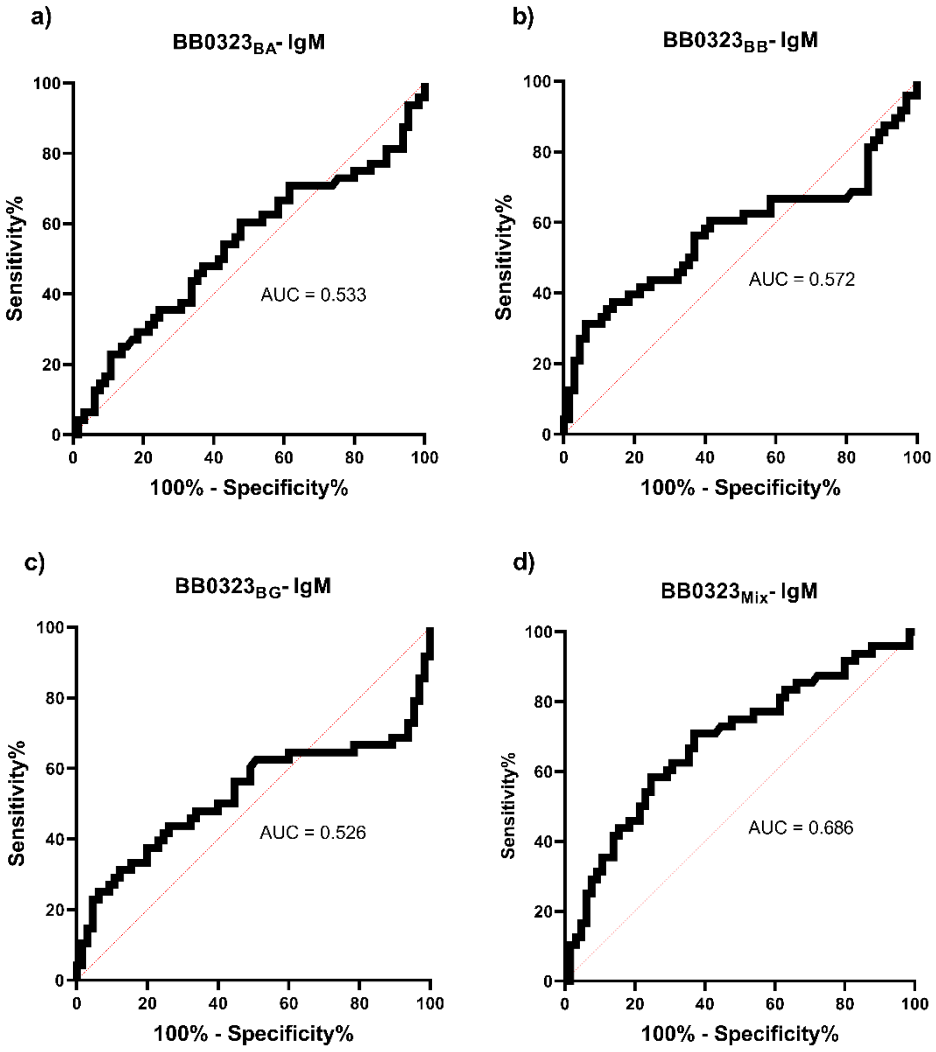

Figure 5. 117 ROC analysis and AUC: a) IgM-ELISA-BB0323$_{BA}$; b) IgM-ELISA-BB0323$_{BB}$; c) IgM-ELISA-BB0323$_{BG}$; d) IgM-ELISA-BB0323$_{Mix}$.

5.1.4.3. ELISA based on multivalent chimeric proteins

The sensitivity and specificity of ELISA based on the BmpA-BBK32-G and BmpA-BBK32-M chimeric proteins were determined using cut-off values obtained by ROC analysis.

The optimal cut-off value was 0.228, 0.223, 0.114 for the IgG-ELISA-BmpA-BBK32-G (IgG-ELISA-B/32-G), IgM-ELISA-BmpA-BBK32-M (IgM-ELISA-B/32-M), and IgG-ELISA-BmpA-BBK32-M (IgG-ELISA-B/32-M), respectively (Table 5.40, Figure 5.118). The highest sensitivity (71%) and specificity (95%) were shown by the IgG-ELISA-B/32-G, what is more, the AUC (0.886) is also the highest. The IgM-ELISA- B/32-M showed identical sensitivity (71%). However, its specificity (89%), and especially AUC (0.780) were lower (Figure 5.119). The IgG-ELISA-B/32-M showed noticeably lower sensitivity and specificity.

Student's t-test showed a statistically significant difference in absorbance between the negative and positive sera for IgG-ELISA-B/32-G, IgM-ELISA-B/32-M, and IgG-ELISA-B/32-M ($P<0.05$). For IgM-ELISA-B/32-G, $P=0.0634$ which proves no statistically significant difference in the absorbance values for the two groups of sera.

Table 5. 40 Results of the IgG and IgM ELISA based on multivalent chimeric proteins

Multivalent protein	Detected Ab isotype	Optimal cut-off	Sensitivity [%]	Specificity [%]	AUC	Mean absorbance	Median absorbance
B/32-G	IgG	0.228	71 (105/148)*	95 (7/150)*	0.886	P[a]: 0.366 N[b]: 0.126	P[a]: 0.330 N[b]: 0.107
B/32-G	IgM	No statistical difference in absorbance for positive and negative sera (P=0.0634)			0.646	P[a]: 0.199 N[b]: 0.162	P[a]: 0.177 N[b]: 0.141
B/32-M	IgM	0.223	71 (34/48)*	89 (7/65)*	0.780	P[a]: 0.353 N[b]: 0.184	P[a]: 0.240 N[b]: 0.170
B/32-M	IgG	0.114	66 (97/148)*	69 (47/150)*	0.722	P[a]: 0.168 N[b]: 0.109	P[a]: 0.136 N[b]: 0.098

*- number of seropositive sera/number of tested sera
AUC - area under the curve
[a] - positive sera
[b] - negative sera

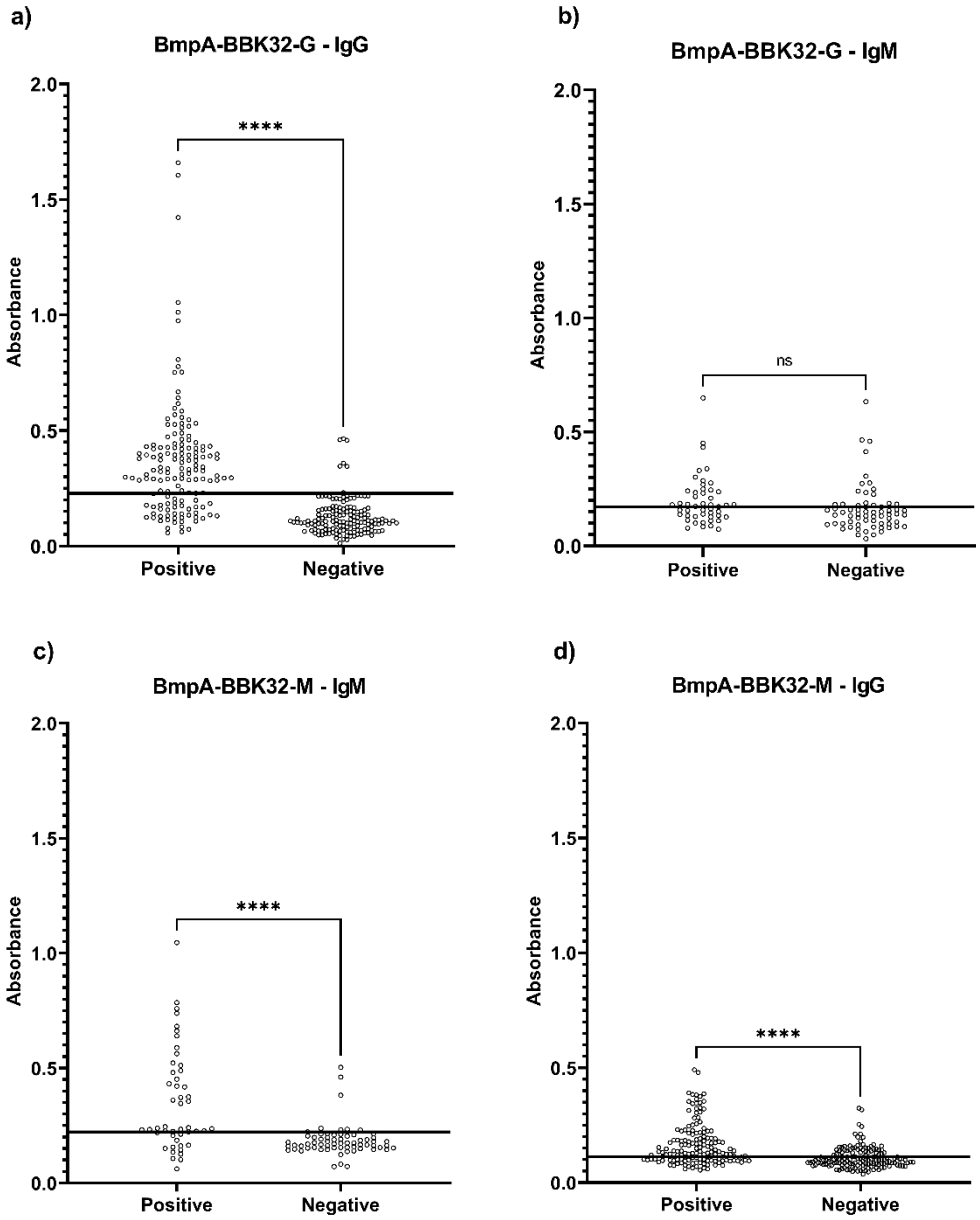

Figure 5. 118 Absorbance for negative and positive sera: a) IgG-ELISA-BmpA-BBK32-G; b) IgM-ELISA-BmpA-BBK32- G; c) IgM-ELISA-BmpA-BBK32-M; d) IgG-ELISA-BmpA-BBK32-M.

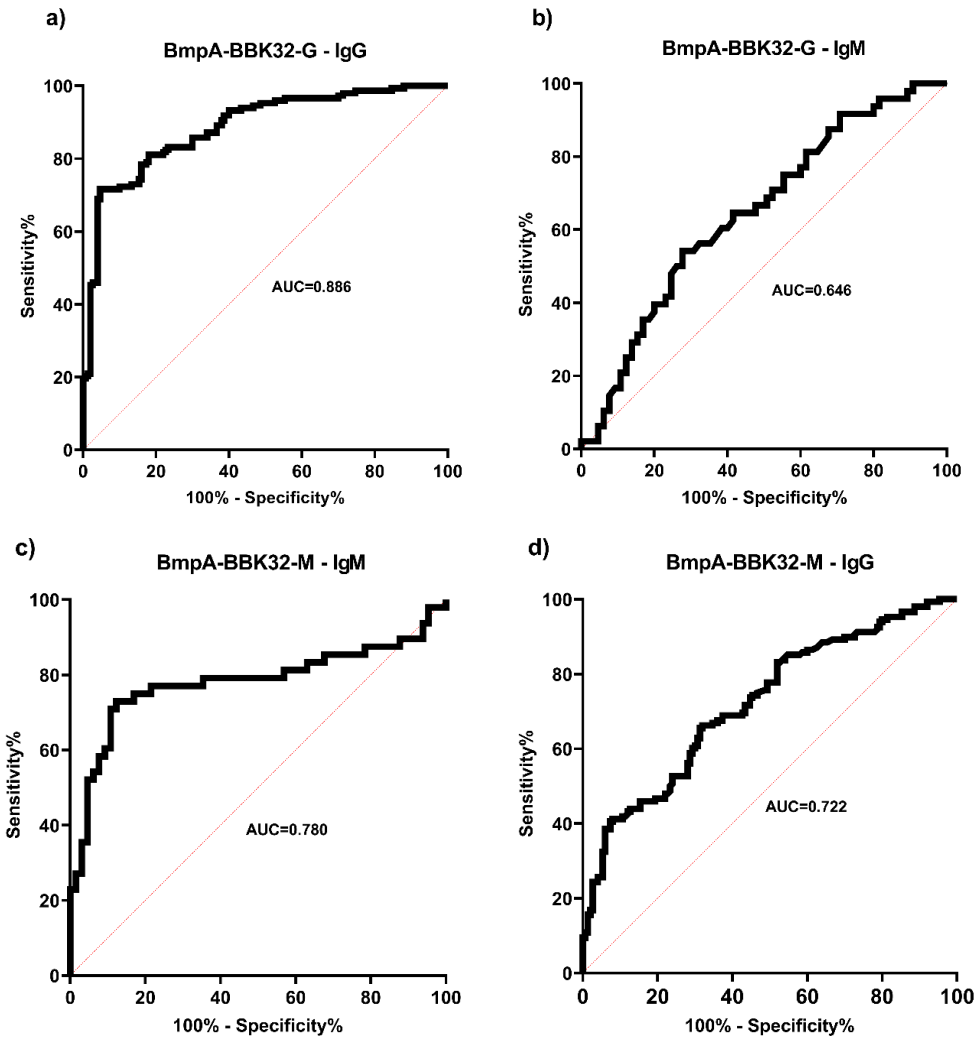

Figure 5. 119 ROC analysis and AUC: a) IgG-ELISA-BmpA-BBK32-G; b) IgM-ELISA-BmpA-BBK32- G; c) IgM-ELISA-BmpA-BBK32-M; d) IgG-ELISA-BmpA-BBK32-M.

6. DISCUSSION

6.1. Selection of *B. burgdorferi* s.l. antigens with potential diagnostic usefulness

Relatively few *B. burgdorferi* s.l. antigens from its extremely large and complex proteome have been characterized for their reactivity with specific antibodies. Only for a few *B. burgdorferi* s.l. antigens, comprehensive studies were performed to determine their diagnostic utility (DbpA, OspC, BmpA, BBK32, BBA64, VlsE, FlaB), and as mentioned earlier, scientists focused mainly on plasmid-encoded surface lipoproteins (DbpA, VlsE, BBK32, OspC). Although these proteins are characterized by very high immunogenicity, their low degree of sequence conservation makes it difficult to use them in the diagnosis of Lyme disease in Europe, where the diversity of *B. burgdorferi* s.l. representatives is very high (Kenedy et al., 2012; Lohr et al., 2018; Purser and Norris, 2000). In addition, many studies have shown that enzyme immunoassays based on recombinant proteins significantly differ in sensitivity depending on the genospecies from which the antigen is obtained (Heikkilä et al., 2002b; Magnarelli et al., 2002; Panelius et al., 2002; Roessler et al., 1997b). This also applies to proteins commonly used in commercial assays, such as DbpA and OspC, characterized by very high immunogenicity and diversity. Therefore, Lyme disease serodiagnosis may be improved by using carefully selected antigens with a conserved sequence. Antigens encoded by the the *B. burgdorferi* s.l. chromosome were chosen for further research as the chromosome is highly conserved. It was decided that the diagnostic utility of these antigens as well as the dependence of reactivity with anti-*B. burgdorferi* s.l. antibodies on the genospecies from which they were obtained, will be determined. For this purpose, a bioinformatic analysis of amino acid sequences of selected (BB0108, BB0126, BB0298, BB0323, and BB0689) antigens was performed to determine their degree of sequence conservation and potential reactivity with specific anti-*B. burgdorferi* s.l. antibodies.

As expected, the chromosomal location of the genes encoding BB0108, BB0126, BB0298, BB0323, and BB0689 antigens ensured that they are fairly well conserved within the *B. burgdorferi* s.l. complex (Table 5.2). The degree of sequence identity for BB0108 and BB0298 within the *B. burgdorferi* s.l. complex was 92%, for BB0126 and BB0323 it was 83% and 85%, respectively. Only in the case of BB0689 this value fell below 80%, reaching 77%. These results significantly exceed those obtained for antigens commonly used in serodiagnostic, such as DbpA, and OspC. The analyses performed for these proteins show that the sequence conservation of DbpA is 41% and OspC's is

59% (Heikkilä et al., 2002b; Roberts et al., 1998; Theisen et al., 1993). There is therefore a possibility that these selected antigens may be useful in the diagnosis of Lyme disease, regardless of the species causing the disease.

However, genes located on the chromosome have certain disadvantages, as there is a high degree of sequence identity with relapsing fever *Borrelia* which may cause false positive results in serodiagnosis. In the USA and Canada, the dominant species is *B. hermsii.* In Europe, relapsing fever is endemic only in its southern parts, where *B. hispanica* is dominant (Rebaudet and Parola, 2006). It seems that the greatest problems in the diagnosis of Lyme disease may be caused by *B. miyamotoi* transmitted by ticks of the *Ixodes* genus similar to *B. burgdorferi* s.l. (Siński et al., 2016).

The next step was to assess the potential reactivity of these antigens with antibodies by identifying immunodominant fragments using bioinformatics methods. The largest number of linear and conformational epitopes was predicted for BB0108, a lipoprotein likely located on the cell surface. In addition, its expression increases during transmission, suggesting that this protein directly interacts with mammalian tissues. This may indicate a high diagnostic potential of this antigen as two independent microarray studies have also shown that it is recognized by anti-*Borrelia* antibodies (Barbour et al., 2008; Xu et al., 2008).

BB0323 is of crucial importance as it seems to be essential for the establishment of *B. burgdorferi* s.l. infection in both ticks and mammalian hosts. Additionally, a significant increase in its production was noticed during tick-mouse transmission. All this information together with results obtained during B-cell epitope mapping suggests that it may be a useful tool in the diagnosis of Lyme disease (Kariu et al., 2015; Zhang et al., 2009).

The performed bioinformatics analysis predicted only a single epitope for BB0698. However, literature data suggest that this protein may have a very high diagnostic value due to the fact that it is an antigen located in the outer cell membrane and its production increases during the tick's feeding. Additionally it has been confirmed that it is an immunogen, as baboons infected with *B. burgdorferi* s.s. produced BB0689-specific bactericidal antibodies (Brangulis et al., 2015a; Brooks et al., 2006).

BB0126, BB0298 are lipoproteins probably presented on the outer membrane surface (Brooks et al., 2006; Caimano et al., 2015; Ojaimi et al., 2003). Conserved linear B-cell epitopes were predicted in their sequences, and in the case of BB0298 for which 3D structures were available, discontinuous B-cell epitopes were also identified. In addition, the production of proteins BB0126 and BB0298 is upregulated when the tick feeds, indicating their potential role in the pathogenesis of Lyme disease (Ojaimi et al. 2003). Therefore, it is presumed that they may induce the production of specific

anti-*B. burgdorferi* antibodies. An additional advantage of BB0126 is its low sequence identity with proteins from other organisms, including relapsing fever *Borrelia*, where it was estimated at about 53%.

Obtained *in silico* results suggest that all these antigens may be useful serodiagnostic tools because potential B-cell epitopes are predicted in their sequence. Moreover, their high degree of conservation indicates that variants of these antigens from different genospecies can be recognized by specific antibodies with the same efficiency. However, to confirm these assumptions, it was necessary to conduct laboratory tests using a large pool of sera to determine the actual reactivity of these antigens with anti-*B. burgdorferi* s.l. antibodies.

6.2. Design of multivalent chimeric proteins *B. burgdorferi* s.s.

The use of molecular biology techniques makes it possible to produce a large quantity of recombinant proteins for the serodiagnosis of Lyme disease in a safe manner with low production costs. However, despite these undeniable advantages, using single recombinant proteins in serodiagnostic assays instead of whole cell lysates may reduce its sensitivity. There are many antigens in the WCL that can be recognized by specific antibodies. Using single proteins significantly lowers the number of epitopes binded by immunoglobulins.

The solution to the problem of insufficient sensitivity may be the use of mixtures of several monovalent recombinant proteins. This approach has been shown to increase the sensitivity of immunoenzymatic assays for diagnosis of diseases caused by other pathogens (Holec-Gąsior, 2013; Holec-Gąsior and Kur, 2010; Holec et al., 2008; Magalhães et al., 2017; Rauer et al., 1998). However, the biotechnological production and purification of many different proteins can be expensive and time-consuming. Furthermore, standardization of tests based on several types of proteins can also be problematic. For this reason, chimeric proteins that contain selected immunodominant fragments from several proteins in a single amino acid chain are favourable. Such a protein could be recognized by antibodies specific to several antigens (Del-Rei et al., 2019; Holec-Gąsior et al., 2012).

For multivalent chimeric proteins to be highly useful in diagnosing Lyme disease, carefully selected fragments of antigens must be used for their construction. They should be highly immunogenic, conserved among the genospecies of *B. burgdorferi* s.l., and not show a similarity of amino acid sequence to proteins of other organisms (i.e., not be a potential source of cross-reactions).

Two approaches to the rational design of multivalent chimeric proteins that are highly reactive with *B. burgdorferi* s.l.-specific antibodies were used in the research

carried out as part of the doctoral dissertation. The first was the selection of appropriate immunodominant fragments based on bioinformatics analysis, the second was the design of chimeric proteins based on data obtained during experimental linear epitope mapping using peptide microarrays. Both methods focused on identifying linear epitopes because it was assumed that the combination of amino acid sequences not naturally occurring in close proximity to each other into one polypeptide chain would disturb the natural conformation of selected protein fragments, which would cause them to lose their conformational epitopes (Bansal and Kundu, 2022). This may seem like a disadvantage since we are not sure whether linear epitopes are exposed on the surface of the protein. However, as shown in example C6, linear epitopes can be located in the protein's internal structure and exposed when antigens are released and/or degraded during infection (Embers et al., 2007). In addition, most identified linear antigenic determinants are presumed to be part of B-cell conformational epitopes, thus it was assumed that despite the focus on linear epitope selection, some conformational ones would still be retained in the structure of the chimeric protein (Assis et al., 2014; Potocnakova et al., 2016).

Three antigens with confirmed immunogenicity BmpA, BBK32, and BBA64 were selected for the construction of multivalent chimeric proteins based on bioinformatics analysis. All of them are surface lipoproteins responsible for adhesion to host cells. Their production begins when the tick takes a blood meal, so these antigens should be well exposed to the immune system (Probert and Johnson, 1998; Verma et al., 2009). Moreover, BmpA shows diagnostic value in detecting IgM and IgG as it is used in Western blot according to official recommendations (Dressler et al., 1993; Engstrom et al., 1995). BBK32 was chosen because of numerous literature reports on its diagnostic usefulness suggesting that it is helpful in diagnosing early Lyme disease (Heikkilä et al., 2003, 2002a; Panelius et al., 2003). While BBA64 was considered interesting because it has been shown that it induces the production of bactericidal antibodies (Brandt et al., 2014).

Sequence analysis showed that of these proteins, BmpA has the highest degree of sequence conservation, which was expected as BmpA is encoded by a chromosome, however the fewest potential linear epitopes were identified in its sequence (Roessler et al., 1997b). The least conserved within the *B. burgdorferi* s.l. group was BBA64, which made it difficult to select highly conserved linear epitopes within its sequence. BBK32 appeared to contain the most extensive immunodominant fragments (Figuras 5.13-5.15).

Based on the obtained results, two multivalent chimeric proteins were designed, both containing an identical fragment from BmpA at their N-terminus, as due to the high conservation of this sequence, the resulting chimeric protein would be reactive with antibodies directed against different genospecies of *B. burgdorferi* s.l. On the other hand,

at the C-terminus, sequences obtained from plasmid-coded BBA64 or BBK32 antigens were introduced, which, according to the performed bioinformatics analysis should show higher immunogenicity.

The mapping of linear epitopes using peptide microarray was limited to two antigens, i.e., BmpA and BBK32. BBA64 was excluded due to its highest variability among *B. burgdorferi* s.l. and the lowest, according to literature data, reactivity with specific antibodies among these proteins (Weiner et al., 2015).

Microarray epitope mapping showed that most of the identified antibody-binding sequences in both proteins were reactive with positive and negative sera. This indicates a high potential for cross-reactivity, even if the antigens are encoded by plasmids. Similar results were obtained when mapping p66 (Arnaboldi and Dattwyler, 2015). This shows why the development of a one-step, highly specific serodiagnostic tests is so difficult and why it is crucial to understand epitope-paratope interactions as best as possible.

The results obtained from the peptide microarray could be compared with a previous study where, 2 regions of B-cell epitopes, recognized by IgG, in BBK32 were identified from amino acids 16 to 30 and from amino acids 51 to 80, by probing overlapping peptide libraries of BBK32 with sera from patients with early Lyme disease (Toumanios et al., 2019). In this study, the amino acid region from 16 to 30 only shared the last 4 amino acids (EMKE) with peptide nº14 that appeared as reactive in the microarray assay (Table S4). The patient populations used in this study were derived from different areas; therefore, it is unclear if the differences in the results of both studies could be due to the use of sera from different geographical locations (Arnaboldi et al., 2013) or because the previous study used serum samples from early Lyme disease for epitope identification. In the study from Tokarz et al. 2018, a chip for the diagnosis of tick-borne diseases was used to identify *B. burgdorferi* s.l. infections among other tick-borne pathogens employing 170 000 peptides from 62 proteins. One peptide from BBK32 was more frequently reactive to IgG in samples from patients with acute neuroborreliosis (-EMKEESPGLFDKGNSILE-). This peptide was also significantly identified during this experiment by IgG from positive serum samples (Table S4 and S5).

Comparing these two methods, more antibody-binding fragments (for both positive and negative sera) were identified using the peptide microarray than bioinformatics tools. This is probably due to the relatively high threshold set to obtain the highest certainty that a given fragment selected by computational methods is indeed a B-cell epitope. This approach seems to be correct because in the case of BmpA all potential epitopes identified by bioinformatics tools partially coincide with those determined experimentally. In the case of BBK32, the agreement between the two methods is not so complete, but it is still relatively high. The polypeptide microarray

confirmed 4 out of 6 of the reactive fragments identified using bioinformatics methods. Unfortunately, their main disadvantage is that they cannot be used to eliminate sequences that are a source of cross-reactions. After analyzing the results, it turns out that most of the predicted epitopes coincided with sequences recognized by antibodies contained in both positive and negative sera. The ability to identify cross-recognition fragments is a great advantage of experimental methods, as it allows the elimination of these problematic epitopes from the sequences of new diagnostic tools. This contributes to an increase in the specificity of antigen-antibody interactions and thus also to the reduction of false positive results in serodiagnosis.

Another advantage of empirical methods is the differentiation of protein fragments that react with different classes of antibodies, which is a much more specific approach to designing multivalent chimeric proteins. Therefore, it was decided to take advantage of this opportunity and create two separate multivalent chimeric proteins dedicated to the detection of IgM or IgG. To check whether serodiagnostic tools with increased IgM detection potential can be constructed. As mentioned, the diagnostic value of serological methods in the early stages of infectious diseases is limited and effective detection of IgM is very problematic, not only in the case of Lyme disease. IgM are produced when the immune response to a foreign antigen is still immature, which causes tests based on IgM detection to give false positive results more often (Molins et al., 2017). A study by Webber et al. (2019) estimated that false positives in IgM-WB account for up to 53% of results, which causes overdiagnosis of Lyme disease.

It was decided to construct multivalent chimeric proteins composed of these short identified immunodominant fragments instead of testing their reactivity as separate constructs because, usually, such short peptides do not have satisfactory diagnostic sensitivity (Durante et al., 2017). Of course, the exception that immediately comes to mind is the C6 peptide, where tests based on it are characterized by even 100% sensitivity in late Lyme disease. However, Arnaboldi et al. 2022 studies suggest that it is very difficult to label such a peptide even if it shows high reactivity during mapping. This research group mapped the linear epitopes of ErpP, BBH32, and FlaB antigens and then checked the reactivity of the identified immunodominant fragments by ELISA. The FlaB fragment provided the highest sensitivity, tests based on it reached a sensitivity of 37.6%, which is insufficient for the effective diagnosis of Lyme disease. Only the addition of a fragment derived from VlsE increased the sensitivity of ELISA (Arnaboldi et al., 2022).

The multivalent chimeric proteins designed by the two approaches differ significantly in size, BmpA-BBK32 and BmpA-BBA64 have a molecular weight of over 50 kDa, while BmpA-BBK32-G and BmpA-BBK32-M are much smaller (about 20 kDa). In the case of designing chimeric proteins based on computational data, large, relatively

well-conserved fragments with a high density of potential epitopes were selected for their construction. This was done to increase the probability of finding real immunodominant fragments in the designed multivalent chimeric proteins because, despite the rapid development of bioinformatics tools, there is still no certainty that the actual location of epitopes is consistent with that determined by the software. However, during the design of BmpA-BBK32-G and BmpA-BBK32-M, thanks to experimental epitope mapping, the exact location of immunodominant fragments was known, therefore it was decided to include these short, well-defined sequences in the construction of multivalent chimeric proteins. This resulted in a significant reduction in the size of recombinant proteins designed based on epitope mapping.

6.3. Production and purification of monovalent and multivalent recombinant proteins

To answer the question of whether the selection of antigens with potential diagnostic value was adequately carried out and whether the applied methods of designing multivalent chimeric proteins make it possible to obtain new useful diagnostic tools, it was necessary to construct expression systems enabling the biotechnological production of these antigens to estimate their reactivity with anti-*B. burgdorferi* antibodies.

The first stage of this process was the construction of recombinant plasmids encoding target proteins. pUET1, constructed at the Gdańsk University of Technology, was chosen as the expression vector, which is a hybrid of two commercially available plasmids, namely pET30 from which the MCS was excised and pUC19, which comprises the rest of the backbone. pUET1 is, therefore, a small, high-copy expression plasmid that enables the production of recombinant proteins under the control of the lactose operon. Only in later stages of work, due to emerging problems with the solubility of target proteins, it was also decided to construct recombinant plasmids based on the pET32a and pET42a backbone.

During the research conducted as part of the doctoral thesis, 25 recombinant plasmids were constructed allowing the production of 15 monovalent recombinant proteins, 4 multivalent chimeric proteins, and 6 monovalent/multivalent recombinant proteins with additional fusion partners TrxA or GST (Table 5.20-5.22). All of them were produced using *E. coli* cells, mainly strain BL21(DE3)pLysS (Results 5.5.3). However, the Origami™, Rosetta(DE3)pLacI and Rosetta(DE3)pLysS were also used in later stages of the work (Results 5.5.7.3).

All produced monovalent and multivalent recombinant proteins are connected with the surface of *B. burgdorferi* s.l., therefore BL21(DE3)pLysS cells were the first

choice during host selection as they are commonly used in the production of membrane proteins which may be particularly challenging. The main reason is their interaction with the components of cell membranes, e.g., with lipids, which leads to membrane function disorders and toxic effects on the *E. coli* cell. BL21(DE3)pLysS due to constitutively expressed T7 lysozyme (carried on the pLysS plasmid) decreases the basal level of T7 RNA polymerase. This reduces transcriptional activity, which is desirable as membrane proteins have been shown to be often toxic to host cells during their biotechnological production (Montigny et al., 2004).

Target proteins such as BB0323s, BB0689s, BmpA-BBK32, and BmpA-BBA64 were produced in the form of inclusion bodies, which consist of dense aggregates of misfolded/denatured proteins. Therefore, it was necessary to use buffers with a high concentration of denaturing agents such as urea or guanidine hydrochloride for their purification. Sometimes a reducing agent such as β-mercaptoethanol is also added along with them. These compounds lead to denaturation and complete unfolding of the polypeptide chain, allowing them to be purified (Singh and Panda, 2005).

The main reason why recombinant prokaryotic proteins are deposited in the form of inclusion bodies is the misfolding of target proteins in bacterial cells.This can be caused by several factors presented in Table 6.1.

Table 6. 1 Reasons for the deposition of proteins in bacterial cells in the form of inclusion bodies

Cause	Description	Reference
High yield of production of heterologous protein	Transcription and translation systems can be overloaded. Cells may struggle to maintain the appropriate conditions for correct protein folding and stabilization, leading to their aggregation and deposition in the form of inclusion bodies. It is generally assumed that expression of heterologous protein above 2% of the cellular protein may lead to the formation of inclusion bodies in *E. coli.*	(Baneyx and Mujacic, 2004; Singh and Panda, 2005)
Toxicity of the protein or its fragments	Produced heterologous proteins can disrupt the structure of *E. coli* cells and lead to their damage. Damaged cells may produce improperly folded or inactive proteins that can aggregate. Additionally, the deposition of recombinant proteins in the form of inclusion bodies prevents their spread within the cell and minimizes their negative impact on its functions. This is a natural defense mechanism of *E. coli*	(Kaur et al., 2018)
Improper cultivation conditions	*E. coli* growth conditions such as temperature, pH, salt concentration, or expression induction can impact the folding of recombinant proteins. Improper conditions can promote protein aggregation and lead to precipitation.	(Kaur et al., 2018)
Lack of proper post-translational modifications	*E. coli* is a prokaryotic organism that lacks the ability to perform complex post-translational modifications such as glycosylation, phosphorylation, or disulfide bond formation. These modifications are essential for the proper folding and stability of many eukaryotic proteins.	(Baneyx and Mujacic, 2004; Singh and Panda, 2005)

Analysis of polyacrylamide gels aimed at estimating the content of individual target proteins in *E. coli* whole cell lysate showed that all monovalent recombinant proteins (BB0108s, BB0126s, BB0298s, BB0323s, and BB0689s) as well as two of the chimeric proteins (BmpA-BBK32-G, and BmpA-BBK32-M) were produced at a much higher level than 2% of the total protein fraction produced by the cell (Table 5.23) [Result 5.5.1 and 5.5.2]. That could cause the formation of inclusion bodies by BB0323s and BB0689s. The production of BmpA-BBK32 and BmpA-BBA64 was at a much lower level (below 2% of the total protein fraction of the cell) (Table 5.23), but they were also produced in an insoluble form. However, it should be noted that chimeric proteins consist of domains or fragments derived from different sources, which can lead to improper folding and conformational instability. This, in turn, increases the likelihood of aggregation and precipitation of such proteins (Buske et al., 2009; George and Heringa, 2003).

As mentioned, heterologous membrane proteins are often toxic to *E. coli* during their biotechnological production. Therefore, host cells often deposit them in the form of inclusion bodies to limit their harmful effects (Montigny et al., 2004). However, in the conducted toxicity assay, the production of any target protein was not observed to cause a statistically significant slowdown in the growth of the *E. coli* strains used, which excludes the toxic effect of these proteins (Results 5.5.4). As *B. burgdorferi* s.l. is a prokaryotic organism, the reason for the formation of inclusion bodies cannot be traced to the absence of appropriate post-translational modifications such as glycosylation or phosphorylation. For these reasons, it is assumed that the overexpression of *B. burgdorferi* s.l. proteins is the most probable cause of the formation of inclusion bodies

It was noticed that BB0689s, BmpA-BBA64, and BmpA-BBK32 formed insoluble aggregates after the renaturation process [Methods 4.17]. It has been shown that recombinant/chimeric proteins produced in the form of inclusion bodies are able to renature after the removal of the denaturing agent while maintaining solubility and reactivity with specific antibodies (Bryksin et al., 2005; Ferra et al., 2019). Interestingly, the same applied to BB0126s and BB0298s. Since they were successfully purified using buffers without the addition of urea, it appears that they were not deposited in the cell as inclusion bodies (Figure 5.76 and 5.77; Table 5.24). However, they aggregated after elution. BB0108s and BB0323s were not affected by this issue. The latter, despite being produced in the form of inclusion bodies, remained dissolved after the removal of the denaturing agent by dialysis into a storage buffer [Methods 4.18.1].

Proteins can form aggregates in aqueous solutions for several reasons, the dominant of which is, as in the case of the formation of inclusion bodies, the lack of proper assembly, which can lead to the exposure of hydrophobic fragments or inappropriate interactions between protein fragments, which in turn promotes aggregation. Other causes are environmental conditions, such as extreme pH, high temperature, high salt concentration, or the presence of detergents, which can also destabilize the structure of proteins and promote their aggregation (Singh and Panda, 2005).

It was believed that the reason for the problems in obtaining BB0689s, BmpA-BBA64, and BmpA-BBK32 in soluble form was their incorrect renaturation. Therefore, the original dialysis protocol was modified, and it was decided to remove the denaturing agent gradually [Methods 4.18.2]. This enabled producing partially folded intermediates that can promote the formation of correct structures in the subsequent protein re-folding process (Yang et al., 2011).

Inappropriate environmental conditions may also contribute to protein aggregation, buffers with a changed composition were used for the purification of

monovalent and multivalent proteins. They were selected based on literature data describing the production and purification of other *B. burgdorferi* s.l. recombinant proteins (Table 5.25). However, this approach did not contribute to solving the problems associated with the aggregation of the obtained proteins from aqueous solutions.

From the obtained results, it is difficult to determine the direct cause of the problems with aggregation of BB0126s and BB0298s after purification. As many as 7 different buffers were used to purify and store these proteins, it was assumed that the incorrect folding of these proteins also causes the aggregation of BB0126s and BB0298s, and although they do not accumulate in the form of inclusion bodies in bacterial cells, their incorrect structure contributes to their precipitation from aqueous solutions after purification. Therefore, it was decided to purify them using standard buffers with 1 M urea content, so as not to lead to their complete denaturation and preserve their native-like secondary structures, which, similarly to the use of gradual dialysis, can contribute to improveing the recovery of correctly folded native protein (Singh and Panda, 2005). However, this approach had no effect in both cases, and the proteins precipitated after dialysis into buffers not containing a denaturing agent.

Because changed purification protocols and changing storage buffers did not improve protein stability, an attempt was made to solve the problem by ensuring the correct folding of proteins during their biotechnological production. The problem with the misfolding of proteins produced in *E. coli* is quite common, it is estimated that only about 30% of recombinant proteins were expressed in soluble forms. Therefore several strategies have been developed to overcome these hurdles (Yang et al., 2011). But still, despite many years of development, there is currently no simple approach that can be applied in all cases, so the production of each recombinant protein should be considered separately (Chen, 2012; Correa and Oppezzo, 2015). Three approaches were used in these studies, namely:

- changing the conditions for the production of monovalent and multivalent recombinant proteins: lowering the temperature [Results 5.5.7.1];
- use of other *E. coli* strains: Origami™(DE3), Rosetta(DE)pLacI, Rosetta(DE)pLysS [Materials 3.2; Results 5.5.7.3];
- addition of domains that improve folding and increase solubility: TrxA, GST [Results 5.5.7.4].

Changing the growth conditions is the easiest way to improve the folding of recombinant proteins produced in *E. coli*. Lowering culture temperature can reduce the

rate of translation, positively affecting protein folding and increasing the final yield of soluble protein (Correa and Oppezzo, 2015; Vera et al., 2007).

The first step to obtaining recombinant proteins in a soluble form was to change the gene expression conditions by lowering the temperature (20ºC, 25ºC, and 30ºC). However, this approach did not bring the expected results. Calculation of production efficiency from one liter of culture indicates that lowering temperature reduced the production level of recombinant proteins but did not affect their solubility. Although analysis of polyacrylamide gels suggests that the total content of target proteins in whole cell lysates decreased with lowering the temperature for BB0126s and BB0298s, these proteins still accounted for more than 10% of the proteome produced by *E. coli.* On the other hand, BB0689s, even in non-optimal conditions, still accounted for more than 40% of proteins separated in a single lane, the same as for production at 37ºC. However, it should be remembered that the question of whether the production efficiency per liter decreases because of slowing down the production of target proteins by *E. coli* at the cellular level or simply as the effect of their slowed-down growth and obtaining a lower cellular mass has not been unequivocally answered. To get an answer to this question, it would be necessary to analyze the transcriptome, e.g., using Real-Time PCR.

As the decrease of temperature in which the biotechnological production of proteins was carried out did not bring any positive result, it was decided to use other strains of *E. coli* whose genetic features could contribute to obtaining recombinant proteins with the correct spatial structure (Mathieu et al., 2019). For this purpose strains Origami^{TM}(DE3), Rosetta(DE3)pLacI oraz Rosseta(DE3)pLysS were selected.

E. coli Origami^{TM}(DE3) has mutations in the glutathione reductase (*gor*) and thioredoxin reductase (*trxB*) genes maintaining a greater oxidative potential of cytoplasm facilitating the formation of disulfide bonds (de Marco, 2009; Salinas et al., 2011). Analysis of the amino acid sequence indicates that none of the target proteins have cysteines in its sequence that can form sulfide bridges. Therefore, it was not decided to produce target proteins in this strain at earlier stages of work. However, in response to emerging problems with solubility, it was decided to use Origami^{TM}(DE3) assuming that perhaps changed conditions of protein expression and folding associated with additional mutations will contribute to improving the solubility of *B. burgdorferi* s.l. antigens. *E. coli* Rosseta(DE3)pLacI and Rosseta(DE3)pLysS were selected for their codon usage adapted to eukaryotic genes. The use of a non-optimal t-RNA set for *B. burgdorferi* s.l. may contribute to the slowdown of translation, which, as has been shown, may affect the correct folding of heterologous proteins and limit the formation of inclusion bodies (Liu et al., 2021). It was assumed that this may have a particularly positive effect on the solubility of BB0126s, BB0298s, BB0689s which were produced at a high level.

Changing the *E. coli* strain also failed to solve the aggregation problem of the obtained monovalent and multivalent recombinant proteins. For this reason, it was decided to add to their sequence fusion tags that increase solubility. Most often, these domains are fragments of proteins with extremely high solubility or chaperone activity and are introduced at the N-terminus of the protein. The mechanism of action of fusion tags has yet to be fully understood. However, it is assumed that the presence of a stable partner promotes the correct folding of the protein, enhancing its solubility (Esposito and Chatterjee, 2006). In the research carried out as part of this doctoral stage, it was decided to check the influence of two fusion tags i.e., GST and TrxA.

The production of all recombinant proteins with additional fusion partners took place in *E. coli* BL21(DE3)pLysS [Materials 3.2; Results 5.5.7.4.2]. However, the incorporation of additional domains in the sequence of target proteins did not allow prevent BB0126s, BB0298s, BB0689s, BmpA-BBK32, and BmpA-BBA64 aggregation. A different solution to this problem is therefore necessary. Unfortunately, due to time constraints, it could not be implemented during the research conducted as part of this doctoral thesis.

There are several potential solutions to the problem of aggregation of recombinant and chimeric proteins that have not been implemented and which could have positive effects. Firstly, so far, only two fusion tags have been used, and it has been shown that not all fusion tags will work efficiently with any protein (Bhatwa et al., 2021). Therefore, it is possible that other fusion partners such as maltose-binding protein (MBP) or small ubiquitin-related modifier (SUMO) would bring better results. MBP is one of the longest used domains to improve the solubility of recombinant proteins. It is a 42 kD protein naturally produced in the periplasm of *E. coli* (di Guana et al., 1988). While SUMO is a relatively small yeast protein (11.2 kDa) that facilitates the correct folding of the target protein, which leads to both an increase in its solubility and production efficiency (Correa and Oppezzo, 2015).

Another possibility is to change the promoter that controls the expression of the target gene, which could help solve this problem. Of particular interest seems to be the popular BAD promoter, which is induced by arabinose. Generally considered to be a weaker promoter than the *lacUV5* used in pUET1, pET32, and pET42 and has been shown to reduce the amount of insoluble protein fraction (Lozano Terol et al., 2021).

A solution to this obstacle could be using *E. coli* strains dedicated to the production of membrane proteins, such as C41(DE3) or C43(DE3) (Mathieu et al., 2019), or transferring the protein maturation process to the periplasm. Both strains C41(DE3) and C43(DE3) have reduced expression levels of T7 RNA polymerase by the introduction of mutations in the *lacUV5* promoter, additionally, the C43 (DE3) also

possesses a mutation in the lac repressor gene. So the general mechanism of reducing the toxic effect of membrane proteins is similar to that found in *E. coli* BL21(DE3)pLysS (Bhatwa et al., 2021).

Another strategy is to introduce mutations into the gene sequence encoding the target protein to produce a variant with stabilized properties or increased solubility, thus being a suitable last resort when all else fails. When structural and functional information is available, these sequence modifications can be achieved by rationally designed site-directed mutagenesis. Most often, this involves the removal/reduction of the hydrophobic amino acid clusters (Dale et al., 1994; Eijsink et al., 2004; Jung and Seongsoon, 2008). However, this approach may be problematic in the case of *B. burgdorferi* s.l. proteins since for many of them the spatial structures are not known.

6.4. Evaluation of the reactivity of monovalent and multivalent recombinant proteins with specific antibodies

Two immunoenzymatic techniques were used, i.e., Western blot and ELISA, which are the basis of the two-tiered serological diagnosis of borreliosis. The reactivity of all produced monovalent and multivalent recombinant proteins (BB0108s, BB0126s, BB0298s, BB0323s, BB0689s, BmpA-BBA64, BmpA-BBK32, BmpA-BBK32-G, BmpA-BBK32-M) with specific anti-*B. burgdorferi* s.l. antibodies was preliminarily determined by Western blot using a small number of sera. Subsequently, the antigens BB0108s, BB0323s, BmpA-BBK32-G and BmpA-BBK32-M were tested by ELISA on a larger pool of sera. ELSA was chosen to test the diagnostic usefulness of the obtained antigens in a wider pool of sera because it is a quantitative method as opposed to WB, which is qualitative and subjective. Additionally, ELISA has a simpler and more automated procedure that allows this immunoenzymatic assay to be performed on a larger scale, with less risk of errors. Western blot is more complex and has many steps, making the process time-consuming and more prone to human error. This makes it difficult to standardize the entire assay, affecting the results' repeatability.

6.4.1. Reactivity of monovalent recombinant proteins with anti-*B. burgdorferi* s.l. antibodies

Recombinant proteins were not characterized by a high reactivity with antibodies in positive serum samples in WB assay. The sensitivity of BB0108s and BB0323s-based WB was approximately 44%, and for BB0126s and BB0298s, it was in the range of 16-24%. The sensitivity reached maximum values for IgG-WB-BB0689s, as it did not fall below 44% for any of the variants, and IgG-WB-BB0689$_{BA}$ was the only one that exceeded the sensitivity of 50%. However, this antigen was also most often recognized

by antibodies in the negative sera (specificity range 72-76%), suggesting that this high reactivity is mainly due to cross-reactivity and not specific interactions with anti-*B. burgdorferi* s.l. IgG.

After performing the analysis using Fisher's exact test, it was shown that statistically significant differences in reactivity with antibodies contained in two groups of sera, i.e., negative, and positive, are found only in WB based on the BB0108s and BB0323s (all variants) and for BB0298 derived from *B. garinii*. These results seem interesting in the context of the previously performed amino acid sequence analysis aimed at estimating the potential diagnostic utility of selected antigens, as the largest number of potential linear epitopes have been identified for BB0108s and BB0323s. Thus, the bioinformatics approach may actually contribute to a easy and quick initial selection of antigens worth empirically testing.

The reactivity of tested antigens with IgM in WB reached a maximum of 20-24% for BB0108s. IgM-WB showed high specificity, over 92%, probably due to the generally low reactivity of antigens with IgM and not due to the higher specificity of epitope-paratope interactions. The statistical analysis suggests that none of the tested recombinant proteins have a diagnostic value in detecting IgM directed against *B. burgdorferi* s.l. using WB.

When analyzing the reactivity of IgG-positive sera, it was noted that the presence of specific antibodies to one antigen of *B. burgdorferi* s.l. does not mean that it contains immunoglobulins specific to its other antigens. For example, in WB only IgG-positive sera number 23 contained antibodies specific to all recombinant proteins tested. On average, the sera contained antibodies against 3 different antigens. This highlights the well-known disadvantage of using single recombinant proteins in enzyme immunoassays - despite the presence of pathogen-specific antibodies, they may be directed only against some of its antigens. Therefore, using a single protein may lead to a significant decrease in the sensitivity of such assays.

Comparing these results to those obtained for recombinant proteins commonly used in commercial Western blot assays, it turns out that the reactivity of BB0108s and BB0323s was at a similar level as that obtained for IgG-DbpA$_{BA}$ (45%; 9/20) in the study by Heikkilä et al. (2002) and exceeded that of the least reactive variant of this protein, *B. burgdorferi* s.s., which was 20% (4/20). However, when the results for the three DbpA variants in the study were added together, the overall sensitivity for detecting late-stage Lyme disease was 80% (16/20), significantly exceeding the value achieved in the case of BB0108s and BB0323s. In addition, WB based on DbpAs was characterized by 100% specificity (0/20), while for BB0108s and BB0323, it was a maximum of 96% (1/25) and 92% (2/25), respectively (Heikkilä et al., 2002b). WB based on the most reactive FlaA

variant derived from *B. garinii*, achieved a sensitivity of 75% (21/28) and a specificity of over 95% (1/23). When the reactivity of the three FlaA variants was added together, the sensitivity increased to 79% (22/28), and specificity decreased to 87% (3/23). FlaA from *B. burgdorferi* s.s. showed the lowest diagnostic utility, and the sensitivity decreased to 39% (11/28) with a sensitivity of 91% (2/23), which was a result comparable to that achieved for IgG-WB based on BB0108s and BB0323s (Panelius et al., 2001).

Since BB0108s and BB0323s were the only recombinant proteins obtained in a soluble form, their reactivity with specific antibodies could also be determined using ELISA.

In the IgG-ELISA, the BB0108s were highly reactive with the antibodies contained in the positive sera. The sensitivity of IgG-ELISA reached even above 80% for the most reactive variant of the antigen, which is similar to that obtained by DbpA in the late stages of Lyme disease (Heikkilä et al., 2003, 2002b). However, it should be noted that the assay's high sensitivity was not matched by its satisfactory specificity, as it was 82%. The use of the BB0108s mix in ELISA did not improve the sensitivity of the test. It turned out to be even slightly lower than that obtained for the most reactive variant of the protein from *B. afzelii*. This can be explained by the lower content of $BB0108_{BA}$ in the wells, as only 0.33 µg of $BB0108_{BA}$ was used to coat the microtiter plates in this case, while it was 1 µg in the single protein assay. However, using the mixture positively affected the specificity and increased the AUC, significantly improving the diagnostic value of such an immunoenzymatic assay. This approach increased the overall difference in absorbance values between the two groups of sera. It is shown through a more significant difference in mean absorbance and median between the negative and positive sera in ELISA based on a protein mix than in those using single antigens. It is possible that by using three antigen variants, more anti-*B. burgdorferi* s.l. antibodies from positive sera recognized specific epitopes. This allowed the determination of a higher value of the optimal cut-off (0.254 compared to values oscillating around 0.195), leading to an increase in the specificity of the test, while only slightly lowering the sensitivity. The validity of this assumption could be checked by increasing the content of $BB0108_{BA}$ relative to $BB0108_{BB}$ and determining whether it increases the assay's sensitivity.

The sensitivity of the IgG-ELISA based on BB0323s was in the range of 62-72%. Similarly, to BB0108s, the protein BB0323 obtained from *B. afzelii* was the most reactive, while IgG-ELISA-$BB0323_{BB}$ was characterized by the lowest sensitivity. The specificity of these assays was 90%, except for the IgG-ELISA-$BB0323_{BA}$ where it dropped to 88%. Using the $BB0323_{Mix}$ in ELISA did not affect the diagnostic usefulness of the enzyme immunoassay. Although sensitivity compared to ELISA based on single antigens obtained from *B. burgdorferi* s.s. and *B. garinii* increased, it did not reach as high a value

as for $BB0323_{BA}$. It is assumed that, similarly to the case of BB0108s, it is related to the lower content of the most reactive protein variant in the microtiter plate wells. The specificity remained unchanged at 90%.

The effectiveness of both proteins in detecting IgM was lower than for IgG. In IgM-ELISA based on single variants of BB0323s, no statistically significant differences were obtained in the absorbance of positive and negative sera. Additionally, the obtained AUC values did not exceed 0.6 (0.533, 0.572, 0.526), which suggests that this protein is not reactive with this class of antibodies. Thus, tests based on BB0323s did not allow distinguishing between IgM-negative and IgM-positive sera. The use of a mixture of three variants of BB0323s had an observable positive effect. The IgM-ELISA-$BB0323_{Mix}$ showed a statistically significant difference in the absorbance of the positive and negative sera and the AUC increased to 0.686. Using a mixture of proteins from three genospecies in the ELISA probably allowed the detection of infections with different representatives of *B. burgdorferi* s.l. in a single assay.

For IgM-ELISA based on all variants of BB0108s, statistically significant differences in absorbance were obtained for both sera groups, which suggests that BB0108s is recognized by specific IgM, which was not observed in Western blot. This implies that conformational epitopes may play a major role in these interactions as in IgM-WB-BB0108s there was no statistically significant difference in the reactivity between negative and positive sera. The use of the $BB0108_{Mix}$ did not improve the sensitivity of the assay but allowed a slight increase in AUC.

Similarly, as in the previous studies, the sensitivity of ELISA and Western blot based on new recombinant *B. burgdorferi* s.l. antigens differed depending on the antigen variant used. It is impornant to note that differences in ELISA sensitivity were up to 11% and 10% for BB0108s and BB0323s, respectively, while in the case of WB, they were even lower. Thus, they were not as meaningful as those observed in studies conducted for DbpA and OspC, where differences in ELISA sensitivity between variants in a single study were 25% and 50%, respectively (Heikkilä et al., 2002b; Panelius et al., 2002). Moreover, in studies by Heikkilä et al. (2002) and Schulte-Spechtel et al. (2006), it was observed that most of the sera were reactive with only one variant of the DbpA. In the present study, antibodies in the positive sera recognized all three antigen variants in most cases. The sensitivity of ELISA and WB, taking into account all individual antigen variants, in most cases did not differ from that obtained for the most reactive form of the protein. Only in the case of IgG-WB-BB0689s, when its three variants were considered, did the total WB sensitivity increase to 60% (15/25). The results suggest that in most cases, when antibodies against one variant of the antigen were present in the serum, they recognized its other forms. The observation that the most diverse reactivity of

different protein variants concerns BB0689 is in line with the bioinformatic analysis, which showed that this antigen had the lowest sequence conservation (Table 5.2). This indicates that the appropriate selection of conserved antigens may make their reactivity independent of the genospecies causing Lyme disease.

In most cases, similar to other research carried out on sera collected from different areas of Europe, the highest reactivity in the IgG class was shown by variants derived from *B. afzelii* or *B. garinii* (Heikkilä et al., 2002b; Magnarelli et al., 2002; Panelius et al., 2002; Roessler et al., 1997b). This allows us to assume that infections with these genospecies were dominant among the patients from whom the sera were collected. However, these are only conjectures as no specific information was available. This observation is not entirely consistent with the research on the prevalence of *B. burgdorferi* s.l. genospecies in Poland, which state that *B. burgdorferi* s.s. is dominant (Cisak et al., 2006; Strzelczyk et al., 2015). However, it agrees with the reports that *B. afzelii* and *B. garinii* are the dominant genospecies in Europe (Estrada-Peña et al., 2011; Strand et al., 2017). The only case where a recombinant protein variant derived from *B. burgdorferi* s.s. showed higher reactivity than those obtained from *B. afzelii,* and *B. garinii* was $BB0108_{BB}$ in the IgM-ELISA.

It seems that the main parameter that reduces the diagnostic usefulness of BB0108s and BB0323s in ELISA is their relatively low specificity compared to the previously characterized recombinant proteins. According to the literature, the specificity of ELISA based on DbpA, VlsE or OspC is very high and in many studies, it reached 100%, even when the immunoassays were performed on sera collected from people infected with pathogens that are the source of cross-reactions with *B. burgdorferi* s.l. (Fung et al., 1994; Gerber et al., 1995; Heikkilä et al., 2003; Liang et al., 1999; Magnarelli et al., 2002; Padula et al., 1994; Panelius et al., 2002; Schulte-Spechtel et al., 2006). This phenomenon may be due to the location of the genes encoding these proteins. DbpA, VlsE, OspC are encoded by low-conserved plasmids and are mainly responsible for the pathogenesis and virulence of *B. burgdorferi* s.l. and are not directly necessary for the proper functioning of the bacterial cell. The *bb0108s* and *bb0323s* genes are located on the chromosome, where there are mainly genes that control the basic life functions of the cell, so there is a possibility that homologs of these proteins may be found in other organisms (Fraser et al., 1997; Schwartz et al., 2021). This means that the encoding of the protein by the chromosome ensures its high conservation and reactivity with antibodies directed against different genospecies of *B. burgdorferi* s.l., however, on the other hand, it may be the cause of increased cross-reactivity of these proteins.

6.4.2. Reactivity of multivalent chimeric proteins with anti-*B. burgdorferi* s.l. antibodies

All tested multivalent chimeric proteins showed very high reactivity with IgG in Western blot. IgG-WB based on BmpA-BBA64 and BmpA-BBK32 achieved 100% sensitivity and specificity. For IgG-WB-BmpA-BBK32-G, the sensitivity decreased to 90% but the specificity of the assay was still 100%. The reactivity of multivalent chimeric proteins with IgM, as in the case of monovalent recombinant proteins, was at a lower level. Only for WB based on BmpA-BBK32-M, statistically significant differences in reactivity were obtained for both groups of sera.

So far, the diagnostic utility of other *B. burgdorferi* s.l. chimeric proteins in diagnosing Lyme disease using WB has not been tested. Comparing these results with single antigens whose fragments have been incorporated into chimeric protein sequences, BmpA-BBA64, BmpA-BBK32 and BmpA-BBK32-G appear to have a higher reactivity with anti-*B. burgdoerferi* s.l. antibodies. WB based on three BBK32 variants showed 67% (10/15) sensitivity in detecting specific antibodies in erythema migrans patients and 100% (15/15) when samples from patients in the convalescent phase were tested. When the most reactive variant of *B. garinii* BBK32 was considered, the sensitivity was 27% (4/15), and 53% (8/15) for early and late Lyme patients, respectively. However, in another study conducted by the same group, IgG-BBK32 achieved 100% sensitivity in detecting late Lyme disease, regardless of the genospecies from which the antigen was obtained (Heikkilä et al., 2002a). The sensitivity of IgG-WB based on BmpA from *B. afzelii* and *B. garinii* was 36.0% (31/86) and 34.9% (30/86), respectively, and dropped to 13.9% for *B. burgdorferi* s.s. derived BmpA. The specificity of these assays was 100% (Roessler et al., 1997a). In a study by Weiner et al. (2015) regarding the diagnostic usefulness of BBA64 in the detection of early Lyme disease, this antigen showed only a slight reactivity with class M antibodies in WB, it was not recognized at all by IgG.

This comparison shows that the construction of multivalent chimeric proteins, including conserved immunodominant fragments from several antigens, is justified and may contribute to improving the diagnosis of Lyme disease since these constructs show higher reactivity with specific antibodies than single parental antigens.

Due to solubility problems, the diagnostic utility of the BmpA-BBA64 and BmpA-BBK32 antigens could not be tested in ELISA, although this would be desirable due to their high reactivity in IgG-WB, exceeding that observed with BmpA-BBK32-G. It is hypothesized that the reason for this difference in reactivity was the significant difference in the molecular mass of these proteins. BmpA-BBK32 and BmpA-BBA64 are

larger and contain more epitopes that specific antibodies could recognize. However, there is also another side to this, which is highlighted by the results of IgM-WB. BmpA-BBK32 and BmpA-BBA64 were recognized by antibodies contained in positive sera more often than BmpA-BBK32-M. Their lack of diagnostic utility in the detection of IgM was mainly determined by their frequent cross-reactions with immunoglobulins contained in negative sera. This shows how important it is not only to know the highly reactive fragments of the protein but also those responsible for cross-reactions. This problem has probably become apparent with IgM because they generally have a lower specificity of interactions as they are first-line antibodies.

IgG-ELISA-BmpA-BBK32-G (IgG-ELISA-B/32-G) showed relatively high sensitivity and specificity for the detection of IgG, 71% and 95%, respectively, and the AUC was 0.88. The sensitivity of IgM-ELISA-BmpA-BBK32-M (IgM-ELISA-B/32-M) was also 71%, however, the specificity and AUC fell to 89% and 0.78.

An attempt to construct multivalent chimeric proteins useful in the diagnosis of Lyme disease has been made before. Gomes-Solecki et al. (2000) produced 17 chimeric proteins composed of antigenic fragments of OspA, OspB, OspC, flagellin and p93. In this case, the scientists had no knowledge of epitope distribution and designed a collection of chimeric proteins composed of different fragments of the same antigens. Subsequently, to select for chimeras containing immunodominant fragments, immunoblot was performed using monoclonal antibodies specific for particular antigens. On this basis, 4 chimeric proteins were selected from the initial 17 for further research. However, only two showed satisfactory diagnostic utility with a sensitivity of 63% and 69% and a specificity of about 85%. This example illustrates how highly useful epitope mapping can be, as it is possible to save a lot of time and human effort by designing chimeric proteins based on the obtained mapping results, in contrast to including random fragments of antigens in their sequence, hoping that they contain specific epitopes (Gomes-Solecki et al., 2000).

It seems that the selection of IgM and IgG-specific epitopes has allowed the production of multivalent chimeric proteins exhibiting increased reactivity with a specific antibody isotype. This particularly applies to BmpA-BBK32-G, which is not reactive with anti-*B. burgdorferi* s.l. IgM. Student's t-test did not show a statistically significant difference in the absorbance obtained for negative and positive sera, and the ROC analysis showed that the AUC is 0.646, which means that the adopted model is only slightly better than the random differentiation of both groups of sera (AUC=0.5). This indicates a very low number of epitopes specifically recognized by IgM antibodies in sequence BmpA-BBK32-G. The results obtained for IgG-ELISA-B/32-M are not so clear. Student's t-test showed a statistically significant difference in the absorbance values

obtained for both groups of tested sera. In addition, the AUC calculated from the ROC is much higher at 0.722, not significantly different from that obtained for IgM-ELISA-B/32-M. The results suggest a lower reactivity of BmpA-BBK32-M with specific IgG compared to BmpA-BBK32-G. This is indicated not only by the lower AUC value, but also by the median and average absorbance values. The same pool of positive sera was used in both tests, and the values obtained for BmpA-BBK32-M IgG detection are more than two times higher than for BmpA-BBK32-G. This suggests that the number of epitopes recognized by IgG antibodies in the BmpA-BBK32-M protein is reduced. The probable reason for the better result for BmpA-BBK32-M in detecting non-dedicated antibodies is that IgG are present in the bloodstream at a much higher titer and show higher affinity. In addition, IgG target a broader spectrum of epitopes, while IgM recognize only those antigens and their fragments exposed in the early stages of infection (Hillerdal and Henningsson, 2021; Keyt et al., 2020; Liu et al., 2019; Mäkelä et al., 1970).

Comparing the results obtained in Western blot and ELISA, it is noticeable that BmpA-BBK32-G and BmpA-BBK32-M show greater reactivity with specific antibodies in the former. This is probably because they were designed based on mapping linear epitopes, which are better exposed in WB than ELISA. In ELISA, the proteins were not denatured, so they probably assumed some spatial structure even though sequences -GGG- were introduced, forcing a linear conformation. The tertiary structure of BmpA-BBK32-G and BmpA-BBK32-M may not contain any naturally occurring structural epitopes as non-contiguous protein sequences in the native proteins have been joined together into a single amino acid chain. In ELISA, it may be advisable to use multivalent chimeric proteins composed of larger fragments of antigens, so as to at least partially preserve their conformational epitopes (Ferra et al., 2015, 2019).

An interesting issue is that the reactivity of the recombinant proteins with specific antibodies suggests that the sera were collected predominantly from patients infected with *B. afzelii* or *B. garinii*. While for the construction of multivalent chimeric proteins, fragments of genes from *B. burgdorferi* s.s. were used based on research carried out in eastern Poland, which show that this genospecies is dominant in Poland. At this point, the question arises whether, the use of *B. afzelii* or *B. garinii* protein fragments in the construction of chimeric proteins, would increase their reactivity.

Pooled positive sera from two regions of Poland (Pomorskie/Warmińsko-Mazurskie and Mazowieckie voivodships) were used to map the linear antigens. Therefore, it seems reasonable to believe that they were collected from people infected with different genospecies of *B. burgdorferi* s.l. Only peptides that were characterized by high reactivity were used for the construction of multivalent chimeric antigens, thus

suggesting that they were recognized by antibodies specific to different genospecies. In addition, the sequential analysis showed that the identified immunodominant fragments were quite well conserved within the *B. burgdorferi* s.l. complex. It therefore seems that the influence of varied amino acid sequences of antigens among different genospecies on the sensitivity of serological diagnosis of Lyme disease was at least partially eliminated. This problem could be more relevant to the BmpA-BBA64 and BmpA-BBK32 chimeras, where longer fragments of proteins with higher sequence diversity were used. To confirm these assumptions, it would be worthwhile to map the epitopes of BmpA and BBK32 obtained from other genospecies and compare whether the same antigen fragments are reactive. Another approach would be to construct multivalent chimeric proteins containing the corresponding fragments from *B. afzelii* or *B. garinii* instead of *B. burgdorferi* s.s. Perhaps then the reactivity of such chimeric antigens would be enhanced.

6.4.3. Reactivity of insoluble proteins in ELISA

BB0126s, BB0298s, BB0689s, BmpA-BBA64, and BmpA-BBK32, showed no reactivity with antibodies in ELISA, this is especially surprising for BmpA-BBA64 and BmpA-BBK32 which in Western blot were recognized by antibodies contained in all tested sera. Therefore, it causes doubts whether these antigens are not recognized by antibodies in ELISA, or whether the reason for their lack of reactivity is their aggregation in aqueous solutions. It is preferable to use antigens in soluble form for ELISA for several reasons. Firstly, it enables even coating of the wells. Aggregates can form clusters that are difficult to control. As a result, some areas of the well may not be sufficiently covered with antigen, leading to inconsistent test results. This also results in problems with optimizing ELISA conditions because it is difficult to determine what amount of antigen is bound to the sorption surface of the plate. In addition, antibodies in the tested sera must have access to the appropriate epitopes located on the surface of the antigen. If the antigen is insoluble, antibodies may have difficulty effectively reaching and binding to epitopes. This may lead to a decrease in the sensitivity and specificity of ELISA (Geumann et al., 2010; Walker, 1987). This problem does not occur in Western blot because during SDS-PAGE the protein is denatured and in this form is transferred to the membrane. For this reason, only linear epitopes are recognized in WB, as the protein loses its spatial structure (Hnasko and Hnasko, 2015).

7. FUTURE PROSPECTS

In order to have a better understanding of how the rational selection and design of new serodiagnostic tools may affect the diagnosis of Lyme disease, it would be worth extending the results presented here in the future with the following issues.

A great complement to the studies carried out so far would be to test BB0108s, BB0323s, BmpA-BBK32-G, and BmpA-BBK32-M using well-defined positive and negative sera. Firstly, it would be helpful to know the symptoms of the patients from whom the serum was collected and their treatment history to be sure that they were suffering from Lyme disease as there is a risk that a positive serodiagnosis could be due to cross-reactions, which are quite common. Information on the duration of symptoms (acute, late) and their form (LA, neuroborreliosis, ACA) would allow for assessing the reactivity of antigens with antibodies in different phases of the disease. Knowing only the IgM and IgG titer does not allow for an unambiguous assessment of the stage of the disease because IgM in some patients is present in circulation for a long time (Markowicz et al., 2021). However, the most desirable in the context of this work would be information on which genospecies of *B. burgdorferi* s.l. caused the infection. Unfortunately, this is very difficult, because the only way to obtain such information would be to sequence the PCR product obtained on the template of *B. burgdorferi* s.l. DNA isolated from clinical samples of an infected patient, and as it is known, molecular methods in the diagnosis of Lyme disease are often characterized by low sensitivity. The simplest method would be to isolate DNA from EM-affected skin fragments. This type of sample provides a fairly high PCR sensitivity of 68% and is easier to collect than synovial fluid, which is the clinical material in which spirochete DNA is most likely to be detected (Grąźlewska et al., 2020). Therefore, in order to obtain sera characterized in this way, it would be necessary to closely cooperate with medical units that collect samples from patients on an ongoing basis. Due to these difficulties, a good alternative in this case would be to use the sera of experimentally infected mice inoculated with different genospecies of *B. burgdorferi* s.l. Then, such sera would allow for a real assessment of whether the reactivity of the obtained antigens does not change depending on which genospecies caused the infection.

It was noted that some negative sera gave false positive results in both enzyme immunoassays regardless of which recombinant or chimeric protein was tested. Unfortunately, the sera used in this study were not tested for antibodies against other pathogens. However, it seems worth checking whether these negative sera giving false positive results contain antibodies against pathogens that are a confirmed source of cross-reactions with *B. burgdorferi* s.l., i.e., *T. pallidum*, relapsing fever *Borrelia*,

cytomegalovirus, parvovirus B19, Epstein-Bar virus, *A. phagocytophilum*, *Yersinia* and the presence of rheumatoid factor (Golkocheva-Markova et al., 2011; Goossens et al., 1999; Magnarelli et al., 2002; Panelius et al., 2002; Rawlins et al., 2005; Smismans et al., 2006; Talagrand-Reboul et al., 2020; Tuuminen et al., 2011; Wojciechowska-Koszko et al., 2022). It would also be worth testing sera collected from people living in non-endemic areas for *B. burgdorferi* s.l. These additional tests would allow broader conclusions about the specificity of the interactions of antibodies with the antigens.

Another issue that should be resolved is how the order of individual domains building a multivalent chimeric protein can affect epitope exposure. This has been proven with chimeric proteins useful in the diagnosis of toxoplasmosis, it is also an important aspect that can affect reactivity with specific antibodies (Ferra et al., 2019). In addition, it would be worth checking the effect of linkers on the reactivity of these proteins. BmpA-BBA64 and BmpA-BBK32 were constructed without introducing any internal sequences to link these two fragments, it is possible that linker introduction, as in the case of BmpA-BBK32-G and BmpA-BBK32-M would affect their conformation and overall reactivity with antibodies. It would also be worth using other linkers, such as -AAY-, used in the construction of multivalent vaccines (Fadhil Hashim et al., 2023). This would make it possible to acquire more comprehensive knowledge on how the rational design of new diagnostic tools can contribute to the improvement of serodiagnostics.

Also of interest is the construction of a multi-epitope assay based on synthetic peptide mapping data. Such solutions are already being developed for several infectious diseases, including Chagas disease and Lyme disease (Mucci et al., 2017). Lahey et al. (2015) developed an assay combining full-sequence recombinant proteins and highly reactive peptides that detected *B. burgdorferi* s.l. infection in a higher proportion of early Lyme patients at baseline and post-treatment visits than the two-tiered algorithm. So perhaps this combined approach is a way to improve the diagnosis of Lyme disease.

8. SUMMARY AND FINAL CONCLUSIONS

Due to climate changes increasing the range of ticks' existence and the length of their feeding period, Lyme disease is becoming a mounting problem (Strand et al., 2017). Although authorities of many developed countries notice this problem and the recommendation to monitor cases of this disease is widespread, there is still a need to improve its diagnosis. The currently used commercial tests are based on a scheme developed in the 1990s, and as the research shows, they are insufficient to ensure an adequate diagnosis of Lyme disease in humans. As has been mentioned many times in this dissertation, the main problem Lyme disease serodiagnosis faces is the complicated antigenic structure of *B. burgdorferi* s.l. and the multitude of its genospecies. Therefore, it is necessary to better understand the spirochete proteome and to continue research to determine the diagnostic utility of the new pool of *B. burgdorferi* s.l. antigens to find those that may contribute to improving the serodiagnosis of Lyme disease. Nowadays, many computational and empirical methods exist for mapping linear and conformational epitopes which appears to be a key step in the rational design of multivalent chimeric proteins. This enables the identification of highly specific epitopes and sequences responsible for cross-reactions, which allows the selection of appropriate fragments for the construction of multivalent chimeric proteins. Previous studies have demonstrated the application of epitope mapping by microarray as a tool that allows the design of multivalent chimeric proteins that may be useful in serodiagnosis and vaccinology (de la Fuente et al., 2022; Pichler, 2002; Potocnakova et al., 2016). This may allow the future to develop a simple, one-stage ELISA test that will significantly improve and reduce the cost of routine diagnosis of Lyme disease.

To sum up, the following stages of work were carried out during the implementation of this doctoral thesis:

- Amino acid sequence analysis of selected *B. burgdorferi* s.l. antigens (BB0108, BB0126, BB0298, BB0323, BB0689) was performed to determine their degree of conservation within genospecies and to identify potential B-cell epitopes to estimate their reactivity with antibodies.
- Four multivalent chimeric proteins were designed using two approaches:
    - *In silico*: conserved immunodominant fragments of the BmpA, BBA64, and BBK32 antigens were identified using bioinformatics tools, and multivalent chimeric proteins containing these selected fragments (BmpA-BBA64 and BmpA-BBK32) were designed;
    - Empirical: using polypeptide microarrays, immunodominant and cross-reactive fragments of BmpA and BBK32 antigens were identified, and

then, based on these results, chimeric proteins BmpA-BBK32-G and BmpA-BBK32-M were designed, dedicated to the detection of IgG and IgM, respectively.

- Expression systems based on *E. coli* were constructed, allowing for the production of:
  - 15 monovalent *B. burgdorferi* s.l. recombinant proteins: BB0108, BB0126, BB0298, BB0323, BB0689 each in three versions derived from the genospecies *B. afzelii, B. burgdorferi* and *B. garinii;*
  - 4 multivalent chimeric proteins: BmpA-BBK32, BmpA-BBA64, BmpA-BBK32-G, BmpA-BBK32-M;
  - 6 recombinant proteins containing TrxA or GST domains: BB0126-TrxA, BB0126-GST, BmpA- BBK32- TrxA, BmpA-BBK32-GST, BmpA-BBA64-GST.
- The reactivity of BB0108s, BB0126s, BB0298s, BB0323s, BB0689s, BmpA-BBK32, BmpA- BBA64, BmpA-BBK32-G, BmpA-BBK32-M with specific IgG and IgM contained in human serum was assessed by Western blot.
- The reactivity of BB0108s, BB0323s, BB0689s, BmpA-BBK32-G, and BmpA-BBK32-M with specific IgG and IgM contained in human serum was assessed by ELISA.

Based on the results obtained as part of the implementation of these research tasks, the following conclusions can be drawn:

- Developing an effective expression system to produce the target protein in a soluble form is crucial to obtain new serodiagnostic tools. Although *E. coli*-based expression systems are widely used, in some cases, it is extremely difficult to obtain soluble recombinant proteins with the correct conformation.
- BB0108s and BB0323s show moderate diagnostic usefulness in the detection of IgG using WB and ELISA, the reactivity of their individual variants did not differ significantly, which suggests that the use of preserved antigens in serodiagnostic assays may contribute to solving the problem caused by the diversity of *B. burgdorferi* s.l. genospecies in Europe.
- BB0108s is recognized by anti-*B. burgdorferi* s.l. specific IgM in ELISA but does not appear to be of significant diagnostic value.
- BmpA-BBK32 and BmpA-BBA64 chimeric proteins are highly reactive with IgG in WB, these assays achieved 100% sensitivity and specificity. While IgG-WB based on BmpA-BBK32-G achieved a sensitivity of 90% and a specificity of

100%. Thus, it seems that multivalent chimeric proteins composed of selected fragments of antigens with proven immunogenicity may improve the serodiagnosis of Lyme disease.

- BmpA-BBK32-M was the only multivalent chimeric protein tested in IgM-WB to show statistically significant differences in reactivity with positive and negative sera. Although IgM-WB based on BmpA-BBK32 or BmpA-BBA64 did not differ in sensitivity, they were less specific. This suggests that in the rational design of multivalent chimeric proteins, it is crucial to identify and remove cross-reacting fragments, which enables empirical epitope mapping.
- BmpA-BBK32-G and BmpA-BBK32-M showed moderate utility in the detection of their dedicated antibodies. However, it was noted that the appropriate selection of linear epitopes allows for the construction of multivalent chimeric proteins showing increased reactivity with a specific antibody isotope. Therefore, it seems that designing multivalent chimeric proteins typically dedicated to IgM detection may improve the diagnosis of early Lyme disease.

REFERENCES

1. Aguero-Rosenfeld, M., Wang, G., Scwartz, I., Wormser, G., 2005. Diagnosis of Lyme borreliosis. Clin. Microbiol. Rev. 18, 484–509. https://doi.org/10.1128/CMR.18.3.484

2. Aguero-Rosenfeld, M.E., Nowakowski, J., McKenna, D.F., Carbonaro, C.A., Wormser, G.P., 1993. Serodiagnosis in early Lyme disease. J. Clin. Microbiol. 31, 3090–3095. https://doi.org/10.1128/JCM.31.12.3090-3095.1993

3. Ahmad, T.A., Eweida, A.E., Sheweita, S.A., 2016. B-cell epitope mapping for the design of vaccines and effective diagnostics. Trials Vaccinol. 5, 71–83. https://doi.org/10.1016/J.TRIVAC.2016.04.003

4. Allen, C., Steere, M., Stephen, E., Malavista, M., John, A., Hardin, M.D., Shaun Ruddy, M., Philip, W., Askenase, M., Warren, A., Andiman, M.. 1977. Erythema chronicum migrans and Lyme arthritis. Ann. Agric. Environ. Med. 86, 685–698. https://doi.org/10.7326/0003-4819-86-6-685.

5. Almagro Armenteros, J.J., Tsirigos, K.D., Sønderby, C.K., Petersen, T.N., Winther, O., Brunak, S., von Heijne, G., Nielsen, H., 2019. SignalP 5.0 improves signal peptide predictions using deep neural networks. Nat. Biotechnol. 2019 374 37, 420–423. https://doi.org/10.1038/s41587-019-0036-z

6. Altschul, S.F., Gish, W., Miller, W., Myers, E.W., Lipman, D.J., 1990. Basic local alignment search tool. J. Mol. Biol. 215, 403–410. https://doi.org/10.1016/S0022-2836(05)80360-2

7. Anderson, C., Brissette, C.A., 2021. The brilliance of *Borrelia*: Mechanisms of host immune evasion by Lyme disease-causing spirochetes. Pathogens 10, 1–17. https://doi.org/10.3390/pathogens10030281

8. Arnaboldi, P.M., Dattwyler, R.J., 2015. Cross-reactive epitopes in *Borrelia burgdorferi* p66. Clin. Vaccine Immunol. 22, 840–843. https://doi.org/10.1128/CVI.00217-15

9. Arnaboldi, P.M., Katseff, A.S., Sambir, M., Dattwyler, R.J., 2022. Linear peptide epitopes derived from ErpP, p35, and FlaB in the serodiagnosis of Lyme disease. Pathogens 11, 1–10. https://doi.org/10.3390/pathogens11080944

10. Arnaboldi, P.M., Seedarnee, R., Sambir, M., Callister, S.M., Imparato, J.A., Dattwylera, R.J., 2013. Outer surface protein C peptide derived from *Borrelia burgdorferi* sensu stricto as a target for serodiagnosis of early Lyme disease. Clin. Vaccine Immunol. 20, 474–481. https://doi.org/10.1128/CVI.00608-12

11. Assis, L.M., Sousa, J.R., Pinto, N.F.S., Silva, A.A., Vaz, A.F.M., Andrade, P.P., Carvalho, E.M., De Melo, M.A., 2014. B-cell epitopes of antigenic proteins in *Leishmania infantum*: an *in silico* analysis. Parasite Immunol. 36, 313–323. https://doi.org/10.1111/PIM.12111

12. Bacon, R.M., Biggerstaff, B.J., Schriefer, M.E., Gilmore, Jr., R.D., Philipp, M.T., Steere, A.C., Wormser, G.P., Marques, A.R., Johnson, B.J.B., 2003. Serodiagnosis of Lyme disease by kinetic enzyme-linked immunosorbent assay using recombinant VlsE1 or peptide antigens of *Borrelia burgdorferi* compared with 2-tiered testing using whole-cell lysates. J. Infect. Dis. 187, 1187–1199. https://doi.org/10.1086/374395

13. Bahrami, A.A., Payandeh, Z., Khalili, S., Zakeri, A., Bandehpour, M., 2019. Immunoinformatics: *in silico* approaches and computational design of a multi-epitope, immunogenic protein. Int. Rev. Immunol. 38, 307–322. https://doi.org/10.1080/08830185.2019.1657426

14. Baneyx, F., Mujacic, M., 2004. Recombinant protein folding and misfolding in *Escherichia coli*. Nat. Biotechnol. 22, 1399–1407. https://doi.org/10.1038/nbt1029

15. Bansal, S., Kundu, B., 2022. Advanced computational tools for quantitative analysis of protein-nucleic acid interfaces. Protein engineering: Methods and applications. Elsevier. https://doi.org/10.1016/B978-0-323-90264-9.00011-8

16. Barbour, A.G., Jasinskas, A., Kayala, M.A., Davies, D.H., Steere, A.C., Baldi, P., Felgner,

P.L., 2008. A genome-wide proteome array reveals a limited set of immunogens in natural infections of humans and white-footed mice with *Borrelia burgdorferi*. Infect. Immun. 76, 3374–3389. https://doi.org/10.1128/IAI.00048-08

17. Barbour, A.G., Zuckert, W.R., 1997. New tricks of tick-borne pathogen. Nature 390, 553–554. https://doi.org/10.1038/37475

18. Bateman, A., Martin, M.J., Orchard, S., Magrane, M., Agivetova, R., Ahmad, S., Alpi, E., Bowler-Barnett, E.H., Britto, R., Bursteinas, B., Bye-A-Jee, H., Coetzee, R., Cukura, A., da Silva, A., Denny, P., Dogan, T., Ebenezer, T.G., Fan, J., Castro, L.G., Teodoro, D., 2021. UniProt: the universal protein knowledgebase in 2021. Nucleic Acids Res. 49, D480–D489. https://doi.org/10.1093/NAR/GKAA1100

19. Bergmann, A.R., Schmidt, B.L., Derler, A.M., Aberer, E., 2002. Importance of sample preparation for molecular diagnosis of Lyme borreliosis from urine. J. Clin. Microbiol. 40, 4581–4584. https://doi.org/10.1128/JCM.40.12.4581-4584.2002

20. Berndtson, K., 2013. Review of evidence for immune evasion and persistent infection in Lyme disease. Int. J. Gen. Med. 6, 291–306. https://doi.org/10.2147/IJGM.S44114

21. Bhatwa, A., Wang, W., Hassan, Y.I., Abraham, N., Li, X.Z., Zhou, T., 2021. Challenges associated with the formation of recombinant protein inclusion bodies in *Escherichia coli* and strategies to address them for industrial applications. Front. Bioeng. Biotechnol. 9, e630551. https://doi.org/10.3389/FBIOE.2021.630551

22. Blanchard, L., Jones-Diette, J., Lorenc, T., Sutcliffe, K., Sowden, A., Thomas, J., 2022. Comparison of national surveillance systems for Lyme disease in humans in Europe and North America: a policy review. BMC Public Health 22, 1–13. https://doi.org/10.1186/S12889-022-13669-w

23. Bradshaw, G.L., Thueson, R.K., Uriona, T.J., 2017. Improved serodiagnostic performance for Lyme disease by use of two recombinant proteins in ELISA as compared to standardized two tier testing. J. Clin. Microbiol. 55, 3046–3056. https://doi.org/10.1128/JCM.01004-17

24. Branda, J.A., Linskey, K., Kim, Y.A., Steere, A.C., Ferraro, M.J., 2011. Two-tiered antibody testing for lyme disease with use of 2 enzyme immunoassays, a whole-cell sonicate enzyme immunoassay followed by a vlse c6 peptide enzyme immunoassay. Clin. Infect. Dis. 53, 541–547. https://doi.org/10.1093/cid/cir464

25. Branda, J.A., Strle, K., Nigrovic, L.E., Lantos, P.M., Lepore, T.J., Damle, N.S., Ferraro, M.J., Steere, A.C., 2017. Evaluation of modified 2-tiered serodiagnostic testing algorithms for early Lyme disease. Clin. Infect. Dis. 64, 1074–80. https://doi.org/10.1093/cid/cix043

26. Brandt, K.S., Patton, T.G., Allard, A.S., Caimano, M.J., Radolf, J.D., Gilmore, R.D., 2014. Evaluation of the *Borrelia burgdorferi* BBA64 protein as a protective immunogen in mice. Clin. Vaccine Immunol. 21, 526–533. https://doi.org/10.1128/CVI.00824-13

27. Brangulis, K., Jaudzems, K., Petrovskis, I., Akopjana, I., Kazaks, A., Tars, K., 2015a. Structural and functional analysis of BB0689 from *Borrelia burgdorferi*, a member of the bacterial CAP superfamily. J. Struct. Biol. 192, 320–330. https://doi.org/10.1016/J.JSB.2015.09.007

28. Brangulis, K., Petrovskis, I., Kazaks, A., Akopjana, I., Tars, K., 2015b. Crystal structures of the Erp protein family members ErpP and ErpC from *Borrelia burgdorferi* reveal the reason for different affinities for complement regulator factor H. Biochim. Biophys. Acta 9, 349–355. https://doi.org/10.1016/j.bbapap.2014.12.025

29. Brisson, D., Drecktrah, D., Eggers, C.H., Samuels, D.S., 2012. Genetics of *Borrelia burgdorferi*. Annu. Rev. Genet. 46, 515–536. https://doi.org/10.1146/annurev-genet-011112-112140

30. Brooks, C.S., Hefty, P.S., Jolliff, S.E., Akins, D.R., 2003. Global analysis of *Borrelia burgdorferi* genes regulated by mammalian host-specific signals. Infect. Immun. 71, 3371–3383. https://doi.org/10.1128/IAI.71.6.3371-3383.2003

31. Brooks, C.S., Vuppala, S.R., Jett, A.M., Akins, D.R., 2006. Identification of *Borrelia*

burgdorferi outer surface proteins. Infect. Immun. 74, 296–304. https://doi.org/10.1128/IAI.74.1.296-304.2006

32. Bruckbauer, H.R., Preac-Mursic, V., Fuchs, R., Wilske, B., 1992. Cross-reactive proteins of *Borrelia burgdorferi*. Eur. J. Clin. Microbiol. Infect. Dis. 11, 224–232. https://doi.org/10.1007/BF02098084

33. Bryksin, A. V., Godfrey, H.P., Carbonaro, C.A., Wormser, G.P., Aguero-Rosenfeld, M.E., Cabello, F.C., 2005. *Borrelia burgdorferi* BmpA, BmpB, and BmpD proteins are expressed in human infection and contribute to P39 immunoblot reactivity in patients with Lyme disease. Clin. Diagn. Lab. Immunol. 12, 935–940. https://doi.org/10.1128/CDLI.12.8.935-940.2005

34. Burgdorfer, W., Bargour, A.G., Hayes, S.F., Benach, J., Grunwaldt, E., Davis, J.P., 1982. Lyme disease a tick-borne spirochetosis? 216, 1317–1319. https://doi.org/10.1126/science.7043737

35. Buske, F.A., Their, R., Gillam, E.M.J., Bode, M., 2009. *In silico* characterization of protein chimeras: relating sequence and function within the same fold. Proteins 77, 111–120. https://doi.org/10.1002/prot.22422

36. Byram, R., Gaultney, R.A., Floden, A.M., Hellekson, C., Stone, B.L., Bowman, A., Stevenson, B., Johnson, B.J.B., Brissette, C.A., 2015. *Borrelia burgdorferi* RevA significantly affects pathogenicity and host response in the mouse model of Lyme disease. Infect. Immun. 83, 3675–3683. https://doi.org/10.1128/IAI.00530-15

37. Caimano, M.J., Dunham-Ems, S., Allard, A.M., Cassera, M.B., Kenedy, M., Radolf, J.D., 2015. Cyclic di-GMP modulates gene expression in Lyme disease spirochetes at the tick-mammal interface to promote spirochete survival during the blood meal and tick-to-mammal transmission. Infect. Immun. 83, 3043–3060. https://doi.org/10.1128/IAI.00315-15

38. Caine, J.A., Coburn, J., 2016. Multifunctional and redundant roles of *Borrelia burgdorferi* outer surface proteins in tissue adhesion, colonization, and complement evasion. Front. Immunol. 7, 1–11. https://doi.org/10.3389/FIMMU.2016.00442

39. Cannon, M.J., Schmid, D.S., Hyde, T.B., 2010. Review of cytomegalovirus seroprevalence and demographic characteristics associated with infection. Rev. Med. Virol. 20, 202–213. https://doi.org/10.1002/RMV.655

40. Carrasco, S.E., Troxell, B., Yang, Y., Brandt, S.L., Li, H., Sandusky, G.E., Condon, K.W., Serezani, C.H., Frank, X., 2015. Outer surface protein OspC is an antiphagocytic factor that protects *Borrelia burgdorderi* from phagocytosis by macrophages. Am. Soc. Microbiol. 83, 4848–4860. https://doi.org/10.1128/IAI.01215-15

41. Carroll, J.A., El-Hage, N., Miller, J.C., Babb, K., Stevenson, B., 2001. *Borrelia burgdorferi* RevA antigen is a surface-exposed outer membrane protein whose expression is regulated in response to environmental temperature and pH. Infect. Immun. 69, 5286–5293. https://doi.org/10.1128/IAI.69.9.5286-5293.2001

42. Casjens, S., Palmer, N., Van Vugt, R., Huang, W.M., Stevenson, B., Rosa, P., Lathigra, R., Sutton, G., Peterson, J., Dodson, R.J., Haft, D., Hickey, E., Gwinn, M., White, O., Fraser, C.M., 2000. A bacterial genome in flux: The twelve linear and nine circular extrachromosomal DNAs in an infectious isolate of the Lyme disease spirochete *Borrelia burgdorferi*. Mol. Microbiol. 35, 490–516. https://doi.org/10.1046/j.1365-2958.2000.01698.x.

43. Casjens, S.R., Gilcrease, E.B., Vujadinovic, M., Mongodin, E.F., Luft, B.J., Schutzer, S.E., Fraser, C.M., Qiu, W.G., 2017. Plasmid diversity and phylogenetic consistency in the Lyme disease agent *Borrelia burgdorferi*. BMC Genomics 18, 1–18. https://doi.org/10.1186/s12864-017-3553-5

44. Casjens, S.R., Mongodin, E.F., Qiu, W.G., Luft, B.J., Schutzer, S.E., Gilcrease, E.B., Huang, W.M., Vujadinovic, M., Aron, J.K., Vargas, L.C., Freeman, S., Radune, D., Weidman, J.F., Dimitrov, G.I., Khouri, H.M., Sosa, J.E., Halpin, R.A., Dunn, J.J., Fraser, C.M., 2012. Genome stability of Lyme disease spirochetes: Comparative genomics of *Borrelia burgdorferi* plasmids. PLoS One 7, 1–24. https://doi.org/10.1371/journal.pone.0033280

45. Centers for Disease Control and Prevention (CDC), 1995. Recommendations for test

performance and interpretation from the second national conference on serologic diagnosis of Lyme disease. JAMA J. Am. Med. Assoc. 274, 937. https://doi.org/10.1001/jama.1995.03530120023018

46. Cerar, T., Strle, F., Stupica, D., Ruzic-Sabljic, E., McHugh, G., Steere, A.C., Strle, K., 2016. Differences in genotype, clinical features, and inflammatory potential *of Borrelia burgdorferi* sensu stricto strains from Europe and the United States. Emerg. Infect. Dis. 22, 818–827. https://doi.org/10.3201/eid2205.151806

47. Cheadle, C., Vawter, M. P., Freed, W. J., & Becker, K. G., 2003. Analysis of microarray data using Z score transformation. J. Mol. Diagn. 5, 73-81. https://doi.org/10.1016/S1525-1578(10)60455-2

48. Chen, R., 2012. Bacterial expression systems for recombinant protein production: *E. coli* and beyond. Biotechnol. Adv. 30, 1102–1107. https://doi.org/10.1016/J.BIOTECHADV.2011.09.013

49. Chung, Y., Zhang, N., Wooten, R.M., Stevenson, B., 2013. *Borrelia burgdorferi* elicited-IL-10 suppresses the production of inflammatory mediators, phagocytosis, and expression of co-stimulatory receptors by murine macrophages and/or dendritic cells. PLoS One 8, e84980. https://doi.org/10.1371/journal.pone.0084980

50. Cisak, E., Wójcik-Fatla, A., Stojek, N.M., Chmielewska-Badora, J., Zwoliński, J., Buczek, A., Dutkiewicz, J., 2006. Prevalence of *Borrelia burgdorferi* genospecies in *Ixodes ricinus* ticks from Lublin region (eastern Poland). Ann. Agric. Environ. Med. 13, 301–306.

51. Cobb, B.A., Kasper, D.L., 2005. Coming of age: carbohydrates and immunity. Eur. J. Immunol. 35, 352–356. https://doi.org/10.1002/EJI.200425889

52. Coburn, J., Leong, J., Chaconas, G., 2013. Illuminating the roles of the *Borrelia burgdorferi* adhesins. Trends Microbiol. 21, 372–379. https://doi.org/10.1016/j.tim.2013.06.005

53. Coleman, A.S., Yang, X., Kumar, M., Zhang, X., Promnares, K., Shroder, D., Kenedy, M.R., Anderson, J.F., Akins, D.R., Pal, U., 2008. *Borrelia burgdorferi* complement regulator-acquiring surface protein 2 does not contribute to complement resistance or host infectivity. PLoS One 3, https://doi.org/10.1371/JOURNAL.PONE.0003010

54. Cook, M., 2014. Lyme borreliosis: a review of data on transmission time after tick attachment. Int. J. Gen. Med. 8, 1–8. https://doi.org/10.2147/IJGM.S73791

55. Correa, A., Oppezzo, P., 2015. Overcoming the solubility problem in *E. coli:* Available approaches for recombinant protein production. Methods Mol. Biol. 1258, 27–44. https://doi.org/10.1007/978-1-4939-2205-5_2

56. Craft, J.E., Grodzicki, R.L., Shrestha, M., Fischer, D.K., Phil, M., Garcfa-Blanco, M., Steere, A.C., 1984. The antibody response in Lyme disease. Yale J. Biol. Med. 57, 561–565.

57. da Silva, B.M., Ascher, D.B., Pires, D.E. V, 2023. epitope1D: accurate taxonomy-aware B-cell linear epitope prediction. Brief. Bioinform. 24, 1–8. https://doi.org/10.1093/bib/bbad114

58. Dąbrowski, S., Kur, J., 1999. Cloning, overexpression, and purification of the recombinant His-tagged SSB protein of *Escherichia coli* and use in polymerase chain reaction amplification. Protein Expr. Purif. 16, 96–102. https://doi.org/10.1006/prep.1999.1044

59. Dai, J., Wang, P., Adusumilli, S., Booth, C.J., Narasimhan, S., Anguita, J., Fikrig, E., 2009. Antibodies against a tick protein, Salp15, protect mice from the Lyme disease agent. Cell Host Microbe 6, 482–492. https://doi.org/10.1016/j.chom.2009.10.006

60. Dale, G.E., Broger, C., Langen, H., Arcy, A.D., Stüber, D., 1994. Improving protein solubility through rationally designed amino acid replacements: Solubilization of the trimethoprim-resistant type S1 dihydrofolate reductase. Protein Eng. Des. Sel. 7, 933–939. https://doi.org/10.1093/protein/7.7.933

61. Davies, D.H., Liang, X., Hernandez, J.E., Randall, A., Hirst, S., Mu, Y., Romero, K.M., Nguyen, T.T., Kalantari-Dehaghi, M., Crotty, S., Baldi, P., Villarreal, L.P., Felgner, P.L., 2005. Profiling the humoral immune response to infection by using proteome microarrays: High-

throughput vaccine and diagnostic antigen discovery. Proc. Natl. Acad. Sci. U. S. A. 102, 547–552. https://doi.org/10.1073/pnas.0408782102

62. de la Fuente, J., Moraga-Fernández, A., Alberdi, P., Díaz-Sánchez, S., García-Álvarez, O., Fernández-Melgar, R., Contreras, M., 2022. A Quantum vaccinomics approach for the design and production of MSP4 chimeric antigen for the control of *Anaplasma phagocytophilum* infections. Vaccines 10, 1995. https://doi.org/10.3390/VACCINES10121995

63. de Libero, G., Mori, L., 2010. How the immune system detects lipid antigens. Prog. Lipid Res. 49, 120–127. https://doi.org/10.1016/j.plipres.2009.10.002

64. de Marco, A., 2009. Strategies for successful recombinant expression of disulfide bond-dependent proteins in *Escherichia coli*. Microb. Cell Fact. 8, 1–18. https://doi.org/10.1186/1475-2859-8-26

65. Dea-Ayuela, M.A., Bolás-Fernández, F., 2005. Two-dimensional electrophoresis and mass spectrometry for the identification of species-specific *Trichinella* antigens. Vet. Parasitol. 132, 43–49. https://doi.org/10.1016/J.VETPAR.2005.05.018

66. Del-Rei, R.P., Leony, L.M., Celedon, P.A.F., Zanchin, N.I.T., dos Reis, M.G., de Miranda Gomes, Y., Schijman, A.G., Longhi, S.A., Santos, F.L.N., 2019. Detection of anti-*Trypanosoma cruzi* antibodies by chimeric antigens in chronic Chagas disease-individuals from endemic South American countries. PLoS One 14, 1–12. https://doi.org/10.1371/journal.pone.0215623

67. Dennis, J., Walker, L., Tyrer, J., Michailidou, K., & Easton, D. F., 2021. Detecting rare copy number variants from Illumina genotyping arrays with the CamCNV pipeline: Segmentation of z-scores improves detection and reliability. Genet. Epidemiol. 45, 237-248. https://doi.org/10.1002/gepi.22367

68. des Vignes, F., Piesman, J., Heffernan, R., Schulze, T.L., Stafford, K.C., Fish, D., 2001. Effect of tick removal on transmission of *Borrelia burgdorferi* and *Ehrlichia phagocytophila* by *Ixodes scapularis* nymphs. J. Infect. Dis. 183, 773–778. https://doi.org/10.1086/318818

69. Desai, P.N., Shrivastava, N., Padh, H., 2010. Production of heterologous proteins in plants: Strategies for optimal expression. Biotechnol. Adv. 28, 427–435. https://doi.org/10.1016/j.biotechadv.2010.01.005

70. Dessau, R.B., van Dam, A.P., Fingerle, V., Gray, J., Hovius, J.W., Hunfeld, K.P., Jaulhac, B., Kahl, O., Kristoferitsch, W., Lindgren, P.E., Markowicz, M., Mavin, S., Ornstein, K., Rupprecht, T., Stanek, G., Strle, F., 2018. To test or not to test? Laboratory support for the diagnosis of Lyme borreliosis: a position paper of ESGBOR, the ESCMID study group for Lyme borreliosis. Clin. Microbiol. Infect. 24, 118–124. https://doi.org/10.1016/J.CMI.2017.08.025

71. di Guana, C., Lib, P., Riggsa, P.D., Inouyeb, H., 1988. Vectors that facilitate the expression and purification of foreign peptides in *Escherichia coli* by fusion to maltose-binding protein. Gene 67, 21–30. https://doi.org/10.1016/0378-1119(88)90004-2

72. Dressler, F., Whalen, J.A., Reinhardt, B.N., Steere, A.C., 1993. Western blotting in the serodiagnosis of Lyme disease. J. Infect. Dis. 167, 392–400. https://doi.org/10.1093/infdis/167.2.392

73. Dunaj, J., Moniuszko, A., Zajkowska, J., Panacewicz, S., 2013. The role of PCR in diagnostics of Lyme borreliosis. Przegl. Epidemiol. 67, 35–39.

74. Durante, I.M., La Spina, P.E., Carmona, S.J., Agü ero, F., Buscaglia, C.A., 2017. High-resolution profiling of linear B-cell epitopes from mucin-associated surface proteins (MASPs) of Trypanosoma cruzi during human infections. Neglected Trop. Dis. 29, e0005986. https://doi.org/10.1371/journal.pntd.0005986

75. Eiffert, H., Hanefeld, F., Thomssen, R., Christen, H.J., 1996. Reinfection in Lyme borreliosis. Infection 24, 437–439. https://doi.org/10.1007/BF01713045

76. Eijsink, V.G.H., Bjørk, A., Gåseidnes, S., Sirevåg, R., Synstad, B., Van Den Burg, B., Vriend,

G., 2004. Rational engineering of enzyme stability. J. Biotechnol. 113, 105–120. https://doi.org/10.1016/j.jbiotec.2004.03.026

77. Eisen, L., 2020. Vector competence studies with hard ticks and *Borrelia burgdorferi* sensu lato spirochetes: A review. Ticks Tick. Borne. Dis. 11, 1–26. https://doi.org/10.1016/J.TTBDIS.2019.101359

78. Eldin, C., Raffetin, A., Bouiller, K., Hansmann, Y., Roblot, F., Raoult, D., Parola, P., 2019. Review of European and American guidelines for the diagnosis of Lyme borreliosis. Med. Mal. Infect. 49, 121–132. https://doi.org/10.1016/j.medmal.2018.11.011

79. Embers, M.E., Jacobs, M.B., Johnson, B.J.B., Philipp, M.T., 2007. Dominant epitopes of the C6 diagnostic peptide of *Borrelia burgdorferi* are largely inaccessible to antibody on the parent VlsE molecule. Clin. Vaccine Immunol. 14, 931–936. https://doi.org/10.1128/CVI.00075-07

80. Emini, E.A., Hughes, J. V, Perlow, D.S., Boger, J., 1985. Induction of hepatitis A virus-neutralizing antibody by a virus-specific synthetic peptide. J. Virol. 55, 836–839. https://doi.org/10.1128/JVI.55.3.836-839.1985

81. Engstrom, S.M., Shoop, E., Johnson, R.C., 1995. Immunoblot interpretation criteria for serodiagnosis of early Lyme disease. J. Clin. Microbiol. 33, 419–427. https://doi.org/10.1128/JCM.33.2.419-427.1995.

82. Esposito, D., Chatterjee, D.K., 2006. Enhancement of soluble protein expression through the use of fusion tags. Curr. Opin. Biotechnol. 17, 353–358. https://doi.org/10.1016/J.COPBIO.2006.06.003

83. Estrada-Peña, A., Ortega, C., Sánchez, N., DeSimone, L., Sudre, B., Suk, J.E., Semenza, J.C., 2011. Correlation of *Borrelia burgdorferi* sensu lato prevalence in questing *Ixodes ricinus* ticks with specific abiotic traits in the Western Palearctic. Appl. Environ. Microbiol. 77, 3838–3845. https://doi.org/10.1128/AEM.00067-11

84. Fadhil Hashim, A., Humadi, S., Ahjel, S., 2023. Design and construction of multi epitope-peptide vaccine candidate for rabies virus. Bioinformation 19, 167–177. https://doi.org/10.6026/97320630019167

85. Ferra, B., Holec-Gąsior, L., Kur, J., 2015. A new *Toxoplasma gondii* chimeric antigen containing fragments of SAG2, GRA1, and ROP1 proteins—impact of immunodominant sequences size on its diagnostic usefulness. Parasitol. Res. 114, 3291–3299. https://doi.org/10.1007/s00436-015-4552-6

86. Ferra, B.T., Holec-Gąsior, L., Gatkowska, J., Dziadek, B., Dzitko, K., Grąźlewska, W., Lautenbach, D., 2019. The first study on the usefulness of recombinant tetravalent chimeric proteins containing fragments of SAG2, GRA1, ROP1 and AMA1 antigens in the detection of specific anti-*Toxoplasma gondii* antibodies in mouse and human sera. PLoS One 14, 1–23. https://doi.org/10.1371/journal.pone.0217866

87. Fikrig, E., Feng, W., Barthold, S.W., Telford, S.R., Flavell, R.A., 2000. Arthropod- and host-specific *Borrelia burgdorferi* bbk32 expression and the inhibition of spirochete transmission. J. Immunol. 164, 5344–5351. https://doi.org/10.4049/jimmunol.164.10.5344

88. Fingerle, V., Schulte-Spechtel, U.C., Ruzic-Sabljic, E., Leonhard, S., Hofmann, H., Weber, K., Pfister, K., Strle, F., Wilske, B., 2008. Epidemiological aspects and molecular characterization of *Borrelia burgdorferi* s.l. from southern Germany with special respect to the new species *Borrelia spielmanii* sp. nov. Int. J. Med. Microbiol. 298, 279–290. https://doi.org/10.1016/j.ijmm.2007.05.002

89. Fischer, J.R., Parveen, N., Magoun, L., Leong, J.M., 2003. Decorin-binding proteins A and B confer distinct mammalian cell type-specific attachment by *Borrelia burgdorferi*, the Lyme disease spirochete. Proc. Natl. Acad. Sci. U. S. A. 10, 7307–7312. https://doi.org/10.1073/pnas.1231043100

90. Flisiak, R., Pancewicz, S., Grygorczuk, S., Knysz, B., Simon, K., Zajkowska, J., 2011. Diagnostyka i leczenie Boreliozy z Lyme - Zalecenia Polskiego Towarzystwa Epidemiologów i Lekarzy Chorób Zakaźnych

91. Fraser, C.M., Casjens, S., Huang, W.M., Sutton, G.G., Clayton, R., Lathigra, R., White, O., Ketchum, K.A., Dodson, R., Hickey, E.K., Gwinn, M., Dougherty, B., Tomb, J.F., Fleischmann, R.D., Richardson, D., Peterson, J., Kerlavage, A.R., Quackenbush, J., Salzberg, S., Hanson, M., Van Vugt, R., Palmer, N., Adams, M.D., Gocayne, J., Weidman, J., Utterback, T., Watthey, L., McDonald, L., Artiach, P., Bowman, C., Garland, S., Fujii, C., Cotton, M.D., Horst, K., Roberts, K., Hatch, B., Smith, H.O., Venter, J.C., 1997. Genomic sequence of a Lyme disease spirochaete, *Borrelia burgdorferi*. Nature 390, 580–586. https://doi.org/10.1038/37551

92. Fung, B.P., McHugh, G.L., Leong, J.M., Steere, A.C., 1994. Humoral immune response to outer surface protein C of *Borrelia burgdorferi* in Lyme disease: role of the immunoglobulin M response in the serodiagnosis of early infection. Infect Immun 62, 3213–3221. https://doi.org/10.1128/iai.62.8.3213-3221.1994.

93. Garcia, B.L., Zhi, H., Wager, B., Höök, M., Skare, J.T., 2016. *Borrelia burgdorferi* BBK32 inhibits the classical pathway by blocking activation of the C1 complement complex. https://doi.org/10.1371/journal.ppat.1005404

94. Gąsiorowski, J., Witecka-Knysz, E., Knysz, B., Gerber, H., Gładysz, A., 2007. Diagnostyka boreliozy. Med. Pr. 58, 439–447.

95. Ge, Y., Li, C., Corum, L., Slaughter, C.A., 1998. Structure and expression of the FlaA Periplasmic flagellar protein of *Borrelia burgdorferi.* J. Bacteriol. 180, 2418–2425. https://doi.org/10.1128/JB.180.9.2418-2425.1998

96. George, R.A., Heringa, J., 2003. An analysis of protein domain linkers : their classification and role in protein folding. Protein Eng. 15, 871–879. https://doi.org/10.1093/protein/15.11.871

97. Gerber, M.A., Shapiro, E.D., Bell, G.L., Sampieri, A., Padula, S.J., 1995. Recombinant outer surface protein-C ELISA for the diagnosis of early Lyme-disease. J. Infect. Dis. 171, 724–727. https://doi.org/10.1093/infdis/171.3.724

98. Geumann, C., Grønborg, M., Hellwig, M., Martens, H., Jahn, R., 2010. A sandwich enzyme-linked immunosorbent assay for the quantification of insoluble membrane and scaffold proteins. Anal. Biochem. 402, 161–169. https://doi.org/10.1016/j.ab.2010.03.037

99. Ghosh, S., Seward, R., Costello, C.E., Stollar, B.D., Huber, B.T., 2006. Autoantibodies from synovial lesions in chronic, antibiotic treatment-resistant Lyme arthritis bind cytokeratin-10. J. Immunol. 177, 2486–2494. https://doi.org/10.4049/JIMMUNOL.177.4.2486

100. Gilmore, R.D., Howison, R.R., Dietrich, G., Patton, T.G., Clifton, D.R., Carroll, J.A., 2010. The *bba64* gene of *Borrelia burgdorferi*, the Lyme disease agent, is critical for mammalian infection via tick bite transmission. Proc. Natl. Acad. Sci. 107, 7515–7520. https://doi.org/10.1073/pnas.1000268107

101. Gilmore, R.D., Mbow, M.L., Stevenson, B., 2001. Analysis of *Borrelia burgdorferi* gene expression during life cycle phases of the tick vector *Ixodes scapularis.* Microbes Infect. 3, 799–808. https://doi.org/10.1016/S1286-4579(01)01435-6

102. Goettner, G., Schulte-Spechtel, U., Hillermann, R., Liegl, G., Wilske, B., Fingerle, V., 2005. Improvement of Lyme borreliosis serodiagnosis by a newly developed recombinant immunoglobulin G (IgG) and IgM line immunoblot assay and addition of VlsE and DbpA homologues. J. Clin. Microbiol. 43, 3602–3609. https://doi.org/10.1128/JCM.43.8.3602-3609.2005

103. Goldstein, S.F., Buttle, K.F., Charon, N.W., 1996. Structural analysis of *Leptospiraceae* and *Borrelia burgdorferi* by high voltage electron microscopy. J. Bacteriol. 178, 6539–6545.

104. Golkocheva-Markova, E., Nenova, R., Stoilov, R., Christova, I., Najdenski, H., 2011. Cross-reactivity between *Yersinia* outer membrane proteins and anti-*Francisella* and anti-*Borrelia* antibodies in serodiagnosis of *Yersinia*-triggered reactive arthritis. Comptes Rendus L'Academie Bulg. des Sci. 64, 61–66.

105. Gomes-Solecki, M.J.C., Dunn, J.J., Luft, B.J., Castillo, J., Dykhuizen, D.E., Yang, X., Glass, D., Dattwyler, R.J., Glass, J.D., 2000. Recombinant chimeric *Borrelia* proteins for diagnosis

of Lyme disease. J. Clin. Microbiol. 38, 2530–2535. https://doi.org/10.1128/JCM.38.7.2530-2535.2000

106. Goossens, H., Nohlmans, M.K., van den Bogaard, E., 1999. Epstein-Barr virus and cytomegalovirus infections cause false-positive results in IgM two-test protocol for early Lyme borreliosis. Infection 27, 231. https://doi.org/10.1007/BF02561539

107. Graves, J., Byerly, J., Priego, E., Makkapati, N., Parish, S., Medellin, B., Berrondo, M., 2020. A Review of deep learning methods for antibodies. Antibodies 9, 12. https://doi.org/10.3390/antib9020012

108. Grążlewska, W., Ferra, B., Holec-Gąsior, L., 2020. Przydatność diagnostyczna reakcji PCR w rozpoznawaniu boreliozy. Adv. Microbiol. 59, 367–377. https://doi.org/10.21307/pm-2020.59.4.28

109. Hagman, K.E., Lahdenne, P., Popova, T.G., Porcella, S.F., Akins, D.R., Radolf, J.D., Norgard, M. V, 1998. Decorin-binding protein of *Borrelia burgdorferi* is encoded within a two-gene operon and is protective in the murine model of Lyme borreliosis. Am. Soc. Microbiol. 66, 2674–2683. https://doi.org/10.1128/iai.66.6.2674-2683.1998

110. Hallström, T., Siegel, C., Mörgelin, M., Kraiczy, P., Skerka, C., Zipfel, P.F., 2013. CspA from *Borrelia burgdorferi* inhibits the terminal complement pathway. MBio 4, 481–494. https://doi.org/10.1128/MBIO.00481-13

111. Hansen, K., Asbrink, E., 1989. Serodiagnosis of erythema migrans and acrodermatitis chronica atrophicans by the *Borrelia burgdorferi* immunodominant 60-kilodalton antigen common to. Infect. Immun 27, 545–551. https://doi.org/10.1128/jcm.27.3.545-551.1989

112. Hansen, K., Hindersson, P., Pedersen, N.S., 1988. Measurement of antibodies to the *Borrelia burgdorferi* flagellum improves serodiagnosis in Lyme disease. J. Clin. Microbiol. 26, 338–346. https://doi.org/10.1128/jcm.26.2.338-346.1988

113. Haste Andersen, P., Nielsen, M., Lund, O., 2006. Prediction of residues in discontinuous B-cell epitopes using protein 3D structures. Protein Sci. 15, 2558–2567. https://doi.org/10.1110/PS.062405906

114. Haupt, K., Kraiczy, P., Wallich, R., Brade, V., Skerka, C., Zipfel, P.F., 2007. Binding of human factor H-related protein 1 to serum-resistant *Borrelia burgdorferi* is mediated by *Borrelial* complement regulator-acquiring surface proteins. J. Infect. Dis. 196, 124–133. https://doi.org/10.1086/518509

115. Hauser, U., Wilske, B., 1997. Enzyme-linked immunosorbent assays with recombinant internal flagellin fragments derived from different species of *Borrelia burgdorferi* sensu lato for the serodiagnosis of Lyme neuroborreliosis. Med. Microbiol. Immunol. 1997 1862 186, 145–151. https://doi.org/10.1007/S004300050057

116. Heikkilä, T., Huppertz, H.I., Seppälä, I., Sillanpää, H., Saxen, H., Lahdenne, P., 2003. Recombinant or peptide antigens in the serology of Lyme arthritis in children. J. Infect. Dis. 187, 1888–1894. https://doi.org/10.1086/375371

117. Heikkilä, T., Seppälä, I., Saxén, H., Panelius, J., Peltomaa, M., Julin, T., Carlsson, S.A., Lahdenne, P., 2002a. Recombinant BBK32 protein in serodiagnosis of early and late Lyme borreliosis. J. Clin. Microbiol. 40, 1174–1180. https://doi.org/10.1128/JCM.40.4.1174-1180.2002

118. Heikkilä, T., Seppälä, I., Saxen, H., Panelius, J., Yrjänäinen, H., 2002b. Species-specific serodiagnosis of Lyme arthritis and neuroborreliosis due to *Borrelia burgdorferi* sensu stricto, *B. afzelii*, and *B. garinii* by using decorin binding protein A. J. Clin. Microbiol. 40, 453–460. https://doi.org/10.1128/JCM.40.2.453

119. Heiss, K., Heidepriem, J., Fischer, N., Weber, L.K., Dahlke, C., Jaenisch, T., Loeffler, F.F., 2020. Rapid response to pandemic threats: immunogenic epitope detection of pandemic pathogens for diagnostics and vaccine development using peptide microarrays. J. Proteome Res. 19, 4339–4354. https://doi.org/10.1021/acs.jproteome.0c00484

120. Helble, J.D., McCarthy, J.E., Hu, L.T., 2021. Interactions between *Borrelia burgdorferi* and

its hosts across the enzootic cycle. Parasite Immunol. 43, e12816. https://doi.org/10.1111/PIM.12816

121. Hillerdal, H., Henningsson, A.J., 2021. Serodiagnosis of Lyme borreliosis—is IgM in serum more harmful than helpful? Eur. J. Clin. Microbiol. Infect. Dis. 40, 1161–1168. https://doi.org/10.1007/s10096-020-04093-2

122. Hnasko, T.S., Hnasko, R.M., 2015. The Western blot. Methods Mol. Biol. 1318, 87–96. https://doi.org/10.1007/978-1-4939-2742-5_9

123. Hofhuis, A., Van De Kassteele, J., Sprong, H., Van Den Wijngaard, C.C., Harms, M.G., Fonville, M., Docters Van Leeuwen, A., Simões, M., Van Pelt, W., 2017. Predicting the risk of Lyme borreliosis after a tick bite, using a structural equation model. PLoS One 12, e0181807. https://doi.org/10.1371/journal.pone.0181807

124. Hofmann, H., Fingerle, V., Hunfeld, K.P., Huppertz, H.I., Krause, A., Rauer, S., Ruf, B., 2017. Cutaneous Lyme borreliosis: Guideline of the German Dermatology Society. Ger. Med. Sci. 15, 1–31. https://doi.org/10.3205/000255

125. Holec-Gąsior, L., 2013. *Toxoplasma gondii* recombinant antigens as tools for serodiagnosis of human toxoplasmosis: Current status of studies. Clin. Vaccine Immunol. 20, 1343–1351. https://doi.org/10.1128/CVI.00117-13

126. Holec-Gąsior, L., Ferra, B., Drapała, D., Lautenbach, D., Kur, J., 2012. A new MIC1-MAG1 recombinant chimeric antigen can be used instead of the *Toxoplasma gondii* lysate antigen in serodiagnosis of human toxoplasmosis. Clin. Vaccine Immunol. 19, 57–63. https://doi.org/10.1128/CVI.05433-11

127. Holec-Gąsior, L., Kur, J., 2010. *Toxoplasma gondii*: Recombinant GRA5 antigen for detection of immunoglobulin G antibodies using enzyme-linked immunosorbent assay. Exp. Parasitol. 124, 272–278. https://doi.org/10.1016/j.exppara.2009.10.010

128. Holec, L., Gąsior, A., Brillowska-Dąbrowska, A., Kur, J., 2008. *Toxoplasma gondii*: Enzyme-linked immunosorbent assay using different fragments of recombinant microneme protein 1 (MIC1) for detection of immunoglobulin G antibodies. Exp. Parasitol. 119, 1–6. https://doi.org/10.1016/j.exppara.2007.12.002

129. Howe, T.R., Laquier, F.W., Barbour, A.G., 1986. Organization of genes encoding two outer membrane proteins of the Lyme disease agent *Borrelia burgdorferi* within a single transcriptional unit. Infect. Immun. 54, 207–212. https://doi.org/10.1128/iai.54.1.207-212.1986

130. Hsieh, Y.F., Liu, H.W., Hsu, T.C., Wei, J.C.C., Shih, C.M., Krause, P.J., Tsay, G.J., 2007. Serum reactivity against *Borrelia burgdorferi* OspA in patients with rheumatoid arthritis. Clin. Vaccine Immunol. 14, 1437–1441. https://doi.org/10.1128/CVI.00151-07

131. Hunter, E.F., RussellL, H., Farshy, C., Sampson, J., 1986. Evaluation of sera from patients with Lyme disease in the fluorescent *Treponemal* antibody-absorption test for syphilis. Sex. Transm. Dis. 13, 232–236. https://doi.org/10.1097/00007435-198610000-00005

132. Hyde, J.A., 2017. *Borrelia burgdorferi* keeps moving and carries on: A review of *Borrelial* dissemination and invasion. Front. Immunol. 8, 1–16. https://doi.org/10.3389/fimmu.2017.00114

133. Hynote, E.D., Mervine, P.C., Stricker, R.B., 2012. Clinical evidence for rapid transmission of Lyme disease following a tickbite. Diagn. Microbiol. Infect. Dis. 72, 188–192. https://doi.org/10.1016/j.diagmicrobio.2011.10.003

134. Jacobs, J.M., Yang, X., Luft, B.J., Dunn, J.J., Camp, D.G., Smith, R.D., 2005. Proteomic analysis of Lyme disease: global protein comparison of three strains of *Borrelia burgdorferi*. Proteomics 5, 1446–1453. https://doi.org/10.1002/PMIC.200401052

135. Jacquot, M., Gonnet, M., Ferquel, E., Abrial, D., Claude, A., Gasqui, P., rie Choumet, V., Charras-Garrido, M., Garnier, M., Faure, B., Sertour, N., Dorr, N., De Goë, J., Vourc, G., Bailly, X., Stevenson, B., 2014. Comparative population genomics of the *Borrelia burgdorferi* species complex reveals high degree of genetic isolation among species and underscores

benefits and constraints to studying intra-specific epidemiological processes. PLoS One 9, e94384. https://doi.org/10.1371/journal.pone.0094384

136. Jakab, Á., Kahlig, P., Kuenzli, E., Neumayr, A., 2022. Tick borne relapsing fever - a systematic review and analysis of the literature. PLoS Negl. Trop. Dis. 16, e0010212. https://doi.org/10.1371/JOURNAL.PNTD.0010212

137. Jaulhac, B., Chary-Valckenaere, I., Sibilia, J., Javier, R.M., Piémont, Y., Kuntz, J.L., Monteil, H., Pourel, J., 1996. Detection of *Borrelia burgdorferi* by DNA amplification in synovial tissue samples from patients with Lyme arthritis. Arthritis Rheum. 39, 736–745. https://doi.org/10.1002/art.1780390505

138. Jespersen, M.C., Peters, B., Nielsen, M., Marcatili, P., 2017. BepiPred-2.0: improving sequence-based B-cell epitope prediction using conformational epitopes. Nucleic Acids Res. 45, W24–W29. https://doi.org/10.1093/NAR/GKX346

139. Johnson, B.J.B., Robbins, K.E., Bailey, R.E., Cao, B.L., Sviat, S.L., Craven, R.B., Mayer, L.W., Dennis, D.T., 1996. Serodiagnosis of Lyme disease: Accuracy of a two-step approach using a flagella-based ELISA and immunoblotting. J. Infect. Dis. 174, 346–353. https://doi.org/10.1093/infdis/174.2.346

140. Jonsson, M., Noppa, L., Barbour, A.G., Bergstrom, S., 1992. Heterogeneity of outer membrane proteins in *Borrelia burgdorferi*: Comparison of *osp* operons of three isolates of different geographic origins. Infect. Immun. 60, 1845–1853. https://doi.org/10.1128/iai.60.5.1845-1853.1992

141. Jung, S., Seongsoon, P., 2008. Improving the expression yield of *Candida antarctica* lipase B in *Escherichia coli* by mutagenesis. Biotechnol. Lett. 30, 717–722. https://doi.org/10.1007/s10529-007-9591-3

142. Kalish, R., McHugh, G., Granquist, J., Shea, B., Ruthazer, R., Steere, A.C., 2001. Persistence of immunoglobulin M or immunoglobulin G antibody responses to *Borrelia burgdorferi* 10-20 years after active Lyme disease. Clin. Infect. Dis. 33, 780–785. https://doi.org/10.1086/322669

143. Karbalaei, M., Rezaee, S.A., Farsiani, H., 2020. *Pichia pastoris*: A highly successful expression system for optimal synthesis of heterologous proteins. J. Cell. Physiol. 235, 5867–5881. https://doi.org/10.1002/jcp.29583

144. Kariu, T., Sharma, K., Singh, P., Smith, A.A., Backstedt, B., Buyuktanir, O., Pal, U., 2015. BB0323 and novel virulence determinant BB0238: *Borrelia burgdorferi* proteins that interact with and stabilize each other and are critical for infectivity. J. Infect. Dis. 211, 462–471. https://doi.org/10.1093/INFDIS/JIU460

145. Kaur, Jashandeep, Kumar, A., Kaur, Jagdeep, 2018. Strategies for optimization of heterologous protein expression in *E. coli*: Roadblocks and reinforcements. Int. J. Biol. Macromol. 106, 803–822. https://doi.org/10.1016/j.ijbiomac.2017.08.080

146. Kenedy, M.R., Lenhart, T.R., Akins, D.R., 2012. The role of *Borrelia burgdorferi* outer surface proteins. FEMS Immunol. Med. Microbiol. 66, 1–19. https://doi.org/10.1111/j.1574-695X.2012.00980.x

147. Keyt, B.A., Baliga, R., Sinclair, A.M., Carroll, S.F., Peterson, M.S., n.d. Structure, function, and therapeutic use of IgM antibodies. Antibodies 2020, 53. https://doi.org/10.3390/antib9040053

148. Khan, A.H., Bayat, H., Rajabibazl, M., Sabri, S., Rahimpour, A., 2017. Humanizing glycosylation pathways in eukaryotic expression systems. World J. Microbiol. Biotechnol. 33, 1–12. https://doi.org/10.1007/s11274-016-2172-7

149. Kondrusik, M., Grygorczuk, S., Skotarczak, B., Wodecka, B., Rymaszewska, A., Pancewicz, S., Zajkowska, J., Świerzbińska, R., Hermanowska-Szpakowicz, T., 2007. Molecular and serological diagnosis of *Borrelia burgdorferi* infection among patients with diagnosed erythema migrans. Ann. Agric. Environ. Med. 14, 209–213.

150. Kraiczy, P., Hartmann, K., Hellwage, J., Skerka, C., Kirschfink, M., Brade, V., Zipfel, P.F.,

Wallich, R., Stevenson, B., 2004a. Immunological characterization of the complement regulator factor H-binding CRASP and Erp proteins of *Borrelia burgdorferi*. Int. J. Med. Microbiol. 293 Suppl 37, 152–157. https://doi.org/10.1016/S1433-1128(04)80029-9

151. Kraiczy, P., Hellwage, J., Skerka, C., Becker, H., Kirschfink, M., Simon, M.M., Brade, V., Zipfel, P.F., Wallich, R., 2004b. Complement resistance of *Borrelia burgdorferi* correlates with the expression of BbCRASP-1, a novel linear plasmid-encoded surface protein that interacts with human factor H and FHL-1 and is unrelated to Erp proteins*. J. Biol. Chem. 279, 2421–2429. https://doi.org/10.1074/jbc.M308343200

152. Kraiczy, P., Rossmann, E., Brade, V., Simon, M.M., Skerka, C., Zipfel, P.F., Wallich, R., 2006. Binding of human complement regulators FHL-1 and factor H to CRASP-1 orthologs of *Borrelia burgdorferi*. Wien Klin Wochenschr 669–676. https://doi.org/10.1007/s00508-006-0691-1

153. Kraiczy, P., Skerka, C., Kirschfink, M., Zipfel, P.F., Brade, V., 2001. Mechanism of complement resistance of pathogenic *Borrelia burgdorferi* isolates. Int. Immunopharmacol. 1, 393–401. https://doi.org/10.1016/S1567-5769(00)00041-2

154. Křupka, M., Mašek, J., Bartheldyová, E., Knötigová, P.T., Plocková, J., Korvasová, Z., Škrabalová, M., Koudelka, Š., Kulich, P., Zachová, K., Czerneková, L., Strouhal, O., Horynová, M., Šebela, M., Miller, A.D., Ledvina, M., Raška, M., Turánek, J., 2012. Enhancement of immune response towards non-lipidized *Borrelia burgdorferi* recombinant OspC antigen by binding onto the surface of metallochelating nanoliposomes with entrapped lipophilic derivatives of norAbuMDP. J. Control. Release 160, 374–381. https://doi.org/10.1016/j.jconrel.2012.02.017

155. Krzyczmanik, D., Sińczuk-Walczak, H., Wittczak, T., Cyran, A., Pałczyński, C., Walusiak-Skorupa, J., 2012. Borreliosis in occupational medicine practice. Med. Pr. 63, 483–92.

156. Kumar, R., Yadav, A.K., Singh, V.K., Vandre, R.K., Singh, P.K., Verma, N., Das, R., Vineeth, M.R., 2015. Transgenic animal technology: Recent advances and applications: A Review. Agric. Rev. 36, 46. https://doi.org/10.5958/0976-0741.2015.00005.7

157. Kurtenbach, K., De Michelis, S., Etti, S., Schäfer, S.M., Sewell, H.-S., Brade, V., Kraiczy, P., 2002. Host association of *Borrelia burgdorferi* sensu lato-the key role of host complement. Trends Microbiol. 10. https://doi.org/10.1016/s0966-842x(01)02298-3

158. Lahey, L.J., Panas, M.W., Mao, R., Delanoy, M., Flanagan, J.J., Binder, S.R., Rebman, A.W., Montoya, J.G., Soloski, M.J., Steere, A.C., Dattwyler, R.J., Arnaboldi, P.M., Aucott, J.N., Robinson, W.H., 2015. Development of a multiantigen panel for improved detection of *Borrelia burgdorferi* infection in early Lyme disease. J. Clin. Microbiol. 53, 3834–3841. https://doi.org/10.1128/JCM.02111-15

159. Lantos, P.M., Lipsett, S.C., Nigrovic, L.E., 2016. False positive Lyme disease IgM immunoblots in children. J. Pediatr. 174, 267–269. https://doi.org/10.1016/j.jpeds.2016.04.004

160. Larkin, M.A., Blackshields, G., Brown, N.P., Chenna, R., Mcgettigan, P.A., McWilliam, H., Valentin, F., Wallace, I.M., Wilm, A., Lopez, R., Thompson, J.D., Gibson, T.J., Higgins, D.G., 2007. Clustal W and Clustal X version 2.0. Bioinformatics 23, 2947–2948. https://doi.org/10.1093/BIOINFORMATICS/BTM404

161. Lawrenz, M.B., Hardham, J.M., Owens, R.T., Nowakowski, J., Steere, A.C., 1999. Human Antibody Responses to VlsE Antigenic variation protein of *Borrelia burgdorferi.* J. Clin. Microbiol. 37, 3997–4004. https://doi.org/10.1128/JCM.37.12.3997-4004.1999

162. Lessard, J.C., 2013. Molecular cloning. Methods Enzymol. 529, 85–98. https://doi.org/10.1016/B978-0-12-418687-3.00007-0

163. Li, X., Liu, X., Beck, D.S., Kantor, F.S., Fikrig, E., 2006. *Borrelia burgdorferi* lacking BBK32, a fibronectin-binding protein, retains full pathogenicity. Infect. Immun. 74, 3305–3313. https://doi.org/10.1128/IAI.02035-05

164. Li, X., Neelakanta, G., Liu, X., Beck, D.S., Kantor, F.S., Fish, D., Anderson, J.F., Fikrig, E., 2007. Role of outer surface protein D in the *Borrelia burgdorferi* life cycle. Infect. Immun. 75,

4237–4244. https://doi.org/10.1128/IAI.00632-07

165. Liang, F.T., Philipp, M.T., 2000. Epitope mapping of the immunodominant invariable region of *Borrelia burgdorferi* VlsE in three host species. Infect. Immun. 68, 2349–2352. https://doi.org/10.1128/IAI.68.4.2349-2352.2000

166. Liang, F.T., Steere, A.C., Marques, A.R., Johnson, B.J., Miller, J.N., Philipp, M.T., 1999. Sensitive and specific serodiagnosis of Lyme disease by enzyme-linked immunosorbent assay with a peptide based on an immunodominant conserved region of *Borrelia burgdorferi* VlsE. J Clin Microbiol 37, 3990–3996. https://doi.org/10.1128/JCM.37.12.3990-3996.1999

167. Lin, J., Sampson, H.A., 2017. IgE epitope mapping using peptide microarray immunoassay. Methods. Mol. Biol. 1592, 177-187. https://doi.org/10.1007/978-1-4939-6925-8_14

168. Lin, Y.-P., Tan, X., Caine, J.A., Castellanos, M., Chaconas, G., Coburn, J., Leong, J.M., 2020. Strain-specific joint invasion and colonization by Lyme disease spirochetes is promoted by outer surface protein C. PLOS Pathog. 16, e1008516. https://doi.org/10.1371/journal.ppat.1008516

169. Liu, J., Wang, Y., Xiong, E., Hong, R., Lu, Q., Ohno, H., Wang, J.Y., 2019. Role of the IgM Fc receptor in immunity and tolerance. Front. Immunol. 10. https://doi.org/10.3389/fimmu.2019.00529

170. Liu, Y., Yang, Q., Zhao, F., 2021. Synonymous but not silent: The codon usage code for gene expression and protein folding. Annu. Rev. Biochem. 90, 375. https://doi.org/10.1146/ANNUREV-BIOCHEM-071320-112701

171. Liveris, D., Schwartz, I., McKenna, D., Nowakowski, J., Nadelman, R., DeMarco, J., Iyer, R., Bittker, S., Cooper, D., Holmgren, D., Wormser, G.P., 2012. Comparison of five diagnostic modalities for direct detection of *Borrelia burgdorferi* in patients with early Lyme disease. Diagn. Microbiol. Infect. Dis. 73, 243–245. https://doi.org/10.1016/j.diagmicrobio.2012.03.026

172. Lohr, B., Fingerle, V., Norris, D.E., Hunfeld, K.-P., 2018. Laboratory diagnosis of Lyme borreliosis: Current state of the art and future perspectives. Crit. Rev. Clin. Lab. Sci. 0, 1–27. https://doi.org/10.1080/10408363.2018.1450353

173. Lozano Terol, G., Gallego-Jara, J., Sola Martínez, R.A., Martínez Vivancos, A., Cánovas Díaz, M., de Diego Puente, T., 2021. Impact of the expression system on recombinant protein production in *Escherichia coli* BL21. Front. Microbiol. 12, 1–12. https://doi.org/10.3389/fmicb.2021.682001

174. Luft, B.J., Dunn, J.J., Dattwyler, R.J., Gorgone, G., Gorevic, P.D., Schubach, W.H., 1993. Cross-reactive antigenic domains of the flagellin protein of *Borrelia burgdorferi*. Res. Microbiol. 144, 251–257. https://doi.org/10.1016/0923-2508(93)90009-Q

175. Luther, B., Moskophidis, M., 1990. Antigenic cross-reactivity between *Borrelia burgdorferi*, *Borrelia recurrentis*, *Treponema pallidum*, and *Treponema phagedenis*. Zentralblatt für Bakteriol. 274, 214–226. https://doi.org/10.1016/S0934-8840(11)80104-0

176. Magalhães, F.B., Castro Neto, A.L., Nascimento, M.B., Santos, W.J.T., Medeiros, Z.M., Lima Neto, A.S., Costa, D.L., Costa, C.H.N., Dos Santos, W.L.C., Pontes de Carvalho, L.C., Oliveira, G.G.S., De Melo Neto, O.P., 2017. Evaluation of a new set of recombinant antigens for the serological diagnosis of human and canine visceral leishmaniasis. PLoS One 12, e0184867. https://doi.org/10.1371/journal.pone.0184867

177. Magnarelli, L. a, Ijdo, J.W., Padula, S.J., Flavell, R. a, Fikrig, E., 2000. Serologic diagnosis of Lyme borreliosis by using enzyme-linked immunosorbent assays with recombinant antigens. J. Clin. Microbiol. 38, 1735–9. https://doi.org/10.1128/JCM.38.5.1735-1739.2000

178. Magnarelli, L.A., Dumler, J.S., Anderson, J.F., Johnson, R.C., Fikrig, E., 1995. Coexistence of antibodies to tick-borne pathogens of babesiosis, ehrlichiosis, and Lyme borreliosis in human sera. J. Clin. Microbiol. 33, 3054–3057. https://doi.org/10.1128/JCM.33.11.3054-3057.1995

179. Magnarelli, L.A., Fikrig, E., Padula, S.J., Anderson, J.F., Flavell, R.A., 1996. Use of

recombinant antigens of *Borrelia burgdorferi* in serologic tests for diagnosis of Lyme borreliosis. J. Clin. Microbiol. 34, 237–240. https://doi.org/10.1128/JCM.34.2.237-240.1996

180. Magnarelli, L.A., Lawrenz, M., Fikrig, E., Norris, S.J., 2002. Comparative reactivity of human sera to recombinant VlsE and other *Borrelia burgdorferi* antigens in class-specific enzyme-linked immunosorbent assays for Lyme borreliosis. J. Med. Microbiol. 51, 649–655. https://doi.org/10.1099/0022-1317-51-8-649

181. Magnarelli, L.A., Miller, J.N., Anderson, J.F., Riviere, G.R., 1990. Cross-reactivity of nonspecific treponemal antibody in serologic tests for Lyme disease. J. Clin. Microbiol. 28, 1276–1279. https://doi.org/10.1128/jcm.28.6.1276-1279.1990

182. Mäkelä, O., Rouslahti, E., Seppälä, I.J.T., 1970. Affinity of IgM and IgG antibodies. Immunochemistry 7, 917–932. https://doi.org/10.1016/0019-2791(70)90053-4

183. Maksimov, P., Zerweck, J., Maksimov, A., Hotop, A., Groß, U., Pleyer, U., Spekker, K., Däubener, W., Werdermann, S., Niederstrasser, O., Petri, E., Mertens, M., Ulrich, R.G., Conraths, F.J., Schares, G., 2012. Peptide microarray analysis of in silico-predicted epitopes for serological diagnosis of Toxoplasma gondii infection in humans. Clin. Vaccine Immunol. 19, 865–874. https://doi.org/10.1128/CVI.00119-12

184. Mannelli, A., Bertolotti, L., Gern, L., Gray, J., 2011. Ecology of *Borrelia burgdorferi* sensu lato in Europe: transmission dynamics in multi-host systems, influence of molecular processes and effects of climate change. FEMS Microbiol. Rev. 36, 837–861. https://doi.org/10.1111/j.1574-6976.2011.00312.x

185. Maraspin, V., Ogrinc, K., Ružić-Sabljić, E., Lotrič-Furlan, S., Strle, F., 2011. Isolation of *Borrelia burgdorferi* sensu lato from blood of adult patients with borrelial lymphocytoma, Lyme neuroborreliosis, Lyme arthritis and acrodermatitis chronica atrophicans. Infection 39, 35–40. https://doi.org/10.1007/s15010-010-0062-8

186. Margos, G., Vollmer, S.A., Ogden, N.H., Fish, D., 2011. Population genetics, taxonomy, phylogeny and evolution of *Borrelia burgdorferi* sensu lato. Infect. Genet. Evol. 11, 1545–1563. https://doi.org/10.1016/j.meegid.2011.07.022

187. Markowicz, M., Reiter, M., Gamper, J., Stanek, G., Stockinger, H., 2021. Persistent anti-*Borrelia* IgM antibodies without Lyme borreliosis in the clinical and immunological context. Microbiol. Spectr. 9, e01020-21. https://doi.org/10.1128/spectrum.01020-21

188. Marques, A., 2008. Chronic Lyme disease: A Review. Infect. Dis. Clin. North Am. 22, 341–360. https://doi.org/10.1016/j.idc.2007.12.011

189. Mathiesen, M.J., Christiansen, M., Holm, A., Åsbrink, E., Theisen, M., Hansen, K., Åsbrink, E.V.A., 1998. Peptide-based OspC enzyme-linked immunosorbent assay for serodiagnosis of Lyme borreliosis. J. Clin. Microbiol. 36, 3474–3479. https://doi.org/10.1128/JCM.36.12.3474-3479.1998.

190. Mathieu, K., Javed, W., Vallet, S., Lesterlin, C., Candusso, M.P., Ding, F., Xu, X.N., Ebel, C., Jault, J.M., Orelle, C., 2019. Functionality of membrane proteins overexpressed and purified from *E. coli* is highly dependent upon the strain. Sci. Rep. 9, e2654. https://doi.org/10.1038/S41598-019-39382-0

191. Matyjasek, A., Zdrojewski, Z., 2016. Borreliosis — the latest recommendations on diagnosis. Forum Reumatol. 2, 58–64.

192. McDowell, J. V., Hovis, K.M., Zhang, H., Tran, E., Lankford, J., Marconi, R.T., 2006. Evidence that the BBA68 protein (BbCRASP-1) of the Lyme disease spirochetes does not contribute to factor H-mediated immune evasion in humans and other animals. Infect. Immun. 74, 3030–3034. https://doi.org/10.1128/IAI.74.5.3030-3034.2006

193. Meriläinen, L., Herranen, A., Schwarzbach, A., Gilbert, L., 2015. Morphological and biochemical features of *Borrelia burgdorferi* pleomorphic forms. Microbiology 161, 516–527. https://doi.org/10.1099/mic.0.000027

194. Molins, C.R., Delorey, M.J., Replogle, A., Sexton, C., Schriefer, M.E., 2017. Evaluation of bioMérieux's dissociated Vidas Lyme IgM II and IgG II as a first-tier diagnostic assay for

Lyme disease. J. Clin. Microbiol. 55, 1698–1706. https://doi.org/10.1128/JCM.02407-16

195. Mongodin, E.F., Casjens, S.R., Bruno, J.F., Xu, Y., Drabek, E.F., Riley, D.R., Cantarel, B.L., Pagan, P.E., Hernandez, Y.A., Vargas, L.C., Dunn, J.J., Schutzer, S.E., Fraser, C.M., Qiu, W.G., Luft, B.J., 2013. Inter- and intra-specific pan-genomes of *Borrelia burgdorferi* sensu lato: Genome stability and adaptive radiation. BMC Genomics 14, 1–25. https://doi.org/10.1186/1471-2164-14-693

196. Moniuszko-Malinowska, A., Czupryna, P., Zajkowska, J., 2016. *Borrelia burgdorferi* – morphological structure and motility as adaptation for transmission and survival in the habitat of a tick - vertebrate setup. Przegl. Epidemiol. 70, 420–427.

197. Montigny, C., Penin, F., Lethias, C., Falson, P., 2004. Overcoming the toxicity of membrane peptide expression in bacteria by upstream insertion of Asp-Pro sequence. Biochim. Biophys. Acta. 1660, 53–65. https://doi.org/10.1016/J.BBAMEM.2003.10.013

198. Motaleb, M.A., Pitzer, J.E., Sultan, S.Z., Liu, J., 2011. A novel gene inactivation system reveals altered periplasmic flagellar orientation in a *Borrelia burgdorferi fliL* mutant. J. Bacteriol. 193, 3324–3331. https://doi.org/10.1128/JB.00202-11

199. Mucci, J., Carmona, S.J., Volcovich, R., Altcheh, J., Bracamonte, E., Marco, J.D., Nielsen, M., Buscaglia, C.A., Agüero, F., 2017. Next-generation ELISA diagnostic assay for Chagas disease based on the combination of short peptidic epitopes. PLoS Negl. Trop. Dis. 11, e0005972. https://doi.org/10.1371/JOURNAL.PNTD.0005972

200. Mygland, Å., Ljøstad, U., Fingerle, V., Rupprecht, T., Schmutzhard, E., Steiner, I., 2010. EFNS guidelines on the diagnosis and management of European Lyme neuroborreliosis. Eur. J. Neurol. 17, 8–16. https://doi.org/10.1111/j.1468-1331.2009.02862.x

201. Nair, S., Kukreja, N., Singh, B.P., Arora, N., 2011. Identification of B-cell epitopes of alcohol dehydrogenase allergen of *Curvularia lunata*. PLoS One 6, e20020. https://doi.org/10.1371/JOURNAL.PONE.0020020

202. Norris, S.J., 2015. *vls* antigenic variation systems of Lyme disease *Borrelia*: eluding host immunity through both random, segmental gene conversion and framework heterogeneity. Microbiol. Spectr. 2, 1–29. https://doi.org/10.1128/microbiolspec.MDNA3-0038-2014

203. Norris, S.J., 2006. The dynamic proteome of Lyme disease *Borrelia*. Genome Biol. 7, 209. https://doi.org/10.1186/gb-2005-7-3-209

204. Nowakowski, J., Schwartz, I., Liveris, D., Wang, G., Aguero-Rosenfeld, M.E., Girao, G., McKenna, D., Nadelman, R.B., Cavaliere, L.F., Wormser, G.P., 2002. Laboratory diagnostic techniques for patients with early Lyme disease associated with erythema migrans: A comparison of different techniques. Clin. Infect. Dis. 33, 2023–2027. https://doi.org/10.1086/324490

205. Nowalk, A., Green, M., 2016. Epstein-Barr virus. Microbiol. Spectr. 4. https://doi.org/10.1128/MICROBIOLSPEC.DMIH2-0011-2015

206. Nowalk, A.J., Gilmore, R.D., Carroll, J.A., 2006. Serologic proteome analysis of *Borrelia burgdorferi* membrane-associated proteins. Infect. Immun. 74, 3864–3873. https://doi.org/10.1128/IAI.00189-06

207. Obert, R., Adelman, B.N., Orowitz, A.W.H., Ze -Chen, T., Sieh, H., Oseph, J., Aria, M., Guero -R Osenfeld, E.A., Ra, I., Chwartz, S., Ohn, J., Owakowski, N., Hobha, S., Arde, V., Ary, G., Ormser, P.W., 2009. Simultaneous human granulocytic ehrlichiosis and Lyme borreliosis. N. Engl. J. Med. 337, 27–30. https://doi.org/10.1056/NEJM199707033370105

208. Ohnishi, J., Piesman, J., de Silva, A.M., 2001. Antigenic and genetic heterogeneity of *Borrelia burgdorferi* populations transmitted by ticks. Proc. Natl. Acad. Sci. 98, 670–675. https://doi.org/10.1073/pnas.98.2.670

209. Ojaimi, C., Brooks, C., Casjens, S., Rosa, P., Elias, A., Barbour, A., Jasinskas, A., Benach, J., Katona, L., Radolf, J., Caimano, M., Skare, J., Swingle, K., Akins, D., Schwartz, I., 2003. Profiling of temperature-induced changes in *Borrelia burgdorferi* gene expression by using whole genome arrays. Infect. Immun. 71, 1689–1705. https://doi.org/10.1128/IAI.71.4.1689

210. Padula, S.J., Dias, F., Sampieri, A., Craven, R.B., Ryan, R.W., 1994. Use of recombinant Ospc from *Borrelia burgdorferi* for serodiagnosis of early Lyme disease. J. Clin. Microbiol. 32, 1733–1738.

211. Panelius, J., Lahdenne, P., Heikkila, T., Peltomaa, M., Oksi, J., Seppala, I., 2002. Recombinant OspC from *Borrelia burgdorferi* sensu stricto *B. afzelii* and *B. garinii* in the serodiagnosis of Lyme borreliosis. J. Med. Microbiol. 51, 731–739. https://doi.org/10.1099/0022-1317-51-9-731

212. Panelius, J., Lahdenne, P., Saxén, H., Carlsson, S.A., Heikkilä, T., Peltomaa, M., Lauhio, A., Seppälä, I., 2003. Diagnosis of Lyme neuroborreliosis with antibodies to recombinant proteins DbpA, BBK32, and OspC, and VIsE IR6 peptide. J. Neurol. 250, 1318–1327. https://doi.org/10.1007/s00415-003-0205-2

213. Panelius, J., Lahdenne, P., Saxen, H., Heikkila, T., Seppala, I., 2001. Recombinant flagellin A proteins from *Borrelia burgdorferi* sensu stricto, *B. afzelii*, and *B. garinii* in serodiagnosis of Lyme borreliosis. J. Clin. Microbiol. 39, 4013–4019. https://doi.org/10.1128/JCM.39.11.4013

214. Panelius, J., Sillanpää, H., Seppälä, I., Sarvas, H., Lahdenne, P., 2007. Antibodies to recombinant decorin-binding proteins A and B in the cerebrospinal fluid of patients with Lyme neuroborreliosis. Scand. J. Infect. Dis. 39, 775–780. https://doi.org/10.1080/00365540701367744

215. Park, J., Throop, A.L., LaBaer, J., 2015. Site-specific recombinational cloning using gateway and In-Fusion cloning schemes. Curr. Protoc. Mol. Biol. 2015, 3.20.1-3.20.23. https://doi.org/10.1002/0471142727.mb0320s110

216. Parker, J.M.R., Guo, D., Hodges, R.S., 1986. New hydrophilicity scale derived from high-performance liquid chromatography peptide retention data: correlation of predicted surface residues with antigenicity and X-ray-derived accessible sites. Biochemistry 25, 5425–5432. https://doi.org/10.1021/BI00367A013

217. Patriquin, G., LeBlanc, J., Heinstein, C., Roberts, C., Lindsay, R., Hatchette, T.F., 2016. Cross-reactivity between Lyme and syphilis screening assays: Lyme disease does not cause false-positive syphilis screens. Diagn. Microbiol. Infect. Dis. 84, 184–186. https://doi.org/10.1016/J.DIAGMICROBIO.2015.11.019

218. Perkins, N.J., Schisterman, E.F., 2006. The inconsistency of “Optimal’ cutpoints obtained using two criteria based on the receiver operating characteristic curve. Am. J. Epidemiol. 163, 670–675. https://doi.org/10.1093/aje/kwj063

219. Pichler, W.J., 2002. Modes of presentation of chemical neoantigens to the immune system. Toxicology 181–182, 49–54. https://doi.org/10.1016/S0300-483X(02)00254-8

220. Ponomarenko, J., Bui, H.H., Li, W., Fusseder, N., Bourne, P.E., Sette, A., Peters, B., 2008. ElliPro: A new structure-based tool for the prediction of antibody epitopes. BMC Bioinformatics 9, 1–8. https://doi.org/10.1186/1471-2105-9-514

221. Potocnakova, L., Bhide, M., Pulzova, L.B., 2016. an introduction to B-cell epitope mapping and *in silico* epitope prediction. J. Immunol. Res. 2016. https://doi.org/10.1155/2016/6760830

222. Probert, W.S., Johnson, B.J.B., 1998. Identification of a 47 kDa fibronectin-binding protein expressed by *Borrelia burgdorferi* isolate B31. Mol. Microbiol. 30, 1003–1015. https://doi.org/10.1046/j.1365-2958.1998.01127.x

223. Purser, J.E., Norris, S.J., 2000. Correlation between plasmid content and infectivity in *Borrelia burgdorferi*. Proc. Natl. Acad. Sci. 97, 13865–13870. https://doi.org/10.1073/pnas.97.25.13865

224. Rahman, M. Saifur, Rahman, M.K., Saha, S., Kaykobad, M., Rahman, M. Sohel, 2019. Antigenic: An improved prediction model of protective antigens. Artif. Intell. Med. 94, 28–41. https://doi.org/10.1016/J.ARTMED.2018.12.010

225. Raoult, D., Hechemy, K.E., Baranton, G., 1989. Cross-reaction with *Borrelia burgdorferi*

antigen of sera from patients with human immunodeficiency virus infection, syphillis, and leptospirosis. J. Clin. Microbiol. 27, 2152–2155. https://doi.org/10.1128/jcm.27.10.2152-2155.1989

226. Rauer, S., Spohn, N., Rasiah, C., Neubert, U., Vogt, A., 1998. Enzyme-linked immunosorbent assay using recombinant OspC and the internal 14-kDa flagellin fragment for serodiagnosis of early Lyme disease. J. Clin. Microbiol. 36, 857–861. https://doi.org/10.1128/JCM.36.4.857-861.1998

227. Rawlins, M.L., Gerstner, C., Hill, H.R., Litwin, C.M., 2005. Evaluation of a Western blot method for the detection of *Yersinia* antibodies: Evidence of serological cross-reactivity between *Yersinia* outer membrane proteins and *Borrelia burgdorferi*. Clin. Diagn. Lab. Immunol. 12, 1269–1274. https://doi.org/10.1128/CDLI.12.11.1269-1274.2005

228. Rebaudet, S., Parola, P., 2006. Epidemiology of relapsing fever borreliosis in Europe. FEMS Immunol. Med. Microbiol. 48, 11–15. https://doi.org/10.1111/j.1574-695X.2006.00104.x

229. Reed, K.D., 2002. Laboratory testing for Lyme disease: possibilities and practicalities. J. Clin. Microbiol. 40 2, 319–24. https://doi.org/10.1128/JCM.40.2.319

230. Renaudineau, Y., JAMIN, C., SARAUX, A., PIERRE, Y., 2005. Rheumatoid factor on a daily basis. Autoimmunity 38, 11–16. https://doi.org/10.1080/08916930400022574

231. Revel, A.T., Blevins, J.S., Almazán, C., Neil, L., Kocan, K.M., Fuente, J. de la, Hagman, K.E., Norgard, M. V., 2005. *bptA* (*bbe16*) is essential for the persistence of the Lyme disease spirochete, *Borrelia burgdorferi*, in its natural tick vector. Proc. Natl. Acad. Sci. U. S. A. 102, 6972–6977. https://doi.org/10.1073/pnas.0502565102

232. Rizzoli, A., Hauffe, H.C., Carpi, G., Vourc'h, G.I., Neteler, M., Rosà, R., 2011. Lyme borreliosis in Europe. Eurosurveillance 16, 1–8. https://doi.org/10.2807/ese.16.27.19906-en

233. Roberts, W.C., Mullikin, B.A., Lathigra, R., Hanson, M.S., 1998. Molecular analysis of sequence heterogeneity among genes encoding decorin binding proteins A and B of *Borrelia burgdorferi* sensu lato. Infect. Immun. 66, 5275–5285. https://doi.org/10.1128/iai.66.11.5275-5285.1998

234. Roessler, D., Hauser, U., Wilske, B., 1997a. Heterogeneity of BmpA (P39) among European isolates of *Borrelia burgdorferi* sensu lato and influence of interspecies variability on serodiagnosis. J. Clin. Microbiol. 35, 2752–2758.

235. Rosa, P., Tilly, K., Stewart, P., 2005. The burgeoning molecular genetics of the Lyme disease spirochaete. Nature 3, 129–143. https://doi.org/10.1038/nrmicro1068

236. Rubinstein, N.D., Mayrose, I., Martz, E., Pupko, T., 2009. Epitopia: A web-server for predicting B-cell epitopes. BMC Bioinformatics 10, 287. https://doi.org/10.1128/AAC.00558-09

237. Ružić-Sabljić, E., Cerar, T., 2017. Progress in the molecular diagnosis of Lyme disease. Expert Rev. Mol. Diagn. 17, 19–30. https://doi.org/10.1080/14737159.2016.1246959

238. Sahdev, S., Khattar, S.K., Saini, K.S., 2008. Production of active eukaryotic proteins through bacterial expression systems: A review of the existing biotechnology strategies. Mol. Cell. Biochem. 307, 249–264. https://doi.org/10.1007/s11010-007-9603-6

239. Salinas, G., Pellizza, L., Margenat, M., Fló, M., Fernández, C., 2011. Tuned *Escherichia coli* as a host for the expression of disulfide-rich proteins. Biotechnol. J. 6, 686–699. https://doi.org/10.1002/BIOT.201000335

240. Salo, J., Loimaranta, V., Lahdenne, P., Viljanen, M.K., Hytönen, J., 2011. Decorin binding by DbpA and B of *Borrelia garinii*, *Borrelia afzelii*, and *Borrelia burgdorferi* sensu stricto. J. Infect. Dis. 204, 65–73. https://doi.org/10.1093/infdis/jir207

241. Sarkar, A., Tilly, K., Stewart, P., Bestor, A., Battisti, J.M., Rosa, P.A., 2009. *Borrelia burgdorferi* resistance to a major skin antimicrobial peptide is independent of outer surface lipoprotein content. Antimicrob. Agents Chemother. 53, 4490–4494. https://doi.org/10.1128/AAC.00558-09

242. Sarma, J.V., Ward, P.A., 2011. The complement system. Cell Tissue Res. 343, 227–235. https://doi.org/10.1007/s00441-010-1034-0

243. Schicht, S., Junge, S., Schnieder, T., Strube, C., 2011. Prevalence of *Anaplasma phagocytophilum* and coinfection with *Borrelia burgdorferi* sensu lato in the hard tick *Ixodes ricinus* in the city of Hanover (Germany). Vector-Borne Zoonotic Dis. 11, 1595–1597. https://doi.org/10.1089/vbz.2011.0699

244. Schmidt, B., 1997. PCR in laboratory diagnosis of human *Borrelia burgdorferi* infections. Clin. Microbiol. Rev. 10, 185–201. https://doi.org/10.1128/CMR.10.1.185

245. Schulte-Spechtel, U., Fingerle, V., Goettner, G., Rogge, S., Wilske, B., 2006. Molecular analysis of decorin-binding protein A (DbpA) reveals five major groups among European *Borrelia burgdorferi* sensu lato strains with impact for the development of serological assays and indicates lateral gene transfer of the *dbpA* gene. Int. J. Med. Microbiol. 296, 250–266. https://doi.org/10.1016/j.ijmm.2006.01.006

246. Schutzer, S.E., Body, B.A., Boyle, J., Branson, B.M., Dattwyler, R.J., Fikrig, E., Gerald, N.J., Gomes-Solecki, M., Kintrup, M., Ledizet, M., Levin, A.E., Lewinski, M., Liotta, L.A., Marques, A., Mead, P.S., Mongodin, E.F., Pillai, S., Rao, P., Robinson, W.H., Roth, K.M., Schriefer, M.E., Slezak, T., Snyder, J.L., Steere, A.C., Witkowski, J., Wong, S.J., Branda, J.A., 2019. Direct diagnostic tests for Lyme disease. Clin. Infect. Dis. 68, 1052–1057. https://doi.org/10.1093/cid/ciy614

247. Schwan, T.G., Piesman, J., 2000. Temporal changes in outer surface proteins A and C of the Lyme disease- associated spirochete, *Borrelia burgdorferi*, during the chain of infection in ticks and mice. J. Clin. Microbiol. 38, 382–388.

248. Schwan, T.G., Piesman, J., Golde, W.T., Dolan, M.C., Rosa, P.A., 1995. Induction of an outer surface protein on *Borrelia burgdorferi* during tick feeding. Proc. Natl. Acad. Sci. U. S. A. 92, 2909–2913. https://doi.org/10.1073/pnas.92.7.2909

249. Schwartz, I., Margos, G., Casjens, S.R., Qiu, W.G., Eggers, C.H., 2021. Multipartite genome of Lyme disease *Borrelia*: Structure, variation and prophages. Curr. Issues Mol. Biol. 42, 409–454. https://doi.org/10.21775/CIMB.042.409

250. Seriburi, V., Ndukwe, N., Chang, Z., Cox, M.E., Wormser, G.P., 2012. High frequency of false positive IgM immunoblots for *Borrelia burgdorfer*i in clinical practice. Clin. Microbiol. Infect. 18, 1236–1240. https://doi.org/10.1111/J.1469-0691.2011.03749.X

251. Shapiro, E.D., 2014. Lyme Disease. N. Engl. J. Med. 370, 1724–1731. https://doi.org/10.1056/NEJMcp1314325

252. Sharma, S., Ciufo, S., Starchenko, E., Darji, D., Chlumsky, L., Karsch-Mizrachi, I., Schoch, C.L., 2018. The NCBI BioCollections Database. Database 2018, 6. https://doi.org/10.1093/DATABASE/BAY006

253. Simpson, W.J., Cieplak, W., Schrumpf, M.E., Barbour, A.G., Schwan, T.G., 1994. Nucleotide-sequence and analysis of the gene in *Borrelia burgdorferi* encoding the immunogenic P39 antigen. Fems Microbiol. Lett. 119, 381–387. https://doi.org/10.1111/j.1574-6968.1994.tb06917.x

254. Singh, S.M., Panda, A.K., 2005. Solubilization and refolding of bacterial inclusion body proteins. J. Biosci. Bioeng. 99, 303–310. https://doi.org/10.1263/JBB.99.303

255. Siński, E., Welc-Falęciak, R., Zajkowska, J., 2016. *Borrelia miyamotoi*: A human tick-borne relapsing fever spirochete in Europe and its potential impact on public health. Adv. Med. Sci. 61, 255–260. https://doi.org/10.1016/j.advms.2016.03.001

256. Smismans, A., Goossens, V.J., Nulens, E., Bruggeman, C.A., 2006. Comparison of five different immunoassays for the detection of *Borrelia burgdorferi* IgM and IgG antibodies. Clin. Microbiol. Infect. 12, 648–655. https://doi.org/10.1111/j.1469-0691.2006.01448.x

257. Stanek, G., Reiter, M., 2011. The expanding Lyme *Borrelia* complex-clinical significance of genomic species? Clin. Microbiol. Infect. 17, 487–493. https://doi.org/10.1111/j.1469-0691.2011.03492.x

258. Stanek, G., Wormser, G.P., Gray, J., Strle, F., 2012. Lyme borreliosis. Lancet 379, 461–473. https://doi.org/10.1016/S0140-6736(11)60103-7

259. Steere, A.C., Coburn, J., Glickstein, L., 2004. The emergence of Lyme disease. J. Clin. Invest. 113, 1093–1101. https://doi.org/10.1172/JCI21681

260. Steere, A.C., Drouin, E.E., Glickstein, L.J., 2011. Relationship between immunity to *Borrelia burgdorferi* outer-surface protein A (OspA) and Lyme arthritis. Clin. Infect. Dis. 52, s259–s265. https://doi.org/10.1093/CID/CIQ117

261. Steinbrink, A., Brugger, K., Margos, G., Kraiczy, P., Klimpel, S., 2022. The evolving story of *Borrelia burgdorferi* sensu lato transmission in Europe. Parasitol. Res. 2022 1213 121, 781–803. https://doi.org/10.1007/S00436-022-07445-3

262. Stephenson, K.E., Neubauer, G.H., Reimer, U., Pawlowski, N., Knaute, T., Zerweck, J., Korber, B.T., Barouch, D.H., 2015. Quantification of the epitope diversity of HIV-1-specific binding antibodies by peptide microarrays for global HIV-1 vaccine development. J. Immunol. Methods 416, 105–123. https://doi.org/10.1016/j.jim.2014.11.006

263. Stevenson, B., El-Hage, N., Hines, M.A., Miller, J.C., Babb, K., 2002. Differential binding of host complement inhibitor factor H by *Borrelia burgdorferi* Erp surface proteins: A possible mechanism underlying the expansive host range of Lyme disease spirochetes. Infect. Immun. 70, 491–497. https://doi.org/10.1128/IAI.70.2.491-497.2002

264. Stevenson, B., Krusenstjerna, A.C., Castro-Padovani, T.N., Savage, C.R., Jutras, B.L., Saylor, T.C., 2022. The consistent tick-vertebrate infectious cycle of the Lyme disease spirochete enables *Borrelia burgdorferi* to control protein expression by monitoring its physiological status. J. Bacteriol. 204. https://doi.org/10.1128/JB.00606-21

265. Strand, M., Hönig, V., Ru˚žek, D., Grubhoffer, L., Regoa, R.O.M., 2017. Europe-wide meta-analysis of *Borrelia burgdorferi* sensu lato prevalence in questing *Ixodes ricinus* ticks. Appl. Environ. Microbiol. 83, 1–16. https://doi.org/10.1128/AEM.00609-17

266. Strle, K., Drouin, E.E., Shen, S., Khoury, J.E., McHugh, G., Ruzic-Sabljic, E., Strle, F., Steere, A.C., 2009. *Borrelia burgdorferi* stimulates macrophages to secrete higher levels of cytokines and chemokines than *Borrelia afzelii* or *Borrelia garinii*. J. Infect. Dis. 200, 1936–1943. https://doi.org/10.1086/648091

267. Strzelczyk, J.K., Gaździcka, J., Cuber, P., Asman, M., Trapp, G., Gołąbek, K., Zalewska-Ziob, M., Nowak-Chmura, M., Siuda, K., Wiczkowski, A., Solarz, K., 2015. Prevalence of *Borrelia burgdorferi* sensu lato in *Ixodes ricinus* ticks collected from southern Poland. Acta Parasitol. 60, 666–674. https://doi.org/10.1515/AP-2015-0095

268. Sykes, R.A., Makiello, P., 2017. An estimate of Lyme borreliosis incidence in Western Europe. J. Public Health. 39, 74–81. https://doi.org/10.1093/pubmed/fdw017

269. Szmyt, A., Dąbrowska, A., Chrzanowska, J., 2015. Alternatywne metody otrzymywania biologicznie aktywnych białek i peptydów. Acta Sci. Pol. Biotechnol. 14, 33–44.

270. Talagrand-Reboul, E., Raffetin, A., Zachary, P., Jaulhac, B., Eldin, C., 2020. Immunoserological diagnosis of human borrelioses: current knowledge and perspectives. Front. Cell. Infect. Microbiol. 10, 241. https://doi.org/10.1128/IAI.00828-15

271. Theel, E.S., 2016. The past, present, and (possible) future of serologic testing for Lyme disease. J. Clin. Gastroenterol. 54, 1191–1196. https://doi.org/10.1128/JCM.03394-15

272. Theisen, M., Frederiksen, B., Lebech, A.M., Vuust, J., Hansen, K., 1993. Polymorphism in ospC gene of *Borrelia burgdorferi* and immunoreactivity of OspC protein: Implications for taxonomy and for use of OspC protein as a diagnostic antigen. J. Clin. Microbiol. 31, 2570–2576. https://doi.org/10.1128/JCM.31.10.2570-2576.1993

273. Tjernberg, I., Krüger, G., Eliasson, I., 2007. C6 peptide ELISA test in the serodiagnosis of Lyme borreliosis in Sweden. Eur. J. Clin. Microbiol. Infect. Dis. 26, 37–42. https://doi.org/10.1007/S10096-006-0239-3

274. Tokarz, R., Mishra, N., Tagliafierro, T., Sameroff, S., Caciula, A., Chauhan, L., Patel, J.,

Sullivan, E., Gucwa, A., Fallon, B., Golightly, M., Molins, C., Schriefer, M., Marques, A., Briese, T., Lipkin, W.I., 2018. A multiplex serologic platform for diagnosis of tick-borne diseases. Sci. Rep. 8, 1–10. https://doi.org/10.1038/s41598-018-21349-2

275. Toumanios, C., Prisco, L., Dattwyler, R.J., Arnaboldi, P.M., 2019. Linear B-cell epitopes derived from the multifunctional surface lipoprotein BBK32 as targets for the serodiagnosis of Lyme disease. mSphere 4. https://doi.org/10.1128/mSphere.00111-19

276. Tuuminen, T., Hedman, K., Söderlund-Venermo, M., Seppälä, I., 2011. Acute parvovirus B19 infection causes nonspecificity frequently in *Borrelia* and less often in *Salmonella* and *Campylobacter* serology, posing a problem in diagnosis of infectious arthropathy. Clin. Vaccine Immunol. 18, 167–172. https://doi.org/10.1128/CVI.00367-10

277. van Dam, P., Kuiper, H., Vos, K., Widjojokusumo, W., de Jongh, B.M., Spanjaard, L., Ramselaar, C., Kramer, M.D., Dankert, J., 1993. Different genospecies of *Borrelia burgdorferi* are associated with distinct clinical manifestations of Lyme borreliosis. Clin. Infect. Dis. 17, 708–717. https://doi.org/10.1093/clinids/17.4.708

278. van Dam, A.P., 2011. Molecular diagnosis of *Borrelia* bacteria for the diagnosis of Lyme disease. Expert Opin. Med. Diagn. 5, 135–149. https://doi.org/10.1517/17530059.2011.555396

279. Vassilopoulos, D., Calabrese, L.H., 2008. Virally associated arthritis 2008: Clinical, epidemiologic, and pathophysiologic considerations. Arthritis Res. Ther. 10, 1–8. https://doi.org/10.1186/AR2480

280. Vera, A., González-Montalbán, N., Arís, A., Villaverde, A., 2007. The conformational quality of insoluble recombinant proteins is enhanced at low growth temperatures. Biotechnol. Bioeng 96, 1101–1106. https://doi.org/10.1002/bit.21218

281. Verma, A., Brissette, C.A., Bowman, A., Stevenson, B., 2009. *Borrelia burgdorferi* BmpA is a laminin-binding protein. Infect. Immun. 77, 4940–4946. https://doi.org/10.1128/IAI.01420-08

282. Wagemakers, A., Coumou, J., Schuijt, T.J., Oei, A., Nijhof, A.M., Van 'T Veer, C., Van Der Poll, T., Bins, A.D., Hovius, J.W.R., 2016. An *Ixodes ricinus* tick salivary lectin pathway inhibitor protects *Borrelia burgdorferi* sensu lato from human complement. Vector-Borne Zoonotic Dis. 16, 223–228. https://doi.org/10.1089/vbz.2015.1901

283. Wager, B., Shaw, D.K., Groshong, A.M., Blevins, J.S., Skare, J.T., 2015. BB0744 affects tissue tropism and spatial distribution of *Borrelia burgdorferi*. Infect. Immun. 83, 3693–3703. https://doi.org/10.1128/IAI.00828-15

284. Walker, J.M., 1987. The enzyme linked immunosorbent assay (ELISA). Tech. Mol. Biol. 82–97. https://doi.org/10.1007/978-1-4615-9799-5_4

285. Wallich, R., Moter, S.E., Simon, M.M., Ebnet, K., Heiberger, A., Kramer, M.D., 1990. The *Borrelia burgdorferi* flagellum-associated 41-kilodalton antigen (Flagellin): Molecular cloning, expression, and amplification of the gene. Infect. Immun. 58, 1711–1719. https://doi.org/10.1128/iai.58.6.1711-1719.1990

286. Wang, G., van Dam, A.P., Schwartz, I., Dankert, J., 1999. Molecular typing of *Borrelia burgdorferi* sensu lato: taxonomic, epidemiological, and clinical implications. Clin. Microbiol. Rev. 12, 633–53. https://doi.org/10.1128/CMR.12.4.633

287. Wang, Y., Zhao, S., Bai, L., Fan, J., Liu, E., 2013. Expression systems and species used for transgenic animal bioreactors. Biomed Res. Int. 9, 580463. https://doi.org/10.1155/2013/580463

288. Webber, B.J., Burganowski, R.P., Colton, L., Escobar, J.D., Pathak, S.R., Gambino-Shirley, K.J., 2019. Lyme disease overdiagnosis in a large healthcare system: a population-based, retrospective study. Clin. Microbiol. Infect. 25, 1233–1238. https://doi.org/10.1016/j.cmi.2019.02.020

289. Weiner, Z.P., Crew, R.M., Brandt, K.S., Ullmann, A.J., Schriefer, M.E., Molins, C.R., Gilmore, R.D., 2015. Evaluation of selected *Borrelia burgdorferi* lp54 plasmid-encoded gene products

expressed during mammalian infection as antigens to improve serodiagnostic testing for early Lyme disease. Clin. Vaccine Immunol. 22, 1176–1186. https://doi.org/10.1128/CVI.00399-15

290. Wielkoszynski, T., Moghaddam, A., Bäckman, A., Broden, J., Piotrowski, R., Mond-Paszek, R., Kozarenko, A., Ny, T., Wilczynska, M., 2018. Novel diagnostic ELISA test for discrimination between infections with *Yersinia enterocolitica* and *Yersinia pseudotuberculosis*. Eur. J. Clin. Microbiol. Infect. Dis. 37, 2301–2306. https://doi.org/10.1007/S10096-018-3373-9

291. Wilske, B., Fingerle, V., Herzer, P., Hofmann, A., Lehnert, G., Peters, H., Pfister, H.W., Preac-Mursic, V., Soutschek, E., Weber, K., 1993. Recombinant immunoblot in the serodiagnosis of Lyme borreliosis - Comparison with indirect immunofluorescence and enzyme-linked immunosorbent assay. Med. Microbiol. Immunol. 182, 255–270. https://doi.org/10.1007/BF00579624

292. Wilske, B., Fingerle, V., Schulte-Spechtel, U., 2007. Microbiological and serological diagnosis of Lyme borreliosis. FEMS Immunol. Med. Microbiol. 49, 13–21. https://doi.org/10.1111/j.1574-695X.2006.00139.x

293. Wilske, Bettina, Habermann, C., Fingerle, V., Hillenbrand, B., Jauris-Heipke, S., Lehnert, G., Pradel, I., Roè Ssler, D., Schulte-Spechtel, U., 1993. An improved recombinant IgG immunoblot for serodiagnosis of Lyme borreliosis. Med Microbiol Immunol 182, 139–144. https://doi.org/10.1128/CDLI.5.4.456-462.1998

294. Wittmann-Liebold, B., Graack, H.R., Pohl, T., 2006. Two-dimensional gel electrophoresis as tool for proteomics studies in combination with protein identification by mass spectrometry. Proteomics 6, 4688–4703. https://doi.org/10.1002/pmic.200500874

295. Wojciechowska-Koszko, I., Kwiatkowski, P., Sienkiewicz, M., Kowalczyk, M., Kowalczyk, E., Dołęgowska, B., 2022. Cross-reactive results in serological tests for borreliosis in patients with active viral infections. Pathogens 11, 203. https://doi.org/10.3390/PATHOGENS11020203

296. Wu, J., Weening, E.H., Faske, J.B., Höök, M., Skare, J.T., 2011. Invasion of eukaryotic cells by *Borrelia burgdorferi* requires β1 integrins and Src kinase activity. Infect. Immun. 79, 1338–1348. https://doi.org/10.1128/IAI.01188-10

297. Xie, J., Zhi Id, H., Garrigues Id, R.J., Keightley, A., Garcia, B.L., Skare, J.T., 2019. Structural determination of the complement inhibitory domain of *Borrelia burgdorferi* BBK32 provides insight into classical pathway complement evasion by Lyme disease spirochetes. PLOS Pathog. 15, e1007659. https://doi.org/10.1371/journal.ppat.1007659

298. Xu, Y., Bruno, J.F., Luft, B.J., 2008. Profiling the humoral immune response to *Borrelia burgdorferi* infection with protein microarrays. Microb. Pathog. 45, 403–407. https://doi.org/10.1016/J.MICPATH.2008.09.006

299. Yang, X., Izadi, H., Coleman, A.S., Wang, P., Ma, Y., Fikrig, E., Anguita, J., Pal, U., 2008. *Borrelia burgdorferi* lipoprotein BmpA activates pro-inflammatory responses in human synovial cells through a protein moiety. Microbes Infect. 10, 1300–1308. https://doi.org/10.1016/j.micinf.2008.07.029

300. Yang, X.F., Pal, U., Alani, S.M., Fikrig, E., Norgard, M. V., 2004. Essential role for OspA/B in the life cycle of the Lyme disease spirochete. J. Exp. Med. 199, 641–648. https://doi.org/10.1084/jem.20031960

301. Yang, Z., Zhang, L., Zhang, Y., Zhang, T., Feng, Y., Lu, X., Lan, W., Wang, J., Wu, H., Cao, C., Wang, X., 2011. Highly efficient production of soluble proteins from insoluble inclusion bodies by a two-step-denaturing and refolding method. PLoS One 6, 1–8. https://doi.org/10.1371/journal.pone.0022981

302. Zhang, J., Tao, A., 2015. Antigenicity, immunogenicity, allergenicity. Allergy Bioinforma. 8, 175. https://doi.org/10.1007/978-94-017-7444-4_11

303. Zhang, J.R., Hardham, J.M., Barbour, A.G., Norris, S.J., 1997. Antigenic variation in Lyme disease *borreliae* by promiscuous recombination of VMP-like sequence cassettes. Cell 89,

275–285. https://doi.org/10.1016/S0092-8674(00)80206-8

304. Zhang, X., Yang, X., Kumar, M., Pal, U., 2009. BB0323 function is essential for *Borrelia burgdorferi* virulence and persistence through tick-rodent transmission Cycle. J. Infect. Dis. 200, 1318–1330. https://doi.org/10.1086/605846

SUPPLEMENTARY MATERIALS

Table S1 Nucleotide sequence of plasmid pUC57-BmpA-BBK32-G

pUC57-BmpA-BBK32-G				
1	AGCTTGGCGT	AATCATGGTC	ATAGCTGTTT	CCTGTGTGAA	ATTGTTATCC
51	GCTCACAATT	CCACACAACA	TACGAGCCGG	AAGCATAAAG	TGTAAAGCCT
101	GGGGTGCCTA	ATGAGTGAGC	TAACTCACAT	TAATTGCGTT	GCGCTCACTG
151	CCCGCTTTCC	AGTCGGGAAA	CCTGTCGTGC	CAGCTGCATT	AATGAATCGG
201	CCAACGCGCG	GGGAGAGGCG	GTTTGCGTAT	TGGGCGCTCT	TCCGCTTCCT
251	CGCTCACTGA	CTCGCTGCGC	TCGGTCGTTC	GGCTGCGGCG	AGCGGTATCA
301	GCTCACTCAA	AGGCGGTAAT	ACGGTTATCC	ACAGAATCAG	GGGATAACGC
351	AGGAAAGAAC	ATGTGAGCAA	AAGGCCAGCA	AAAGGCCAGG	AACCGTAAAA
401	AGGCCGCGTT	GCTGGCGTTT	TTCCATAGGC	TCCGCCCCCC	TGACGAGCAT
451	CACAAAAATC	GACGCTCAAG	TCAGAGGTGG	CGAAACCCGA	CAGGACTATA
501	AAGATACCAG	GCGTTTCCCC	CTGGAAGCTC	CCTCGTGCGC	TCTCCTGTTC
551	CGACCCTGCC	GCTTACCGGA	TACCTGTCCG	CCTTTCTCCC	TTCGGGAAGC
601	GTGGCGCTTT	CTCATAGCTC	ACGCTGTAGG	TATCTCAGTT	CGGTGTAGGT
651	CGTTCGCTCC	AAGCTGGGCT	GTGTGCACGA	ACCCCCCGTT	CAGCCCGACC
701	GCTGCGCCTT	ATCCGGTAAC	TATCGTCTTG	AGTCCAACCC	GGTAAGACAC
751	GACTTATCGC	CACTGGCAGC	AGCCACTGGT	AACAGGATTA	GCAGAGCGAG
801	GTATGTAGGC	GGTGCTACAG	AGTTCTTGAA	GTGGTGGCCT	AACTACGGCT
851	ACACTAGAAG	AACAGTATTT	GGTATCTGCG	CTCTGCTGAA	GCCAGTTACC
901	TTCGGAAAAA	GAGTTGGTAG	CTCTTGATCC	GGCAAACAAA	CCACCGCTGG
951	TAGCGGTGGT	TTTTTTGTTT	GCAAGCAGCA	GATTACGCGC	AGAAAAAAAG
1001	GATCTCAAGA	AGATCCTTTG	ATCTTTTCTA	CGGGGTCTGA	CGCTCAGTGG
1051	AACGAAAACT	CACGTTAAGG	GATTTTGGTC	ATGAGATTAT	CAAAAAGGAT
1101	CTTCACCTAG	ATCCTTTTAA	ATTAAAAATG	AAGTTTTAAA	TCAATCTAAA
1151	GTATATATGA	GTAAACTTGG	TCTGACAGTT	ACCAATGCTT	AATCAGTGAG
1201	GCACCTATCT	CAGCGATCTG	TCTATTTCGT	TCATCCATAG	TTGCCTGACT
1251	CCCCGTCGTG	TAGATAACTA	CGATACGGGA	GGGCTTACCA	TCTGGCCCCA
1301	GTGCTGCAAT	GATACCGCGA	GACCCACGCT	CACCGGCTCC	AGATTTATCA
1351	GCAATAAACC	AGCCAGCCGG	AAGGGCCGAG	CGCAGAAGTG	GTCCTGCAAC
1401	TTTATCCGCC	TCCATCCAGT	CTATTAATTG	TTGCCGGGAA	GCTAGAGTAA
1451	GTAGTTCGCC	AGTTAATAGT	TTGCGCAACG	TTGTTGCCAT	TGCTACAGGC
1501	ATCGTGGTGT	CACGCTCGTC	GTTTGGTATG	GCTTCATTCA	GCTCCGGTTC
1551	CCAACGATCA	AGGCGAGTTA	CATGATCCCC	CATGTTGTGC	AAAAAAGCGG
1601	TTAGCTCCTT	CGGTCCTCCG	ATCGTTGTCA	GAAGTAAGTT	GGCCGCAGTG
1651	TTATCACTCA	TGGTTATGGC	AGCACTGCAT	AATTCTCTTA	CTGTCATGCC
1701	ATCCGTAAGA	TGCTTTTCTG	TGACTGGTGA	GTACTCAACC	AAGTCATTCT
1751	GAGAATAGTG	TATGCGGCGA	CCGAGTTGCT	CTTGCCCGGC	GTCAATACGG
1801	GATAATACCG	CGCCACATAG	CAGAACTTTA	AAAGTGCTCA	TCATTGGAAA
1851	ACGTTCTTCG	GGGCGAAAAC	TCTCAAGGAT	CTTACCGCTG	TTGAGATCCA
1901	GTTCGATGTA	ACCCACTCGT	GCACCCAACT	GATCTTCAGC	ATCTTTTACT
1951	TTCACCAGCG	TTTCTGGGTG	AGCAAAAACA	GGAAGGCAAA	ATGCCGCAAA
2001	AAAGGGAATA	AGGGCGACAC	GGAAATGTTG	AATACTCATA	CTCTTCCTTT
2051	TTCAATATTA	TTGAAGCATT	TATCAGGGTT	ATTGTCTCAT	GAGCGGATAC
2101	ATATTTGAAT	GTATTTAGAA	AAATAAACAA	ATAGGGGTTC	CGCGCACATT
2151	TCCCCGAAAA	GTGCCACCTG	ACGTCTAAGA	AACCATTATT	ATCATGACAT
2201	TAACCTATAA	AAATAGGCGT	ATCACGAGGC	CCTTTCGTCT	CGCGCGTTTC
2251	GGTGATGACG	GTGAAAACCT	CTGACACATG	CAGCTCCCGG	AGACGGTCAC
2301	AGCTTGTCTG	TAAGCGGATG	CCGGGAGCAG	ACAAGCCCGT	CAGGGCGCGT
2351	CAGCGGGTGT	TGGCGGGTGT	CGGGGCTGGC	TTAACTATGC	GGCATCAGAG
2401	CAGATTGTAC	TGAGAGTGCA	CCATATGCGG	TGTGAAATAC	CGCACAGATG
2451	CGTAAGGAGA	AAATACCGCA	TCAGGCGCCA	TTCGCCATTC	AGGCTGCGCA
2501	ACTGTTGGGA	AGGGCGATCG	GTGCGGGCCT	CTTCGCTATT	ACGCCAGCTG
2551	GCGAAAGGGG	GATGTGCTGC	AAGGCGATTA	AGTTGGGTAA	CGCCAGGGTT
2601	TTCCCAGTCA	CGACGTTGTA	AAACGACGGC	CAGTGAATTC	GAGCTCGGTA
2651	CCTCGCGAAT	GCATCTAGAT	ATCGGATCCA	TGCAGCGGTA	AAGGCAGCCT
2701	GGGTAGCGAA	ATTCCGAAAG	TGAGCCTGAT	CATTGACGGC	ACCTTCGACG
2751	ATAAGAGCTT	CAACGAGAGC	GCGCTGAACG	GTGTGAAGAA	AGTTAAAGAG
2801	GAATTCAAGA	TCGAACTGGT	TCTGAAGGAG	AGCAGCAGCG	GTGGCGGTCA

```
2851 GGAAGGTGCG TTTCTGACCG GCTACATTGC GGCGAAGCTG AGCAAAACCG
2901 GCAAGATCGG CTTCCTGGGC GGTATCGAGG GTGAAATTGT GGATGCGTTT
2951 CGTTACGGTT ATGAAGCGGG TGCGAAATAT GCGGGCGGTG GCGTGGGCTT
3001 CGTTCGTAAC CCGAAAATGA TCAGCTTTGA GCTGGAAAAG GAGATTGACG
3051 GTGGTGGTGA CCTGTTCATC CGTTACGAAA TGAAAGAGGA GAGCCCGGGT
3101 CTGGGCGGTG GCGAACAGAG CGAGACCCGT AAGGAAAAGA TCCAAAAGCA
3151 GCAAGACGAG TACAAGGGTA TGACCCAAGG CAGCCTGA
```

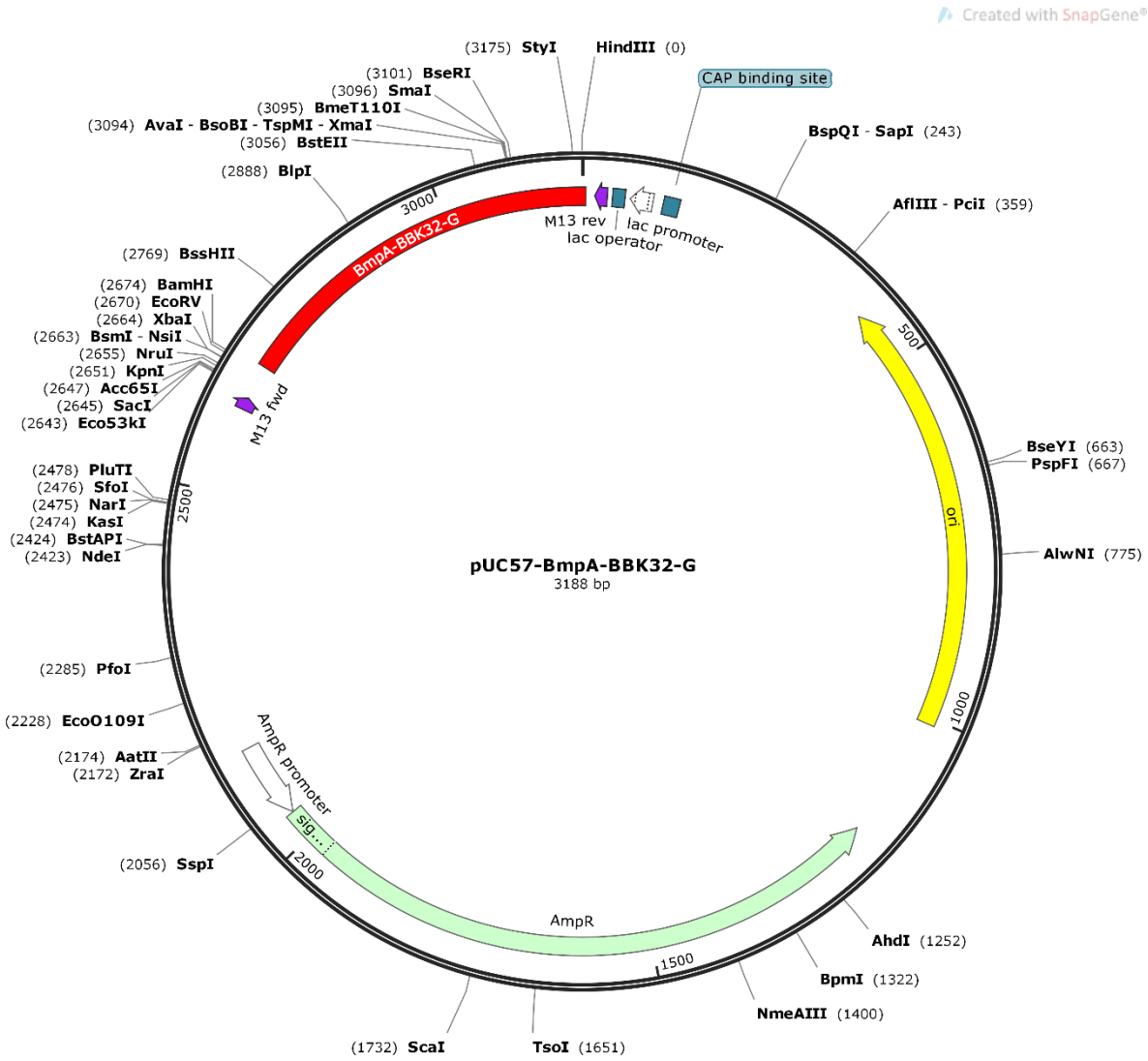

Figure S1 Map of plasmid pUC57-BmpA-BBK32-G.

Table S2 Nucleotide sequence of plasmid pUC57-BmpA-BBK32-G

pUC57-BmpA-BBK32-M
1 AGCTTGGCGT AATCATGGTC ATAGCTGTTT CCTGTGTGAA ATTGTTATCC
51 GCTCACAATT CCACACAACA TACGAGCCGG AAGCATAAAG TGTAAAGCCT
101 GGGGTGCCTA ATGAGTGAGC TAACTCACAT TAATTGCGTT GCGCTCACTG
151 CCCGCTTTCC AGTCGGGAAA CCTGTCGTGC CAGCTGCATT AATGAATCGG
201 CCAACGCGCG GGGAGAGGCG GTTTGCGTAT TGGGCGCTCT TCCGCTTCCT
251 CGCTCACTGA CTCGCTGCGC TCGGTCGTTC GGCTGCGGCG AGCGGTATCA
301 GCTCACTCAA AGGCGGTAAT ACGGTTATCC ACAGAATCAG GGGATAACGC
351 AGGAAAGAAC ATGTGAGCAA AAGGCCAGCA AAAGGCCAGG AACCGTAAAA
401 AGGCCGCGTT GCTGGCGTTT TTCCATAGGC TCCGCCCCCC TGACGAGCAT

```
 451 CACAAAAATC GACGCTCAAG TCAGAGGTGG CGAAACCCGA CAGGACTATA
 501 AAGATACCAG GCGTTTCCCC CTGGAAGCTC CCTCGTGCGC TCTCCTGTTC
 551 CGACCCTGCC GCTTACCGGA TACCTGTCCG CCTTTCTCCC TTCGGGAAGC
 601 GTGGCGCTTT CTCATAGCTC ACGCTGTAGG TATCTCAGTT CGGTGTAGGT
 651 CGTTCGCTCC AAGCTGGGCT GTGTGCACGA ACCCCCCGTT CAGCCCGACC
 701 GCTGCGCCTT ATCCGGTAAC TATCGTCTTG AGTCCAACCC GGTAAGACAC
 751 GACTTATCGC CACTGGCAGC AGCCACTGGT AACAGGATTA GCAGAGCGAG
 801 GTATGTAGGC GGTGCTACAG AGTTCTTGAA GTGGTGGCCT AACTACGGCT
 851 ACACTAGAAG AACAGTATTT GGTATCTGCG CTCTGCTGAA GCCAGTTACC
 901 TTCGGAAAAA GAGTTGGTAG CTCTTGATCC GGCAAACAAA CCACCGCTGG
 951 TAGCGGTGGT TTTTTTGTTT GCAAGCAGCA GATTACGCGC AGAAAAAAAG
1001 GATCTCAAGA AGATCCTTTG ATCTTTTCTA CGGGGTCTGA CGCTCAGTGG
1051 AACGAAAACT CACGTTAAGG GATTTTGGTC ATGAGATTAT CAAAAAGGAT
1101 CTTCACCTAG ATCCTTTTAA ATTAAAAATG AAGTTTTAAA TCAATCTAAA
1151 GTATATATGA GTAAACTTGG TCTGACAGTT ACCAATGCTT AATCAGTGAG
1201 GCACCTATCT CAGCGATCTG TCTATTTCGT TCATCCATAG TTGCCTGACT
1251 CCCCGTCGTG TAGATAACTA CGATACGGGA GGGCTTACCA TCTGGCCCCA
1301 GTGCTGCAAT GATACCGCGA GACCCACGCT CACCGGCTCC AGATTTATCA
1351 GCAATAAACC AGCCAGCCGG AAGGGCCGAG CGCAGAAGTG GTCCTGCAAC
1401 TTTATCCGCC TCCATCCAGT CTATTAATTG TTGCCGGGAA GCTAGAGTAA
1451 GTAGTTCGCC AGTTAATAGT TTGCGCAACG TTGTTGCCAT TGCTACAGGC
1501 ATCGTGGTGT CACGCTCGTC GTTTGGTATG GCTTCATTCA GCTCCGGTTC
1551 CCAACGATCA AGGCGAGTTA CATGATCCCC CATGTTGTGC AAAAAAGCGG
1601 TTAGCTCCTT CGGTCCTCCG ATCGTTGTCA GAAGTAAGTT GGCCGCAGTG
1651 TTATCACTCA TGGTTATGGC AGCACTGCAT AATTCTCTTA CTGTCATGCC
1701 ATCCGTAAGA TGCTTTTCTG TGACTGGTGA GTACTCAACC AAGTCATTCT
1751 GAGAATAGTG TATGCGGCGA CCGAGTTGCT CTTGCCCGGC GTCAATACGG
1801 GATAATACCG CGCCACATAG CAGAACTTTA AAAGTGCTCA TCATTGGAAA
1851 ACGTTCTTCG GGGCGAAAAC TCTCAAGGAT CTTACCGCTG TTGAGATCCA
1901 GTTCGATGTA ACCCACTCGT GCACCCAACT GATCTTCAGC ATCTTTTACT
1951 TTCACCAGCG TTTCTGGGTG AGCAAAAACA GGAAGGCAAA ATGCCGCAAA
2001 AAAGGGAATA AGGGCGACAC GGAAATGTTG AATACTCATA CTCTTCCTTT
2051 TTCAATATTA TTGAAGCATT TATCAGGGTT ATTGTCTCAT GAGCGGATAC
2101 ATATTTGAAT GTATTTAGAA AAATAAACAA ATAGGGGTTC CGCGCACATT
2151 TCCCCGAAAA GTGCCACCTG ACGTCTAAGA AACCATTATT ATCATGACAT
2201 TAACCTATAA AAATAGGCGT ATCACGAGGC CCTTTCGTCT CGCGCGTTTC
2251 GGTGATGACG GTGAAAACCT CTGACACATG CAGCTCCCGG AGACGGTCAC
2301 AGCTTGTCTG TAAGCGGATG CCGGGAGCAG ACAAGCCCGT CAGGGCGCGT
2351 CAGCGGGTGT TGGCGGGTGT CGGGGCTGGC TTAACTATGC GGCATCAGAG
2401 CAGATTGTAC TGAGAGTGCA CCATATGCGG TGTGAAATAC CGCACAGATG
2451 CGTAAGGAGA AAATACCGCA TCAGGCGCCA TTCGCCATTC AGGCTGCGCA
2501 ACTGTTGGGA AGGGCGATCG GTGCGGGCCT CTTCGCTATT ACGCCAGCTG
2551 GCGAAAGGGG GATGTGCTGC AAGGCGATTA AGTTGGGTAA CGCCAGGGTT
2601 TTCCCAGTCA CGACGTTGTA AAACGACGGC CAGTGAATTC GAGCTCGGTA
2651 CCTCGCGAAT GCATCTAGAT ATCGGATCCA GACCTGATCT GGCTGATTGG
2701 CTACCGTTTC AGCGATGTGG CGAAAGTTGC GGCGCTGCAG AACGGTGGCG
2751 GTAGCAACCG TTACCAAAGC TATCTGGAGG GTGTGAAGTA CAACGTTGAC
2801 AGCGCGATCC AGACCATTAC CAAAATCTAC AACACCTATA CCCTGTTCAG
2851 CACCAAGCTG ACCCAAATGT ATAGCACCCG TCTGGACAAC TTTGCGAAGG
2901 CGAAAGCGAA GGAAGAGGCG GCGAAATTCA CCAAAGAGGA CCTGGAGAAG
2951 AACTTTAAGA CCCTGCTGAA CTACATTCAA GTGAGCGTTA AAACCGCGGC
3001 GAACTTTGTG TATATCAACG ATACCCACGC GAAGCGTAAG CTGGAGAACA
3051 TTGAGGCGGA AATCAAAACC CTGATTGCGA AAATCAAGGA GCAGAGCAAC
3101 CTGTACGAAG CGTATAAGGC GATTGTTACC AGCATCCTGC TGATGCGTGA
3151 CAGCCTGAAA GAAGTGCAAG GCATCATTGA TAAGAACGGT GTTTGGTATA
```

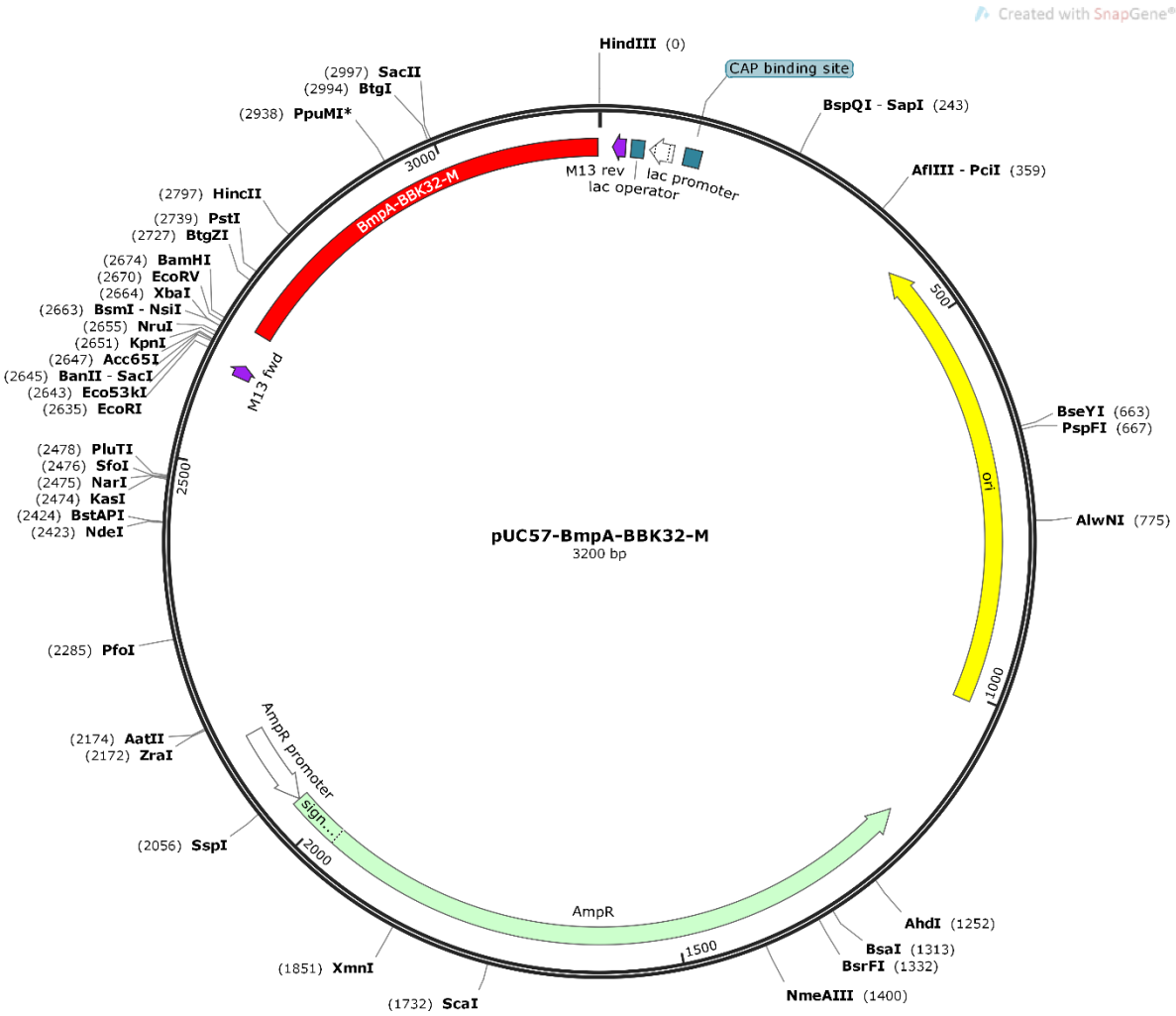

Figure S2 Map of plasmid pUC57-BmpA-BBK32-M.

Table S3 BmpA overlapping peptides identified as reactive in each of the study groups

BmpA			Serum groups					
Peptide nº	**Position in protein sequence**	**Peptide sequence**	**IgG Negative (Control)**	**IgG Positive**	**IgM positive**	**IgM negative (Control)**	**IgG mix (IgG+/IgM+)**	**IgM mix (IgG+/IgM+)**
17	27-41	EIPKVSLIIDGTFDD						X
20	30-44	KVSLIIDGTFDDKSF					X∗ϕ	
25	35-49	IDGTFDDKSFNESAL						X∗ϕ
26	36-50	DGTFDDKSFNESALN			X			X
40	50-64	NGVKKVKEEFKIELV	X					
47	57-71	EEFKIELVLKESSSN	X	X∗			X	
48	58-72	EFKIELVLKESSSNS		X∗				
54	64-78	VLKESSSNSYLSDLE	X					
59	69-83	SSNSYLSDLEGLKDA						∗
60	70-84	SNSYLSDLEGLKDAG						∗
61	71-85	NSYLSDLEGLKDAGS	X					
62	72-86	SYLSDLEGLKDAGSD						X∗
64	74-88	LSDLEGLKDAGSDLI	X					X∗
82	92-106	GYRFSDVAKVAALQN			X∗			
93	103-117	ALQNPDMKYAIIDPI				X		

BmpA			Serum groups					
Peptide nº	**Position in protein sequence**	**Peptide sequence**	**IgG Negative (Control)**	**IgG Positive**	**IgM positive**	**IgM negative (Control)**	**IgG mix (IgG+/IgM+)**	**IgM mix (IgG+/IgM+)**
94	104-118	LQNPDMKYAIIDPIY				X		
95	105-119	QNPDMKYAIIDPIYS				X		
96	106-120	NPDMKYAIIDPIYSN				X		
97	107-121	PDMKYAIIDPIYSND			X	X		X
98	108-122	DMKYAIIDPIYSNDP				X		
99	109-123	MKYAIIDPIYSNDPI				X		
100	110-124	KYAIIDPIYSNDPIP				X		
102	112-126	AIIDPIYSNDPIPAN			X	X		X
103	113-127	IIDPIYSNDPIPANL			X	X		
106	116-130	PIYSNDPIPANLVGM				X		
109	119-133	SNDPIPANLVGMTFR	X					
110	120-134	NDPIPANLVGMTFRA	X					
112	122-136	PIPANLVGMTFRAQE	X					
116	126-140	NLVGMTFRAQEGAFL	X					
142	152-166	GKIGFLGGIEGEIVD				X	X	
144	154-168	IGFLGGIEGEIVDAF					X*	
145	155-169	GFLGGIEGEIVDAFR					X*	

BmpA			Serum groups					
Peptide nº	**Position in protein sequence**	**Peptide sequence**	**IgG Negative (Control)**	**IgG Positive**	**IgM positive**	**IgM negative (Control)**	**IgG mix (IgG+/IgM+)**	**IgM mix (IgG+/IgM+)**
146	156-170	FLGGIEGEIVDAFRY					X∗ϕ	
149	159-173	GIEGEIVDAFRYGYE						X
151	161-175	EGEIVDAFRYGYEAG		X∗				
173	183-197	IKISTQYIGSFADLE						X∗
186	196-210	LEAGRSVATRMYSDE					X	
220	230-244	KELGSGHYIIGVDED						X∗
221	231-245	ELGSGHYIIGVDEDQ			X			X
228	238-252	IIGVDEDQAYLAPDN				X		
242	252-266	NVITSTTKDVGRALN	X					
255	265-279	LNIFTSNHLKTNTFE	X					
257	267-281	IFTSNHLKTNTFEGG	X					
261	271-285	NHLKTNTFEGGKLIN	X					
265	275-289	TNTFEGGKLINYGLK						∗ϕ
266	276-290	NTFEGGKLINYGLKE						X∗ϕ
267	277-291	TFEGGKLINYGLKEG						X∗ϕ
268	278-292	FEGGKLINYGLKEGV						X∗ϕ

BmpA			Serum groups					
Peptide nº	**Position in protein sequence**	**Peptide sequence**	**IgG Negative (Control)**	**IgG Positive**	**IgM positive**	**IgM negative (Control)**	**IgG mix (IgG+/IgM+)**	**IgM mix (IgG+/IgM+)**
269	279-293	EGGKLINYGLKEGVV		∗				
286	296-310	VRNPKMISFELEKEI					X∗ϕ	
297	307-321	EKEIDNLSSKIINKE		X∗				
299	309-323	EIDNLSSKIINKEII				X		
302	312-326	NLSSKIINKEIIVPS	X					
304	314-328	SSKIINKEIIVPSNK	X					
309	319-333	NKEIIVPSNKESYEK	X					
317	327-339	NKESYEKFLKEFIGS	X					

x, reactive peptides with Z-score >2. ∗, peptides that showed significant differences with Z-ratio >1.96 when are compared with the negative immunoglobulin isotype group (Control), ϕ peptides that showed significant differences with Z-ratio >1.96 when are compared with positive IgG or IgM samples depending on the immunoglobulin isotype.

Serum groups= IgG in the Negative samples (Control); IgG in the samples positive to IgG (IgG Positive); IgM in the samples positive to IgM (IgM Positive); IgM in the Negative samples (Control); IgG in samples positive to IgG and IgM (IgG mix (IgG+/IgM+)); IgM in samples positive to IgG and IgM (IgM mix (IgG+/IgM+)).

Table S4 BBK32 overlapping peptides identified as reactive in each of the study groups

BBK32			Serum groups					
Peptide nº	**Position in protein sequence**	**Peptide sequence**	**IgG Negative (Control)**	**IgG Positive**	**IgM positive**	**IgM negative (Control)**	**IgG mix (IgG+/IgM+)**	**IgM mix (IgG+/IgM+)**
14	27-41	EMKEESPGLFDKGNS		X*				
23	36-50	FDKGNSILETSEESI	X					
27	40-54	NSILETSEESIKKPM	X					
35	48-62	ESIKKPMNKKGKGKI			*			
38	51-65	KKPMNKKGKGKIARK			X*			
39	52-66	KPMNKKGKGKIARKK			X*			
40	53-67	PMNKKGKGKIARKKG				X		
42	55-69	NKKGKGKIARKKGKS			X*			
43	56-70	KKGKGKIARKKGKSK			X*			
44	57-71	KGKGKIARKKGKSKV			X*			
45	58-72	GKGKIARKKGKSKVS			X	X		
46	59-73	KGKIARKKGKSKVSR				X		
47	60-74	GKIARKKGKSKVSRK				X		
49	62-76	IARKKGKSKVSRKEP				X		
86	99-113	EEESLKTELLKEQSE						ϕ
88	101-115	ESLKTELLKEQSETR		X*				
93	106-120	ELLKEQSETRKEKIQ		X*				
100	113-127	ETRKEKIQKQQDEYK		*				
112	125-139	EYKGMTQGSLNSLSG		X*				

BBK32			Serum groups					
Peptide nº	**Position in protein sequence**	**Peptide sequence**	**IgG Negative (Control)**	**IgG Positive**	**IgM positive**	**IgM negative (Control)**	**IgG mix (IgG+/IgM+)**	**IgM mix (IgG+/IgM+)**
122	136-149	NSLSGESGELEEPIE	X					
125	139-152	SGESGELEEPIESNE						X
127	141-154	ESGELEEPIESNEID	X	X*				X
130	143-157	ELEEPIESNEIDLTI		X*			*	X*ϕ
134	147-161	PIESNEIDLTIDSDL						*
135	148-162	IESNEIDLTIDSDLR	X					
136	149-163	ESNEIDLTIDSDLRP		X*		X		
157	170-184	IAGSNSISYTDEIEE					X	
160	173-187	SNSISYTDEIEEEDY	X				X	
161	174-188	NSISYTDEIEEEDYD	X					
162	175-189	SISYTDEIEEEDYDQ				X		
163	176-190	ISYTDEIEEEDYDQY				X		
164	177-191	SYTDEIEEEDYDQYY	X		X	X		
165	178-192	YTDEIEEEDYDQYYL				X		
166	179-193	TDEIEEEDYDQYYLD	X	X		X	X*ϕ	
167	180-194	DEIEEEDYDQYYLDE			X	X	X	
168	181-195	EIEEEDYDQYYLDEY	X	X	X*		X	
169	182-196	IEEEDYDQYYLDEYD	X	X	X*	X	X	
170	183-197	EEEDYDQYYLDEYDE	X	X	X	X	X	
171	184-198	EEDYDQYYLDEYDEE	X	X	X	X	X	

BBK32			Serum groups					
Peptide nº	**Position in protein sequence**	**Peptide sequence**	**IgG Negative (Control)**	**IgG Positive**	**IgM positive**	**IgM negative (Control)**	**IgG mix (IgG+/IgM+)**	**IgM mix (IgG+/IgM+)**
172	185-199	EDYDQYYLDEYDEED	X	X	X	X		
173	186-200	DYDQYYLDEYDEEDE	X		X	X		X
174	187-201	YDQYYLDEYDEEDEE	X	X	X	X		
175	188-202	DQYYLDEYDEEDEEE	X		X	X	X	X
176	189-203	QYYLDEYDEEDEEEI	X		X	X		X
177	190-204	YYLDEYDEEDEEEIR	X	X	X	X	X	
178	191-205	YLDEYDEEDEEEIRL	X		X	X	X	X
179	192-206	LDEYDEEDEEEIRLS	X			X		
180	193-207	DEYDEEDEEEIRLSN			X	X		X
181	194-208	EYDEEDEEEIRLSNR		X*			X	X
184	197-211	EEDEEEIRLSNRYQS		X				X
185	198-212	EDEEEIRLSNRYQSY		X				X*ϕ
187	200-214	EEEIRLSNRYQSYLE						X
236	249-263	LDNFAKAKAKEEAAK			*			X*ϕ
238	251-265	NFAKAKAKEEAAKFT			*			X*ϕ
239	252-266	FAKAKAKEEAAKFTK			*			*
240	253-267	AKAKAKEEAAKFTKE			*			X*ϕ
241	254-268	KAKAKEEAAKFTKED			*			X*ϕ
243	256-270	KAKEEAAKFTKEDLE			*			X*
279	292-306	YINDTHAKRKLENIE						*
282	295-309	DTHAKRKLENIEAEI						X*ϕ
284	297-311	HAKRKLENIEAEIKT						X*ϕ

x, reactive peptides with Z-score >2. ∗, peptides that showed significant differences with Z-ratio >1.96 when are compared with the negative immunoglobulin isotype group (Control), ϕ peptides that showed significant differences with Z-ratio >1.96 when are compared with positive IgG or IgM samples depending on the immunoglobulin isotype.

Serum groups= IgG in the Negative samples (Control); IgG in the samples positive to IgG (IgG Positive); IgM in the samples positive to IgM (IgM Positive); IgM in the Negative samples (Control); IgG in samples positive to IgG and IgM (IgG mix (IgG+/IgM+)); IgM in samples positive to IgG and IgM (IgM mix (IgG+/IgM+)).

SCIENTIFIC ACHIEVEMENTS

Publications in Journals indexed by Journal Citation Report (list A)

1. Mazuecos, L., Contreras, M., Kasaija, P. D., Manandhar, P., **Grąźlewska, W**., Guisantes-Batan, E., de la Fuente, J. Natural Clerodendrum-derived tick repellent: learning from Nepali culture, *Experimental and Applied Acarology* (2023). https://doi.org/10.1007/s10493-023-00804-4 (IF[1]: 2.171; MEiN[3]: 100 Q2)
2. **Grąźlewska, W**., Ferra, B., Holec-Gąsior, L. *Borrelia burgdorferi* BmpA-BBK32 and BmpA-BBA64: new recombinant chimeric proteins with potential diagnostic value. *Pathogens*, 10, 767 (2021) https://doi.org/10.3390/pathogens10060767 (IF[1]: 3.806; MEiN[3]: 100 Q2)
3. **Grąźlewska, W**., Ferra, B., Holec-Gąsior, L. Przydatność diagnostyczna reakcji PCR w rozpoznawaniu boreliozy. *Advancements of Microbiology*, *59*, 367-377 (2020). https://doi.org/10.21307/pm-2020.59.4.28 (IF[2]: 1.106; MEiN[3]: 20 Q4)
4. Ferra, B., Holec-Gąsior, L., **Grąźlewska, W**. *Toxoplasma gondii* recombinant antigens in the serodiagnosis of toxoplasmosis in domestic and farm animals. *Animals*, *10*, 1-27 (2020). https://doi.org/10.3390/ani10081245 (IF[1]: 3.177; MEiN[3]: 100 Q1)
5. **Grąźlewska, W.,** & Holec-Gąsior, L. Antygeny rekombinantowe w diagnostyce serologicznej boreliozy. *Advancements of Microbiology, 58*, 399-413 (2019). https://doi.org/10.21307/pm-2019.58.4.399 (IF[2]: 1.106; MEiN[3]: 20 Q4)
6. Ferra, B., Holec-Gąsior, L., Gatkowska, J., Dziadek, B., Dzitko, K., **Grąźlewska, W**., Lautenbach, D. The first study on the usefulness of recombinant tetravalent chimeric proteins containing fragments of SAG2, GRA1, ROP1 and AMA1 antigens in the detection of specific anti-*Toxoplasma gondii* antibodies in mouse and human sera. *PLOS ONE*, *14*, 1-23 (2019). https://doi.org/10.1371/journal.pone.0217866 (IF[1]: 3.747; MEiN[3]: 100 Q1)
7. Holec-Gąsior, L., Ferra, B., **Grąźlewska, W**. *Toxoplasma gondii* tetravalent chimeric proteins as novel antigens for detection of specific immunoglobulin G in sera of small ruminants. *Animals*, 9, 1-8 (2019) https://doi.org/10.3390/ani9121146 (IF[1]: 3.177; MEiN[3]: 100 Q1)

[1]2-year Impact Factor (IF) according to Journal Citation Report for the 2022 year. All numbers are based on Scimago Journal & Country Rank (https://www.scimagojr.com, accessed May 2023).

[2]Impact Factor (IF) according to Journal Citation Report for the 2022 year based on the official website of the journal (http://am-online.org/about-the-journal, accessed May 2023).

[3]Journal ratings according to the Ministry of National Education (MEiN) for the 2022 year. All numbers are based on the publicly available search engine (https://punktacjaczasopism.pl/, accessed May 2023).

Conferences

1. Poster session, **Grąźlewska, W.**, Holec-Gąsior, L., Sołowińska, K., Rudzińska, M. ,,Evaluation of the diagnostic utility of recombinant proteins BB0323 and BB0108 obtained from three genospecies of *Borrelia burgdorferi* sensu lato**" -** 33rd European Congress of Clinical Microbiology & Infectious Diseases, Copenhagen, 15-18.04.2023.

2. Oral presentation, **Grąźlewska, W.**, Holec-Gąsior, L., Contreras-Rojo, M. ,,Identification of immunodominant fragments of BmpA and BBK32 *Borrelia burgdorferi* sensu stricto antigens with the use of peptide microarray-based immunoassay" - 26th Congress of the Polish Parasitological Society, Olsztyn, 11-15.09.2022.
3. Oral presentation, **Grąźlewska, W**., Holec-Gąsior, L., Ferra, B. ,,*Borrelia burgdorferi* s.l. jako groźny patogen środowiskowy - analiza problemu oraz nowe możliwości diagnostyczne" - VI Pomorskie Spotkania z Mikrobiologią, Online conference, 24-25.06.2021.
4. Poster session, **Grąźlewska, W**., Ferra, B., Holec-Gąsior, L., Gatkowska, J., Dziadek, B., Dzitko, K. „Evaluation of the diagnostic value of tri- and tetravalent chimeric proteins in a murine model of toxoplasmosis" - 8th International Weigl Conference, Łódź, 26-28.06.2019.
5. Poster session, Ferra, B., Holec-Gąsior, L., **Grąźlewska, W**., Gatkowska, J., Dziadek, B., Dzitko, K. ,,*Toxoplasma gondii* recombinant tetravalent chimeric antigens as an alternative to the native antygen in serodiagnosis of human toxoplasmosis" - 8th International Weigl Conference, Łódź, 26-28.06.2019.
6. Oral presentation, **Grąźlewska, W**., Holec-Gąsior, L. ,,Analiza sekwencji aminokwasowej białek antygenowych *Borrelia burgdorferi* sensu lato o potencjalnej użyteczności diagnostycznej" - Nowe Wyzwania Dla Polskiej Nauki. III Edycja, Sobieszewo, 8.09.2018.

Participation in grant projects

- ,,New diagnostic tests for the detection of anti-*Toxoplasma gondii* antibodies in animal serum samples based on recombinant chimeric proteins" The National Centre for Research and Development, Poland. Lider X. Financing: 1 428 850 zł. Reference: LIDER/34/0188/L-10/18/NCBR/2019.

Internships

- Research internship under the InterPhD2 program ,,Identification of *Anaplasma phagocytophilum* virulence factors transported by type IV secretion system" - Spanish Institute of Game and Wildlife Research (IREC), 4.10.2021-4.04.2022.

Other

- Oral presentation, **Grąźlewska, W**., Holec-Gąsior L. "Antygeny rekombinantowe *Borrelia burgdorferi* sesnu lato w diagnostyce serologicznej boreliozy", Seminar of the Polish Parasitological Society, 26.10.2022.